RADIOLOGY AND ONCOLOGY

vol.45 no.2
june 2011

AROMASIN®
eksemestan

ENDOKRINO ZDRAVLJENJE BOLNIC Z RAKOM DOJK PO MENOPAVZI

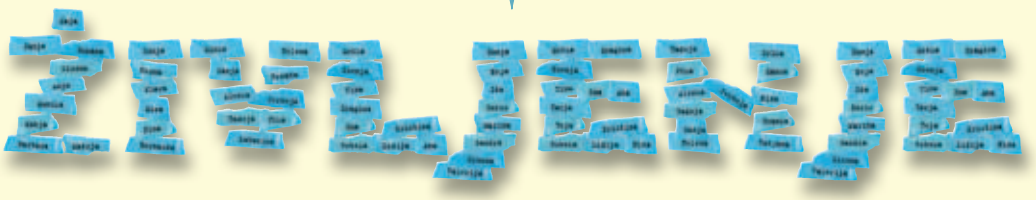

BISTVENE INFORMACIJE IZ POVZETKA GLAVNIH ZNAČILNOSTI ZDRAVILA

AROMASIN 25 mg obložene tablete
Sestava in oblika zdravila: obložena tableta vsebuje 25 mg eksemestana. **Indikacije:** Adjuvantno zdravljenje žensk po menopavzi, ki imajo invazivnega zgodnjega raka dojke s pozitivnimi estrogenskimi receptorji in so se uvodoma vsaj 2 do 3 leta zdravile s tamoksifenom. Zdravljenje napredovalega raka dojke pri ženskah z naravno ali umetno povzročeno menopavzo, pri katerih je bolezen napredovala po antiestrogenskem zdravljenju. Učinkovitost še ni bila dokazana pri bolnicah, pri katerih tumorske celice nimajo estrogenskih receptorjev. **Odmerjanje in način uporabe:** 25 mg enkrat na dan, najbolje po jedi. Pri bolnicah z zgodnjim rakom dojke je treba zdravljenje nadaljevati do dopolnjenega petega leta adjuvantnega hormonskega zdravljenja oz. do recidiva tumorja. Pri bolnicah z napredovalim rakom dojke je treba zdravljenje nadaljevati, dokler ni razvidno napredovanje tumorja. **Kontraindikacije:** znana preobčutljivost na učinkovino zdravila ali na katero od pomožnih snovi, ženske pred menopavzo, nosečnice in doječe matere. **Posebna opozorila in previdnostni ukrepi:** predmenopavzni endokrini status, jetrna ali ledvična okvara, bolniki z redko dedno intoleranco za fruktozo, malabsorpcijo glukoze/galaktoze ali pomanjkanjem saharoza-izomaltaze. Lahko povzroči alergijske reakcije ali zmanjšanje mineralne gostote kosti ter večjo pogostnost zlomov. Ženskam z osteoporozo ali tveganjem zanjo je treba na začetku zdravljenja izmeriti mineralno kostno gostoto s kostno denzitometrijo. Čeprav še ni dovolj podatkov, kako učinkujejo zdravila za zdravljenje zmanjšane mineralne kostne gostote, ki jo povzroča Aromasin, je treba pri bolnicah s tveganjem uvesti zdravljenje ali profilakso osteoporoze ter bolnice natančno spremljati. **Medsebojno delovanje z drugimi zdravili:** Sočasna uporaba zdravil – npr. rifampicina, antiepileptikov (npr. fenitoina ali karbamazepina) ali zdravil rastlinskega izvora s šentjaževko – ki inducirajo CYP 3A4, lahko zmanjša učinkovitost Aromasina. Uporabljati ga je treba previdno z zdravili, ki se presnavljajo s pomočjo CYP 3A4 in ki imajo ozek terapevtski interval. Kliničnih izkušenj s sočasno uporabo zdravila Aromasin in drugih zdravil proti raku ni. Ne sme se jemati sočasno z zdravili, ki vsebujejo estrogen, saj bi ta izničila njegovo farmakološko delovanje. **Vpliv na sposobnost vožnje in upravljanja s stroji:** Po uporabi zdravila je lahko psihofizična sposobnost za upravljanje s stroji ali vožnjo avtomobila zmanjšana. **Neželeni učinki:** neželeni učinki so bili v študijah, v katerih so uporabljali standardni odmerek 25 mg, ponavadi blagi do zmerni. Zelo pogosti (> 10 %): vročinski oblivi, bolečine v sklepih, mišicah in kosteh, utrujenost, navzea, nespečnost, glavobol, močnejše znojenje, ginekološke motnje. **Način in režim izdajanja:** zdravilo se izdaja le na recept, uporablja pa se po navodilu in pod posebnim nadzorom zdravnika specialista ali od njega pooblaščenega zdravnika. **Imetnik dovoljenja za promet:** Pfizer Luksembourg SARL, 51, Avenue J. F. Kennedy, L-1855, Luksemburg.
Datum zadnje revizije besedila: 11.12.2009
Pred predpisovanjem se seznanite s celotnim povzetkom glavnih značilnosti zdravila.

"SAMO ZA STROKOVNO JAVNOST"

AR0-01-11

Pfizer

Pfizer Luxembourg SARL, Grand Duchy of Luxembourg, 51, Avenue J.F. Kennedy, L-1855,
PFIZER, Podružnica za svetovanje s področja farmacevtske dejavnosti, Ljubljana, Letališka 3c, 1000 Ljubljana, SLOVENIJA

RADIOLOGY AND ONCOLOGY

June 2011
Vol. 45 No. 2
Pages 75-158
ISSN 1318-2099
UDC 616-006
CODEN: RONCEM

Publisher
Association of Radiology and Oncology

Affiliated with
Slovenian Medical Association – Slovenian Association of Radiology, Nuclear Medicine Society,
Slovenian Society for Radiotherapy and Oncology, and Slovenian Cancer Society
Croatian Medical Association – Croatian Society of Radiology
Societas Radiologorum Hungarorum
Friuli-Venezia Giulia regional groups of S.I.R.M.
Italian Society of Medical Radiology

Aims and scope
Radiology and Oncology is a journal devoted to publication of original contributions in diagnostic and interventional radiology, computerized tomography, ultrasound, magnetic resonance, nuclear medicine, radiotherapy, clinical and experimental oncology, radiobiology, radiophysics and radiation protection.

Editorial office

Radiology and Oncology
Zaloška cesta 2
P. O. Box 2217
SI-1000 Ljubljana
Slovenia
Phone: +386 1 5879 369
Phone/Fax: +386 1 5879 434
E-mail: gsersa@onko-i.si

Reader for English
Vida Kološa

Secretary
Mira Klemenčič
Zvezdana Vukmirović

Design
Monika Fink-Serša, Samo Rovan, Ivana Ljubanović

Layout
Matjaž Lužar

Printed by
Tiskarna Ozimek, Slovenia

Published quarterly in 600 copies

Beneficiary name: DRUŠTVO RADIOLOGIJE IN ONKOLOGIJE
Zaloška cesta 2
1000 Ljubljana
Slovenia

Beneficiary bank account number: SI56 02010-0090006751
IBAN: SI56 0201 0009 0006 751
Our bank name: Nova Ljubljanska banka, d.d.,
Ljubljana, Trg republike 2,
1520 Ljubljana; Slovenia

SWIFT: LJBASI2X

Subscription fee for institutions EUR 100, individuals EUR 50

The publication of this journal is subsidized by the Slovenian Book Agency.

Indexed and abstracted by:
Science Citation Index Expanded (SciSearch®)
Journal Citation Reports/Science Edition
Scopus
EMBASE/Excerpta Medica
DOAJ
Open J-gate
Chemical Abstracts
Biomedicina Slovenica

This journal is printed on acid- free paper

On the web: ISSN 1581-3207
http://versitaopen.com/ro
http://versita.com/science/medicine/ro/
http://www.onko-i.si/radioloncol/

contents

clinical oncology

radiophysics

special communication

RADIOLOGY AND ONCOLOGY is covered in Science Citation Index Expanded (SciSearch®),Journal Citation Reports/Science Edition, Scopus, DOAJ, EMBASE/Excerpta Medica, Open J-gate, Chemical Abstracts, Biomedicina Slovenica

review

Microsatellite instability in colorectal cancer

Matej Horvat[1], Borut Stabuc[2]

[1] University Medical Centre Maribor, Maribor, Slovenia

[2] Department of Gastroenterology, University Medical Centre Ljubljana, Slovenia

Correspondence to: Matej Horvat MD, Sobetinci 45, 2281 Markovci; Phone: +386-41-872-147; E-mail: matejhorvat@onko-i.si

Received 30 November 2010
Accepted 15 January 2011

Disclosure: No potential conflicts of interest were disclosed.

Background. Colorectal cancer (CRC) is the third most common cancer in the world. In 75% CRC develops sporadically, in 25% hereditary or as a consequence of inflammatory bowel disease. CRC carcinogenesis develops over many years. The cause of CRC in 85% is chromosomal instability (CIN) and in 15% microsatellite instability (MSI-H), where hereditary nonpolyposis colorectal cancer (HNPCC) represents 10-20%. Microsatellite sequences (MS) are repeated sequences of short stretches of DNA all over the genome. Microsatellite stability (MSS) means MS are the same in each cell of an individual, whereas microsatellite instability (MSI-H) means MS differ in normal and cancer cells of an individual. The cause of MSI-H is a damaged mismatch repair mechanism (MMR), with the most important MMR proteins being MSH2, MLH1 and MSH6.

Conclusions. MSI-H seems to be an important prognostic factor in CRC and an important predictive factor of CRC chemotherapeutic treatment efficacy. Clinical trials conducted until now have shown contradictory findings in different chemotherapeutic settings, adjuvant and palliative; therefore MSI-H is going to be the object of the future research. The future of cancer treatment is in the individualized therapy based on molecular characteristics of the tumour, such as MSI-H in CRC.

Key words: colorectal cancer; microsatellite instability; chemotherapy

Introduction

Colorectal cancer (CRC) is the third most common cancer and the fourth most common cause of cancer related deaths in the world.[1] CRC incidence in last decades is steadily growing.[2] CRC incidence in Slovenia in 2007 was 1392 new cases. It was the third most common cancer in males and second most common cancer in females.[3] CRC is a significant public health problem.[4] CRC develops in 75% sporadically because of mutations acquired during a person's lifetime and in 25% as a combination of hereditary syndromes, a higher risk because of CRC familial burden without criteria for a hereditary syndrome or as consequence of inflammatory bowel disease (IBS).[1,5]

Colorectal cancer carcinogenesis

20 years ago Fearon and Vogelstein developed a theory about CRC carcinogenesis on the genetical level they called multistep carcinogenesis.[6] With this theory they explained the progress of normal colon and rectum mucosa through adenomas to malignant growth. A normal balance of mucosa cells in colon and rectum is maintained by their origin in the colonic crypt, their migration to the surface epithelia and finally apoptosis in the surface epithelia. This process reverts in adenomatous polyps and in malignant growth. There is less apoptosis in the surface epithelia and more in the colonic crypt, both is proportional to the level of malignancy. Mucosa cells become more susceptible to DNA damage, DNA methylation and reverse levels of apoptosis.[7] CRC carcinogenesis is promoted by mutations in genes involved in cellular differentiation, mitosis, growth and cellular death.[8] CRC cancerogensis is a process that lasts 5-10 years. With presence of malignant growth the quantity of genetic mutations potentiates.[9,10] The growth of CRC from a local to a disseminated form lasts further 3-5 years.[11]

CRC develops because of the genomic instability as a consequence of mutations in gatekeeper and

caretaker genes.[12] There are two forms of genomic instability: chromosomal instability (CIN) and microsatellite instability (MSI).[8,13] CIN represents 85% of genomic instability. CIN develops because of chromosomal translocations, rearrangements of parts of chromosomes and gene multiplication.[14,15] CIN develops in genes participating in chromosomal condensation, centrosome and microtubule formation and cell cycle checkpoints.[16] CRC developing through CIN pathway is aneuploid. The most common affected genes in CIN are protooncogene KRAS, tumour suppressor genes APC and p53 and BUB family genes that regulate cell cycle.[17,18]

Microsatellite instability

CRC developing because of MSI has smaller genomic abnormalities, CRC is diploid without major chromosomal abnormalities.[19] Present are point mutations, substitutions, insertions or deletions of one or a smaller number of nucleotides.[20] Microsatellite sequences (MS) are repeating stretches of DNA located throughout the entire genome: intronic parts of genes, gene promotors, untranslated terminal regions and exonic parts of genes.[21] MS are one to six base pairs long and are repeated many thousand times.[13] MS are identical in each cell of an individual, normal and malignant, condition referred to as microsatellite stability (MSS). MSI is a condition where MS differ in normal and malignant cells of an individual.[22] MSI is defined according to the presence of five Bethesda markers, three of them are dinucleotide markers (D2S123, D5S346 and D17S250) and two of them are mononucleotide markers (BAT25 in BAT26). There is an arbitrary agreement that MSI is present if normal and malignant cells of an individual differ in at least one of the Bethesda markers. MSI high (MSI-H) is present if they differ in at least two of the markers and MSI low (MSI-L) is present if they differ in one of the markers.[23] MS are susceptible to insertions or deletions at the point of replication. Replication is a process requiring the highest level of fidelity, because a replication error might induce mutations in every daughter cell.[24] The fidelity of replication is ensured by complementarities of nucleotide base pairs and the enzyme DNA polymerase with its proofreading activity. They reduce the possibility of mismatched base pairs to one in one million. With the size of human genome being $3x10^9$ base pairs the rate of mutation would be more than thousand errors with each cell replication.[25] Because of this, human cells need another proofreading mechanism enabling the highest fidelity of replication. This mechanism is called mismatch repair mechanism (MMR). An intact MMR lowers the rate of mutation for another one hundred to six hundred times.[26]

In cells with MMR genes mutation replication errors occur, MS develop mutations and in some cells MSI-H occurs. MSI-L CRC does not appear to differ clinically or pathologically from MSS CRC.[27] The lack of an intact MMR mechanism is a cause of the tumour suppressor gene inactivation and of the occurrence of either sporadic or hereditary CRC. The hereditary form of CRC developing in this manner is hereditary nonpolyposis colorectal cancer (HNPCC) - Lynch syndrome and it represents 1-3% of all CRC incidence.[28] The other form of MSI-H related CRC with the lack of intact MMR mechanism develops sporadically without hereditary mutations. The cause of this are epigenetic changes in the genome, CpG promoter hipermethylation of MMR genes, lowering the rate of their expression.[29,30] The consequence are base pair insertions or deletions and frame shift mutations.[21] MSI-H also effects TGFßRII gene mutation, a gene participating in cell signalization, and BAX gene mutation, a gene participating in the apoptosis regulation.[31] Sporadic forms of CRC develop in this manner in approximately 15%. MSI-H is a cause of some other cancers; it affects the development of 5% of endometrial, ovarian and stomach cancer.[32]

The functions of MMR proteins are recognition of mis-incorporated base pairs, the recognition of mother and daughter DNA strand and repairing mis-incorporated base pairs with the base excision. In bacteria MMR mechanism is comprised out of three MMR proteins: MutS, MutL and MutH (Figure 1).[33]

MutS protein forms a dimmer and recognizes mismatched base pairs on the daughter strand or nucleotides not being paired. MutL protein binds to the MutS - the daughter DNA strand complex and enables binding of MutH protein. MutH recognizes the daughter DNA strand that is not methylated. The daughter strand is split at the nearest GATC sites in 5′ and 3′ direction. MutH also has an endonuclease activity; it excises the daughter DNA strand between the both restriction sites. DNA polymerase and ligase complete the missing daughter strand and enzyme methylase finishes the process of replication by methylating it.[34] MMR mechanism is a process that has been highly conserved during the evolution from bacteria to human, the latter being far more complex. Each bacterial Mut protein has many human homologs.

Bacterial MutS protein has three human homologs: hMSH2, hMSH3 and hMSH6. Bacterial MutL protein has also three human homologs: hMLH1, hPMS1 and hPMS2. Human homologs of bacterial MutH protein have not been discovered yet, their function is performed by MutL homologs.[35,36]

In hereditary form of CRC HNPCC most commonly mutated genes are hMSH2, hMSH6 in hMLH1. In the sporadic form of CRC the most commonly present mutation is an epigenetic alteration, hMLH1 promotor hypermethylation, and its subsequent lower expression.[29] MSI-H is an early event in CRC carcinogenesis, it is present in 57% of HNPCC adenomas and in 3% of sporadic adenomas.[37]

Pathohistological characteristics of MSI-H colorectal cancer

CRC is defined as MSI-CRC because of mutations present in the MS of CRC cancer cells. MSI-H and MSI-L are further characterized by the number of positive Bethesda markers as noted earlier in this article. CRC is defined as being MSS if there are no mutations in the MS of CRC cancer cells. Apart from its genetic origin MSI-H CRC differs from MSS CRC in many other features.[38] MSI-H CRC is in a big proportion of 86-100% located proximally to the splenic flexure, MSS CRC is located there in 25% of cases.[39,40] Upon the pathohistological examination MSI-H tumours are poorly differentiated, mucinous and have an intensive lymphocytic infiltration in the region surrounding the tumour in comparison to MSS tumours.[38,40] MSI-H tumours have a larger primary local mass.[41] MSI-H tumours have a better prognosis.[42] MSI-H tumours rarely metastize.[43] MSI-H tumours develop from hyperplastic adenomas with already present mutations and lower expression of hMLH1 gene.[38] MSI-H tumours have a highly homogenous cell population.[43] Better MSI-H CRC prognosis is attributed to a high proportion of mutations that act self destructively on tumour cells and cause the further mutation in genes the cell needs for its survival. Mutated proteins may also incorporate in the cell membrane of MSI-H tumour cells causing an immune reaction by the organism and the destruction of the tumour cell; a fact that may also explain the intensive lymphocytic infiltration in MSI-H tumours.[41] Cell line trials conducted on CRC tumour cells have shown that MSI-H tumour cells next to all its genetic and patomorphological differences, also have characteristics of a predictive factor for the chemotherapeutic treatment efficacy. Trials conducted on cell lines have shown resistance of cell lines with defective MMR system and MSI-H to some chemotherapeutic regimens.[38,44-48]

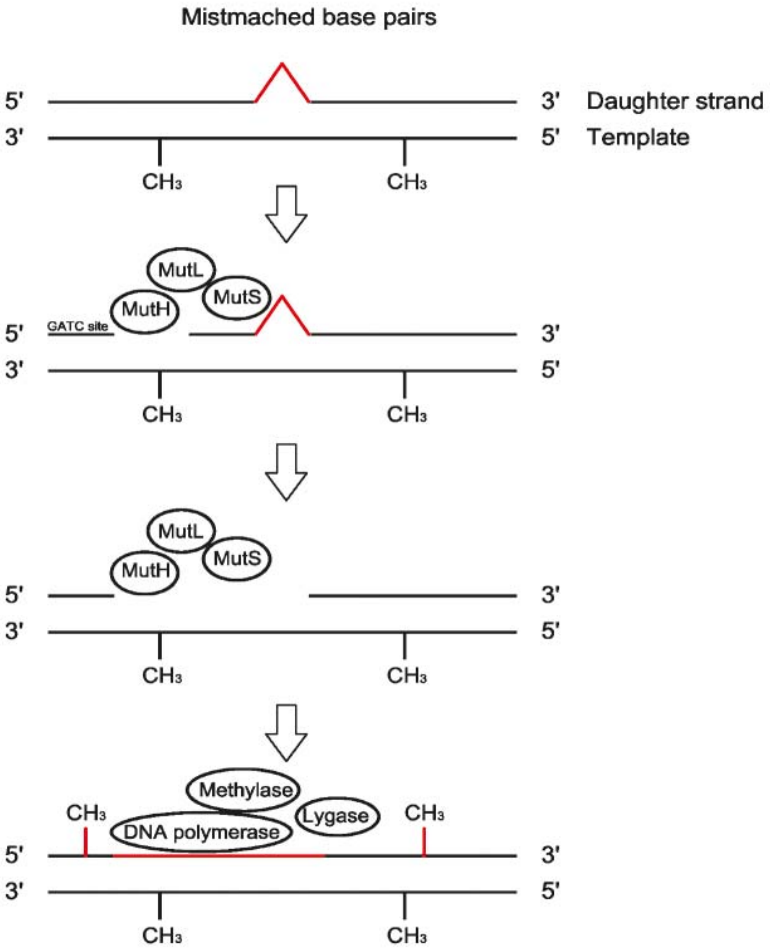

FIGURE 1. Mismatch repair. MutS protein binds to mismatched base pairs. MutL and MutH bind to the complex. MutH recognizes the daughter DNA strand which is not methylated, splits it at nearest GATC sites and excises the DNA strand. DNA polymerase, ligase and methylase complete the daughter strand.

MSI-H as a prognostic factor in colorectal cancer and predictive factor in colorectal cancer chemotherapy

The chemotherapeutic treatment carries with its adverse effects that are more or less expressed in an individual.[49] Clinical trials currently conducted are trying to elucidate the efficacy of the treatment and also the causes of chemotherapeutic regimens toxicity.[50] The chemotherapeutic treatment is effective in a certain proportion of patients; with dis-

seminated CRC the treatment response to 5-FU regimens is 20-25%, in combination of 5-FU with novel chemotherapeutics irinotecan and oxaliplatin the response rate is 45-50%.[51] This means that chemotherapy is not only ineffective, but also causes many adverse effects for a large group of patients with no benefit.[52] Clinical trials wish to elucidate predictive factors for the chemotherapeutic treatment and predictive factors for adverse effects, that could be used in everyday clinical setting. Cancers in the same stage of the TNM staging system according to their clinicopathological characteristic, differ in their clinical course, because of heterogeneity of their molecular characteristics.[42] Toxicity of chemotherapeutics is influenced by patient comorbidity and by individual molecular variability.[50] One of the potential predictive factors for the chemotherapeutic treatment efficacy and for the adverse effects level in an individual is MSI-H.[50,52] Many clinical trials about MSI-H as a prognostic factor for CRC and as a predictive factor with adjuvant and palliative CRC chemotherapy have been conducted in last ten years.

Three classes of chemotherapeutic agents are used in CRC treatment: antimetabolites, alkylating agents and topoisomerase inhibitors.[29,38] Antimetabolite used is called 5-flourouracil (5-FU). 5-FU is converted in the cell in two active forms that affect RNA synthesis and enzyme thymidylate syntethase (TS).[53] Enzyme TS induces synthesis of thymidine monophosphates, 5-FU inhibits its action. MSI-H tumours cells (with defective MMR system) do not recognize the mutations caused by 5-FU on the DNA strand and they do not induce apoptosis.[54,55] The resistance of MSI-H cell lines to 5-FU is explained by the fact that 5-FU sensitivity depends on the effective MMR system to induce apoptosis. *In vitro* cell line trials concerning MSI-H cells have shown the resistance to the treatment with 5-FU.[56,57] Clinical trials concerning MSI-H patients and 5-FU treatment have shown contradicting results.[30,58] The first clinical trial of MSI-H patients with adjuvant chemotherapy (5-FU monotherapy) has shown a better survival for patients receiving adjuvant chemotherapy, but clinical trials following have not shown that benefit.[41,59]

Chemotherapeutic irinotecan causes with inhibition of enzyme topoisomerase I brakes of DNA strand and apoptosis of cancer cell. *In vitro* cell line trials concerning MSI-H cells have shown higher sensitivity to irinotecan.[46,60] Clinical trials have confirmed those results.[38,48,61]

Chemotherapeutic oxaliplatin is an alkylating agent and is a platinum analog. Platinum analogs form covalent bonds with DNA strand stopping the cell cycle and causing apoptosis.[62,63] Cell lines with defective MMR system have a lower sensitivity to platinum analogs, because there is no effective MMR system to recognize DNA strand defects and induce apoptosis.[44-47]

In the recent 5 years several metaanalyses concerning MSI-H as a prognostic and predictive factor of CRC chemotherapeutic treatment were performed (Table 1). In 2005 Popat *et al.* have conducted the first metaanalysis of clinical trials about MSI-H as a prognostic factor in CRC.[42] Metaanalysis included 32 clinical trials with 7642 patients, 1277 of them were MSI-H, representing 16.7% of all patients. The conclusion of the metaanalysis was that patients with MSI-H have a better survival than MSS patients in the same stage of the disease. In 2009 Des Guetz *et al.* have conducted a metaanalysis of 7 clinical trials of MSI-H as a predictive factor in adjuvant chemotherapeutical setting in stage II and III of the disease after the surgical treatment.[64] Metaanalysis included 7 clinical trials with 3690 patients, 454 of them were MSI-H, representing 14% of all patients. Patients received adjuvant 5-FU based chemotherapy. MSI-H patients receiving adjuvant chemotherapy did not have a better survival than MSI-H patients not receiving chemotherapy. MSS patients receiving adjuvant chemotherapy had a better survival than MSS patients not receiving adjuvant chemotherapy. These results show an appearance of chemoresistance of MSI-H patients to adjuvant 5-FU based chemotherapy. In 2009 Des Guetz *et al.* have also conducted a metaanalysis of 6 clinical trials of MSI-H as a predictive factor in palliative chemotherapeutical setting in stage IV of the disease.[65] Metaanalysis included 6 clinical trials with 964 patients, 91 of them were MSI-H, representing 9.4% of all patients. The conclusion of the metaanalysis was that patients with MSI-H have a statistically significantly better survival than MSS patients in the same stage of the disease. The efficacy of the chemotherapeutical treatment did not differ in MSI-H and MSS patients in five trials, in one of the trials MSI-H patients had a better survival than MSS patients.[30] In one of the trials the better efficacy of higher doses of chemotherapy was observed among MSI-H patients.[66] Both metaanalyses by Des Guetz included clinical trials with chemotherapeutical regimens that differed from each other, which made it difficult to objectively compare the results. From the results we conclude that there is an appearance of chemoresistance of MSI-H patients to adjuvant 5-FU based chemotherapy, making MSI-H a negative predictive factor for 5-FU

TABLE 1. Summary of metaanalysis performed concerning MSI-H as a prognostic and predictive factor in CRC

Metaanalysis (year)	Number of clinical trials/ Number of patients	Patients with MSI-H/%	Conclusion
Popat *et al.* (2005)	32/7642	1277/16,7 %	MSI-H a positive prognostic factor
DesGuetz *et al.* (2009) Adjuvant chemotherapy setting	7/3690	454/14,0 %	MSI-H a negative predictive factor in adjuvant setting
DesGuetz *et al.* (2009) Metastatic chemotherapy setting	6/964	91/9,4 %	MSI-H a positive prognostic factor. No clear conclusion concerning MSI-H as a predictive factor
Guastadisegni *et al.* (2010)	31/12872	1972/15,4 %	MSI-H a positive prognostic factor. No clear conclusion concerning MSI-H as predictive factor, due to trial heterogenity

adjuvant chemotherapy. In metastatic setting there was no clear conclusion about MSI-H as a predictive factor. The incidence of MSI-H in stages II and III was higher than in metastatic setting. In 2010 Guastadisegni *et al.* have conducted a metaanalysis of 31 clinical trials with 12872 patients, 1972 of them were MSI-H, representing 15.4% of all patients in all stages of the disease.[67] The conclusion of the metaanalysis regarding MSI-H as a prognostic factor was the same as in the previous metaanalysis that patients with MSI-H have a better survival than MSS patients in the same stage of the disease. Metaanalysis included clinical trials with chemotherapeutical regimens that differed from each other, what made it difficult to objectively compare results and to come to a clear conclusion about MSI-H as a predictive factor. The authors concluded that regarding the complexity of 5-FU in the treatment of CRC MSI-H was only one of the important predictive factors that functioned with others that still had to be elucidated.

CRC develops through MSI-H pathway in 15%. It, therefore, would not be cost efficient to determine the MSI-H status in each CRC patient. In 2010 Sinicrope *et al.* have conducted a trial where they developed a prognostic model of determining probability of MSI-H in CRC regarding the clinical and pathological characteristics of patients diagnosed with CRC.[68] When the tumour is proximally localized, poorly differentiated and when the patient is female, there is a 51% probability of MSI-H CRC incidence in comparison to 15% MSI-H CRC in general CRC population. When they considered lymphocytic infiltration the probability got even higher. Using this prognostic model it would make determining MSI-H status more cost efficient.

Conclusions

Cancer patients nowadays have more and more diagnostic and therapeutic possibilities. The future of their treatment is an individualized therapy determined by patient characteristics and by tumour molecular characteristics that influence survival, chemotherapeutic treatment efficacy and incidence of adverse effects. MSI status is one of those prognostic and predictive factors in CRC.

References

1. Weitz J, Koch M, Debus J, Höhler T, Galle PR, Büchler MW. Colorectal cancer. *Lancet* 2005; **365:** 153-65.
2. Primic-Žakelj M, Zadnik V, Žagar T, Zakotnik B. *Survival of cancer patients, diagnosed in 1991-2005 in Slovenia.* Ljubljana: Institute of Oncology Ljubljana, Cancer Registry of Republic of Slovenia; 2009.
3. Cancer incidence in Slovenia 2007. Ljubljana: Institute of Oncology Ljubljana, Cancer Registry of Republic of Slovenia; 2010.
4. Velenik V. Post-treatment surveillance in colorectal cancer. *Radiol Oncol* 2010; **44:** 135-41.
5. Zhou YL, Boardman LA, Miller RC. Genetic testing for young-onset colorectal cancer: case report and evidence-based clinical guidelines. *Radiol Oncol* 2010; **44:** 57-61.
6. Fearon ER, Vogelstein B. A genetic model for colorectal tumourogenesis. *Cell* 1990; **61:** 759-67.
7. West NJ, Courtney EDY, Poullis AP, Leicester RJ. Apoptosis in the colonic crypt, colorectal adenomata, and manipulation by chemoprevention. *Cancer Epidemiol Biomarkers Prev* 2009; **18:** 1680-7.
8. Duval A, Hamelin R. Mutations at coding repeat sequences in mismatch repair-deficient human cancers: toward a new concept of target genes for instability. *Cancer Res* 2002; **62:** 2447-54.
9. Lynch JP, Hoops TC. The genetic pathogenesis of colorectal cancer. *Hemat Oncol Clin N Am* 2002; **16:** 775-810.
10. Kondo Y, Issa JPJ. Epigenetic changes in colorectal cancer. *Cancer Met Rev* 2004; **23:** 29-39.
11. Kozuka S, Nogaki M, Ozeki T, Masumori S. Premalignancy of the mucosal polyp in the large intestine. Estimation of the periods required for malignant transformation of mucosal polyps. *Dis Colon Rectum* 1975; **18:** 494-500.
12. Kinzler K, Vogelstein B. Gatekeepers and caretakers. *Nature* 1997; **386:** 761-3.
13. Grady WM. Genomic instability and colon cancer. *Cancer Metast Rev* 2004; **23:** 11-27.
14. Stoler DL, Chen N, Basik M, Kahlenberg MS, Rodriguez-Bigas MA, Petrelli NJ, et al. The onset and extent of genomic instability in sporadic colorectal tumour progression. *Proc Natl Acad Sci USA* 1999; **96:** 15121-6.
15. Law DJ, Olschwang S, Monpezat J-P. Concerted nonsystemic allelic loss in human colorectal carcinoma. *Science* 1988; **241:** 961-5.

16. Paulovich AG, Toczyski DP, Hartwell LH. When checkpoints fail. *Cell* 1997; **88:** 315-21.

17. Vogelstein B, Fearon ER, Hamilton SR, Kern SE, Preisinger AC, Leppert M, et al. Genetic alterations during colorectal tumour development. *N Engl J Med* 1988; **319:** 525-32.

18. Powell SM, Zilz N, Beazer-Barclay Y. APC mutations occur early during colorectal oncogenesis. *Nature* 1992; **359:** 235-7.

19. Lenglauer C, Kinzler KW, Vogelstein B. Genetic instability in colorectal cancers. *Nature* 1997; **386:** 623-7.

20. Jass JR, Whitehall VLJ, Young J, Leggett BA. Emerging concepts in colorectal neoplasia. *Gastroenterology* 2002; **123:** 862-76.

21. Thibodeau SN, Bren G, Schaid D. Microsatellite instability in cancer of the proximal colon. *Science* 1993; **260:** 816-9.

22. Worthley DL, Leggett BA. Colorectal cancer: Molecular features and clinical opportunities. *Clin Biochem Rev* 2010; **31:** 31-8.

23. De la Chapelle A, Hampel H. Clinical relevance of microsatellite instability in colorectal cancer. *J Clin Oncol* 2010; **28:** 3380-7.

24. Radman M, Wagner R. Carcinogenesis. Missing mismatch repair. *Nature* 1993; **366:** 722.

25. McClulloch SD, Kunkel TA. The fidelity of DNA synthesis by eukaryotic replicative and translesion synthesis polymerases. *Cell Res* 2008; **18:** 148-61.

26. Eshleman JR, Markowitz SD. Mismatch repair defects in human carcinogenesis. *Hum Mol Genet* 1996; **5:** 1489-94.

27. Umar A, Boland CR, Terdiman JP. Revised Bethesda guidelines for hereditary non-poliposis colorectal cancer (Lynch syndrome) and microsatellite instability. *J Natl Cancer Inst* 2004; **96:** 261-8.

28. Jover R, Zapater P, Castells A, Llor X, Andreu M, Cubiella J, et al. Mismatch repair status in the prediction of benefit from adjuvant Flourouracil chemotherapy in colorectal cancer. *Gut* 2006; **55:** 848-55.

29. Niv Y. Microsatellite instability and MLH1 promoter hypermetalition in colorectal cancer. *World J Gastroenterol* 2007; **13:** 1767-9.

30. Liang JT, Huang KC, Lai HS, Lee PH, Cheng YM, Hsu HC, et al. High frequency microsatellite instability predicts better chemosensitivity to high dose 5-fluorouracil plus Leucovorin chemotherapy for stage IV sporadic colorectal cancer after palliative bowel resection. *Int J Cancer* 2002; **101:** 519-25.

31. Markowitz S, Wang J Myeroff L, Parsons R, Sun L, Lutterbaugh J, et al. Inactivation of the type II TGF-beta receptor in colon cancer cells with microsatellite instability. *Science* 1995; **268:** 1336-8.

32. Lawes DA, SenGupta S, Boulos PB. The clinical importance and prognostic implications of microsatellite instability in sporadic cancer. *Eur J Surg Oncol* 2003; **29:** 201-12.

33. Modrich P. Mechanisms and biological effects of mismatch repair. *Ann Rev Genet* 1991; **25:** 229-53.

34. Joseph N, Duppatla V, Rao DN. Prokaryotic DNA mismatch repair. *Prog Nucleic Acid Res* 2006; **81:** 1-49.

35. Iyer R, Pluciennik A, Modrich P, Modrich PL. DNA mismatch repair: functions and mechanisms. *Chem Rev* 2006; **106:** 302-23.

36. Hsieh P, Yamane K. DNA mismatch repair: Molecular mechanisms, cancer and ageing. *Mech Ageing Dev* 2008; **129:** 391-407.

37. Shibata D, Peinado MA, Ionov Y, Malkhosyan S, Perucho M. Genomic instability in repeated sequences is an early somatic event in colorectal tumorogenesis that persists after transformation. *Nat Genet* 1994; **6:** 273-81.

38. Warusavitarne J, Schnitzler M. The role of chemotherapy in microsatellite unstable (MSI-H) colorectal cancer. *Int J Colorectal Dis* 2007; **22:** 739-48.

39. Aaltonen LA, Peltomaki P, Leach FS, Sistonen P, Pylkkänen L, Mecklin JP, et al. Clues to the pathogenesis of familial colorectal cancer. *Science* 1993; **260:** 812-6.

40. Gryfe R, Kim H, Hsieh ETK, Aronson MD, Holowaty EJ, Bull SB et al. Tumor microsatellite instability and clinical outcome in young patients with colorectal cancer. *N Engl J Med* 2000; **342:** 69-77.

41. Hemminki A, Mecklin JP, Jarvinen H, Aaltonen LA, Joensuu H. Microsatellite instability is a favorable prognostic indicator in patients with colorectal cancer receiving chemotherapy. *Gastroenterology* 2000; **119:** 921-8.

42. Popat S, Hubner R, Houlston RS. Systematic review of microsatellite instability and colorectal cancer prognosis. *J Clin Oncol* 2005; **23:** 609-18.

43. Lim SB, Jeong SY, Lee MR, Ku JL, Shin YK, Kim WH, et al. Prognostic signifance of microsatellite instability in sporadic colorectal cancer. *Int J Colorectal Dis* 2004; **19:** 533-7.

44. Fink D, Nebel S, Aebi S, Zheng H, Cenni B, Nehmé A, et al. The role of DNA mismatch repair in platinum drug resistance. *Cancer Res* 1996; **56:** 4881-6.

45. Vaisman A, Varchenko M, Umar A, Kunkel TA, Risinger JI, Barrett JC, et al. The role of hMLH1, hMSH3 and hMSH6 defects in Cisplatin and Oxaliplatin resistance: correlation with replicative bypass of platinum-DNA adducts. *Cancer Res* 1998; **58:** 3579-85.

46. Bras-Goncalves RA, Rosty C, Laurent-Puig P, Soulié P, Dutrillaux B, Poupon MF. Sensitivity to CPT-11 of xenografted human colorectal cancers as a function of microsatellite instability and p53 status. *Br J Cancer* 2000; **82:** 913-23.

47. Aebi S, Kurdi-Haidar B, Gordon R, Cenni B, Zheng H, Fink D, et al. Loss of DNA mismatch repair in acquired resistance to Cisplatin. *Cancer Res* 1996; **56:** 3087-90.

48. Fallik D, Borrini F, Boige V, Viguier J, Jacob S, Miquel C, et al. Microsatellite instability is a predictive factor of the tumor response to Irinotecan in patients with advanced colorectal cancer. *Cancer Res* 2003; **63:** 5738-44.

49. Rothenberg ML, Meropol NJ, Poplin EA, Van Cutsem E, Wadler S. Mortality associated with Irinotecan plus bolus Flourouracil/Leucovorin. Summary findings of an independent panel. *J Clin Oncol* 2001; **19:** 3801-7.

50. Braun MS, Richman SD, Thompson L, Daly CL, Meade AM, Adlard JW, et al. Association of molecular markers with toxicity outcomes in a randomized trial of chemotherapy for advanced colorectal cancer: The FOCUS trial. *J Clin Oncol* 2009; **27:** 5519-28.

51. Ocvirk J. Advances in the treatment of metastatic colorectal carcinoma. *Radiol Oncol* 2009; **43:** 1-8.

52. Adlard JW, Richman SD, Seymour MT, Quirke P. Prediction of the response of colorectal cancer to systemic therapy. *Lancet Oncol* 2002; **8:** 75-82.

53. Fischer F, Baerenfaller K, Jiricny J. 5-flourouracil is efficiently removed from DNA by the base excision and mismatch repair systems. *Gastroenterology* 2007; **133:** 1858-68.

54. Ricciardiello L, Ceccarelli C, Angiolini G, Pariali M, Chieco P, Paterini P, et al. High tymidylate synthase expression in colorectal cancer with microsatellite instability: implications for chemotherapeutic strategies. *Clin Cancer Res* 2005; **11:** 4234-40.

55. Tajima A, Hess MT, Cabrera BL, Kolodner RD, Carethers JM. The mismatch repair complex hMutS alpha recognizes 5-flourouracil modified DNA: implications for chemosensitivity and resistance. *Gastroenterology* 2004; **127:** 1678-84.

56. Carethers JM, Chauhan DP, Fink D, Nebel S, Bresalier RS, Howell SB, et al. Mismatch repair proficiency and in vitro response to 5-flourouracil. *Gastroenterology* 1999; **117:** 123-31.

57. Kirchner T, Jung A. Pathologische Diagnostik fuer die individualisierte Therapie des Dickdarmkarzinoms. *Pathologe* 2010; **31:** 16-21.

58. Jover R, Zapater P, Castells A, Llor X, Andreu M, Cubiella J, et al. The efficacy of adjuvant chemotherapy with 5-flourouracil in colorectal cancer depends on the mismatch repair status. *Eur J Cancer* 2009; **45:** 365-73.

59. Ribic CM, Sargent DJ, Moore MJ, Thibodeau SN, French AJ, Goldberg RM, et al. Tumor microsatellite-instability status as a predictor of benefit from Flourouracil-based adjuvant chemotherapy for colon cancer. *N Eng J Med* 2003; **349:** 247-57.

60. Magrini R, Bhonde MR, Hanski M, Notter M, Scherübl H, Boland CR. Cellular effects of CPT-11 on colon carcinoma cells: dependence on p53 and hMLH1 status. *Int J Cancer* 2002; **101:** 23-31.

61. Chamara M, Edmonston TB, Burkholder S, Walters R, Anne P, Mitchell E, et al. Microsatellite status and cell cycle associated markers in rectal cancer patients undergoing combined regimen of 5-FU and CPT-11 chemotherapy and radiotherapy. *Anticancer Res* 2004; **24:** 3161-7.

62. Fink D, Aebi S, Howell SB. The role of DNA mismatch repair in drug resistance. *Cancer Res* 1998; **4:** 1-6.

63. Claij N, te Riele H. Microsatellite instability in human cancer: a prognostic marker for chemotherapy? *Exp Cell Res* 1999; **246:** 1-10.

64. Des Guetz G, Schischmanoff O, Nicolas P, Perret GY, Morere JF, Uzzan B. Does microsatellite instability predict the efficacy of adjuvant chemotherapy in colorectal cancer? A systematic review with meta-analysis. *Eur J Cancer* 2009; **45:** 1890-6.

65. Des Guetz G, Uzzan B, Nicolas P, Schischmanoff O, Perret GY, Morere JF. Microsatellite instability does not predict the efficacy of chemotherapy in metastatic colorectal cancer. A systematic review and meta-analysis. *Anticancer Res* 2009; **29:** 1615-20.

66. Des Guetz G, Mariani P, Cucherousset J, Benamoun M, Lagorce C, Sastre X et al. Microsatellite instability and sensitivity to FOLFOX treatment in metastatic colorectal cancer. *Anticancer Res* 2007; **27:** 2715-19.

67. Guastadisegni C, Colafranceschi M, Ottini L, Dogliotti E. Microsatellite instability as a marker of prognosis and response to therapy. A meta analysis of colorectal cancer survival data. *Eur J Cancer* 2010; **46:** 2788-98.

68. Sinicrope F, Foster NR, Sargent DJ, Thibodeau SN, Smyrk TC, O'Connell MJ et al. Model-based prediction of defective DNA mismatch repair using clinicopathological variables in sporadic colon cancer patients. *Cancer* 2010; **116:** 1691-8.

research article

Analysis of peripheral artery velocity tracing in a porcine model

Qingxin Meng[1], Weiwei Ding[2], Bin Yang[1], Ninghua Fu[1], Guangming Lu[3]

[1] Department of Ultrasound, Jinling Hospital, School of Medicine, Nanjing University, Nanjing, China
[2] Research Institute of General Surgery, Jinling Hospital, School of Medicine, Nanjing University, Nanjing, China
[3] Department of Medical Imaging, Jinling Hospital, School of Medicine, Nanjing University, Nanjing, China

Received 19 December 2010
Accepted 17 January 2011

Correspondence to: Guangming Lu, M.D., Department of Medical Imaging, Jinling Hospital, School of Medicine, Nanjing University, 305 East Zhongshan Road, Nanjing 210002, Jiangsu Province, China. Phone: +86-25-80860314; E-mail: lucyok@mspil.edu.cn

Disclosure: No potential conflicts of interest were disclosed.

Background. The aim of the study was to trace the peripheral artery velocity with ultrasound in pigs and provide inference on diagnosis of the type, location and severity of vascular diseases.

Materials and methods. Limb tightening, adrenaline administration and arterial wall pinching were performed independently in six pigs, and then the evolution of the external iliac artery or femoral artery velocity tracing were monitored.

Results. With the increase of the extents of hindlimb tightening, peak systolic velocity (PSV) of ipsilateral external iliac artery turned from 36.33±1.77 cm/s to 59.72±2.67 cm/s, minimum post-principal wave velocity (MPV from 13.68±1.11 cm/s to -7.48±0.82 cm/s, peak diastolic velocity (PDV) from 19.31±0.86 cm/s to 8.98±0.45 cm/s, and, end diastolic velocity (EDV) from 13.2±0.45 cm/s to 0. With the increase of the dose of the epinephrine injection, PSV increased from 36.33±1.77 cm/s to 43.97±2.15 cm/s but then decreased to 35.43±3.01 cm/s, and MPV negatively increased to -23.53±0.82 cm/s after decreasing from 13.68±1.11 cm/s to 0. PDV and EDV gradually decreased to zero. With the increase of the stenosis severity in the abdominal aortic wall pinching, PSV was reduced and had a linearly negative correlation with the stenosis severity (R=0.983, R2=0.967). MPV gradually increased, and its direction reversed when the stenosis severity increased, then diminished when the blood flow was occluded by more than 2/3.

Conclusions. The formation of peripheral artery velocity is the result of concurrent effects of cardiac ejection, vascular resistance, effective circulating blood volume and elastic recoil. Vascular resistance exerts pronounced effects on the diastolic waveform, and the occurrence of backward wave indicates that the downstream circulation resistance significantly increases.

Key words: velocity tracing; resistance; effective circulating blood volume; elastic recoil; principal wave; backward wave

Introduction

The morbidity and mortality of cardiovascular diseases are growing with the increase of hypertension, hyperglycaemia and hyperlipidemia. They are still the main causes of death and the determinants of the decreased quality of life. Most of these diseases can cause the alteration of local or distant hemodynamics because of lumen stenosis or dilatation.[1] The changes in the hemodynamics may alter the magnitude and distribution of regional shearing force, damage the vascular endothelium cells and result in local intimal proliferation, finally leading to the formation of atheromatous plaques. The shape, location and stability of atheromatous plaques are closely associated with the way in which regional shearing force acts, playing an important role in thrombosis.[2-7] It is important, as early as possible, to identify lumen stenosis or dilatation, analyze the changes in hemodynamics, and applied effective strategies to control its aggravation or even eliminate the lesions.[8,9]

Some researchers have studied the changes in hemodynamics caused by arterial stenosis, and proposed the ways in which the hemodynamics is evaluated in experiments *in vivo* or *in vitro*.[4,10-13]

Ultrasound can be used to detect blood vessels in every direction and is dynamical, non-invasive, economical and convenient modality.[9,14] Therefore, hemodynamics can be monitored with ultrasound through the velocity tracing. Apart from pulsatility index (PI) and resistant index (RI)[15-18], peak systolic velocity (PSV) and ratio of PSV at stenosis to PSV at proximal artery are generally regarded as the important indexes in predicting stenosis and its severity.[19-24] However, the valve of velocity is related to many factors such as the site of sampling and the correction angle.

In addition, content in the enteric cavity, scar, muscles, fat tissues and tissue oedema may lead to pronounced acoustic attenuation in deep tissues resulting in ambiguous image of blood vessels. It is critical to determine the site of arterial lesion and its severity in the upstream or downstream of the detection site according to the alteration of local velocity, which is superficial or limpid to be revealed. The waveform of "*tardus-parvus*" has been used to detect serious stenosis in the upstream of renal, hepatic and intracranial artery[29,30], and similarly, the velocity of extremity arteries may also be altered strikingly if there is serious stenosis in the upstream.[28-30] Not only the morphous and the level of stenosis, but the pressure, velocity, physical property and resistance of vessels are crucial factors involving in the changes in hemodynamics in the upstream or/and downstream of stenosis.[11,34-40]

To investigate the mechanisms and contributing factors underlying the formation of peripheral artery velocity, we analyzed the evolution of external iliac artery and femoral artery velocity through tightening limb, administration of adrenaline or pinching the lateral walls of the end of abdominal aorta in pigs. Thus, we determined the type, location and severity of vascular diseases according to local hemodynamics detected by velocity tracing.

Materials and methods

Animals

Six female or male juvenile susscrota domesticas weighing 24 ± 1 kg (range: 20~26 kg) were purchased from the Animal Experiment Center of Jinling Hospital. The whole study was approved by the Animal Research Committee of Jinling Hospital. All procedures were carried out in accordance with the "Principles of Laboratory Animal Care" (NIH publication No.85-23, revised 1985).

Main instruments

The haemostatic clip with concave and convex *dentes* (lot number: X20870) was purchased from Surgical Instruments Factory, Shanghai Medical Instruments (Group) Corp. Ltd., the micro-pump from B. Braun AG, and the animal monitor from Spacelabs Healthcare, Inc. The ultrasonic instrument was purchased from GE logiq I, with the frequency of 10 MHz.

Animal processing

The animals were fasted with access to water *ad libitum* for 24 h before the operation, and housed in a room with controlled temperature (28°C). After an overnight fast, the swine was injected with ketamine (20 mg/kg). Droperidol and atropine (0.06 mg/kg), and then fixed in a supine position. After endotracheal intubation and ventilating mechanically, anaesthesia was remained with intravenous injection of 150 μg/kg/min propofol (Disoprivan 2%, emulsion, Astra Zeneca, Wedel, Germany) and bolus injection of 2~5 μg/kg fentanyl (Janssen Cilag, Neuss, Germany). The vital signs were closely monitored, and the anaesthesia was adjusted according to the blood pressure aiming to ensure the stable circulation.

The hindlimbs were tightened with gauze until blood flow signal was undetectable by ultrasound in the downstream of pressure point, which mimics femoral artery stenosis to different extents. Then, the velocity in the upstream (external iliac artery) was monitored.

Epinephrine administration; about 1/3, 1/2 and 1 dose of ampoule epinephrine hydrochloride (1 ml: 1 mg) were administered intravenously in sequence. The external iliac artery velocity was determined after every injection until it returned to that before experiment. Subsequently, the dose was adjusted and the experiment continued.

Abdominal aortic wall pinching

After anaesthesia, the animal was fixed in a supine position. After sterilizing and skin preparation, laparotomy was performed and the end of abdominal aorta was exposed. The blood vessels were covered with warm and moist saline gauze after the separation. The end of abdominal aorta served as stenotic site. The blood flow of abdominal aorta was blocked with a haemostatic clip. Then, abdominal aortic wall was partially pinched. Finally, the haemostatic clip was released slowly. This process

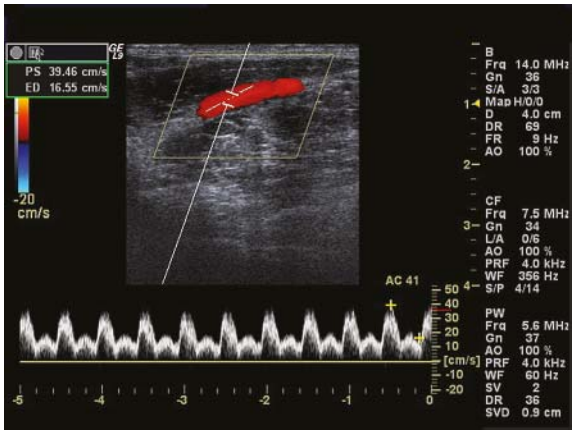

FIGURE 1. Velocity wave of external iliac artery after anaesthesia.

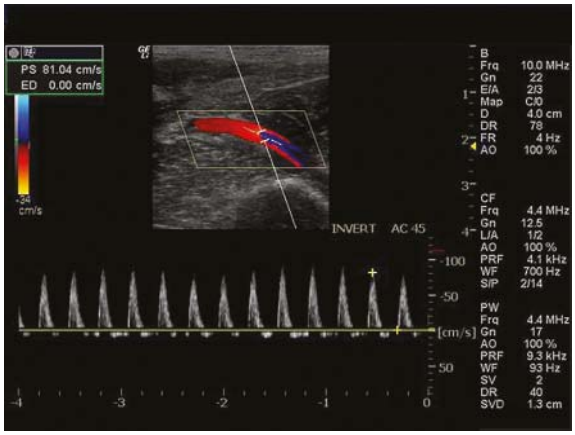

FIGURE 2. Velocity wave of common femoral artery after anaesthesia.

can produce 1/3, 1/2, 2/3 and 3/4 occlusion in sequence which was demonstrated by the detection of internal diameter of lumen by ultrasound). All haemostatic clips were released each time and the following experiment was carried out after the velocity of common femoral artery returned to that before operation.

Animals were sacrificed by intravenous injection of 100 mg/kg pentobarbital sodium at the end of experiments.

Instrument regulation and observation indexes

Two-dimensional images could clearly display the vascular lumens. In the colour Doppler flow imaging, the blood flow signals exactly suffused the vascular lumen with soft colour. The sampling frame steer was consistent with the direction of blood stream, the sampling gate located at the center of lumen whose width was 2 mm, and the correction line paralleled with the direction of bloodstream.

A group of similar velocities in different cardiac cycle were detected. Three velocities were randomly selected and calculated. The average represented the velocity of external iliac artery or femoral artery in the state. The PSV, minimum post-principal wave velocity (MPV, peak reverse velocity was considered as MPV in two-phase velocity tracing), PSV/MPV (P/M), MPV/PSV (M/P), peak diastolic velocity (PDV), and end diastolic velocity (EDV) were used to estimate the hemodynamics of external iliac artery or femoral artery.

Statistical analysis

All quantitative data were presented as means±standard deviation (±s) and processed with SPSS 13.0 statistic software package. Comparisons between multiple groups were done with one way analysis of variance. Intra-group comparisons were performed with LSD test at the homogeneity of variance (the size of test was 0.10), or with Tamhane's-t test at the heterogeneity of variance. A value of $P < 0.05$ was considered statistically significant.

Results

Alteration of velocity wave

After successful anaesthesia, the waveform of external iliac artery velocity was composed of systolic principal wave with steep ascent and descent, and diastolic wave with persistent low-amplitude fluctuation (Figure 1). The waveform of common femoral artery velocity consisted of systolic principal wave with steep ascent and slow descent, and diastolic wave with persistent low-amplitude fluctuation backward (Figure 2).

In terms of the velocity of external iliac artery during the limb tightening, with the increase of pressure, the systolic waveform tended to be acuminate, and the amplitude of diastolic wave was lowered. MPV gradually diminished to zero, and subsequently, the backward wave emerged with the increase of wave amplitude. EDV dropped to zero by degrees. Under the pressure to certain extent, the triphasic wave appeared and resembled the wave of artery of lower extremity in health adults. The waveform gradually returned to that before experiment after the pressure was removed (Figure 3).

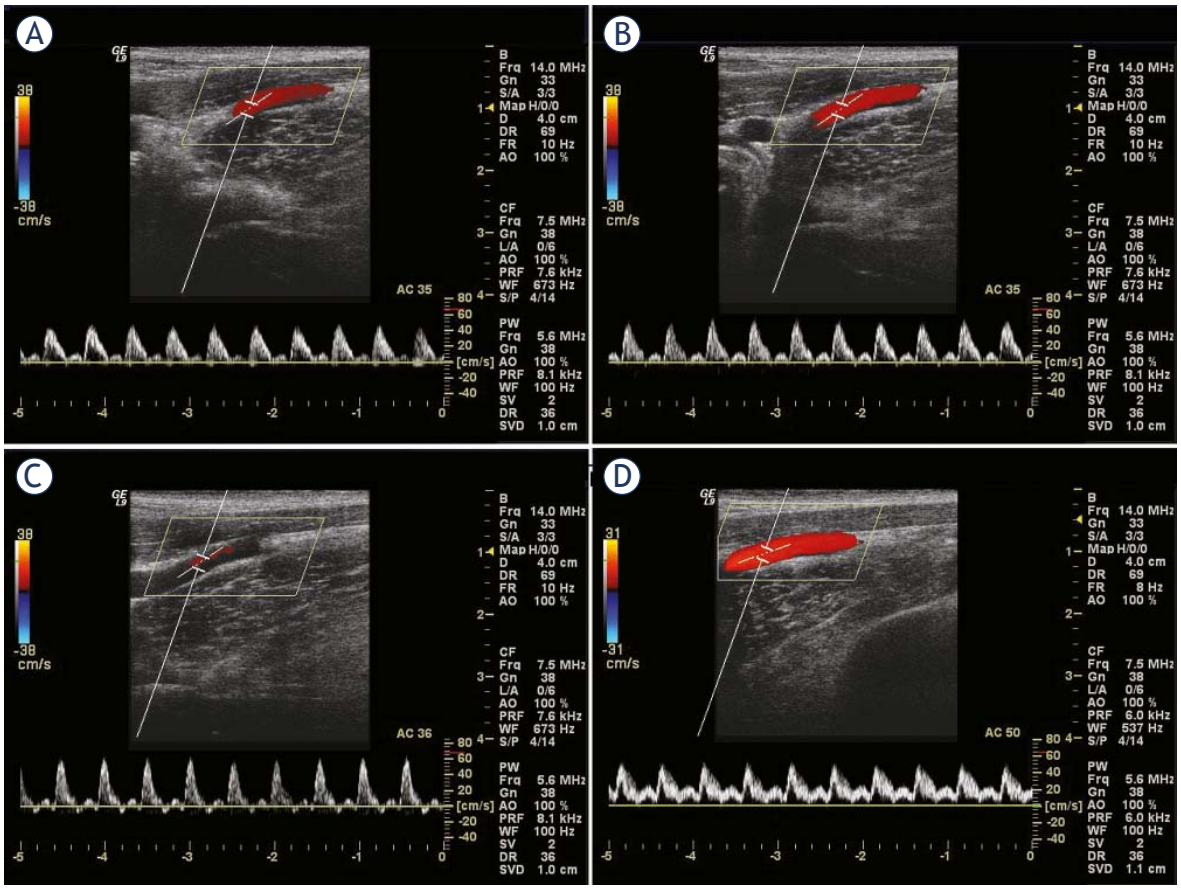

FIGURE 3. Velocity wave (A-C) of external iliac artery with the increase of pressure in limb tightening; D: velocity wave of external iliac artery after removal of pressure.

For the velocity of external iliac artery after the intravenous injection of epinephrine, with the increase in dose, the changes in waveform were similar to those after limb tightening, but these changes were more obvious. After the injection of 1 ampoule epinephrine hydrochloride, the waveform presented diphasic and consisted of systolic positive principal wave and diastolic negative wave. However, after the injection discontinuation, the waves were at opposite direction at several time points when compared with waves before the experiment (Figure 4).

For the velocity of common femoral artery in limb tightening, the systolic principal wave changed slightly and the duration of backward wave was shortened or even disappeared at 1/3 lumen stenosis (Figure 5A). The persistent low amplitude with slight fluctuation, whose direction was coincident with the principal wave, appeared in the diastolic phase at 1/2 lumen stenosis (Figure 5B). The window below the systolic wave vanished at 2/3 lumen stenosis (Figure 5C). The tracing approximately levelled at 3/4 lumen stenosis (Figure 5D).

Alteration of hemodynamic parameters

The hemodynamic parameters of PSV, MPV, PDV and EDV at the stenosis of different degrees are present in Tables 1,2,3. With the increase of pressure in limb tightening, PSV showed a slightly ascendant tendency, MPV negatively increased after gradually descended to zero, PDV declined to different degrees, and EDV gradually decreased to zero. With the increase of dose in the epinephrine injection, PSV increased slightly at a low dose and then slightly decreased, and MPV negatively increased after gradually decreasing to zero. PDV and EDV gradually decreased to zero. With the increase of stenosis severity in the abdominal aortic wall pinching, there was no statistically significant difference between left and right in changed tendency. PSV was reduced and had linearly negative correlation with stenosis severity (R=0.983, R2=0.967). MPV gradually increased, and its direction reversed when the stenosis severity increased, then diminished when the blood flow was occluded by more than 2/3. However, hemodynam-

TABLE 1. Hemodynamic parameters of ipsilateral external iliac artery when a hindlimb was tightened in 6 pigs

Tightening degree	PSV (cm/s)	MPV (cm/s)	PDV (cm/s)	EDV (cm/s)
pre-experiment	36.33±1.77	13.68±1.11	19.31±0.86	13.2±0.45
1	45.87±1.89	6.75±1.24	10.83±1.17	0
2	51.90±3.47	-4.37±0.57	12.27±0.57	0
3	59.72±2.67	-7.48±0.82	8.98±0.45	0
4	51.05±2.52	16.92±1.79	23.17±0.52	15.73±1.03

PSV = peak systolic velocity; MPV = minimum post-principal wave velocity; PDV = peak diastolic velocity; EDV = end diastolic velocity

Note: Group 1, 2, and 3 represent different extents of hindlimb tightening in the experiment on the basis of aesthesis. In addition, no downstream bloodstream was displayed in Group 3, and the constraint was removed in Group 4. For PSV of external iliac artery, there was statistically significant difference except Group 1 and Group 2, Group 2 and Group4 ($P<0.05$); For MPV and EDV, the difference among these groups was statistically significant ($P<0.05$); For PDV, there was statistically significant difference except Group 1 and Group 2, Group 1 and Group 3 ($P<0.05$).

TABLE 2. Hemodynamic parameters of external iliac artery after intravenous epinephrine hydrochloride administration in 6 pigs

Dose	PSV (cm/s)	MPV (cm/s)	PDV (cm/s)	EDV (cm/s)
pre-experiment	36.33±1.77	13.68±1.11	19.31±0.86	13.2±0.45
1/3 ampul	43.97±2.15	10.62±1.38	16.87±0.83	9.57±0.74
1/2 ampul	32.23±1.31	6.12±0.63	13.63±0.65	8.28±0.70
1 ampul	35.43±3.01	-23.53±0.82	0	0
Discontinuation	76.58±8.37	20.68±0.79	24.7±1.49	16.21±2.51

PSV = peak systolic velocity; MPV = minimum post-principal wave velocity; PDV = peak diastolic velocity; EDV = end diastolic velocity

For PSV of external iliac artery, there was statistically significant difference except Group 1/2 ampoule and Group 1 ampoule ($P<0.05$); For MPV and PDV, the difference among these groups was statistically significant ($P<0.05$); For EDV, there was statistically significant difference except Group 1/2 ampoule and Group 1/3 ampoule, pre-experiment group and discontinuation group ($P<0.05$).

TABLE 3. Hemodynamic parameters of bilateral common femoral artery in the experiment of abdominal aortic stenosis in 6 pigs

Degree of stenosis	PSV (cm/s)		MPV (cm/s)	
	right	left	right	left
pre-experiment	90.43±6.31	82.71±6.64	-12.51±0.96	-11.23±0.90
1/3	64.29±3.17	54.42±1.88	-8.51±1.23	-7.35±0.72
1/2	41.57±3.01	36.19±2.84	12.61±1.15	10.88±0.62
2/3	18.06±1.60	14.74±1.60	11.66±1.08	9.67±1.21
3/4	4.24±0.61	4.42±0.25	3.33±0.44	3.49±0.19

PSV = peak systolic velocity; MPV = minimum post-principal wave velocity

For PSV of ipsilateral common femoral artery, there was significant difference among these groups ($P<0.05$); For MPV, there was statistically significant difference except Group 1/2 stenosis and Group 2/3 stenosis ($P<0.05$).

ics was slightly changed when the blood flow was occluded by 1/2 or 2/3.

Discussion

Porcine systolic pressure, diastolic pressure, heart rate and cardiac output, which reflect the characteristics of cardiovascular system, are more similar to those in humans than other experimental animals. Thus, pigs were used in previous studies and the present study.[41,42]. When the environmental temperature lowers or the vessels are revealed, the vessels will contract. However, the vessel will dilate if the depth of anaesthesia was altered. The changes in the velocity at the detection site can be

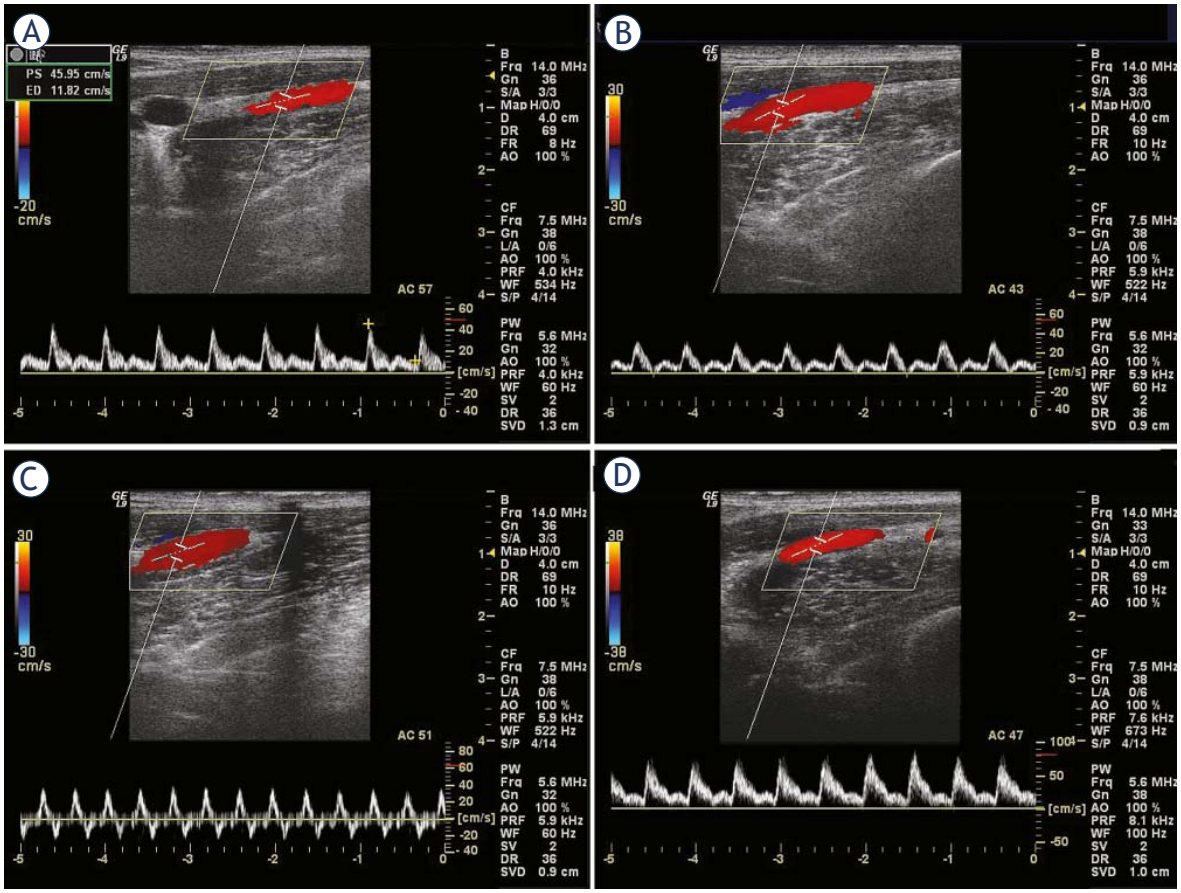

FIGURE 4. Velocity wave (A-C) of external iliac artery after epinephrine administration. A: 1/3 ampoule, B: 1/2 ampoule, C: 1 ampoule, D: soon after injection discontinuation.

detected by ultrasound. In order to achieve the similar velocity to humans, some measures were taken in the operation. A warmer was put besides the animals during the experiment aiming to keep consistent ambient temperature at operation site; the dose of anaesthetic was controlled by a micropump after anaesthesia induction aiming to maintain stable effective concentration; the vessels were covered with warm saline gauze once they were exposed aiming to maintain consistent temperature and humidity of the vessels. We all observed repeatedly the velocity tracing in each stage of the experiment for different swine, which removed the runner's cause of transforming the velocity tracing.

Under normal condition, blood flow produces tension on vessel wall, which varies with the changes in the effective circulating blood volume.[43] The cardiovascular movement has its own periodicity. On the one hand, the blood flow in the peripheral artery abruptly accelerates with the kinetic energy supplied by the cardiac ejection, and so the velocity wave displays steep ascent in the systolic phase. On the other hand, the cyclic strain of vessel wall increases with a great quantity of blood inflowing the great artery of proximal end rapidly, which promotes the elastic distension of vessel wall because of its elasticity. In the diastolic phase, the heart stops ejecting when the aortic valve closes. The hemokinesis of peripheral artery mainly depends on the inertia at this time. However, the elastic recoil of proximal great artery impulses downstream blood to accelerate, resulting in low amplitude in the velocity wave in the diastolic midanaphase. Peripheral blood loses partial kinetic energy in the process of flow because it does work to overcome the peripheral resistance. The rapid cardiac ejection supplies maximal kinetic energy to the blood in the peripheral artery. Therefore, the velocity waves display systolic principal wave, diastolic secondary wave and wave trough among them.

If the resistance of downstream circulation increases, on one hand, the upstream blood does more work to overcome this resistance simultane-

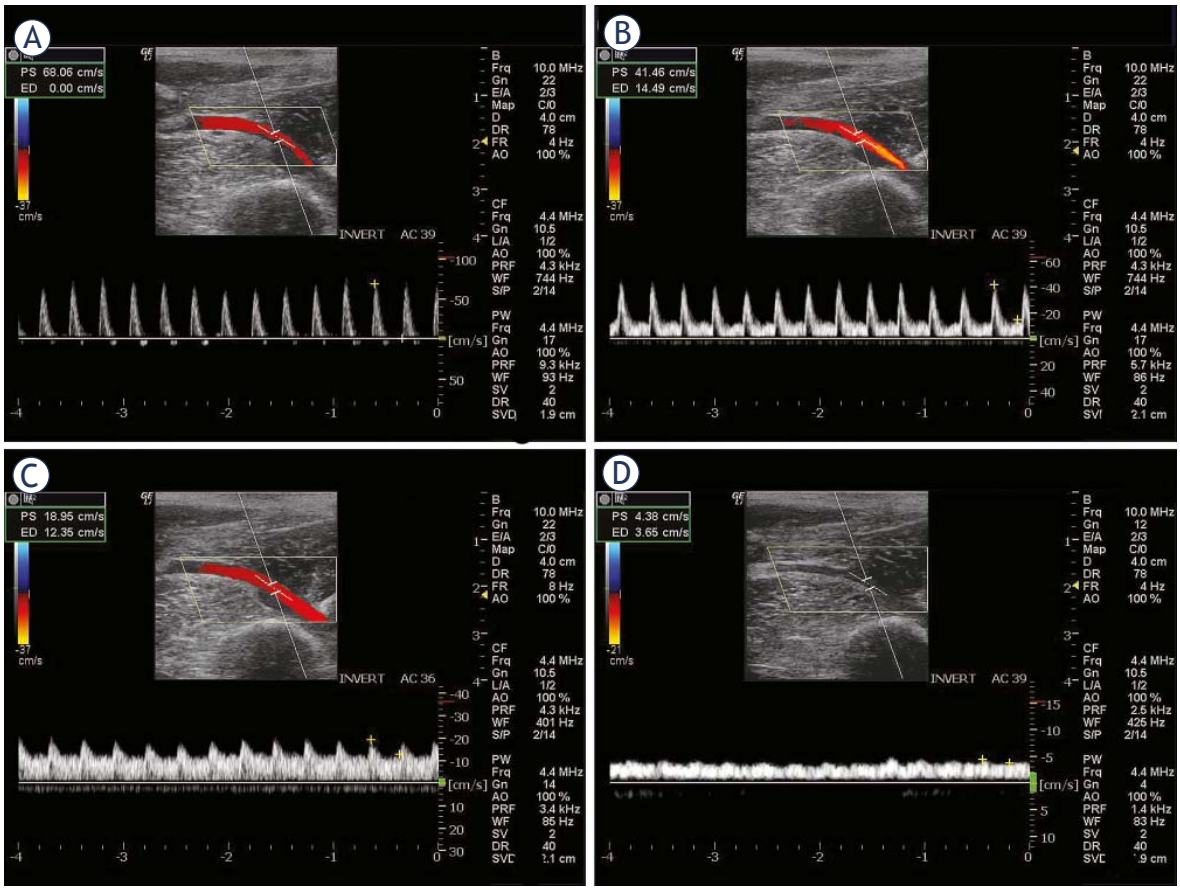

FIGURE 5. Velocity wave (A-C) of right common femoral artery after experimental abdominal aortic stenosis. A: 1/3 lumen stenosis, B: 1/2 lumen stenosis, C: 2/3 lumen stenosis, D: 3/4 lumen stenosis.

ously resulting in lose of more kinetic energy in the process of flow, which further slows the blood flow; on the other hand, the flow of upstream artery is blocked, and its effective circulating blood volume increases accompanied by strengthening of its cyclic strain synchronously, which leads to its elastic expansion. Once the velocity of systolic blood decreases to zero, the vessels elastically contract, producing a reverse blood flow. We identified the diastolic velocity with constant waveform but lowered wave amplitude with the increase of downstream circulation resistance by tightening distal limbs, and the transient reverse velocity wave following the principal wave presented after circulation resistance increased to a certain degree, which resembled the triphasic wave of lower extremity artery in healthy adults.

Adrenaline hydrochloride possesses agonistic effects on α-acceptor and β-receptor. The activated α-acceptor provokes vasoconstriction of skin, mucous membrane and internal organs; the activated β-acceptor excites the skeletal muscle and myocardium, relaxes the tracheal smooth muscle and gastrointestinal smooth muscle, dilates the coronary artery and increases the heart rate. The effect on blood pressure depends on the dose, and the commonly used dose causes the increase of systolic pressure and a slight decline of diastolic pressure, but the high dose significantly increases the blood pressure.[44] Generally, the dose of agonist leads to increase of systolic and diastolic pressure. On the one hand, it can also result in vasoconstriction of skin, mucous membrane and internal organs, leading to increase of systemic vascular resistance; on the other hand, it enables the contraction of the vessel wall. Our results showed the velocity wave remained constant but the diastolic wave amplitude lowered, and the conspicuous reverse velocity behind the principal wave appeared when the dose increased a certain level.

Both limb tightening and adrenalin hydrochloride can cause the increase of peripheral vascular resistance. Thus, the diastolic wave amplitude lowered but the velocity wave remained constant. The

reverse velocity wave appeared after MPV gradually decreased to zero accompanied by the increase of peripheral vascular resistance. These two experiments verified the assumption that peripheral vascular resistance and the elastic recoil of blood vessel had impact on the peripheral artery velocity. Otherwise, the wave amplitude of reverse velocity as a result of a large dose of adrenalin hydrochloride was higher than that after limb tightening, which illustrated the wave amplitude of reverse velocity correlated with vasoconstriction.

When the downstream circulation resistance decreased, the upstream blood did less work to surmount the resistance and subsequently, the drop of kinetic energy in the process of flow was decreased simultaneously, which, in turn, slowed the decrease of blood flow down. Soon after the removal of pressure in limb tightening or discontinuation of adrenalin hydrochloride injection, the reverse velocity wave disappeared because the circulation resistance dropped due to vasodilatation, and the velocity wave restored to the form before experiment. These results demonstrated the diastolic velocity correlated with the downstream circulation resistance, and the reverse velocity appeared because of the elastic recoil of downstream artery.

When the regional effective circulating blood volume diminishes, on one hand, the cyclic strain of vessel wall decreases, as a result of which the elastic recoil of vessel wall weakens; on the other hand, the circulation resistance reduces with the decrease of the vessel pressure. Arterial stenosis is a common cause resulting in the vanishment of distal effective circulating blood volume. The velocity wave of normal lower limb artery displays triphasic. In the experiment, abdominal aortic stenosis of different degrees induced the decrease of effective circulating blood volume of lower extremity, resulting in decrease of the amplitude and the duration of the reverse velocity wave. When the downstream effective circulating blood volume diminishes to a certain degree, the cyclic strain of vessel wall disappears, and then the reverse velocity wave vanishes. If it still diminishes, the circulation resistance decreases because the vessel pressure is reduced, and then the energy loss of hemokinesis decreases, the persistent forward blood emerges in the diastolic phase, presenting nearly flat velocity wave. The characteristics and changes of peripheral artery velocity wave are the results of interactions between systolic function, blood vessel elasticity, effective circulating blood volume and peripheral vascular resistance. The heart rapid ejection produces systolic wave whose altitude is affected by systolic function. The acceleration and deceleration of systolic wave are associated with the circular resistance. The vascular elastic recoil, which pertains to effective circulating blood volume and circular resistance, produces a forward wave in the diastolic midanaphase and a backward wave in the systolic phase. The reverse bloodstream wave in straight artery is a kind of distinctive waveform and hints that the downstream circulating resistance is relatively high. As the result of the interaction between downstream circular resistance and vascular elastic recoil, this wave can be employed to analyze the changes in hemodynamics on the basis of the velocity waves, which may signify some pathological changes of some diseases and their severity, such as stenosis, fistula, and aneurysm.

References

1. Nam KH, Paeng DG, Choi MJ, Shung KK. Ultrasonic observation of blood disturbance in a stenosed tube: effcects of flow acceleration and turbulence downstream. *Ultrasound Med Biol* 2008; **34:** 114-22.
2. Haruguchi H, Teraoka S. Intimal hyperplasia and hemodynamic factors in arterial bypass and arteriovenous grafts: a review. *J Artif Organs* 2003; **6:** 227-35.
3. Ariff B, Stanton A, Barratt D, Augst A, Glor F, Poulter N, et al. Comparison of the effects of antihypertensive treatment with angiotensin II blockade and beta-blockade on carotid wall structure and haemodynamics: protocol and baseline demographics. *J Renin Angiotensin Aldosterone Syst* 2002; **3:** 116-22.
4. Poepping TL, Nikolov HN, Rankin RN, Lee M, Holdsworth DW. An in vitro system for Doppler ultrasound flow studies in the stenosed carotid artery bifurcation. *Ultrasound Med Biol* 2002; **28:** 495-506.
5. Stein PD, Sabbah HN. Measured turbulence and its effect on thrombus formation. *Circ Res* 1974; **35:** 608-14.
6. Grigioni M, Daniele C, Morbiducci U, D'Avenio G., Di Benedetto G., Barbaro V. Morphological analysis of in vivo velocity field in the alteration of the vasomotor tone. *Int J Artif Organs* 2004; **27:** 868-81.
7. Meng QX, Yang B. The haemodynamics caused by arterial stenosis. *Chin J Med Imaging Technol* 2008; **24:** 297-300.
8. Caluk J, Osmanovic E, Barakovic F, Kusljugic Z, Terzic I, Caluk S, et al. Direct coronary stenting in reducing radiation and radiocontrast consumption. *Radiol Oncol* 2010; **44:** 153-7.
9. Gjikolli B, Hadžihasanović B, Jaganjac S, Herceglija E, Nikšić M, Hadzimehmedagić A, et al. Treatment of complicated case with subclavia steal syndrome and stenosis of common iliac artery. *Radiol Oncol* 2008; **42:** 1-12.
10. Shortland AP, Cochrane T. Doppler spectral waveform generation in vitro: an aid to diagnosis of vascular disease. *Ultrasound Med Biol* 1989; **15:**737-48.
11. Khir AW, Parker KH. Wave intensity in the ascending aorta: effects of arterial occlusion. *J Biomechanics* 2005; **38:** 647-55.
12. Hutchison KJ, Karpinski E. Stability of flow patterns in the in vivo post-stenotic velocity field. *Ultrasound Med Biol* 1988; **14:** 269-75.
13. Pawson P, Nolan AM, Reid J, Boyd JS, Paterson C. Changes in the Doppler waveform of the ovine femoral artery following infusion of vasoactive agents: a preliminary study. *Res Vet Sci* 2002; **73:** 215-21.
14. Yilmaz C, Erkan N, Arslan M, Yildirim Y, Kalaycioglu S. Budd-Chiari syndrome associated with liver hydatid disease: retrospective evaluation of color Doppler US findings with emphasis on intrahepatic venous collateralization. *Radiol Oncol* 2009; **43:** 225-32.

15. Fukuhara T, Hida K. Pulsatility index at the cervical internal carotid artery as a parameter of microangiopathy in patients with type 2 diabetes. *J Ultrasound Med* 2006; **25:** 599-605.

16. Ohta Y, Fujii K, Arima H, Matsumura K, Tsuchihashi T, Tokumoto M, et al. Increased renal resistive index in atherosclerosis and diabetic nephropathy assessed by Doppler sonography. *J Hypertens* 2005; **23:** 1905-11.

17. Jorgensen JJ, Stranden E, Gjolberg T. The femoral arterial flow velocity pattern in patients with aortoiliac atherosclerosis. Studies with a pulsed Doppler ultrasound flowmeter. *Acta Chir Scand* 1986; **152:** 257-61.

18. Staub D, Canevascini R, Huegli RW, Aschwanden M, Thalhammer C, Imfeld S, et al. Best duplex-sonographic criteria for the assessment of renal artery stenosis—correlation with intra-arterial pressure gradient. *Ultraschall Med* 2007; **28:** 45-51.

19. Cardoso CM, Xavier SS, Lopez GE, Brunini TM. Direct duplex scanning parameters in the diagnosis of renal artery stenosis: a study to validate and optimize cut-off points. *Arq Bras Cardiol* 2006; **87:** 321-8.

20. Kawarada O, Yokoi Y, Takemoto K, Morioka N, Nakata S, Shiotani S. The performance of renal duplex ultrasonography for the detection of hemodynamically significant renal artery stenosis. *Catheter Cardiovasc Interv* 2006; **68:** 311-8.

21. Smet AA, Ermers EJ, Kitslaar PJ. Duplex velocity characteristics of aortoiliac stenoses. *J Vasc Surg* 1996; **23:** 628-36.

22. Miralles M, Cairols M, Cotillas J, Giménez A, Santiso A. Value of Doppler parameters in the diagnosis of renal artery stenosis. *J Vasc Surg* 1996; **23:** 428-35.

23. Cooperberg E. Ultrasound Doppler spectral analysis in the diagnosis of occlusive lesions of the carotid arteries. *Ultrasound Med Biol* 1992; **18:** 421-5.

24. Leng GC, Whyman MR, Donnan PT, Ruckley CV, Gillespie I, Fowkes FG, et al. Accuracy and reproducibility of duplex ultrasonography in grading femoropopliteal stenoses. *J Vasc Surg* 1993; **17:** 510-7.

25. Choi JY, Lee JY, Lee JM, Kim SH, Lee MW, Han JK, et al. Routine intraoperative Doppler sonography in the evaluation of complications after living-related donor liver transplantation. *J Clin Ultrasound* 2007; **35:** 483-90.

26. Hoff WV. Erratum in: Pediatr Radiol. *Pediatr Radiol* 2007; **37:** 310-2.

27. Kriaa S, Zbidi M, Hafsa C, Brahem R, Majdoub S, Golli M, et al. Tardus-parvus Doppler waveform in the renal arteries of an adult patient suggesting aortic coarctation. *J Clin Ultrasound* 2006; **34:** 458-60.

28. Richardson D, Foster J, Davison AM, Irving HC. Parvus tardus waveform suggesting renal artery stenosis-remember the more proximal stenosis. *Nephrol Dial Transplant* 2000; **15:** 539-43.

29. Hartmann A, Mast H, Thompson JL, Sia RM, Mohr JP. Transcranial Doppler waveform blunting in severe extracranial carotid artery stenosis. *Cerebrovasc Dis* 2000; **10:** 33-8.

30. O'Boyle MK, Vibhakar NI, Chung J, Keen WD, Gosink BB. Duplex sonography of the carotid arteries in patients with isolated aortic stenosis: imaging findings and relation to severity of stenosis. *Am J Roentgenol* 1996; **166:** 197-202.

31. Bagi P, Sillesen H, Hansen HJ. Quantitative Doppler ultrasound evaluation of occlusive arterial disease in the lower limb. *Eur J Vasc Surg* 1988; **2:** 409-15.

32. de Morais Filho D, Miranda F Jr, Del Carmen Janeiro Peres M, Barros N Jr, Buriham E, Salles-Cunha SX. Segmental waveform analysis in the diagnosis of peripheral arterial occlusive diseases. *Ann Vasc Surg* 2004; **18:** 714-24.

33. Fontcuberta J, Flores A, Langsfeld M, Orgaz A, Cuena R, Criado E, et al. Screening algorithm for aortoiliac occlusive disease using duplex ultrasonography-acquired velocity spectra from the distal external iliac artery. *Vascular* 2005; **13:** 164-72.

34. Steinman DA, Poepping TL, Tambasco M, Rankin RN, Holdsworth DW. Flow patterns at the stenosed carotid bifurcation: Effect of concentric versus eccentric stenosis. *Ann Biomed Eng* 2000; **28:** 415-23.

35. Stergiopulos N, Spiridon M, Pythoud F, Meister JJ. On the wave transmission and reflection properties of stenoses. *J Biomech* 1996; **29:** 31-8.

36. Higgins D, Santamore WP, Walinsky P, Nemir P Jr. Hemodynamics of human arterial stenoses. *Inter J Cardiol* 1985; **8:** 177-92.

37. Ahmed SA, Giddens DP. Flow disturbance measurements through a constricted tube at moderate Reynolds numbers. *ERS J Biomech* 1983; **16:** 955-63.

38. Hutchison KJ, Campbell JD, Karpinski E. Decreased poststenotic flow disturbance during drag reduction by polyacrylamide infusion without increased aortic blood flow. *Microvasc Res* 1989; **38:** 102-9.

39. Baker AR, Prytherch DR, Evans DH, Bell PR. Characterisation of aorto-iliac arterial stenoses in terms of pressure and flow. *Cardiovasc Res* 1985; **19:** 559-66.

40. Nielsen TG, Djurhuus C, Pedersen EM, Laustsen J, Hasenkam JM, Schroeder TV. Arteriovenous fistulas aggravate the hemodynamic effect of vein bypass stenoses: An in vitro study. *J Vascul Surg* 1996; **24:** 1043-9.

41. Shi Y, Mei SC. *Medical animal experiment practical manual*.1st ed. Beijing: China Agriculture Press; 2002. p. 233-9.

42. Rice J, Philbin N, McGwin G, Arnaud F, Johnson T, Flournoy WS, et al. Bovine polymerized hemoglobin versus Hextend resuscitation in a swine model of severe controlled hemorrhagic shock with delay to definitive care. *Shock* 2006; **26:** 302-10.

43. Draney MT, Arko FR, Alley MT, Markl M, Herfkens RJ, Pelc NJ, et al. Quantification of vessel wall motion and cyclic strain using cine phase contrast MRI: in vivo validation in the porcine aorta. *Magn Reson Med* 2004; **52:** 286-95.

44. Yang BF. *Pharmacology*.7st ed. Beijing: People's Health Publishing House; 2008. p. 89-91.

research article

Comparison of CT and MRI in diagnosis of cerebrospinal leak induced by multiple fractures of skull base

Xuhui Wang, Minhui Xu, Hong Liang, Lunshan Xu

Department of Neurosurgery, Research Institute of Surgery & Daping Hospital, Third Military Medical University, Chongqing, China

Received 28 November 2010
Accepted 10 January 2011

Correspondence: Dr. Lunshan Xu, Department of Neurosurgery, Daping Hospital, Third Military Medical University, Chongqing 400042, China.
E-mail: david0608@yeah.net

Disclosure: No potential conflicts of interest were disclosed.

Background. Multiple basilar skull fracture and cerebrospinal leak are common complications of traumatic brain injury, which required a surgical repair. But due to the complexity of basilar skull fracture after severe trauma, preoperatively an exact radiological location is always difficult. Multi-row spiral CT and MRI are currently widely applied in the clinical diagnosis. The present study was performed to compare the accuracy of cisternography by multi-row spiral CT and MRI in the diagnosis of cerebrospinal leak.

Methods. A total of 23 patients with multiple basilar skull fracture after traumatic brain injury were included. The radiological and surgical data were retrospectively analyzed. 64-row CT (mm/row) scan and three-dimensional reconstruction were performed in 12 patients, while MR plain scan and cisternography were performed in another 11 patients. The location of cerebrospinal leak was diagnosed by 2 experienced physicians majoring neurological radiology. Surgery was performed in all patients. The cerebrospinal leak location was confirmed and repaired during surgery. The result was considered as accurate when cerebrospinal leak was absent after surgery.

Results. According to the surgical exploration, the preoperative diagnosis of the active cerebrospinal leak location was accurate in 9 out of 12 patients with CT scan. The location could not be confirmed by CT because of multiple fractures in 2 patients and the missed diagnosis occurred in 1 patient. The preoperative diagnosis was accurate in 10 out of 11 patients with MRI examination.

Conclusions. MRI cisternography is more advanced than multi-row CT scan in multiple basilar skull fracture. The combination of the two examinations may increase the diagnostic ratio of active cerebrospinal leak.

Key words: CT; MRI; diagnosis; multiple basilar skull fracture; cerebrospinal leak

Introduction

The incidence of cerebrospinal leak is about 2-9% after the traumatic brain injury.[1] It is even higher after multiple basilar skull fracture. Secondary intracranial infection, as one of the severe complications, may occur in 30-40% of the patients with prolonged cerebrospinal leak.[2] A surgical repair is the most effective therapy for most traumatic cerebrospinal leak, which requires the preoperative exact radiological location. The severe craniocerebral injury always results in multiple basilar skull fracture and followed by cerebrospinal leak. The complexity of multiple basilar fractures greatly increases the difficulty of the surgical repair. Preoperatively exact location of cerebrospinal leak is the precondition of surgery, especially in patients undergoing reoperation after the failed surgical repair.

Many examinations have been tried by the radiological experts to diagnose cerebrospinal leak, including radiological cisternography and CT cisternography. However, radioactivity is present in the former, while the latter is time-consuming and the suitable time of scan is hard to choose. Besides, patients may be uncomfortable because of the invasion and the risk of intracranial infection cannot be neglected. With the wide application of multi-row high-resolution spiral CT and MRI, they are being

the two main approaches diagnosing cerebrospinal leak. Previous studies have been performed to compare the accuracy of the two examinations in diagnosing cerebrospinal leak. But recently CT and MR techniques are improved greatly. They have not been compared in traumatic cerebrospinal leak, either. Patients with cerebrospinal leak in our hospital were included retrospectively in the present study. The accuracy of CT and MRI cisternography was determined by comparing them with the surgical exploration, so as to provide evidence for the surgical repair of cerebrospinal leak.

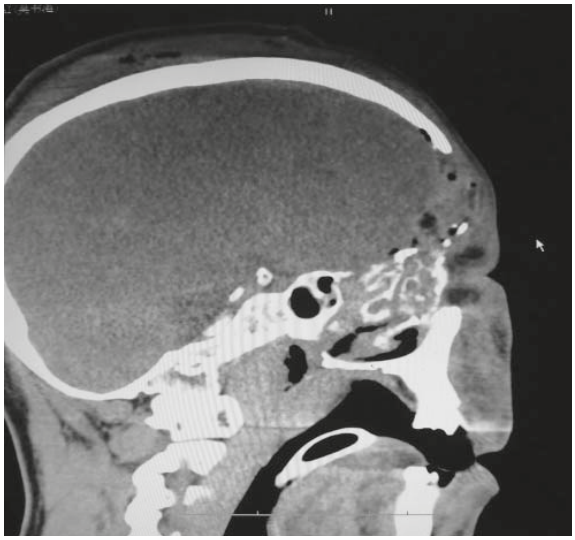

A

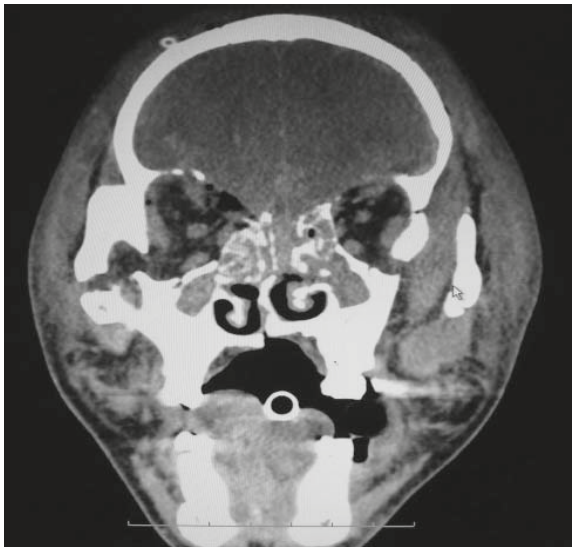

B

FIGURE 1. A 43-year-old patient diagnosed with multiple basilar skull fracture induced by severe craniocerebral injury. Partial frontal bone and superficial arch were resected and cerebrospinal rhinorrhea was present 10 days after surgery (Right). CT showed multiple basilar skull fracture. The cerebrospinal leak location could not be determined because of the several defects in ethmoid and sphenoidal sinus. It was demonstrated by surgery that meninges defect was present at the site of ethmoid sinus (A, sagittal view; B, coronal view). Rhinorrhea disappeared after the surgery repair.

Methods

Twenty-three patients with traumatic cerebrospinal leak from 2006 in our hospital were retrospectively reviewed. There were 19 males and 4 females, aging from 13 to 40 years, with an average age of 28 ± 3.6 years. All patients were manifested with clear liquid leaking from nose or ear after a trauma, among which rhinorrhea was present in 20 cases and otorrhea in 3 cases. The course of disease was as long as 3 weeks to half a year. Cerebrospinal leak was diagnosed according to the positive ß-2 transferrin in leakage of all patients and finally confirmed by surgery. CT plain scan demonstrated fractures in anterior or middle cranial fossa at 2 or more sites. Then high-resolution spiral CT was performed in 12 patients and MR cisternography was performed in 11 patients. The results of radiological examinations were provided by 2 radiological experts independently. The patient was included in the study only if the 2 radiological experts made a consensus on the diagnosis. The diagnosis was then compared with the actual results identified by the surgical exploration (Figure 1).

High-resolution multiple-row CT scan (64-row, with a thickness of 0.625 mm) was performed in 12 patients. The field of view was 25cm and the matrix size was 512×512. Details of bone substance were shown by the reconstruction. The scanning range included ethmoid, sphenoid and temporal bone, as well as all other sites with potential cerebrospinal fluid leak. 30-50% overlapping was applied for the reconstruction. The site of cerebrospinal leak was suspected when CT scan showed skull base defect, air fluid level and image opacification in adjacent paranasal sinus.[3]

MR cisternography was performed in 1.5T MRI SP 6000 system. T1-weighted imaging in coronal, axial and sagittal planes was scanned as routine. T2-weighted spinecho sequence with fat saturation was obtained in coronal, axial and sagittal planes with parameters of 6000/90/1(TR/TE/excitation). MRI was scanned in both supine and prone position to evaluate the influence of position on the distribution of cerebrospinal fluid. The site of cerebrospinal leak was suspected when cerebrospinal fluid was linked with subarachnoid space outside the skull, or herniation of cerebrospinal fluid was present.

Due to the Chinese system of medical care, the examination fees should be paid by the patients' own expense. Thus, MR examination was not performed if the diagnostic objective was obtained with CT scan. CT or MR cisternography were rec-

TABLE 1. Coincidence ratio of CT and MRI examinations with the surgical exploration in diagnosing sites of cerebrospinal leak

Sites	Number	CT			MR		
		Coincidence with surgery	Missed diagnosis	Wrong diagnosis	Coincidence with surgery	Missed diagnosis	Wrong diagnosis
Ethmoid bone	14	8		2	5	1	
Frontal sinus	10	6	1	1	3		
Sphenoid bone	8	3	1	1	5		
Petrous bone	3	1			1		
Temporal bone	1	1			0		
Accuracy		90.48%			93%		

ommended by the physicians according to the result of primary CT scan and the medical history. Therefore, there were few direct comparisons of CT and MRI results in the same patient.

Results

In 12 patients who underwent high-resolution CT examinations, 47 suspected skull defects or fractures were observed and 25 sites of cerebrospinal leak were diagnosed after the analysis: there was a fluid level in the accessory nasal sinuses and the fluid contained glucose and were ß-2 transferrin positive. In comparison with the results of the surgical exploration, 21 sites of cerebrospinal leak were present in 12 patients. A further comparison showed that among 25 sites of cerebrospinal leak, which was seen with the CT examinations, 19 were correctly, 4 was wrong and 2 was missed diagnosed, respectively. The accuracy of CT examination was 90.48%. The diameters of leak site missed diagnosed were about 2 mm, and all missed diagnoses happened in fracture-type defects. Fracture was present in all wrongly-diagnosed sites but no leak was found and diagnosis of cerebrospinal leak was denied during surgery (Table 1).

MR cisternography was performed in 2 patients who underwent CT examination because of the disagreement of the diagnosis between the 2 neuroradiologists. Surgery failure was present in 1 patient after CT examination, in whom cerebrospinal leak in frontal sinus was diagnosed afterward MR cisternography and the secondary surgical repair was successfully performed. (Figure 2)

In 11 patients who underwent MR cisternography, 14 sites of cerebrospinal leak were suspected before the surgery. According to the surgical exploration, there were 15 sites of cerebrospinal leak, while 1 site was missed in the MR cisternography.

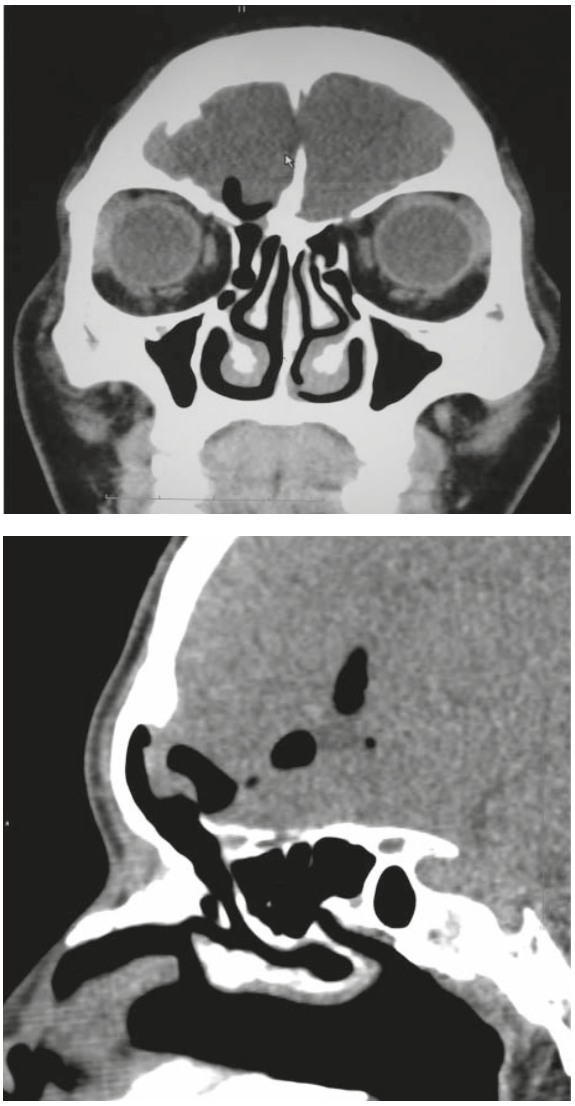

FIGURE 2. Cerebrospinal fluid rhinorrhea was present after brain trauma in a male patient of 37 year old. CT scan showed multiple basilar skull fracture. Thin layer scan of high-resolution CT showed that frontal sinus communicated with nasal cavity and cerebrospinal leak in frontal sinus was the diagnosis (A, coronal view; B, sagittal view). The surgical exploration confirmed that frontal sinus was impaired and communicated with intracalvarium and rhinorrhea disappeared after the surgical repair.

The accuracy was 93% (Table 1). Intermittent cerebrospinal leak was present in the patients missed diagnosed. The diagnostic rate of intermittent and non-active cerebrospinal leak by MR cisternography was not high (Figure 3).

It was demonstrated by surgery that 36 sites of cerebrospinal leak communicated with the paranasal sinus defects, the tympanic cavity, etc, among which 14 sites were in the madreporite, 10 in the frontal sinus and 8 in the sphenoidal sinus. Tympanic cavity of middle ear communicated with defects in petrous and temporal bones in 3 cases and with petrous in 1 case. *Dura mater* was usually thickened and immersed into fracture gap, which was always irregular and slit-like (Table 1).

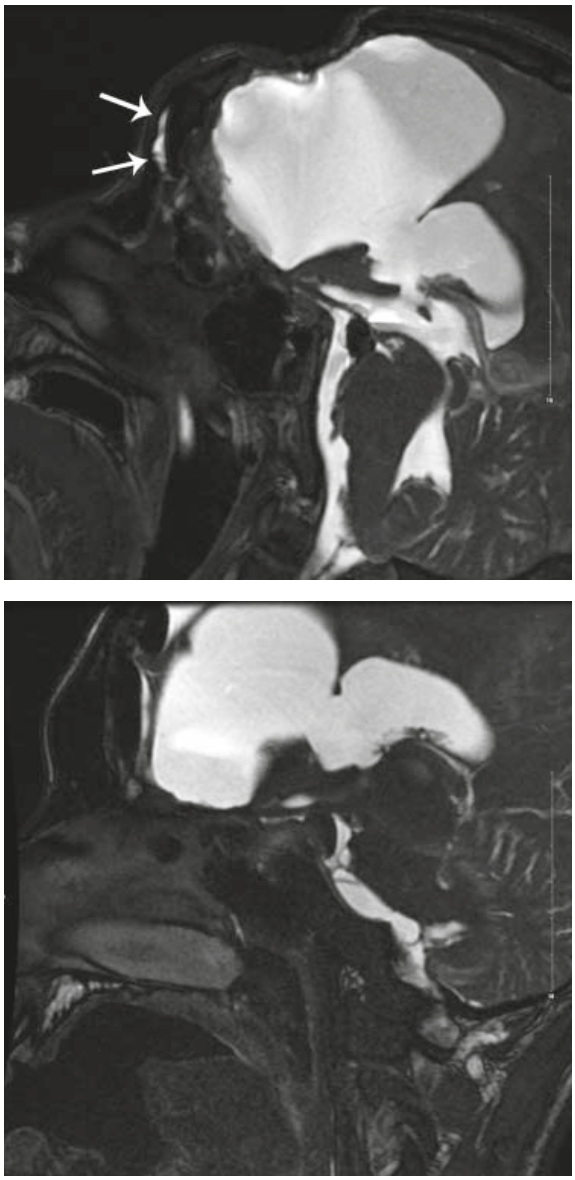

Ⓐ

Ⓑ

FIGURE 3. A male patient aged 21 years with severe craniocerebral injury. Surgery was performed to remove part of the frontal bone and contused brain tissue of frontal lobe. One week after surgery, cerebrospinal fluid rhinorrhea was present in left nose. CT scan showed multiple basilar skull fracture and failure in ethmoid sinus repair. MR cisternography showed that high-signal liquid was present in frontal sinus in the prone position (3A) but not in the supine position (3B) in T2-weighted image, thus cerebrospinal leak in frontal sinus was diagnosed. It was observed during surgery that the crack fracture was present in the posterior side of frontal sinus with damaged *dura mater*, which communicated with nasal cavity, and rhinorrhea disappeared after the surgery.

Discussion

The severe traumatic brain injury always results in multiple basilar skull fracture, and cerebrospinal leak is one of the most important complications. Cerebrospinal leak may be complicated with bacterial meningitis, and sometimes encephalitis and cerebral abscess.[4] Although cerebrospinal leak in some cases recovers spontaneously, long-term cerebrospinal leak increases the risk of intracranial infection greatly, with an incidence as high as 40%.[5] Therefore, the surgical repair is usually required to treat cerebrospinal leak. Location of cerebrospinal leak is essential for the successful surgical repair, especially in patients with cerebrospinal leak after intranasal mini-invasive repair surgery. Many examinations have been applied to locate the cerebrospinal leak, such as radioactive cisternography, which is now seldom used because of the radioactivity, time-consuming, invasion, mild risk, low diagnostic rate and relatively high false positive rate.[2] With the progress of CT, CT cisternography significantly improves the diagnostic rate of cerebrospinal leak site. Its diagnostic rate is as high as 92% in diagnosing active cerebrospinal leak, while it is just 40% in diagnosing intermittent or non-active cerebrospinal leak.[6] The application of CT cisternography is also restricted because of lumbar puncture induced infection, hemorrhage and hypotensive cranial pressure headache.

With the rapid popularity of multiple-row high-resolution CT [7], it has currently been regarded as a routine examination and preferred the method for location of cerebrospinal leak because of the safety and convenience. A layer thickness of 0.5 mm is routinely chosen in the modern CT examination and the image reconstruction can be accomplished in random planes[8,9], thus the diagnostic rate of cerebrospinal leak by high-resolution CT is much higher than CT cisternography.[10] In the present study, 64-row high-resolution CT was applied for thin-layer scan with a layer thickness of 0.625 mm in coronal plane and the multiplanar reconstruction was performed in the scan region to search the

leak site. Many basilar skull defects and crack fractures were found out in these 12 patients, but it was difficult to identify which defect was the real cerebrospinal leak site and several wrong or missed diagnoses were made. Several previous studies were performed to evaluate the role of high-resolution CT in identifying cerebrospinal leak site, but the study reporting the leak site location in complicated basilar skull fracture is rare. Many factors made it hard to locate the leak site, including the complication of basilar skull fracture induced by severe traumatic brain injury, thickening *dura mater* in injury site and injury of paranasal sinus. It was easy for CT to find out suspected leak site, but it remained to be difficult to correctly locate the leak site, which depended on the experience and good communication between radiologists and physicians.

Another diagnostic approach was MRI, which is widely used in the case of brain or spinal injuries.[6,11,12] Cerebrospinal fluid is present as high signal in T2-weighted spinecho sequence with fat saturation and cerebrospinal leak site is visualized by a non-invasive method. Meanwhile, cephalocele and meningocele are also easily diagnosed. The intrathecal injection of contrast media may also increase the diagnostic rate of MRI cisternography.[11] Cerebrospinal leak site can also be visualized by changing the position of patients to compare the distribution of cerebrospinal fluid in cranium and paranasal sinuses in different positions.[6] In the present study, 14 sites of cerebrospinal leak were diagnosed in 11 patients who underwent MRI cisternography and 15 sites were diagnosed by the surgical exploration. The accuracy was as high as 93%. The correct diagnosis was made in 10 out of the 11 patients. Cerebrospinal leak was non-active in the other patient, and the inappropriate timing for MRI cisternography might be the cause of the negative result.

The principle of MR cisternography is similar to CT cisternography and radionuclide cisternography that basilar skull site of cerebrospinal leak was determined by observing current direction of cerebrospinal fluid. Therefore, MR cisternography is good at diagnosing active cerebrospinal leak, while its diagnostic rate was significantly reduced in diagnosing non-active or intermittent cerebrospinal leak.[6] Trauma induced basilar skull fracture is usually very severe and most of cerebrospinal leaks are active. Therefore, MR cisternography showed high accuracy in our present study. Moreover, MR cisternography has a high demand for positions, and changing position according to the menifestations of patients may improve the diagnostic rate[3], which requires participation and good communication between physicians and radiologists. MR cisternography after the intrathecal administration of gadopentate dimeglumine represents an effective and minimally invasive method for evaluating suspected cerebrospinal fluid (CSF) fistulas along the skull base. It provides multiplanar capabilities without risk of radiation exposure and is an excellent approach to depict the anatomy of CSF spaces and CSF fistulas.[13] Brain injury induced by traffic accidents is always accompanied by severe injury in other sites of the body[14], thus the position of patients may be strictly restricted. One kind of MRI equipment accommodating multiple positions of patients may solve this problem greatly.

High-resolution CT and MRI cisternography were compared systematically to evaluate their roles in diagnosing cerebrospinal leak site. The sensitivity, specificity and accuracy of high-resolution CT were 92%, 100% and 93%, while that of MR cisternography were 87%, 100% and 89% respectively.[6] It seemed that high-resolution CT was better than MR cisternography and CT showed details of bone defects better. In the present study, the accuracy of MR cisternography was higher than CT. The reasons were listed as follows. First, less multiple basilar skull fracture was included in our study, which made it difficult to diagnose by CT because of the complicated fracture line. Second, most of cerebrospinal leaks in our present study were active, which might increase the diagnostic accuracy of MR. But CT scan has an advantage of visualizing skull defects better in the surgical repair, especially in providing evidence for intranasal endoscopic repair surgery.[5] Advantages of MR including dynamical display of cerebrospinal fluid flow when changing the position and the correct diagnosis of active leak. But the diagnostic rate of MR in non-active leak is low and MR cannot show basilar skull defect in details. Preoperative CT scan is always required in leak region. Thus, the two examinations have their own advantages and can be applied complementing each other when necessary. We suggested that multiple-row high-resolution CT examinations should be used to locate the suspected leak sites in multiple basilar skull fracture induced by traumatic brain injury. MR cisternography was not necessary if the distributions of leak sites could be involved in one surgical exploration. Cerebrospinal leak sites would be determined by explorations in sequence. When the distributions of leak sites could not be involved in one surgical exploration, MR cisternography should be

performed to determine the location which warranted repair in preference.

In conclusion, in multiple basilar skull fracture induced by traumatic brain injury, high-resolution is preferred in identifying multiple basilar skull defects and fractures, but on the other hand, this may lead to difficulty in diagnosing the real cerebrospinal leak sites. MR cisternography shows a current flow of cerebrospinal fluid and thereby determines the leak sites, which covers the insufficiency of high-resolution CT. But it is difficult for MR cisternography to diagnose the sites of non-active cerebrospinal leak, and the diagnosis of non-active leak remains to be further investigated.

References

1. Hilinski JM, Kim T, Harris JP. Posttraumatic pseudo-cerebrospinal fluid rhinorrhea. *Otol Neurotol* 2001; **22:** 701-5.
2. Schlosser RJ, Bolger WE. Nasal cerebrospinal fluid leaks: critical review and surgical considerations. *Laryngoscope* 2004; **114:** 255-65.
3. Lloyd KM, DelGaudio JM, Hudgins PA. Imaging of skull base cerebrospinal fluid leaks in adults. *Radiology* 2008; **248:** 725-36.
4. Brodie HA. Prophylactic antibiotics for posttraumatic cerebrospinal fluid fistulae. A meta-analysis. *Arch Otolaryngol Head Neck Surg* 1997; **123:** 749-52.
5. McMains KC, Gross CW, Kountakis SE. Endoscopic management of cerebrospinal fluid rhinorrhea. *Laryngoscope* 2004; **114:** 1833-7.
6. Shetty PG, Shroff MM, Sahani DV, Kirtane MV. Evaluation of high-resolution CT and MR cisternography in the diagnosis of cerebrospinal fluid fistula. *AJNR Am J Neuroradiol* 1998; **19:** 633-9.
7. Stanic K, Kovac V. Prophylactic cranial irradiation in patients with small-cell lung cancer: the experience at the Institute of Oncology Ljubljana. *Radiol Oncol* 2010; **44:** 180-6.
8. Prokop M. General principles of MDCT. *Eur J Radiol* 2003; **45 Suppl 1:** S4-10.
9. La Fata V, McLean N, Wise SK, DelGaudio JM, Hudgins PA. CSF leaks: correlation of high-resolution CT and multiplanar reformations with intraoperative endoscopic findings. *AJNR Am J Neuroradiol* 2008; **29:** 536-41.
10. Stone JA, Castillo M, Neelon B, Mukherji SK. Evaluation of CSF leaks: high-resolution CT compared with contrast-enhanced CT and radionuclide cisternography. *AJNR Am J Neuroradiol* 1999; **20:** 706-12.
11. Arbeláez A, Medina E, Rodríguez M, Londoño AC, Castillo M. Intrathecal administration of gadopentetate dimeglumine for MR cisternography of nasoethmoidal CSF fistula. *Am J Roentgenol* 2007; **188:** 560-4.
12. Rajer M, Kovač V. Malignant spinal cord compression. *Radiol Oncol* 2008; **42:** 23-31.
13. Selcuk H, Albayram S, Ozer H, Ulus S, Sanus GZ, Kaynar MY, Kocer N, Islak C. Intrathecal Gadolinium-Enhanced MR cisternography in the evaluation of CSF leakage. *AJNR Am J Neuroradiol* 2010; **31:** 71-5.
14. Ho KM, Burrell M, Rao S. Extracranial injuries are important in determining mortality of neurotrauma. *Crit Care Med* 2010; **38:** 1562-8.

research article

Diffusion differences between pilocytic astrocytomas and grade II ependymomas

Goran Pavlisa[1], Gordana Pavlisa[2], Marko Rados[1]

[1] Department of Radiology, University Hospital Center Zagreb, University of Zagreb School of Medicine, Zagreb, Croatia
[2] Intensive Care Unit, Special Hospital for Pulmonary Diseases, Zagreb, Croatia

Received 20 January 2011
Accepted 2 March 2011

Correspondence to: Goran Pavliša, Department of Radiology, University Hospital Center Zagreb, University of Zagreb School of Medicine, Kišpatičeva 12, 10000 Zagreb, Croatia. Tel: +385 1 2388118; Fax: +385 1 2388250; E-mail: gpavlisa@net.amis.hr

Disclosure: No potential conflicts of interest were disclosed.

Background. The aim of our study was to differentiate between cerebellar pilocytic astrocytomas and grade II ependymomas on the basis of their diffusion properties.
Patients and methods. The study prospectively included 12 patients with pilocytic astrocytomas and 5 with ependymomas. Apparent diffusion coefficients (ADC) were compared between tumour types.
Results. ADC values were significantly higher in pilocytic astrocytomas than ependymomas, with almost no overlapping of the range of measured ADCs between the two tumour types.
Conclusions. Significant diffusion differences between pilocytic astrocytomas and grade II ependymomas enable their preoperative distinction, in combination with conventional magnetic resonance images.

Key words: pilocytic astrocytoma; ependymoma; apparent diffusion coefficient

Introduction

Infratentorially located pilocytic astrocytomas and grade II ependymomas may have similar magnetic resonance imaging (MRI) appearance. Pilocytic astrocytoma (PA) is a World Health Organization (WHO) grade I tumour, with the low mitotic activity and very low potential for malignant transformation.[1] Solid portions of PA have low cell density with bipolar „piloid" astrocytes and characteristic microcytic component and Rosenthal fibers[2], which represents an environment with a relatively unrestricted diffusion of water molecules in extracellular space. One of the common locations of PAs in children and young adults is cerebellum, near the fourth ventricle, which is also a predilection site for ependymomas (EPN). EPNs usually have a higher cell density compared to PAs, and according to their histological characteristics they may be classified as WHO grades I – III.[1,3] Although these two tumour types are readily differentiated on the basis of MRI morphology in a majority of patients, in cases of a solid PA without typical cystic component, differential diagnosis may be difficult.[4] Diffusion properties of intracranial tumours have been extensively studied, however, with disparate results.

The aim of our study was to differentiate between cerebellar pilocytic astrocytomas and grade II ependimomas on the basis of their diffusion properties. We hypothesised that pilocytic astrocytomas have higher values of apparent diffusion coefficient (ADC) than more cellular ependymomas.

Patients and methods

The study prospectively included 17 patients; 12 with newly discovered and subsequently histopathologicaly proven pilocytic astrocytomas (WHO grade I), and 5 with ependymomas (WHO grade II). The neuropathologist was blinded to the MRI findings and ADC values. The adequate study power was calculated based on the pilot study, which included 8 patients, four with PAs and four with EPNs. The required sample size was 5 patients with PAs and EPNs, respectively, based on a level of reliability $1\text{-}\alpha \geq 0.95$ and statistical power $1\text{-}\beta \geq 0.8$. We excluded patients with tumours smaller than 1 cm in largest diameter, because such size did not en-

TABLE 1. Description of continuous variables

Tumour type	ADC (N x 10^{-5} mm^2/s)				
	Mean	Range	SD	VC	SE
Pilocytic astrocytoma	156.7	117.5 – 226.9	38	0.244	11
Ependymoma	97.6	80.4 – 121.9	17	0.181	8

ADC = apparent diffusion coefficient, SD = standard deviation, VC = variability coefficient, SE = standard error

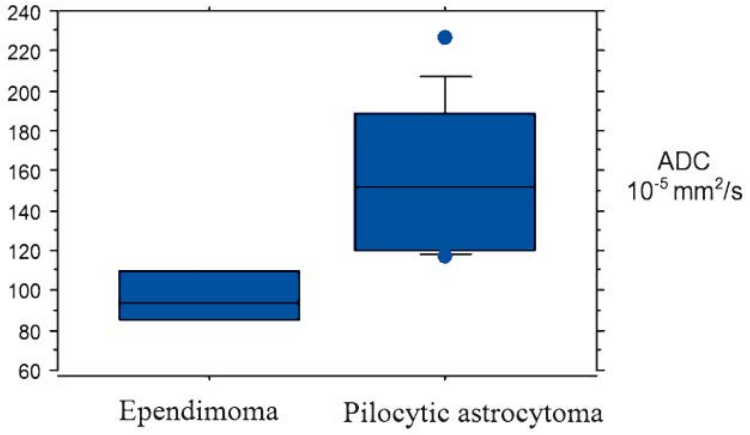

FIGURE 1. The range of apparent diffusion coefficient (ADC) values of ependymomas and pilocytic astrocytomas. ADCs of these tumours were minimally overlapping, between values of 117.5 x 10^{-5} mm^2/s and 121.9 x 10^{-5} mm^2/s.

able precise ADC measurements and the avoidance of partial volume effect. We also excluded patients with extensive artefacts of diffusion-weighted images (DWI) and those with other pathological processes besides tumour, which did not allow for the precise measurement of the control ADC sample.

MR imaging was performed on a 1.5-T system (Symphony, Siemens Medical Systems, Erlangen, Germany) with 30-mT/m gradients and a slew rate of 125 T/m/s. Single-shot echo-planar DW images were acquired in a transverse plain with the acquisition of a diffusion trace, with the following parameters: FOV, 22.8×22.8 cm; matrix, 128×128; slice thickness, 5 mm; slice gap, 1.5 mm; three b values (0, 500, and 1000 s/mm^2); TR, 3200 ms; TE, 94 ms; Nex, 1; TA, 1 min 12 s. ADC maps were automatically calculated, according to the following equation: $ADC=\ln (S_0/S_1)/(b_1-b_0)\times 10^{-5}$ mm^2/s.[5] DWI was performed before the administration of gadolinium-DTPA in all cases. The imaging protocol also included conventional sequences: in all cases, axial FSE T2WI and axial nonenhanced and contrast-enhanced SE T1WI. Two neuroradiologists separately defined the following areas on conventional images, with a consensus in cases of disagreement:

1. solid tumour, as an area with a mass effect and contrast enhancement;
2. normal brain tissue, as an area with normal signal intensities in all sequences, without mass effect;
3. cystic/necrotic area, as an area with a hypointense signal in T1WI and a hyperintense signal in T2WI, without contrast enhancement;
4. haemorrhage, as an area with a hyperintensity in nonenhanced T1WI; and
5. calcified tumours, as hypointense areas in DWI b=0 images.

Cystic/necrotic areas and areas containing haemorrhage and calcifications were excluded from further analysis. ADC measurements were performed using a region-of-interest (ROI) method, with uniform ellipsoid ROIs of 0.2 cm^2, containing approximately 10 pixels. ADC measurements were performed using e-Film Workstation 2.1 (Merge Healthcare, Milwaukee, WI, USA), with a simultaneous display of contrast-enhanced T1WI, T2WI, isotropic DWI, and ADC map. We placed three ROIs in the areas corresponding to each tumour. The representative value used in data and statistical analysis was the mean value±S.D. One control ROI was placed in normal tissue. We additionally preformed ADC measurements bilaterally in deep white matter to exclude any laterality differences of the healthy tissue. The mean tumour ADC values±S.D. were compared to normal tissue, and between PAs and EPNs. The comparison of differences in mean ADC values was performed using the Mann–Whitney U test. $P<0.05$ was considered statistically significant. A statistical analysis was performed using StatView software (SAS Institute Inc. Version 5.0.1) and Statistica 7 (StatSoft, Inc., Netherlands).

All the patients gave their informed consent, and the study was approved by the institutional review board.

Results

There were no significant differences of ADC of normal deep white matter between brain hemi-

TABLE 2. Differences of tumour ADC in patients with pilocytic astrocytomas and ependymomas

Tumor type	ADC (N x 10^{-5} mm^2/s) ± SD		p
	Tumor	Normal tissue	
Pilocytic astrocytoma	156.7 ± 38	85.7 ± 9	<0,0001
Ependimoma	97.6 ± 17	83.8 ± 12	0.3858
p	0.0212	0.9035	

ADC = apparent diffusion coefficient, Underlined = statistically significant difference.

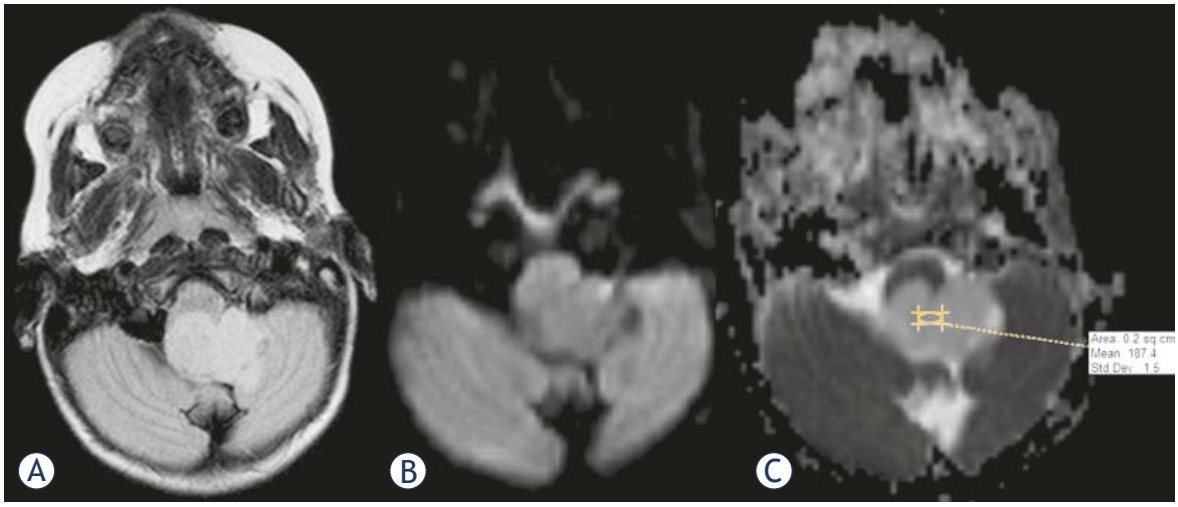

FIGURE 2. MR images in axial plane of a patient with pilocytic astrocytoma. A: Fluid-attenuated inversion recovery (FLAIR) image with a homogenous, slightly hyperintense tumour in the fourth ventricle and left foramen of Luschka. Diffusion-weighted image (B), and map of apparent diffusion coefficient (ADC) (C) without restriction of the diffusion. Intratumoural diffusion coefficient is 187.4 x 10^{-5} mm^2/s.

spheres in patients with both investigated tumour types; it was 80 - 85 x 10^{-5} mm^2/s. Continuous variables are described in Table 1.

The average age was 19 in patients with PAs, and 20 years in patients with EPNs.

The difference of ADCs between tumour and normal brain tissue of patients with PAs was statistically highly significant. In patients with EPNs, there was no significant difference of ADC between tumour and normal tissue. ADC was significantly higher in PAs compared to EPNs (Table 2). The mean ADC of PAs was 156.7 x 10-5 mm^2/s, while the mean ADC of EPNs was 97.6.

The range of ADCs of investigated tumours is displayed graphically (Figure 1).

Discussion

Pilocytic astrocytoma and ependymoma, together with medulloblastoma, are the most common cerebellar tumours in children and young adults.[6] Since these tumours have different biologic potential, the preoperative differentiation among them has important consequences on treatment planning. Conventional MRI, although being the most important diagnostic tool in brain imaging, is not sufficiently specific for the differentiation of these tumour types in all patients. Pilocytic astrocytomas are typically characterized by strongly contrast-enhancing *nodus* and the variably large cystic component, filled with rare proteinaceous fluid which resembles the signal from cerebrospinal fluid. They are usually well-delineated from the surrounding brain tissue, and located in posterior fossa. Ependymomas often share the same location with pilocytic astrocytomas in pediatric patients, but are mostly solid tumours, typically with ependymal spread through the fourth ventricle and into ventricular foramina. However, both tumour types may have morphologically very similar appearance, since not all pilocytic astrocytomas have a pronounced cystic component (Figure 2,3).

Therefore, we aimed to differentiate between PAs and EPNs by measuring intratumoural apparent diffusion coefficient. This method is currently

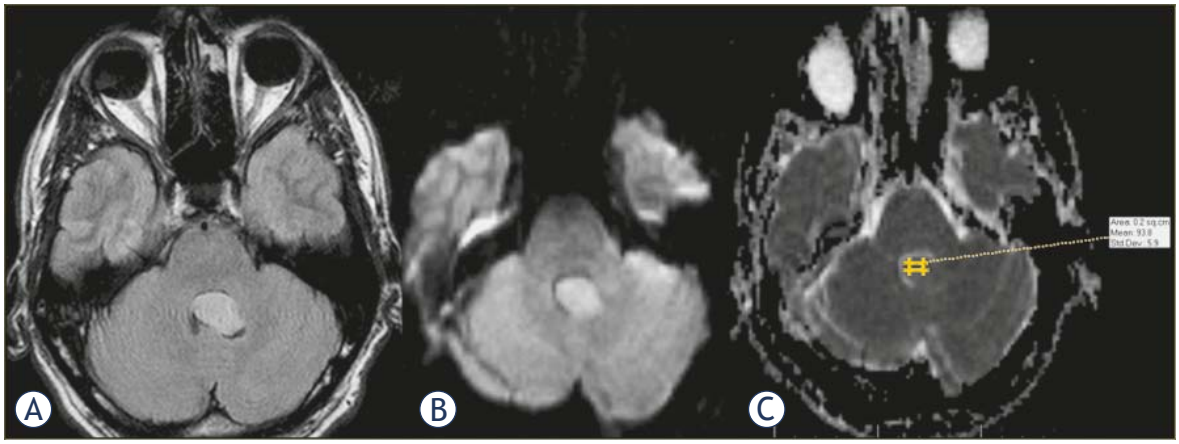

FIGURE 3. Axial MRI of a patient with grade II ependymoma shows morphologically similar tumour to the one seen in Figure 1A, with moderate hyperintensity in FLAIR image. Diffusion-weighted image and ADC map reveal relatively restricted diffusion, with coefficient of 93.8 x 10^{-5} mm^2/s.

available on virtually all MRI scanners; it is non-invasive, with short acquisition times and is free from motion artefacts compared to other imaging sequences. It is widely used in diagnostics of stroke, as well as other pathological conditions.[7,8] Differentiation of intracranial tumours on the basis of their ADC values has been relatively extensively studied, however, with disparate results.[9-16]

We investigated ADC differences in 12 patients with pilocytic astrocytomas and 5 patients with ependymomas. We did not include patients with medulloblastomas in the study, since the literature results on diffusion in highly cellular medulloblastomas are rather clear, with signs of restricted diffusion in previous studies.[14-17] Ependymomas included in the study were WHO grade II. Tumours of grade I, myxopapillary ependymoma and subependymoma, were excluded since they have distinct morphological, biological and demographic features, the first presenting almost exclusively in *cauda equina* region, and the second in an older age group and with different MRI characteristics than ependymoma grade II.[18] PAs have low cell density with relatively large volume of extracellular space, unlike EPNs, therefore, we hypothesised that the diffusion of water molecules in PAs is of a higher order compared to EPNs. Our results confirmed that assumption, with significantly higher ADC values in PAs than EPNs and with almost no overlapping of the range of measured ADCs between the two tumour types. The intratumoural ADC values of our patients were in line with some previous investigations[15], while others found higher ADC in EPNs[14], or lower ADC in PAs[19], compared to our patients. The ADC differences among these studies may be due to the retrospective character of previous studies, different designs without a direct comparison of these tumour types, a single measurement in each tumour, thicker DWI slice used in imaging or due to the investigation of exclusively paediatric population.

Apparent diffusion coefficients of pilocytic astrocytomas and ependymomas in our patients were reliable indicators of tumour type. The level of ADC above 120 x 10^{-5} mm^2/s was indicative of PA, while the ADC between 80 and 120 x 10^{-5} mm^2/s was characteristically for EPN. We believe that this difference of diffusion properties is due to histological features of investigated tumours. The structure of PAs is „biphasic", consisting of vacuolated low density areas and areas of relatively higher density, however even in the latter areas, the overall cellularity is low to moderate, with small nuclei and microcytic stroma.[20] This enables relatively unrestricted diffusion of water molecules, unlike in EPNs, which is of uniformly moderate cell density. The brain tissue which was normal on conventional MRI had very similar ADC levels in both brain hemispheres of our patients, excluding any laterality differences.

In conclusion, a significantly higher apparent diffusion coefficient in pilocytic astrocytomas compared to WHO grade II ependymomas probably reflects the differences in cell density of these tumours, and enables their preoperative distinction, in combination with conventional magnetic resonance images.

References

1. Louis DN, Ohgaki H, Wiestler OD, Cavenee WK. *World Health Organization Classification of tumours of the central nervous system.* Lyon: IARC Press; 2007.

2. Okazaki H, Scheithauer BW. *Atlas of Neuropathology.* New York: Gower Medical Publishing; 1988.

3. Graham DI, Lantos PL. *Greenfield's neuropathology.* 7th Edition. London: Hodder Arnold; 2002.

4. Lin E, Escott E, Garg K, Bleicher A. *Practical differential diagnosis for CT and MRI*. New York: Theme Medical Publishers Inc; 2008.

5. Stejskal E, Tanner J. Spin diffusion measurements: spin echoes in the presence of a time-dependent field gradient. *J Chem Phys* 1965; **42:** 288-92.

6. Becker L. Pathology of pediatric brain tumours. *Neuroimag Clin N Am* 1999; **9:** 671-90.

7. Inan N, Kilinc F, Sarisoy T, Gumustas S, Akansel G, Demirci A. Diffusion weighted MR imaging in the differential diagnosis of haemangiomas and metastases of the liver. *Radiol Oncol* 2010; **44:** 24-9.

8. Oztekin O, Calli C, Kitis O, Adibelli ZH, Eren CS, Apaydin M, et al. Reliability of diffusion weighted MR imaging in differentiating degenerative and infectious end plate changes *Radiol Oncol* 2010; **44:** 97-102.

9. Schaefer PW, Grant PE, Gonzalez RG. Diffusion-weighted MR imaging of the brain. *Radiology* 2000; **217:** 331-45.

10. Aronen H, Cohen M, Belliveau J, Fordham J, Rosen B. Ultrafast imaging of brain tumors. *Top Magn Reson Imaging* 1993; **5:** 14-24.

11. Brunberg JA, Chenevert TL, McKeever PE, Ross DA, Junck LR, Muraszko KM, et al. In vivo MR determination of water diffusion coefficients and diffusion anisotropy: Correlation with structural alteration in gliomas of the cerebral hemispheres. *AJNR Am J Neuroradiol* 1995; **16:** 361-71.

12. Eis M, Els T, Hoehn-Berlage M. High resolution quantitative relaxation and diffusion MRI of three different experimental brain tumors in rats. *Magn Reson Med* 1995; **34:** 835-44.

13. Bulakbasi N, Kocaoglu M, Ors F, Tayfun C, Ucoz T. Combination of single-voxel proton MR spectroscopy and apparent diffusion coefficient calculation in the evaluation of common brain tumors. *AJNR Am J Neuroradiol* 2003; **23:** 225-33.

14. Yamasaki F, Kurisu K, Satoh K, Arita K, Sugiyama K, Ohtaki M, et al. Apparent diffusion coefficient of human brain tumors at MR imaging. *Radiology* 2005; **235:** 985-91.

15. Rumboldt Z, Camacho DLA, Lake D, Welsh CT, Castillo M. Apparent diffusion coefficients for differentiation of cerebellar tumors in children. *AJNR Am J Neuroradiol* 2006; **27:** 1362-9.

16. Chen HJ, Panigrahy A, Dhall G, Finlay JL, Nelson MD, Blüml S. Apparent diffusion and fractional anisotropy of diffuse intrinsic brain stem gliomas. *AJNR Am J Neuroradiol* 2010; **31:** 1879-85.

17. Yamashita Y, Kumabe T, Higano S, Watanabe M, Tominaga T. Minimum apparent diffusion coefficient is significantly correlated with cellularity in medulloblastomas. *Neurol Res* 2009; **31:** 940-46.

18. Applegate GL, Marymont MH. Intracranial ependymomas: a review. *Cancer Invest* 1998; **16:** 588-93.

19. Gauvain KM, McKinstry RC, Mukherjee P, Perry A, Neil JJ, Kaufman BA, et al. Evaluating pediatric brain tumor cellularity with diffusion-tensor imaging. *AJR Am J Roentgenol* 2001; **177:** 449-54.

20. Perry A. Pathology of low-grade gliomas: an update of emerging concepts. *Neurooncology* 2003; **5:** 168-78.

research article

CD133/prominin1 is prognostic for GBM patient's survival, but inversely correlated with cysteine cathepsins' expression in glioblastoma derived spheroids

Seyed Y. Ardebili[1], Irena Zajc[2], Boris Gole[2], Benito Campos[3], Christel Herold-Mende[3], Sara Drmota[2,4], Tamara T. Lah[2,4]

[1] Department of Neurosurgery, University Medical Centre, Ljubljana, Slovenia
[2] Department of Genetic Toxicology and Cancer Biology, National Institute of Biology, Ljubljana, Slovenia
[3] Division of Neurosurgical Research, Department of Neurosurgery, University of Heidelberg, Heidelberg, Germany
[4] Department of Chemistry and Biochemistry, Faculty of Chemistry and Chemical Technology, University of Ljubljana, Ljubljana, Slovenia

Received 27 February 2011
Accepted 11 April 2011

Correspondence to: Prof. Dr. Tamara T. Lah, National Institute of Biology, Večna pot 111, SI-1000, Slovenia. Phone: +386 59 232 703; Fax: +386 1 241 2980; E-mail: tamara.lah@nib.si

Disclosure: No potential conflicts of interest were disclosed.

Introduction. CD133 is a marker for a population of glioblastoma (GBM) and normal neural stem cells (NNSC). We aimed to reveal whether the migratory potential and differentiation of these stem cells is associated with CD133 expression and with cathepsin proteases (Cats).

Materials and methods. The invasiveness of normal NNSC, GBM/CD133+ cell lines and GBM spheroids was evaluated in 3D collagen, as well as of U87-MG and normal astrocytes (NHA) grown in monolayers in 2D Matrigel. Expression of Cats B, L and S was measured at mRNA and activity levels and their relation to invasiveness, to CD133 mRNA in 26 gliomas, and to the survival of these patients.

Results. The average yield of CD133+ cells from GBM samples was 9.6 %. Survival of patients with higher CD133 mRNA expression was significantly shorter ($p < 0.005$). Invasion, associated with proteolytic degradation of matrix, was higher in normal stem cells and GBM spheroids and cells than in isolated GBM CD133+ cells. In glioma samples, there was no correlation between CD133 mRNA expression and Cat mRNAs, but there was an inverse correlation with Cat activities.

Conclusions. The study confirms CD133 as a prognostic marker for the survival of GBM patients. We demonstrated that NNSC have higher invasion potential and invade the collagen matrix in a mode different from that of GBM, initiating stem cell spheres. This result could have implications for the design of new therapeutics, including protease inhibitors that specifically target invasive tumour stem cells. Increased activity of cathepsins in CD133– cells suggests their role in the invasive behaviour of GBM.

Key words: CD133/prominin1; cysteine cathepsins; glioblastoma; glioma stem cells; invasion; neural stem cells

Introduction

Gliomas are the most abundant brain tumours, progressing from benign astrocytomas *via* anaplastic astrocytomas to the most malignant form, glioblastoma multiformae (GBM). The poor prognosis and short life expectancy for GBM patients is partly related to the high invasiveness of the tumour cells. In contrast to carcinoma, GBM cells infiltrate the normal brain parenchyma as single cells, making this tumour extremely difficult to target by conventional therapy.[1-3] GBM is highly heterogenous, consisting of various types of cells. According to the hierarchical model of tumourigenesis, only a small fraction of tumour cells, the cancer stem cells (CSC), are capable of initiating tumour growth, and renewing the tumour in the same or other organ after incomplete surgical removal.[4-6] When injected orthotopi-

cally, these cells were phenotypically characterised as capable of self renewal, asymmetric division and tumour formation in animal models of the same growth characteristics. These cells are also highly resistant to chemo- or radio-therapy[6,7] and presumably they and/or their immediate progenitors have high invasive potential to seed at a distance from the tumour.[8]

In a selective GBM stem cell population, plasma membrane associated protein CD 133/prominin-1 is considered as a cell surface marker of stemness and has been widely used for identifying putative stem cells from a variety of untransformed and cancerous tissues. However, CD133 is also expressed in differentiated epithelial cells in various organs, as well as in hematopoietic cells.[9] From its first use for identification of cancer stem cells in brain tumours[10], CD133 is still the most commonly used brain cancer stem cell marker, despite the many contradictions regarding the methods used to detect the expression of a surface marker in brain tumours. Some studies have shown that not all high grade gliomas express CD133[11] and also, that CD133 negative cell populations from GBM may have tumour initiating potential[12], giving rise to CD133+ tumours.[13-15] The role of this marker in further steps of tumour progression is not known.

Cancer stem cells are, presumably, not only associated with high resistance to therapy but also with higher invasion and metastatic potential, as proposed by Brabletz *et al.*[8] Proteolytic enzymes, including lysosomal cathepsins, participate in many normal and pathological processes and have been associated with cancer progression, mostly with invasion.[16-19] Cysteine cathepsins B, L and S (CatB, CatL and CatS) and the aspartic cathepsin D are over-expressed in many tumour tissues and cells, and have been reported to be mediators of glioma invasion.[19-21] Cysteine cathepsins comprise the largest family of lysosomal enzymes, with 11 proteases structurally grouped in CatB-like and CatL-like enzymes (http://www.merops.ec.uk).[22] We have demonstrated the prognostic impact of CatB, but not of CatL, on survival of glioma patients.[23,24] *In vitro*, we have recently confirmed the inhibition of the invasion of permanent GBM cell lines, as well as primary GBM spheroids by synthetic CatB inhibitors, emphasizing the role of CatB activity that was induced posttranslationally in the invasive GBM subpopulation.[25]

Although the homologous enzyme, CatL, is also correlated with glioma progression[26-28], it appeared to be more relevant to proliferation and apoptosis than to the invasion process.[29] Flannery *et al.*[30] demonstrated that expression of CatS was an independent predictor of survival in GBM tumours, presumably also being related to invasion. However, the proteolytic efficacy of cysteine cathepsins is regulated at all levels of their expression, ultimately by their endogenous inhibitors, the cystatins (http://www.merops.ec.uk).[22] Cystatin superfamily comprises two different families, cystatin family (with extracellular cystatins) and stefin family (with intracellular stefins), all these playing a role in cancer progression.[17,31] A specific role for lysosomal cathepsins in stem cells biology has not been reported.

The first aim of the present study was to demonstrate CD133 mRNA expression in cancerous and normal neurospheres and GBM primary spheroids, and to assess whether there is any prognostic value of this marker for GBM patients treated with standard therapeutic protocols. Secondly, we aimed to establish whether there is any correlation between CD133 and the lysosomal cysteine cathepsins, CatB, CatL and CatS and their inhibitors stefin B and cystatin C, at various levels of expression in these tumours. Finally, we were interested in correlation between proteolysis and the invasion of a variety of CD133 expressing normal and cancerous cells under *in vitro* conditions.

Materials and methods

Glioblastoma patients

The patients were operated at the Department of Neurosurgery, University Clinical Centre of Ljubljana, Slovenia. Tumour samples were collected from 26 patients (16 male, 10 female, median age 60 years, Table 1). 24 patients were diagnosed with WHO grade IV glioblastoma and the remaining two with WHO grade III anaplastic astrocytoma by standard histopathology protocols at the Institute of Pathology, Faculty of Medicine in Ljubljana. These patients were all treated by standard protocols as shown in Table 1. The study was approved by the National Medical Ethics Committee of the Republic of Slovenia (Approval no. 109, 204-6/10/07).

Tumour samples and primary tumour culture preparation

Immediately after removal from the patients, the tumour samples were placed in sterile ice-cold "stem cell buffer" (124 mM NaCl, 5.0 mM KCl, 1.3 mM $MgCl_2$, 2.0 mM $CaCl_2$, 26 mM $NaHCO_3$,

TABLE 1. Patient characteristics, therapy and overall survival

Tumour sample			Patients		
NIB No.	histopathol. diagnosis	Gender	Age	Survival (days)	Additional therapies
AA 060726	AA	female	58	51	NAT
AA 080424	AA	female	34	*463	ChT/RT + ChT + DITEM
GBM 061017	GBM	male	57	548	ChT/RT + ChT
GBM 061123	GBM	female	68	175	ChT/RT
GBM 061206	GBM	male	80	215	NAT
GBM 070103	GBM	male	37	366	ChT/RT + ChT + BCNU
GBM 070322	GBM	female	74	84	NAT
GBM 070402	GBM	male	74	60	NAT
GBM 070904	GBM	female	70	273	ChT/RT
GBM 070912	GBM	male	58	218	ChT/RT + ChT
GBM 070926A	GBM	male	65	67	unfinished RT
GBM 070926B	GBM	female	60	271	ChT/RT
GBM 071017A	GBM	male	43	297	ChT/RT + ChT + c.pr.
GBM 071017B	GBM	male	27	284	ChT/RT + ChT
GBM 071115A	GBM	male	48	371	ChT/RT + ChT + BCNU
GBM 080107	GBM	male	68	110	palRT
GBM 080110	GBM	male	45	*568	ChT/RT + ChT + BCNU
GBM 080129	GBM	female	78	125	NAT
GBM 080512	GBM	female	72	*445	palRT
GBM 080521	GBM	male	66	131	ChT/RT + ChT + BCNU
GBM 080528	GBM	male	50	143	ChT/RT
GBM 080603	GBM	male	43	184	ChT/RT + ChT + AVA
GBM 080612	GBM	male	78	354	ChT/RT
GBM 080619	GBM	male	60	1	NAT
GBM 090909	GBM	female	50	110	palRT
GBM 090921	GBM	female	59	*394	ChT/RT + ChT + DITEM

Histopathological diagnosis of the tumours: AA- anaplastic astrocytoma (WHO grade III), GBM- glioblastoma (WHO grade IV). **Age:** age of the patients at the time of the operation in years. **Survival:** survival of the patients after the first operation in days (*- the patients were still alive at the end of data collection). **Additional therapy** (all the patients were operated, most also received additional therapies): NAT - no additional therapy used, ChT/RT- standard combination of chemotherapy (temozolomide) and radiotherapy (60 Gy), ChT- standard chemotherapy repeated, BCNU- additional chemotherapy with bis-chloronitrosourea, c.pr.- complementary medicine program, palRT- palliative radiotherapy, DITEM- dose dense chemotherapy with temozolomide, AVA- additional chemotherapy with avastin, palRT- palliative radiotherapy.

10 mM D-glucose, pH 7.35) and transferred on ice to the cell-culture laboratory within one hour post-operation. The samples were finely cut. One part of each tissue sample was processed for magnetic bioseparation and the rest used for RNA and protein sample preparation as described below. The cut tumour tissue was washed twice in 1×PBS (PAA, Austria) and resuspended in stem cell buffer with added 1.33 mg/mL trypsin, 0.67 mg/mL hyaluronidase and 0.20 mg/mL kinurenic acid (all Sigma-Aldrich, Germany). After 90 min of incubation at 35°C, 5 % CO_2, >95 % relative humidity with shaking, the samples were centrifuged for 10 min at 300×g (20°C). The supernatant was removed and the tissue resuspended in DMEM/F12 medium (PAA, Austria), supplemented with 0.7 mg/mL ovomucoid (Sigma-Aldrich). The tissue was finely dissociated with a thin glass Pasteur pipette and the tissue suspension was filtered through a 40 μm nylon mesh (BD Falcon, USA).

Isolation of CD133+ glioblastoma cells

The single-cell suspension obtained was ten fold diluted in erythrocyte lysis-buffer (155 mM NH_4Cl, 10 mM $KHCO_3$, 0.1 mM EDTA), incubated for 5 min at 20°C, and centrifuged for 10 min at 300×g (20°C). The supernatant was removed and

the cells resuspended in MACS buffer (1×PBS supplemented with 0.5 % w/v BSA and 2.0 mM EDTA, pH 7.2).

The prepared erythrocyte-free tumour cell suspension was used for direct magnetic bioseparation of CD133+ cells with miniMACS System (Miltenyi Biotec, Germany) according to the manufacturer's protocol. The cell suspension was labelled with CD133+ MicroBeads in the presence of Fc reagent (both Miltenyi Biotec) for 30 min at 4°C, then diluted in 10×V MACS buffer, centrifuged for 10 min at 300×g (20°C), and resuspended in 500 μL MACS buffer. The cell suspension was applied to a magnetic separation column in a magnetic miniMACS™ Separation Unit. The CD133 negative fraction was eluted into a centrifuge tube without applying pressure. The separation column was then removed from the magnetic unit and the CD133+ fraction retained in the column washed out by applying pressure into a separate tube. The percentage of CD133+ cells in tumour samples was calculated as the ratio of the number of cells in the CD133+ fraction to the sum of the cells in the two fractions.

The efficacy of the separation was estimated by quantitative RT-PCR for CD133 as described below. Only separations in which the expression of CD133 mRNA was significantly higher in the CD133 positive fraction than in the negative fraction (F≥1.50) were considered successful, and taken into the study.

Primary cultures of GBM biopsy

Primary cultures of unsorted cells and their CD133- cell populations from GBM samples 071017A and 071115 were prepared and grown as monolayers in DMEM/F12 medium, supplemented with 10 % foetal bovine serum, 4 mM L-glutamine, 1 % penicillin/streptomycin (all PAA) and 1M HEPES (Sigma-Aldrich). GBM spheroids were prepared from human glioblastoma biopsies as described elsewhere.[32] Tumour biopsies were finely cut, resuspended in an appropriate volume of medium and seeded on agar coated cell culture dishes in a complete cell culture medium containing DMEM High Glucose (4.5 g/l), supplemented with 10 % foetal bovine serum, 1 % penicillin/streptomycin, 4 mM L-glutamine (all PAA) and 0.4 mM NEAA (Sigma-Aldrich). When the majority of the spheres reached 200 μm, they were dissociated by addition of 0.25 % trypsin -EDTA (Invitrogen, USA). The cell suspension was centrifuged for 10 min at 300×g, 10°C. The supernatant was removed and the cells distributed to new dishes in 1:3 dilutions. These cells started to form spheres after approximately 24 h.

Normal neural stem cells (NNSC)

Neural stem cells were grown from subventricular zones of brain tissue collected *post-mortem* as described.[33] The collection and use of brain tissue was approved by the Medical Ethics Committee of the Republic of Slovenia (156/07/09). The tissue samples were finely cut, degraded by trypsin (0.13 % w/V in water, Sigma-Aldrich) for 30 min at 37°C. Degradation was then blocked by 1 % foetal bovine serum in DMEM medium (both PAA). The tissue suspension was filtered through 40 μm nylon mesh, centrifuged for 5 min at 300×g, and resuspended in 10 mL of neurobasal medium, supplemented by basic fibroblast growth factor bFGF (20 ng/mL), EGF (20 ng/mL), serum supplement B27 (all Invitrogen, USA), heparin (1U/mL; Sigma-Aldrich), 1 % penicillin/streptomycin and 4 mM L-glutamine (both PAA). NNSC were grown in the form of spheres on non-adhesive culture dishes (Sarstedt, Germany).

Established cell lines

Normal human astrocytes (NHA cells) and human glioblastoma cell line U87-MG were obtained commercially from Cambrex (USA) and American Type Culture Collection, respectively. Both cell lines were grown in monolayers in DMEM High Glucose (4.5 g/l), supplemented with 10 % foetal bovine serum, 1 % penicillin/streptomycin and 4 mM L-glutamine (all PAA). The NHA medium also contained 20 mM HEPES (Sigma-Aldrich, Germany). Cells were harvested by 0.25 % trypsin -EDTA (Invitrogen).

In addition we made use of two GBM stem-like cell cultures that were previously established at the Division of Neurosurgical Research, Heidelberg, Germany. These CD133+ GBM stem cell spheroids were grown from cells NCH644 and NCH421k, obtained as described by Campos *et al.*[34], on non-adhesive culture dishes (Sarstedt) in serum-free DMEM/F12 medium, 1 % penicillin/streptomycin and 4 mM L-glutamine (all PAA), supplemented by bFGF (20 ng/mL) and EGF (20 ng/mL) (both Invitrogen, USA), and BIT-supplement (Provitro, Germany).

All cells and spheroids were cultured under standard conditions at 37°C in humidified atmosphere with 5 % CO_2. Unless otherwise specified, plastic-ware was purchased from Corning Costar Corporation, USA.

2D invasion assay of monolayers in Boyden chambers

Cells were tested for their invasion potential in a two dimensional invasion assay as described previously.[29] Transwell chambers (Corning) with 8 μm pores were coated on the upper surface with Matrigel (0.25 mg/mL, BD Bioscience, USA) and 10^5 cells were seeded. Fibronectin and conditioned serum free medium were used as chemoatractants. After 21 h incubation, MTT (1-(4,5-dimethylthiazol-2-yl)-2,5-diphenyl tetrazolium bromide, (Sigma-Aldrich) at 0.5 mg/mL final concentration was added to each chamber. After 3 h at 37°C, the formazan crystals that formed were collected separately from the upper and lower chambers, pelleted and dissolved in dimethyl sulphoxide, and the absorbance at 570 nm (reference filter 690 nm) measured on a spectrofluorimeter (Tecan). The percentage of cells penetrating Matrigel (invasive cells) was calculated as the ratio of the number of cells in the lower compartment to the sum of cells in both compartments. Invasion was normalised to that of normal neural stem cells NNSC.

3D invasion assay of spheres

Spheroids of NNSC, CD133+GBM stem cells NCH644 and NCH421k and GBM biopsy spheroids were tested for proliferation and invasive potential as described previously.[25] Spheres (150-300 μm in diameter) were embedded in 50μL drops of type I collagen matrix (1.0 mg/mL, BD Bioscience). After incubating for 30–45 min at 37°C, the collagen was covered with cell culture medium. The spheroid diameter and cell invasion distance were measured under a light microscope using an ocular micrometer. Invasion distance was defined as the distance from the edge of the spheroid to the population of the cells most distant from the spheroid. Invasion was monitored for up to 21 days. Cell culture medium was changed every 3 days.

DQ collagen degradation

Matrix degradation is one of the important features of the invasion process. To test the ability cells and spheroids to degrade the extracellular matrix, fluorescently labelled type IV collagen (DQ collagen IV, Invitrogen) was added to a Matrigel matrix (8.5 mg/mL). The spheroids were imbedded into 50 μL drops of Matrigel with 1 % DQ collagen IV as for the 3D invasion assay, whereas the cells grown in monolayer were plated on Lab-Tek Chamber Slides (Nunc, USA) pre-coated with Matrigel mixed with 2.5 % DQ collagen IV. After 24 h incubation, the green fluorescence of degraded DQ collagen IV was observed under a Zeiss LSMS10 confocal microscope. To visualise the cells/spheroids the visual light pictures of the same areas were superimposed.

Quantitative real-time PCR

Samples were homogenized in TRIzol reagent (Invitrogen) and RNA isolated as suggested by the manufacturer. 1.0 μg of each RNA sample was reverse transcribed to cDNA using High Capacity cDNA Reverse Transcription Kit (Applied Biosystems, USA) following the manufacturer's protocol.

Quantitative real-time-PCR assays were performed on ABI Prism 7900 HT Sequence Detection System using TaqMan Universal PCR Master Mix. Human GAPDH was used as internal control (all Applied Biosystems). Forward, reverse primers and probes sequences (in this order) were as follows: for CatB: 5′-CTC TATg AAT CCC ATg Tag ggT gC-3′, 5′-CCT gTT TgT Agg TCg ggC Tg-3′ and 5′-CCC TgT gAg CAC CAC gTC AAC gg-3′; for CatL: 5′-TCA ggA ATA Cag ggA Agg gAA A-3′, 5′-TCC Tgg gCT TAC ggT TTT gA-3′ and 5′-CAC Tgg TCA TgT CTC CAA Agg CgT TCA T-3′; for StefA: 5′-ggA ggC TTA TCT gAggCC AAA-3′, 5′-CAA gCT gTg gTT TAA CCT TAT CAA CA-3′ and 5′-CCg CCA CTC CAg AAA TCC Agg AgA-3′; for StefB: 5′-gCC gAg ACC CAg CAC ATC-3, 5′-ggC CTT AAA CAC Agg gAA CTT CT-3 and 5′-ACC Agg TgA ggT CCC AgC TTg AAg AgA-3; for CysC: 5′-gAC AAC TgC CCC TTC CAT gA-3, 5′-gCA CAg CgT AAA TCT ggA AAg A-3 and 5′-CAg CCA CAT CTg AAA Agg AAA gCA TTC Tg-3. The probes were 5′-FAM 3′-TAMRA modified. For CD133 (PROM1), Hs00195682_m1 and for CatS, Hs00175403_m1 TaqMan Gene Expression Assays (both Applied Biosystems) were used.

Due to the low expression of the CD133 mRNA, the pre-amplification step was performed before quantitative RT-PCR using the PreAmp Master Mix (Applied Biosystems) as suggested by the manufacturer.

mRNA data were calculated as $2^{-\Delta\Delta Ct}$ values. Fold differences in mRNA expression levels (F) between CD133+ and CD133- populations were calculated as in Demuth *et al.*[35], where $F = 2^{(\Delta CtCD133+ - \Delta CtCD133-)}$ and $Ct_{CD133+} = Ct_{GAPDH} - Ct_{target\ gene}$ in the CD133+ cell population, and $Ct_{CD133-} = Ct_{GAPDH} - Ct_{target\ gene}$ in the CD133- cell population. $F \geq 1.50$ is considered as significantly higher and $F \leq 0.75$ lower expression of the selected gene in CD133+ cells. F values be-

tween 1.50 and 0.75 are regarded as non-significant differences.

Protein extraction and enzyme activity assays

Cells, grown in spheres were homogenized by sonication for 2 min in 50 mM Tris buffer, pH 6.9, supplemented with 0.05 % (V/V) Brij 35, 0.5 mM dithiothreitol, 5 mM EDTA, 0.5 mM paramethylsulphonyl fluoride and 10 mM pepstatin A (all Sigma-Aldrich). The homogenates were centrifuged for 30 min at 12.000×g (4°C) and the supernatants stored at -80°C until used.

CatB and CatL activities were measured as described previously.[25] Duplicates of water diluted protein samples were supplemented with activation buffer (0.4 M phosphate buffer pH 6.0, 2.5 mM fresh ditiothreitol for CatB; 0.34 M acetate buffer, pH 4.2, 2.0 mM fresh DTE for CatL; all Sigma-Aldrich) and incubated for 30 min at 37°C. To measure specific cathepsin activity, water was added to one of the duplicates and specific inhibitor (60μM Ca-074, Peptide Institute, Japan, for CatB; 2μM Clik 148, provided by N. Katunuma, Tokushima Bunri University, Tokyo, Japan, for CatL) to the other. Activity buffer (0.4 M phosphate buffer pH 6.0, 2.5 mM fresh DTE for CatB; 0.34 M acetate buffer pH 5.5, fresh 2.5 mM DTE for CatL; all Sigma-Aldrich) was then added and the reaction started by adding specific substrate (100 μM Z-RR-AMC for CatB, 100 μM Z-FR-AMC for CatL; both Bachem, Switzerland). After 90 min at 37°C the reaction was stopped with 1 mM iodoacetic acid and the released 7-AMC measured on a spectrofluorimeter (Tecan). Specific cathepsin activity was calculated as the difference in 7-AMC release in the presence and the absence of the specific cathepsin inhibitor.

CatS activity was measured as described by Flannery *et al*.[30] Water diluted protein samples were supplemented with inactivation buffer (100 mM phosphate buffer, pH 7.5) for 60 min at 37°C to fully inactivate CatB and CatL. The pH was then returned to 6.0 using 500 mM MES buffer. Reaction buffer (200 mM MES, 200 mM EDTA, pH 6.0, fresh 1 mM DTT, all Sigma-Aldrich) was added and the reaction started by adding specific substrate (100μM Z-VVR-AMC, Peptide Institute). After 90 min at 37°C the reaction was stopped with 100 mM acetate buffer, pH 4.3 and the released 7-AMC measured on a spectrofluorimeter.

Each activity assay was performed in triplicate, with controls with omitting the sample. Specific activities were expressed in enzyme units (E.U.) per mg of total protein, with one E.U. being the amount of the enzyme releasing 1 nm of 7-AMC per minute.

Statistical analysis

All statistical analysis was performed with Excel 2002 (Microsoft Corp., USA) and Prism 5.01 (GraphPad Software Inc., USA). The statistical significances of the differences observed were calculated as standard t-test with assumed two-tailed distribution and unequal variance. For correlation studies, Spearman's nonparametric method was used. Prognostic impact of CD133 expression for patient survival was calculated by relating it to overall survival by the Kaplan-Meier univariate analysis. To assess the association between survival period (from initial operation of the tumour to death of the patient) and other variables the Gehan-Breslow-Wilcoxon test was used.

Results

Prognostic value of CD133 mRNA in human GBM

Patient characteristics and survival after the operation are summarised in Table 1. 24 patients were diagnosed with WHO grade IV glioblastoma. In 19 of these, CD133+ mRNA expression in GBM tumour samples was compared with overall survival to assess the prognostic impact of CD133 mRNA (Figure 1). Survival of patients with higher CD133 mRNA levels ($2^{-\Delta\Delta Ct}$ > 30.000) was significantly shorter (median 81 days) than that of patients with lower CD133 mRNA levels (median 284 days, p 0.005).

Separation of CD133+ and CD133- cell populations from GBM samples

The cell suspensions prepared from GBM samples were subjected to direct magnetic bioseparation. In 15 samples the separation was successful, based on the difference in the CD133 mRNA expression being at least 1.5 time higher (F≥1.50) in the CD133+ than in the $CD133^-$ fraction (see Materials & Methods). Only such samples were included in the further analysis. The abundance of the CD133+ cell fractions ranged from 2.0 % to 38.8 % of atotal cell population in individual tumour samples with an average of 9.6 ± 9.5 %.

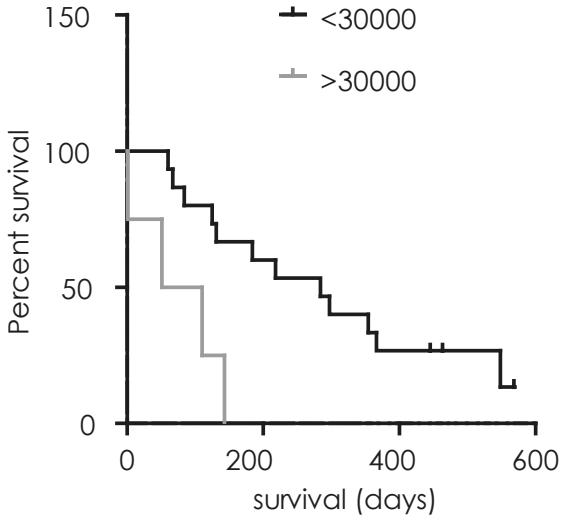

FIGURE 1. Prognostic impact of CD133 mRNA level on survival of the patients. CD133 mRNA expression was measured by QRT PCR in glioma samples of 19 patients and compared to their survival time post-operation. Survival of patients with higher CD133 mRNA levels above a cut-off of 30 000 (—, $2^{-\Delta\Delta Ct}$ > 30.000) was significantly shorter (median 81 days) than survival of patients with CD133 mRNA levels below the cut off (—, $2^{-\Delta\Delta Ct}$ < 30.000; median 284 days, p = 0.005).

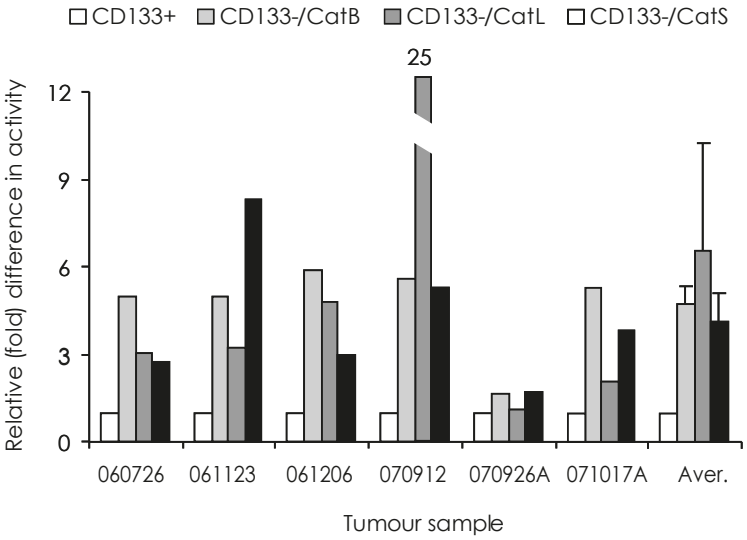

FIGURE 2. Differences in cathepsins' activities in CD133+ and CD133- cell fractions. In each of the six GBM samples, a relative activity of 1 was assigned to all the CD133+ cell fractions (white bars). Fold differences in activity of cathepsins between CD133- and CD133+ cell fractions were calculated as described in Material and Methods. CatB activity (light grey bars) was 1.7-5.9 times (average 3.9) higher, CatL activity (dark grey bars) 1.1-25 times (average 2.6) higher and CatS activity (black bars) 1.7-8.3 times (average 3.2) higher in the CD133- cell fractions than in CD133+ fractions.

Comparison of CD133 with other tumour markers at mRNA levels

In mRNA extracts of CD133+ vs CD133- cells from 13 GBM patients we also compared the expression of other genes characteristics of neural and glioma cancer stem cells and their progenitors, such as nestin, and the markers for more differentiated cells, such as glial fibrillar acidic protein (GFAP) indicating astrocyte lineage differentiation, and β-tubulin 3 (β-TUB 3), the marker of neural differentiation. Table 2A shows that there was no correlation of their expression with CD133 within the group of samples.

Comparison of CD133 with cathepsin expression at the mRNA level

In mRNA extracts of CD133+ vs CD133- cell fractions from 13 GBM patients we also measured mRNA levels of CatB, CatL, CatS, StefA, StefB and CysC (Table 2B). There was no significant correlation between these values. However, we observed that, in more than half the samples, the ratios of expression of CD133+ to CD133- are lower (F≤1) in the three cathepsins. A similar trend was observed for the stefins, but an opposite one for cystatin C, for which increased levels in CD133+ samples were observed. This indicates that expression of the cathepsins increases with differentiation of CD133+ stem cells into the mature GBM cells.

Cathepsin activity in CD133+ and CD133- cell populations

In 6 tumour samples sufficient cellular material was obtained from the successful separation of CD133+ and CD133- cell fractions to assay cathepsin activities. In all the samples, CD133+ cell fractions contained significantly lower CatB, CatL and CatS activities than the CD133- cell fractions (Figure 2).

In parallel to their mRNA expression, the activities of CatB and CatL were higher, by 25 % and 37 %, in the spheroids of NNSC than in GBM stem cells NCH644.

Relative expression of cathepsins and CD133 in various cell lines *in vitro*

Due to the very high variability of CD133 mRNA measurements, the difference between its concentrations in the spheroids of NNSC and NCH644 cells was not significant. In primary cell cultures of two GBM samples, CD133 mRNA expression was similar in unsorted GBM cell populations, but below the limit of detection in CD133- cells remaining after CD133+ cell separation (Figure 3A).

CatB and CatL mRNA expression are presented in Figure 3B. NNSC expressed 7-fold and 18-fold

higher levels of CatB and CatL than the GBM stem cells NCH644. The expression of Cats B and L in primary GBM samples was similar to or nonsignificantly higher than that in NNSC. However, there was no consistent difference in cathepsin expression in unsorted GBM and CD133- cells from the same GBM samples.

Invasion assays

2D invasion assay

Normal NNSC and NHA cells and the GBM cells NCH644 and U87-MG, unsorted, and their respective CD133- cell populations from GBM samples, were tested for invasive potential in a two dimensional (Boyden chamber) invasion assay. The results were normalised to the invasiveness of NNSC (Figure 3C). Unsorted GBM cells were always more invasive than the CD133- cell population from the same tumour. Interestingly, NNSC exhibited higher invasive potential than the GBM stem cells CD133+ NCH644, and NHA appeared to be more invasive than the malignant U87-MG cells, although the differences were not significant. These data correlate approximately with the expression of Cats B and L (Figure 3B).

3D invasion assay in collagen type I

The invasion and proliferation of the spheroids of NNSC, GBM stem cells and GBM biopsy spheroids were monitored in a 3D assay (Figure 4). The mode of invasion of NNSC spheres differed from that of the GBM stem cells. The average invasion distance after 21 days in collagen was 1359±216 μm for spheres of NNSC and 253±95 μm for spheres of GBM stem cells (Figure 4A). The NNSC proliferate slowly, with the size of their spheroids decreasing slightly throughout the experiment (from 170±26 μm to 153±27 μm, Figures 4B and C). In contrast, the spheroids of GBM stem cells NCH644 and NCH421k all grew in size from about 200 μm to an average of 598±340 μm (Figure 4B and D). The high S.D. was due to the variation observed among individual spheroids; about half of them grew to a diameter of over 800 μm in 21 days, whereas the others appeared to proliferate only in the first week of the experiment. The invasiveness of GBM biopsy spheroids appeared very limited; only a few cells invaded the surrounding collagen matrix, and we observed almost no change in spheroid size (Figure 4E). Due to adhesive interactions, GBM spheroids, containing a heterogeneous cell popula-

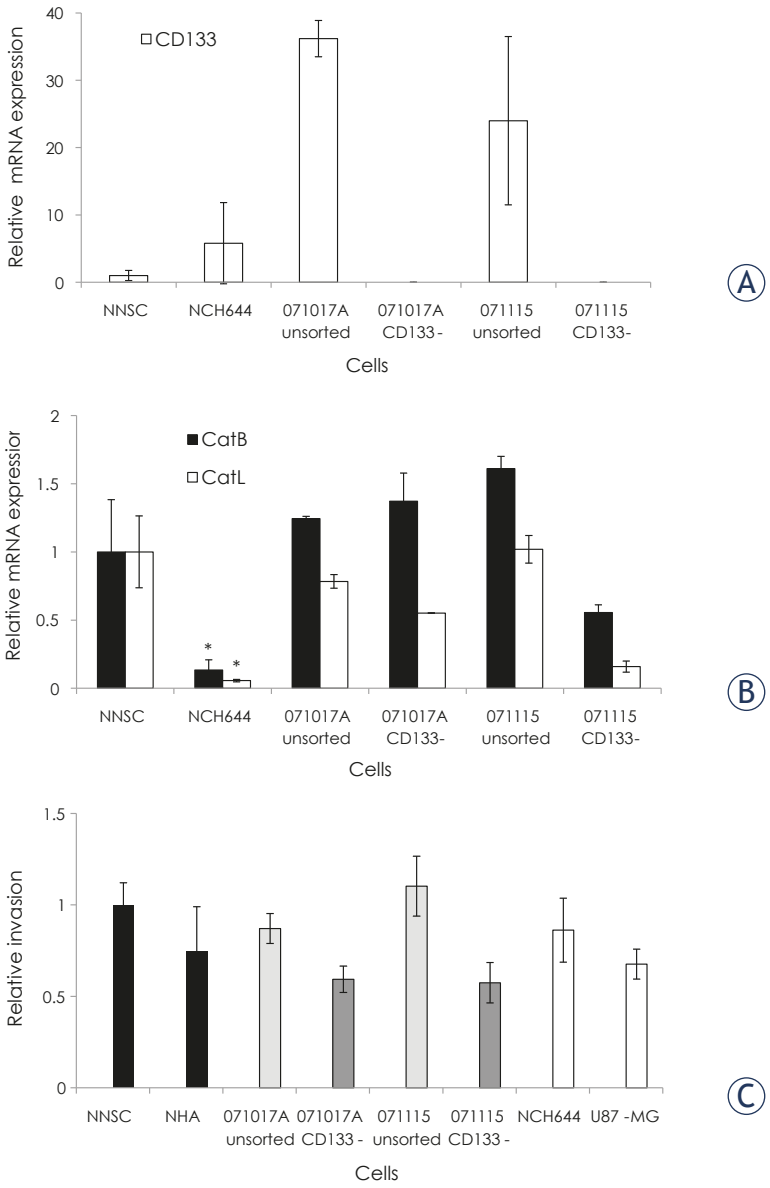

FIGURE 3. Correlation between expression of cathepsins and 2D invasion in Matrigel. CD133 mRNA expression *in vitro*. CD133 mRNA expression was determined by QRT PCR in NNSC and NCH644 spheroids, and in unsorted GBM samples and in CD133- fractions from same GBM samples. A relative mRNA expression of 1 was assigned to NNSC. Cancer stem cells NCH644 cells were positive for CD133, however CD133 expression in (unsorted) GBM neurospheres was significantly higher (Student *t*-test, $p<0.05$) in spite of high variability between the three independent cell cultures, whereas in CD133- fractions from the same tumours, CD133 mRNA was below the detection limit. **Cathepsin B and Cathepsin L mRNA expression *in vitro*.** Cathepsin B and Cathepsin L mRNA expression was determined by QRT PCR in NNSC and NCH644 spheroids, and unsorted GBM samples and CD133- fractions from the same GBM samples. Relative mRNA expressions of 1 were assigned to NNSC. Cancer stem cells NCH644 cells expressed CatB and CatL at a significantly lower level than the NNSC (Student *t*-test, $p<0.05$). **Two dimensional cell invasion.** Two dimensional cell invasion of NNSC, NHA, unsorted GBM cells and CD133- GBM cell populations, NCH644 and U87-MG cells, into Matrigel was carried out as described in Material and Methods. The percentage of invasive cells in NNSC was adjusted to 1 and other values were expressed as invasion relative to NNSC cells. The high variability in three independent experiments is reflected by relatively high inter assay S.D. values, whereas within each experiment the S.D. was always less than 10 %.

TABLE 2. A: Correlation between CD133 and other differentiation markers

Tumour Samples (n=13)	F			
	CD133	nestin	GFAP	TUB3
GBM 061123	**3,19**	1,46	**0,66**	**1,66**
GBM 061206	**32,9**	**2,27**	**2,48**	0,92
GBM 070103	**2,65**	**2,03**	**1,53**	1,36
GBM 070402	**3,43**	**0,65**	**0,20**	0,98
GBM 070904	**6,82**	**0,59**	1,22	**0,46**
GBM 070912	4,85	2,80	3,21	0,69
GBM 070926A	**2,34**	1,09	1,36	1,08
GBM 070926B	**1,66**	**0,70**	**0,68**	1,13
GBM 071017A	**3,67**	1,02	**2,02**	1,42
GBM 071017B	5,14	5,72	3,48	2,05
GBM 071115A	**5,55**	**2,18**	**4,74**	0,91
GBM 080110	**5,60**	0,94	**1,98**	**0,12**
GBM 080512	**2,11**	**1,99**	1,46	0,80

tion, were less invasive than established cultured cells. Taken together, these data show that cell proliferation is higher in cancerous cells, and that invasion and proliferation appear to be inversely correlated.

DQ collagen degradation

The ability of NNSC, GBM stem cells, GBM biopsy spheroids, and the permanent cell lines U87-MG and NHA to degrade the extracellular matrix was demonstrated by breakdown of DQ collagen, monitored by green fluorescence (Figure 5). In spheroids of NNSC, green fluorescence, indicating matrix degradation, was dispersed radially from the sphere centre, most propably along the migration paths of the cells leaving the sphere (Figure 5A). In spheroids of CD133+ GBM stem cells, the cells had not migrated from the sphere after 24 hours, and matrix degradation was localized to small areas on the surface of the sphere (Figure 5B). In GBM biopsy spheroids, the green fluorescence was dispersed over the whole surface of the spheroid (Figure 5C). When grown in monolayers, fluorescence was less intense and more dispersed in GBM cells U87-MG (Figure 5D) than in the normal human astrocytes NHA (Figure 5E). This shows that, in spite of significantly different patterns and rates of invasion between normal and cancer SC and between more differentiated normal and cancer cells, the process involves proteolysis. This may be more extracellular in normal neural cell spheroids and to a larger extent intracellular in tumour cells at the GBM spheroid surface.

Discussion

Transmembrane protein CD133, alone or in combination with other markers, is the most common marker of stem cells in glioma. In this study, CD133+ cells were isolated from the most malig-

TABLE 2. B: Correlation between CD133 and expression of cathepsins and stefins

Tumour Samples (n=13)	F						
	CD133	CatB	CatL	CatS	StefA	StefB	CysC
GBM 061123	3,19	0,40	0,13	0,20	**0,09**	**0,61**	1,33
GBM 061206	**32,9**	**1,60**	**2,50**	**3,87**	**1,73**	1,35	1,28
GBM 070103	**2,65**	0,88	0,92	1,00	0,76	**0,69**	**0,68**
GBM 070402	**3,43**	1,14	**0,73**	**0,43**	1,09	**0,71**	**0,44**
GBM 070904	**6,82**	**0,15**	**0,18**	**0,03**	*	**0,45**	*
GBM 070912	4,85	0,11	0,14	0,08	**0,06**	**0,32**	0,90
GBM 070926A	**2,34**	1,03	0,76	**0,74**	**0,70**	0,86	0,92
GBM 070926B	**1,66**	1,39	1,16	0,99	1,24	0,93	1,26
GBM 071017A	3,67	0,61	0,33	0,10	0,08	0,51	1,57
GBM 071017B	**5,14**	**4,50**	**3,09**	**2,32**	1,38	**2,28**	**3,29**
GBM 071115A	**5,55**	**0,32**	**0,42**	**0,28**	*	0,85	*
GBM 080110	**5,60**	1,14	**0,61**	**0,45**	**0,31**	0,90	**2,87**
GBM 080512	**2,11**	**0,36**	**0,67**	**1,81**	**0,41**	1,30	0,78

The relation factor F represents the ratio of the expression of mRNA of the CD133/prominin 1 to that of other markers in a and to cathepsins B, L and S and stefins A and B in b in CD133 positive and negative cells. The cells were separated from primary GBM by magnetic separation, as described in Material and methods. All significantly altered values are in bold: F ≥1.50 means significantly higher levels of expression in $CD133^+$ cells, F≤0.75 means signficantly lower expression in $CD133^+$ cells. (*) means that the levels were below the limit of detection.

nant brain tumour glioblastoma (GBM). As in other studies[36,37], rather variable amounts of these cells were obtained, ranging from 2 % to 38 %. Further, we confirmed that the survival of GBM patients with higher CD133 mRNA expression was significantly shorter than in those with lower CD133 levels. Zeppernick *et al*.[38] also found that both the proportion of CD133+ cells and their topological organization using immunohistochemitry (IHC), were prognostic factors for adverse, progression-free survival and that the proportion of CD133+ cells was an independent risk factor for GBM re-growth. In a prospective study of GBM patients, it was demonstrated that CD133+/Ki67+ was a considerable prognostic factor of disease progression and poor clinical outcome.[39] High CD133 expression in high-grade oligodendroglial tumours was reported to indicate shorter survival and to be more

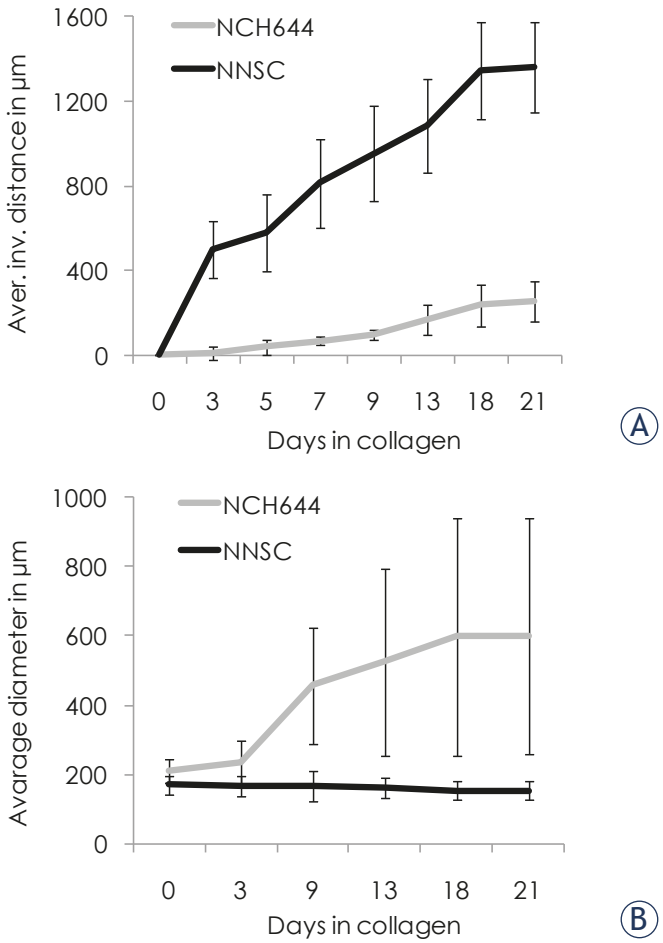

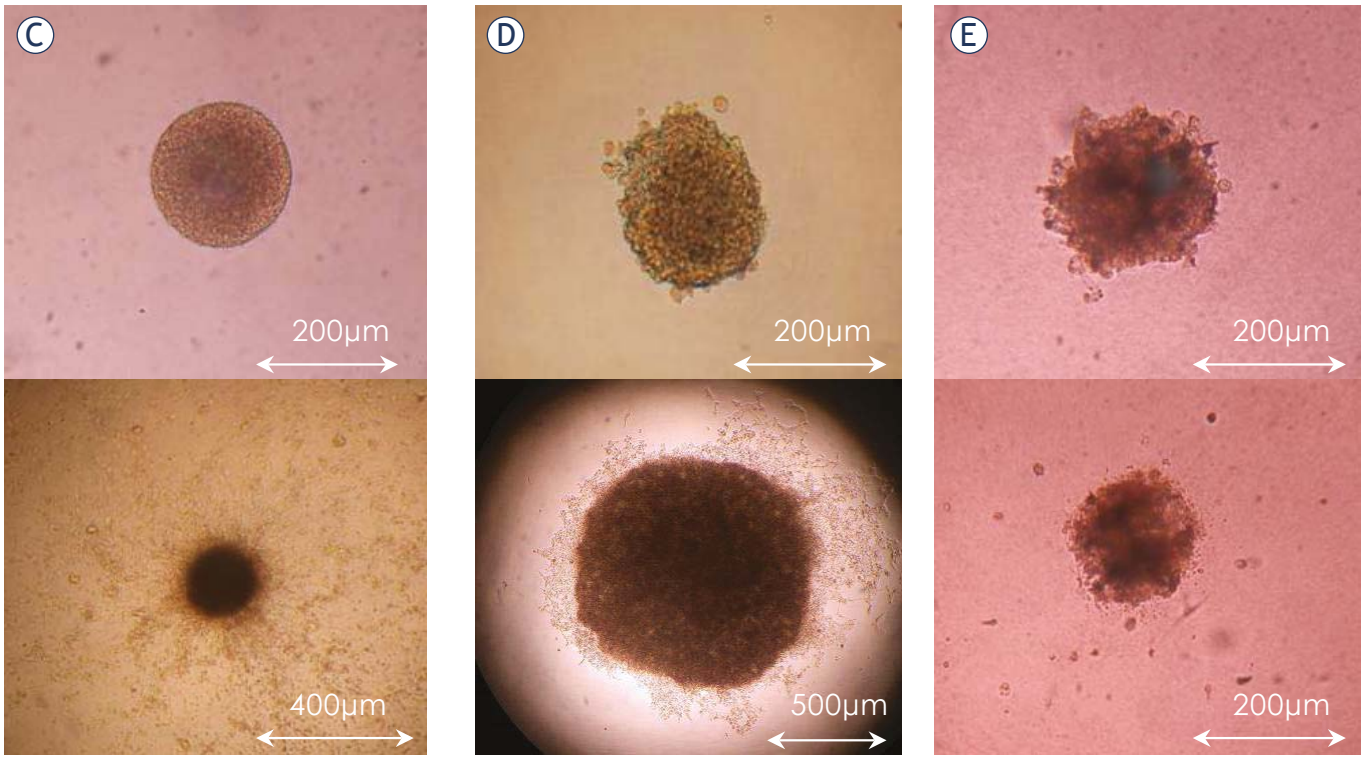

FIGURE 4. 3D spheroid invasion assay. Spheroids were imbedded into collagen I and the invasion distance (panel A) and diameter (panel B) measured under the light microscope for up to 21 days. The average invasion distance was significantly higher ($p<0.05$) for spheres of NNSC than for spheres of NCH644. The average spheroid size did not change significantly in NNSC, but increased ($p=0.009$) in spheres of GBM stem cells, NCH644. GBM biopsy spheroids did not change in size and very few cells invaded the surrounding collagen. Panels C, D and E show the spheroids of NNCS, NCH644 cells and GBM spheroid, respectively at the start (upper panel) and after 21 days (lower panel) of the experiment.

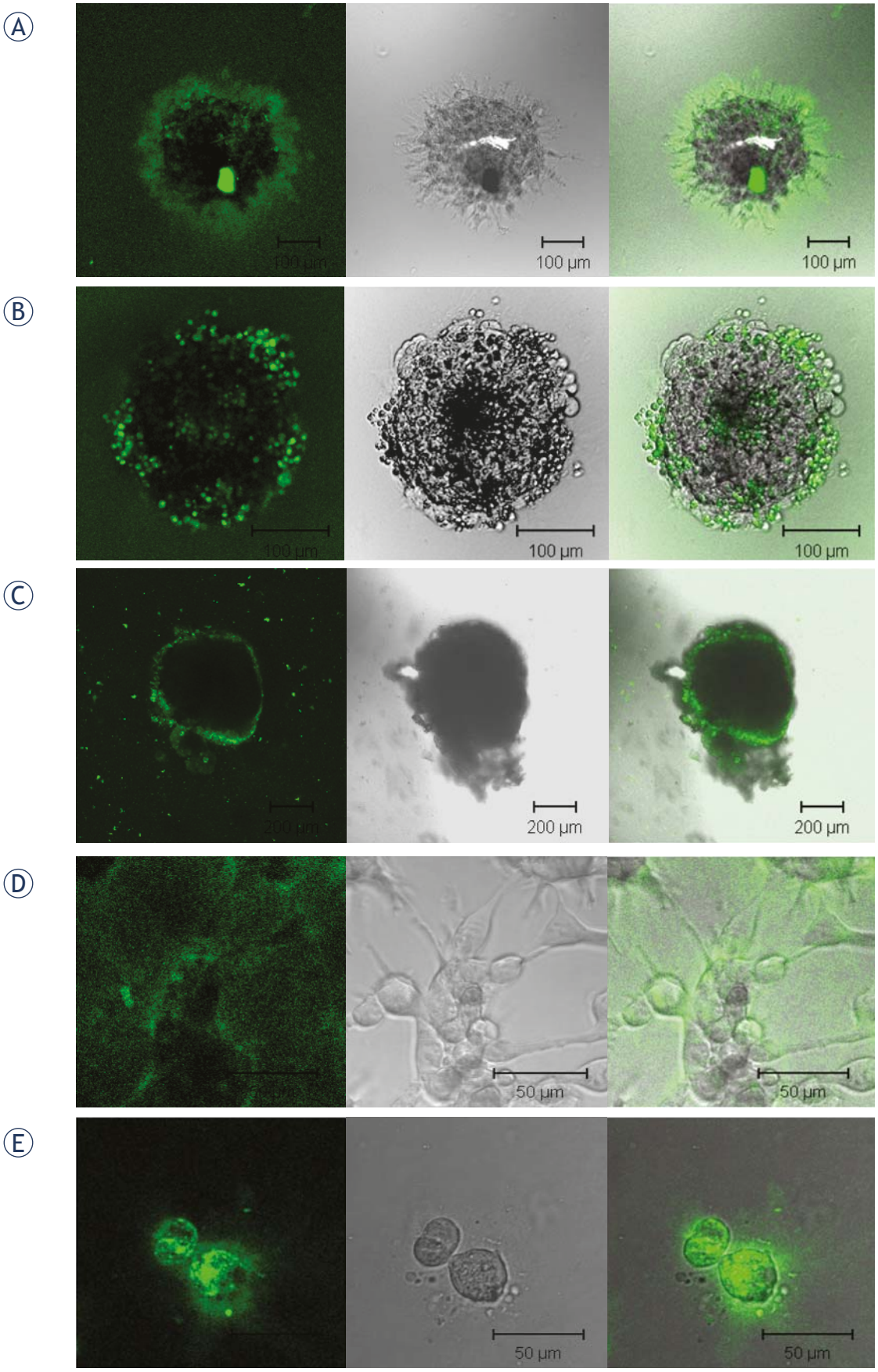

FIGURE 5. Matrix (DQ collagen) degradation by neurospheres and cells grown in monolayers. 1 % (for neurospheres) and 2.5 % (for the permanent cell lines grown in monolayers) DQ collagen type IV was added to Matrigel and matrix degradation observed after 24 h. Left: green fluorescence of degraded DQ collagen under Zeiss LSMS10 confocal microscope. Middle: visual light images of the same areas. Right: green fluorescence and visual light images combined. A: Spheroid of normal neural stem cells NNSC, B: Spheroid of GBM stem cells NCH644, C: GBM spheroid, D: U87-MG cells and E: NHA cells.

reliable than histological assessment.[13] Although it was postulated that CD133 could not be evaluated so accurately by real-time PCR[40] as by IHC, in our hands mRNA CD133 levels had a prognostic impact similar to that of CD133 protein expression in the above studies. We believe that the reliability was due to inclusion of a pre-amplification step in cell mRNA analysis because of the low levels of CD133 transcript.

Comparing CD133 expression with other differentiation markers and markers of lysosomal proteolysis in CD133+ cells, such as nestin and CatB, no correlation in the cohort of 13 GBM patients was found. In our previous studies nestin and Cat B correlated and were both highly prognostic, as proven by IHC[23,41] and mRNA analysis.[24] This indicates, therefore, that CD133 is a prognostic factor independent of nestin and cathepsins, indicating its specific biological impact on survival.

It has been postulated that cancer stem cells can develop a migratory phenotype and are responsible for the metastatic potential of tumours, such as colon carcinoma.[8] In this study we questioned whether CD133+ stem cells are also responsible for the high invasiveness of GBM. Two dimensional (2D) invasion assays showed that the invasion of various normal and cancerous cells was not correlated to their expression of CD133. Being aware of the limits of 2D invasion assay[25,42], we also monitored invasion distance and sphere diameter in a three dimensional (3D) invasion assay on spheres of NNSC, NCH644, NCH421k and GBM biopsy spheroids. Normal neurospheres were undoubtedly more invasive than the spheres of GBM stem cells. However, the latter were more proliferative, since the sphere diameter tripled within the first week of experiment, while it was shrinking in the spheres of NNSC. GBM spheroids also showed a more limited invasive potential than U87-GM spheroids[25], most probably due to the heterogeneous cell population within tumour samples, with higher intercellular adhesion. In our hands, we found higher migratory potential of normal than cancerous spheroids and this was inversely related to CD133 expression, suggesting that its expression does not play a role in cell invasion.

However, according to a current hypothesis[15], only tumour stem cells (also called tumour initiating cells) are capable of tumour renewal, therefore they must acquire migratory properties. Migratory stem cells were clearly visualised in the 3D assays and these cells may represent the invasive malignant GBM cell phenotype. However, there was no evidence that the migratory cell subpopulation of CD133+ cell and GBM biopsy spheroids still expressed this marker. High plasticity of GBM tumour initiating (stem) cells with respect to CD133 expression was suggested, as not only CD133+[11,38,43] but also CD133- spheroids[15,32] were tumorigenic in animals. On the other hand, U87 cells which, when treated with neural stem cell medium, altered their phenotype towards more stem like cells, increasing the levels of CD133 and nestin, and induced highly infiltrative tumours in animals.[44] A model has been proposed in which $CD133^+$ cells constitute a non-invading GBM SC population with the potential to switch reversibly between an invasive and stationary phenotype. This involves an epithelial to mesenchymal transition, followed by a mesenchymal to epithelial transition when seeded to the secondary site.[8] This transition, associated with reversible loss and gain of CD133 marker and possibly associated with a set of migratory proteins like Cats (B, S), is an attractive hypothesis that could explain our results.

Here we have demonstrated for the first time that radial cellular migration from the spheres is accompanied by proteolysis of DQ collagen. Invasion of the cells was therefore associated with the activation of proteases required for matrix degradation. Presumably, cathepsins are involved in the initial steps of a proteolytic cascade[45], leading to pericellular proteolysis, although alternative pathways of migration and interplay of proteases and inhibitors are possible.[18,46,47] In high grade tumours higher expression of Cats B and S has been mostly linked to tumour invasion.[18,19,22,30,48] We recently reported higher levels of all three Cats in invading than in non-invading cells separated from collagen embedded U87-MG spheroids, however only increased activation of CatB contributed to higher invasion.[25] Here, significantly higher Cats levels were observed in the more migratory NNSC than in GBM NCH644 cells at mRNA levels. Normal neurospheres appear to migrate by extracellular dissolution of collagen matrix, whereas its degradation is to a greater extent intracellular within tumour cells, as suggested also for other tumor cells previously[49] when compared with normal neural cells. This suggests that different modes of invasion may be associated with the different proteolysis pathways activated in normal and tumour cell migration.[46]

Inverse correlation of CD133 with invasion (Figure 3) corresponds to our clinical data, where we showed no correlation of Cat mRNA levels with CD133 and lower Cat activity in CD133+ cell fractions from GBM tumours. Cat activation in CD133- cells may be explained by their up-regulation and/

or the downregulation of their inhibitors, such as cystatin C and/or stefins (A and B)[48], during the process of GBM stem cell differentiation. Similarly, CatB was reported to be upregulated after the differentiation of monocytes into tissue macrophages, but not earlier in hematopoetic differentiation[49] and CatL expression was upregulated during angiogenesis from endothelial progenitor cells.[50] These results suggest that GBM stem cells are not as invasive as their progenitors, losing CD133 and acquiring migratory properties by activation of a set of proteolytic enzymes, including Cats.

In conclusion, this study confirms that CD133 is a prognostic marker for survival of GBM patients. We have demonstrated that NNSC have higher invasion potential and invade the collagen matrix in a mode which differs from that of GBM initiating stem spheres. This result could have implications for designing new therapeutics, including protease inhibitors that may be specifically delivered by novel technologies, developing for drug delivery, to target invasive tumour stem cells. Increased expression of cathepsin activities in CD133 negative cells suggests their role in the invasive GBM stem cell progenitors.

Acknowledgements

The authors thank Dr. Maria Beatriz Duran Alonso for scientific and technical contributions to this work; Prof. Dr. Nobuhiko Katunuma, Japan, for providing CLIK-148; Prim. Dr. Jasna Šinkovec, Gynecology Clinic, University Medical Centre Ljubljana and Dr. Uroš Rajčević, National Institute of Biology, for samples of NNSC; Prof. Dr. Janko Kos, Faculty of Pharmacy, UL, Ljubljana, for the polyclonal and monoclonal antibodies for cathepsins, stefins and cystatin C; Dr. Marko Kreft, Medical Faculty, Ljubljana, for his help with confocal microscopy, and Dr. Roger Pain, UK-Slovenia, for critical reading of the manuscript. The project was supported by the Slovenian Research Agency Programme P1-0245 (granted to T.L.).

References

1. Louis DN, Ohgaki H, Wiestler OD, Cavenee WK, Burger PC, Jouvet A, et al. The 2007 WHO classification of tumours of the central nervous system. *Acta Neuropathol* 2007; **114:** 97-109.
2. Pilkington GJ. Cancer stem cells in the mammalian central nervous system. *Cell Prolif* 2005; **38:** 423-33.
3. Baur M, Preusser M, Piribauer M, Elandt K, Hassler M, Hudec M. Frequent MGMT (0(6)-methylguanine-DNA methyltransferase) hypermethylation in long-term survivors of glioblastoma: a single institution experience. *Radiol Oncol* 2010; **44: 113-20.**
4. Reya T, Morrison SJ, Clarke MF, Weissman IL. Stem cells, cancer, and cancer stem cells. *Nature* 2001; **414:** 105-11.
5. Bjerkvig R, Tysnes BB, Aboody KS, Najbauer J, Terzis AJ. Opinion: the origin of the cancer stem cell: current controversies and new insights. *Nat Rev Cancer* 2005; **5:** 899-904.
6. Huse JT, Holland EC. Targeting brain cancer: advances in the molecular pathology of malignant glioma and medulloblastoma. *Nature Rev Cancer* 2010; **10:** 319- 31.
7. Bao S, Wu Q, McLendon RE, Hao Y, Shi Q, Hjelmeland AB, et al. Glioma stem cells promote radioresistance by preferential activation of the DNA damage response. *Nature* 2006; **444:** 756-9.
8. Brabletz T, Jung A, Spaderna SW, Hlubek F, Kirchner T. Migrating cancer stem cells - an integrated concept of malignant tumour progression. *Nat Rev Cancer* 2005; **5:** 744-9.
9. Cheng JX, Liu BL, Zhang X. How powerful is CD133 as a cancer stem cell marker in brain tumors? *Cancer Treat Rev* 2009; **35:** 403-8.
10. Singh SK, Clarke ID, Terasaki M, Bonn VE, Hawkins C, Squire J, et al. Identification of a cancer stem cell in human brain tumors. *Cancer Res* 2003; **63:** 5821-8.
11. Das S, Srikanth M, Kessler JA. Cancer stem cells and glioma. *Nat Clin Pract Neurol* 2008; **4:** 427-35.
12. Joo KM, Kim SY, Jin X, Song SY, Kong DS, Lee JI, et al. Clinical and biological implications of CD133-positive and CD133-negative cells in glioblastomas. *Lab Invest* 2008; **88:** 808-15.
13. Beier D, Hau P, Proeschold M, Lohmeier A, Wischhusen J, Oefner PJ, et al. CD133+ and CD133- glioblastoma-derived cancer stem cells show differential growth characteristics and molecular profiles. *Cancer Res* 2007; **67:** 4010-5.
14. Wang J, Sakariassen PØ, Tsinkalovsky O, Immervoll H, Bøe SO, Svendsen A, et al. CD133 negative glioma cells form tumors in nude rats and give rise to CD133 positive cells. *Int J Cancer* 2008; **122:** 761-8.
15. Prestegarden L, Svendsen A, Wang J, Sleire L, Skaftnesmo KO, Bjerkvig R, et al. Glioma cell populations grouped by different cell type markers drive brain tumor growth. *Cancer Res* 2010; **70:** 4274-9.
16. Koblinski JE, Ahram M, Sloane BF. Unraveling the role of proteases in cancer. *Clin Chim Acta* 2000; **291:** 113-35.
17. Lah TT, Durán Alonso MB, Van Noorden CJ. Antiprotease therapy in cancer: hot or not? *Expert Opin Biol Ther* 2006; **6:** 257-79.
18. Gocheva V, Joyce JA. Cysteine cathepsins and the cutting edge of cancer invasion. *Cell Cycle* 2007; **6:** 60-4.
19. Levicar N, Nutall RK. Lah TT. Proteases in brain tumour progression. *Acta Neurochir* 2003; **145:** 825-38.
20. Vranic A. Antigen expression on recurrent meningioma cells. *Radiol Oncol* 2010; **44:** 107-12.
21. Lah T, Obermajer N, Duran-Alonso MB, Kos J. Cysteine cathepsins and cystatins as cancer biomarkers. In: Edwards DR, editor. *The cancer degradome: proteases and cancer biology*. New York: Springer; 2008. p. 585-23.
22. http://www.merops.ec.uk
23. Strojnik T, Kavalar R, Trinkaus M, Lah TT. Cathepsin L in glioma progression: comparison with cathepsin B. *Cancer Detect Prev* 2005; **29:** 448-55.
24. Colin C, Voutsinos-Porche B, Nanni I, Fina F, Metellus PH, Intagliata D, et al. High expression of cathepsin B and plasminogen activator inhibitor type-1 are strong predictors of survival in glioblastomas. *Acta Neuropathol* 2009; **118:** 745-54.
25. Gole B, Durán Alonso MB, Dolenc V, Lah TT. Post-translational regulation of cathepsin B, but not other cysteine cathepsins, contributes to increase glioblastoma cell invasion in vitro. *Pathol Oncol Res* 2009; 15: 711-23.
26. Sivaparvathi M, Yamamoto M, Nicolson GL, Gokaslan ZL, Fuller GN, Liotta LA, et al. Expression and immunohistochemical localization of cathepsin L during the progression of human gliomas. *Clin Exp Metastasis* 1996; 14: 27-34.

27. Lah TT, Strojnik T, Levicar N, Bervar A, Zajc I, Pilkington G, et al. Clinical and experimental studies of cysteine cathepsins and their inhibitors in human brain tumors. *Int J Biol Markers* 2000; **15:** 90-3.

28. Levičar N, Dewey RA, Daley E, Bates TE, Davies D, Kos J, et al. Selective suppression of cathepsin L by antisense cDNA impairs human brain tumor cell invasion in vitro and promotes apoptosis. *Cancer Gene Ther* 2003; **10:** 141-51.

29. Zajc I, Hreljac I, Lah T. Cathepsin L affects apoptosis of glioblastoma cells: a potential implication in the design of cancer therapeutics. *Anticancer Res* 2006; **26:** 3357-64.

30. Flannery T, McQuaid S, McGoohan C, McConnell RS, McGregor G, Mirakhur M, et al. Cathepsin S expression: An independent prognostic factor in glioblastoma tumours-A pilot study. *Int J Cancer* 2006; **119:** 854-60.

31. Kos J, Lah TT. Cystatins in cancer. In: Žerovnik E, Kopitar-Jerala N (eds). *Human Stefins and Cystatins*. New York: Nova Science Publishers Inc; 2006. p. 152-65.

32. Sakariassen PØ, Prestegarden L, Wang J, Skaftnesmo KO, Mahesparan R, Molthoff C, et al. Angiogenesis-independent tumor growth mediated by stem-like cancer cells. *Proc Natl Acad Sci USA* 2006; **103:** 16466-71.

33. Palmer TD, Schwartz PH, Taupin P, Kaspar B, Stein SA, Gage FH. Progenitor cells from human brain after death. *Nature* 2001; 411: 42-3.

34. Campos B, Wan F, Farhadi M, Ernst A, Zeppernick F, Tagscherer KE, et al. Differentiation therapy exerts antitumour effects on stem-like glioma cells. *Clin Cancer Res* 2010; **16:** 2715-28.

35. Demuth T, Rennert JL, Hoelzinger DB, Reavie LB, Nakada M, Beaudry C, et al. Glioma cells on the run - the migratory transcriptome of 10 human glioma cell lines. *BMC Genomics* 2008; **9:** 54.

36. Campos B, Herold-Mende CC. Insight into the complex regulation of CD133 in glioma. *Int J Cancer* 2010; **128:** 501-10.

37. Wu Y, Wu PY. CD133 as a marker for cancer stem cells: progresses and concerns. *Stem Cell Dev* 2009; **18:** 1127-34.

38. Zeppernick F, Ahmadi R, Campos B, Dictus C, Helmke BM, Becker N, et al. Stem cell marker CD133 affects clinical outcome in glioma patients. *Clin Cancer Res* 2008; **14:** 123-9.

39. Pallini R, Ricci-Vitiani L, Banna GL, Signore M, Lombardi D, Todaro M, et al. Cancer stem cell analysis and clinical outcome in patients with glioblastoma multiforme. *Clin Cancer Res* 2008; **14:** 8205-12.

40. Kong D-S, Kim MH, Park W-Y, Suh Y-L, Lee J-I, Park K, et al. The progression of gliomas is associated with cancer stem cell phenotype. *Oncol Rep* 2008; **19:** 639-43.

41. Strojnik T, Røsland GV, Sakariassen PO, Kavalar R, Lah Turnsek T. Neural stem cell markers, nestin and musashi proteins, in the progression of human glioma: correlation of nestin with prognosis of patient survival. *Surg Neurol* 2007; **68:** 133-43.

42. Birgersdotter A, Sandberg R, Ernberg I. Gene expression perturbation in vitro-a growing case for three-dimensional (3D) culture systems. *Semin Cancer Biol* 2005; **15:** 405-12.

43. Karcher S, Steiner HH, Ahmadi R, Zoubaa S, Vasvari G, Bauer H, et al. Different angiogenic phenotypes in primary and secondary glioblastomas. *Int J Cancer* 2006; **118:** 2182-9.

44. Yu SC, Ping YF, Yi L, Zhou ZH, Chen JH, Yao XH, et al. Isolation and characterization of cancer stem cells from a human glioblastoma cell line U87. *Cancer Lett* 2008; **265:** 124-34.

45. Schmitt M, Jaenicke F, Graeff H. Protease, matrix degradation and tumour-cell spread. *Fibrinolysis* 1992; **6:** 1-17.

46. Friedl P, Wolf K. Tumour cell invasion and migration. Diversity and escape mechanisms. *Nat Rev Cancer* 2003; 3: 362-74.

47. Zajc I, Bervar A, Lah Turnšek T. Cysteine cathepsins, stefins and extracellular matrix degradation during invasion of transformed human breast cell lines. *Radiol Oncol* 2006; **40:** 259-71.

48. Strojan P. Cysteine cathepsins and stefins in head and neck cancer: an update of clinical studies. *Radiol Oncol* 2008; **42:** 69-81.

49. Berquin LM, Sloane BF. Cathepsin B expression in human tumours. *Adv Exp Med Biol* 1996; **389:** 281-94.

50. Urbich C, Heeschen C, Aicher A, Sasaki K, Bruhl T, Farhadi MR, at al. Cathepsin L is required for endothelial progenitor cell-induced neovascularization. *Nat Med* 2005; **11:** 206-13.

research article

Chemotherapy increases caspase-cleaved cytokeratin 18 in the serum of breast cancer patients

Engin Ulukaya[1], Esra Karaagac[1], Ferda Ari[2], Arzu Y. Oral[1], Saduman B. Adim[3], Asuman H. Tokullugil[1], Türkkan Evrensel[4]

[1] Medical School of Uludag University, Clinical Biochemistry Department, Bursa, Turkey
[2] Science and Art Faculty of Uludag University, Biology Department, Bursa, Turkey
[3] Medical School of Uludag University, Pathology Department, Bursa, Turkey
[4] Medical School of Uludag University, Medical Oncology Department, Bursa, Turkey

Received 5 January 2011
Accepted 25 January 2011

Correspondence to: Prof. Dr. Engin Ulukaya, Medical School of Uludag University, Department of Medical Biochemistry 16059 Gorukle, Bursa, Turkey. Phone: +90 (0)224 295 39 13; Fax: +90 (0)224 442 82 45; E-mail: eulukaya@uludag.edu.tr

Disclosure: No potential conflicts of interest were disclosed.

Background. Apoptosis is thought to be induced by chemotherapy in cancer patients. Therefore, the measurement of its amplitude may be a useful tool to predict the effectiveness of cancer treatment sooner than conventional methods do.

Patients and methods. In the study presented, apoptosis was assessed with an ELISA-based assay in which caspase-cleaved cytokeratin 18 (M30-antigen), a novel specific biomarker of apoptosis, is measured. Thirty seven patients with malignant (nonmetastatic and metastatic) breast cancer, 35 patients with benign breast disease, and 34 healthy subjects were studied. Cancer patients received neoadjuvant chemotherapy consisting of either fluorouracil, epirubicin, and cyclophosphamide (FEC) or epirubicin plus docetaxel (ED). Apoptosis was detected before chemotherapy, 24 and 48 h after chemotherapy in the malignant group.

Results. It was found that the baseline apoptosis level in either malignant but nonmetastatic group or benign group was not statistically different from that in the control group ($p>0.05$). However, it was statistically significantly higher in the metastatic group than that in the control group ($p<0.05$). Following the drug application, M30-antigen levels significantly increased at 24 h ($p<0.05$). The baseline M30-antigen levels increased about 3-times in patients showing tumor regression.

Conclusions. M30-antigen level is increased after chemotherapy and its measurement may help clinicians to predict the effectiveness of chemotherapy sooner in breast cancer cases although confirmative larger trials are needed.

Key words: apoptosis; chemotherapy; M30; response to chemotherapy; breast cancer

Introduction

Breast cancer is the leading cancer type which accounts for the highest mortality rate among woman cancers.[1-3] Although new chemotherapeutic agents have been introduced into the market, the patient outcome is still not satisfactory.[3] The improvement of the outcome may be achieved by an early prediction of the response to chemotherapy. For this aim, new biomarker(s), which provide information of the effectiveness of chemotherapy, are required.[4] Apoptosis-related biomarkers may be of importance in this regard.

The mechanism by which chemotherapy kills the cancer cells is mainly the induction of the apoptotic pathway.[5] Because the effects of anti-cancer drugs is based on the induction of apoptosis, *in vitro* evaluation of apoptosis has been used for testing the efficacy of anti-cancer agents.[6-8] If apoptosis in serum can be measured by a biomarker which results from its induction, this may be of great importance for the clinicians to predict the response to

TABLE 1. The characteristics of participants

Characteristics	n
Control	**34**
Mean age ±S.D. (47.2±10.6)	
Malignant group	**37**
Mean age ±S.D. (51.1 ± 12)	
Invasive ductal carcinoma	29
Invasive lobuler carcinoma	3
Metastatic breast cancer	5
Benign group	**35**
Mean age ±S.D. (40.6 ± 8.2)	
Fibrocystic	31
Fibroadenoma	4
Sex	All women
Stage	
I	4
II	17
III	11
IV	5
ER (+)	14
ER (-)	8
PR (+)	18
PR (-)	4

ER, estrogen receptor status; PR, progesterone receptor status

chemotherapy they apply to their patients. It seems that there is such a biomarker which is found in the cytoskeleton.

Cytokeratin 18 (CK 18) is a member of cytoskeletal protein family which is present in epithelial cells.[9] When apoptosis is induced, CK 18 is cleaved from aspartate amino acids localized at position 238 and 396. Monoclonal antibody M30 recognizes the neoepitope of CK 18 formed after cleavage by the caspases. This newly-formed neoepitope can be regarded as a selective biomarker of apoptosis.[10,11] In fact, it was reported that the M30-antigen assay, which detects this neoepitope, reflects apoptosis accurately.[12] It is also reported that M30-antigen is used as a marker for pharmocodynamic studies in cancer.[13] Because deregulated apoptosis is a common feature of malignancies[14], its assessment via circulating apoptotic markers have recently been made in some tumor types, such as gastrointestinal cancers.[15] Recently, it was reported that serum M30-antigen levels may also be a prognostic marker in some tumor types.[16,17] In another study, M30-antigen was reported to be associated with the survival in advanced gastric carcinoma patients.[18]

In addition to its being used as a prognostic marker in tumors, M30-antigen may provide important information regarding the response to therapy. Thus, it may be useful for the estimation of the efficacy of therapy.[19] Kramer *et al*. presented that serum M30-antigen levels increased after docetaxel regimen in prostate cancer.[20] Similarly, it was demonstrated that M30-antigen levels increased after chemotherapy in testicular cancer patients.[16] Our group previously showed that M30-antigen levels increased as a response to therapy in breast cancer patients but we did not measure its levels in benign breast diseases and healthy subjects.[21]

Therefore, we investigated if M30-antigen is increased in breast cancer patients as well as in benign breast diseases in comparison with healthy subjects. We also measured its level after the application of chemotherapy in neoadjuvant setting. We found that chemotherapy leads to a significant increase in M30-antigen levels in serum of breast cancer patients. Thus, it may be used as a biomarker for the prediction of response to chemotherapy in breast cancer patients.

Patients and methods

Patient selection, treatment and assessment of clinical tumor response

The characteristics of the study participants are presented in Table 1. Patients with previously untreated, histological confirmed invasive breast cancer were eligible. The patient selection and eligibility criteria to be enrolled to the study were made according to the previous study performed by our group.[21] Briefly, their performance status ≤ 2 by ECOG. Core needle biopsy was used for the histological confirmation of the tumor. The patients were treated with FEC or ED regimens: FEC regimen consisted of 5-fluorouracil (EBEWE Pharma, Austria) 500 mg/m^2, epirubicin (EBEWE Pharma, Austria) 100 mg/m^2, cyclophosphamide (BAXTER, Germany) 500 mg/m^2 while ED regimen consisted of epirubicin 75 mg/m^2 and docetaxel (EBEWE Pharma, Austria) 80 mg/m^2. All drugs were administered on day 1, at every 21 days.

The response to treatment was assessed after the completion of four cycles of neoadjuvant chemotherapy by standard breast calipers and graded into: (a) clinical complete response (no tumor measurable); (b) clinical partial response (≥50% reduction in tumor size); (c) clinical stable disease (<50% reduction or an increase in tumor size of ≤50%); and (d) clinical progressive disease (>50% increase in tumor size or suspicious new lesion). According to the classification above, the complete and partial responses were defined as a regressive group. The other two groups were the stable group showing stable disease and the

TABLE 2. M30-antigen levels in different groups

M30-antigen	Control group (n = 34)	Benign group (n = 35)	Nonmetastatic group (n = 32)	Metastatic group (n = 5)
Mean ± S.D.	127 ± 46	173 ± 224	182 ± 336	333 ± 184
(min-max)	71-340	68-1295	58-2010	159-607
Median	114	107	118	350
p-Value		>0.05*	>0.05**	<0.05***

*Comparison of control group and benign group, Mann-Whitney U test
** Comparison of control group and nonmetastatic group, Mann-Whitney U test
***Comparison of control group and metastatic group, Mann-Whitney U test

progressive group showing progression as given above. The informed consent was obtained from the participants and the local ethic committee approved the study.

M30-antigen detection

The serum samples of malignant cases were collected prior to chemotherapy (baseline M30-antigen level), and 24 and 48 h after the treatment. Therefore, the acute (short term) effect of the therapy was actually assessed ignoring the long term effects. The sera of benign and healthy control subjects were collected at the time of admission only. The sera were stored at -80ºC until the assessment. An ELISA assay (a solid phase, two-site immunosorbent assay) was used to measure M30-antigen by using a commercial kit (M30-Apoptosense ELISA kit, Peviva, Sweden). Measurement was performed according to the instructions of the manufacturer. The absorbance was finally measured in a microplate reader (FlashScan, Jena, Germany) at 450 nm and the M30-antigen levels were estimated by the standard curve. The concentration of the M30-antigen was expressed as unit per liter (U/L).

Histopathological evaluation

Tissue specimens were fixed in 10% buffered formalin (pH 7.4) and embedded in paraffin. 5 µm thick sections were cut and stained with hematoxylin and eosin. Estrogen (ER) and progesterone (PgR) receptor status were assessed by immunohistochemistry. All specimens were examined by an experienced pathologist who was unaware of the clinical data. Only 22 patients' samples were accessible. The proportion of ER and PgR positive cells was determined as the percentage of invasive tumor cells. The threshold of 10% positivity was chosen as a cut-off value.

Statistical analysis

The statistical analysis was performed using SPSS 13.0 (SPSS Inc., Chicago, IL, USA). All values are presented as mean (± standard deviation- S.D.) and median. In the case of the distribution of parameters did not show normal distribution, nonparametric statistics (Kruskal-Wallis and Mann Whitney-*U* tests) were used. Wilcoxon Rank Sum test was also used to compare two dependent samples represented by M30-antigen levels before and after chemotherapy. The relationship between M30-antigen levels and parameters were analyzed by Pearson Correlation. Statistical significance was assigned to *p*-values less than 0.05.

Results

Characteristics of the study groups

The characteristics of participants are given in Table 1. The healthy control group included 34 people, while the malignant (metastatic and nonmetastatic) group and the benign group included 37 and 35 patients, respectively. Among the malignant group, most of them had invasive ductal carcinoma (n=29), while only 5 of them were metastatic breast cancer cases.

Serum M30-antigen levels are elevated in metastatic breast cancer patients

The baseline level of serum M30-antigen was measured in control, benign and malignant groups. It was found that the mean M30-antigen levels in control, benign, nonmetastatic and metastatic group were 127 ± 46, 173 ± 224, 182 ± 336, and 333 ± 184, respectively. A statistically significant difference between the groups was observed ($p<0.05$; Kruskal-Wallis and Mann-Whitney U tests) (Table 2). The mean of the metastatic malignant group

TABLE 3. M30-antigen levels after chemotherapy (n=11)

M30-antigen level (U/L)	Before chemotherapy (baseline level)	24 h after chemotherapy	48 h after chemotherapy
Mean ±S.D	316 ± 564	809 ± 1526	584 ± 874
(min-max)	96-2010	98-4986	82-2586
Median	136	143	150
p-Value		<0.05*	>0.05**

* Comparison of M30-antigen levels before chemotherapy and those 24 h after chemotherapy, Wilcoxon Sign Rank test
** Comparison of M30-antigen levels before chemotherapy and those 48 h after chemotherapy, Wilcoxon Sign Rank test.

TABLE 4. The M30-antigen levels in ER(-), ER(+) and PgR(-), PgR(+) groups

M30-antigen level (U/L)	ER (+) n=14	ER (-) n=8	PgR (+) n=18	PgR (-) n=4
Mean ±S.D	153 ± 39	183 ± 31	148 ± 30	235 ± 51
(min.-max.)	58-607	86-383	58-607	146-383
p-Value	<0.05*		<0.05**	

Only 22 patients' data were obtained for the evaluation of ER and PgR status.
*Comparison of ER(-) group and ER(+) group, Mann-Whitney U test
** Comparison of PgR(-) group and PgR(+) group, Mann-Whitney U test

was significantly higher than either benign or control group ($p<0.05$). There was no significant difference between the control group and either the nonmetastatic malignant group or the benign group. The mean M30-antigen level of the metastatic group was significantly higher than that in the nonmetastatic group.

M30-antigen level increases following chemotherapy

Eleven nonmetastatic breast cancer patients accepted to donate serum sample after chemotherapy. Blood samples were collected prior to chemotherapy and 24 and 48 h after the application of chemotherapy. The baseline, 24 h and 48 h after chemotherapy levels were 316 ± 564, 809 ± 1526, and 584 ± 874, respectively. The baseline M30-antigen levels increased more than 2-fold 24 h after chemotherapy ($p<0.05$) (Table 3). In addition, M30-antigen level at 48 h following chemotherapy was still higher than the baseline level but it was not statistically significant ($p>0.05$).

Relationship between M30-antigen level and receptor status, stage, and routine tumor markers

It has been found that M30-antigen levels differ depending on the ER or PgR status. ER negative (183 ± 31) or PgR negative (235 ± 51) cases had higher M30-antigen levels compared to those in ER (153 ± 39) or PgR (148 ± 30) positive cases ($p<0.05$), respectively (Table 4).

M30-antigen levels differ depending on the stage (Table 5). Stage IV patients seem to have the highest levels. There was no significant difference between stage II and III but stage IV cases had significantly higher levels compared to those in either stage II or III.

The correlation between M30-antigen and the routine clinical chemistry parameters was analyzed. But there was no significant correlation between them (data not shown). In addition, there was no correlation between baseline M30-antigen levels and age ($r=0.045$, $p=0.647$). The levels of lactate dehydrogenase (LDH), alkaline phosphatase and platelet count were measured in patients with malignant breast cancer and healthy controls. There was no statistically significant difference between the groups (data not shown).

Relationship between M30-antigen and tumor response to chemotherapy in neoadjuvant setting

Eleven malignant cases were classified into three groups according to their responses to chemotherapy: regressive group (n=5) consisting of clinical complete or partial responses, stable group (n=4), and progressive group (n=1). One patient's response was not evaluated although post-chem-

TABLE 5. Comparison of the M30-antigen levels according to the stage of disease

M30-antigen level (U/L)	Stage II (n=17)	Stage III (n=11)	Stage IV (n=5)
Mean ±S.D	242 ± 110	117 ± 15	333 ± 184
(min-max)	72-2010	59-211	159-607
Median	131	113	351
p-Value	p<0.05*	p<0.05**	

* Comparison of the M30-antigen levels between stage 2 and 4, Mann-Whitney U test
** Comparison of the M30-antigen levels between stage 3 and 4, Mann-Whitney U test

TABLE 6. Classification into the responses to chemotherapy in the neoadjuvant setting and their M30-antigen values (U/L, ± SS)

	Stable group, (n=4)	Regressive group, (n=5)	Progressive group, (n=1)
Before Chemotherapy	137 ± 46	544 ± 820	110
24 h after Chemotherapy	115 ± 11	1633 ± 407	143
48 h after Chemotherapy	116 ± 23	1076 ± 1150	502

The statistical evaluation was not performed due to the low number of cases.

otherapy M30-antigen level of that patient was available. As it is shown on Table 6, M30-antigen level of both the stable group and the progressive group did not significantly change after chemotherapy, while it sharply increased in the regressive group 24 h after chemotherapy. It increased about 3-fold (from 544 to 1633 U/L) in this group, implying the apoptosis-inducing effect of drugs applied. However, the differences were not statistically evaluated due to a low number of cases.

Discussion

In the study presented, we measured the M30-antigen levels before and after chemotherapy to investigate its relation with response to treatment. We found that M30-antigen significantly increased following chemotherapy. This may give an idea of the effectiveness of chemotherapy applied in neoadjuvant setting. Neoadjuvant chemotherapy is increasingly being applied in the management of patients with large (≥ 3 cm) and locally advanced breast cancer. Although neoadjuvant chemotherapy may lead to similar disease-free and overall survival rates with those obtained with adjuvant chemotherapy, the response of breast cancer patients to neoadjuvant chemotherapy was found as the most important predictive factor for the survival.[22-24] However, which patient would response to the neoadjuvant chemotherapy is still unpredictable. That is why we believe that the measurement of apoptosis, which is induced by anticancer drugs, may be of great importance in the prediction of response to therapy. This may be achieved by measuring the M30-antigen levels in serum and the clinicians may thus predict better the outcome of their patients by using this tool.

Death of tumor cells generates detectable protein products in the patient's circulation, which may be used for cancer diagnostics and/or monitoring of therapy efficacy.[25] Apoptosis is a form of regulated cell death that is characterized by specific structural changes, mediated by proteases of the caspase family.[26] Caspase activity itself or the presence of specific degradation products can be used for the detection of tumor cell apoptosis. The M30 antibody detects a caspase-degraded product, CK18-Asp396 (also called M30-antigen), of the important cytoskeletal protein called cytokeratin 18 of epithelial cells. Cytokeratin 18 is expressed by most carcinomas, including those of breast, prostate, lung and colon.[11]

Treatment-induced changes in growth dynamics (apoptosis and proliferation) in breast cancer are essential to determine the response or resistance of tumors to chemotherapy. The early detection of chemosensitive tumor with the assessment of apoptosis or different techniques may facilitate the individualized-chemotherapy. It has previously been shown that circulating M30-antigen levels increased in patients with various cancer types and, furthermore, it increased during chemotherapy.[21,27,28] For instance, the docetaxel treatment increased levels of M30-antigen in the serum of breast cancer patients, indicating apoptotic

death of tumor cells, while the cyclophosphamide/epirubicin/5-fluorouracil treatment led to a heterogenous response with regard to cell death mode.[29] Our group previously reported that M30-antigen increased 4-fold after chemotherapy in lung cancer patients.[30] In accordance with this finding, in this study presented, we observed that M30-antigen level was significantly increased 24 and 48 h after the chemotherapy in breast cancer patients. In fact, preclinical and clinical studies have shown that apoptosis significantly increases 1 to 3 days after chemotherapy administration.[31-33]

In the present study, we found that there was no statistically significant difference between the non-metastatic and the control group in terms of M30-antigen levels ($p>0.05$). In supporting this finding, there was no statistically significant difference between the malignant group (202 ± 84) and the control group (187 ± 58) in terms of baseline LDH level, which also represents cell death in serum. However, this may depend on the type of tumor. In the patients with disseminated testicular germ cell tumor, circulating M30-antigen levels were found to be correlated with classic prognostic markers including LDH probably reflecting tumor load.[16]

In contrast to inexistence of M30-antigen increase in the non-metastatic group compared to the control group, M30-antigen level was significantly higher in the metastatic group than that in the control group ($p<0.05$). This implies that the aggressiveness (metastatic ability) of tumor mass may have an impact on the serum level of M30-antigen. This increase may also be explained by the differentiation level of the tumor cells. It is highly possible that the stage or the total size of the tumor mass seems to affect the M30-antigen levels in serum. In fact, in the Olofsson's study, there was a clear relationship between the tumor size and the M30-antigen levels.[29] In this study, stage IV patients had much higher M30 antigen levels than those either stage II or III patients. Thereby, there must be a close link between apoptosis and both malignancy itself and the extension of malignancy. In agreement with this, we did not find any statistically significant increase in M30-antigen levels in the benign group, compared to the control group.

Several studies demonstrated that M30-antigen levels were higher in ER negative breast tumors than ER-positive tumors[21,28], consistent with our results. Furthermore, we also found that M30-antigen levels were higher in PgR negative tumors, compared to PgR-positive ones. However, this needs to be confirmed by larger clinical studies. In fact, the weakness of our study was the low number of patients studied although the results were interesting.

Conclusions

These findings indicate that serum M30-antigen is increased following FEC-based or ED-based chemotherapy. Thus, the measurement of its serum level may be a useful tool to predict the effectiveness of chemotherapy sooner in breast cancer patients. However, larger clinical studies are required to use it in the clinics routinely.

Acknowledgement

We thank to Uludag University Research Fund for providing us with the kits.

References

1. Benson JR, Jatoi I, Keisch M, Esteva FJ, Makris A, Jordan VC. Early breast cancer. *Lancet* 2009; **373:** 1463-79.
2. Plesnicar A, Golicnik M, Fazarinc IK, Kralj B, Kovac V, Plesnicar BK. Attitudes of midwifery students towards teaching breast-self examination. *Radiol Oncol* 2010; **44:** 52-6.
3. Ovcaricek T. Frkovic SG, Matos E, Mozina B, Borstnar S. Triple negative breast cancer – prognostic factors and survival. *Radiol Oncol* 2011; **45:** 46-52.
4. Strojan P. Cysteine cathepsins and stefins in head and neck cancer: an update of clinical studies. *Radiol Oncol* 2008; **42:** 69-81.
5. Hickman JA, Beere HM, Wood AC, Waters CM, Parmar R. Mechanisms of cytotoxicity caused by antitumour drugs. *Toxicol Lett* 1992; **64:** 553-61.
6. Ohmori T, Podack ER, Nishio K, Takahashi M, Miyahara Y, Takeda Y, et al. Apoptosis of lung cancer cells caused by some anti-cancer agents (MMC, CPT-11, ADM) is inhibited by bcl-2. *Biochem Biophys Res Commun* 1993; **192:** 30-6.
7. Walton MI, Whysong D, O'Connor PM, Hockenbery D, Korsmeyer SJ, Kohn KW. Constitutive expression of human Bcl-2 modulates nitrogen mustard and camptothecin induced apoptosis. *Cancer Res* 1993; **53:** 1853-61.
8. Hagg M, Bivén K, Ueno T, Rydlander L, Björklund P, Wiman KG, et al. A novel high-through-put assay for screening of pro-apoptotic drugs. *Invest New Drugs* 2002; **20:** 253-9.
9. Linder S. Cytokeratin markers come of age. *Tumour Biol* 2007; **28:** 189-95.
10. Ueno T, Toi M, Linder S. Detection of epithelial cell death in the body by cytokeratin 18 measurement. *Biomed Pharmacother* 2005; **59** (Suppl): S359-62.
11. Leers MP, Kölgen W, Björklund V, Bergman T, Tribbick G, Persson B, et al. Immunocytochemical detection and mapping of a cytokeratin 18 neo-epitope exposed during early apoptosis. *J Pathol* 1999; **187:** 567-72.
12. Zhang L, Kavanagh BD, Thorburn AM, Camidge DR. Preclinical and clinical estimates of the basal apoptotic rate of a cancer predict the amount of apoptosis induced by subsequent proapoptotic stimuli. *Clin Cancer Res* 2010; **16:** 4478-89.
13. Linder S, Olofsson MH, Herrmann R, Ulukaya E. Utilization of cytokeratin-based biomarkers for pharmacodynamic studies. *Expert Rev Mol Diagn* 2010; **10:** 353-9.
14. Holdenrieder S, Stieber P. Circulating apoptotic markers in the management of non-small cell lung cancer. *Cancer Biomarkers* 2010; **6:** 197-210.

15. Brandt D, Volkmann X, Anstätt M, Länger F, Manns MP, Schulze-Osthoff K, et al. Serum biomarkers of cell death for monitoring therapy response of gastrointestinal carcinomas. *Eur J Cancer* 2010; **46:** 1464-73.

16. de Haas EC, di Pietro A, Simpson KL, Meijer C, Suurmeijer AJ, Lancashire LJ, et al. Clinical evaluation of M30 and M65 ELISA cell death assays as circulating biomarkers in a drug-sensitive tumor, testicular cancer. *Neoplasia* 2008; **10:** 1041-8.

17. Wu YX, Wang JH, Wang H, Yang XY. Study on expression of Ki-67, early apoptotic protein M30 in endometrial carcinoma and their correlation with prognosis. *Zhonghua Bing Li Xue Za Zhi* 2003; **32:** 314-8.

18. Yaman E, Coskun U, Sancak B, Buyukberber S, Ozturk B, Benekli M. Serum M30 levels are associated with survival in advanced gastric carcinoma patients. *Int Immunopharmacol* 2010; **10:** 719-22.

19. Beachy SH, Repasky EA. Using extracellular biomarkers for monitoring efficacy of therapeutics in cancer patients: an update. *Cancer Immunol Immunother* 2008; **57:** 759-75.

20. Kramer G, Erdal H, Mertens HJ, Nap M, Mauermann J, Steiner G, et al. Differentiation between cell death modes using measurements of different soluble forms of extracellular cytokeratin 18. *Cancer Res* 2004; **64:** 1751-6.

21. Demiray M, Ulukaya EE, Arslan M, Gokgoz S, Saraydaroglu O, Ercan I, et al. Response to neoadjuvant chemotherapy in breast cancer could be predictable by measuring a novel serum apoptosis product, caspase-cleaved cytokeratin 18: a prospective pilot study. *Cancer Invest* 2006; **24:** 669–76.

22. Fisher B, Bryant J, Wolmark N, Mamounas E, Brown A, Fisher ER, et al. Effect of preoperative chemotherapy on the outcome of women with operable breast cancer. *J Clin Oncol* 1998; **16:** 2672-85.

23. Bonadonna G, Valagussa P, Brambilla C, Ferrari L, Moliterni A, Terenziani M et al. Primary chemotherapy in operable breast cancer: eight-year experience at the Milan Cancer Institute. *J Clin Oncol* 1998; **16:** 93-100.

24. Scholl SM, Beuzeboc P, Harris AL, Pierga JY, Asselain B, Palangié T, et al. Is primary chemotherapy useful for all patients with primary invasive breast cancer? Recent results. *Cancer Res* 1998; **152:** 217-26.

25. Holdenrieder S,Stieber P. Apoptotic markers in cancer. *Clin Biochem* 2004; **37:** 605-617.

26. Degterev A, Yuan J. Expansion and evolution of cell death programmes. *Nat Rev Mol Cell Biol* 2008; **9:** 378-90.

27. Ozturk B, Coskun U, Sancak B, Yaman E, Buyukberber S, Benekli M. Elevated serum levels of M30 and M65 in patients with locally advanced head and neck tumors. *Int Immunopharmacol* 2009; **9:** 645-8.

28. Ueno T, Toi M, Bivén K, Bando H, Ogawa T, Linder S. Measurement of an apoptotic product in the sera of breast cancer patients. *Eur J Cancer* 2003; **39:** 769-74.

29. Olofsson MH, Ueno T, Pan Y, Xu R, Cai F, van der Kuip H, et al. Cytokeratin-18 is a useful serum biomarker for early determination of response of breast carcinomas to chemotherapy. *Clin Cancer Res* 2007; **13:** 3198-206.

30. Ulukaya E, Yilmaztepe A, Akgoz S, Linder S, Karadag M. The levels of caspase cleaved cytokeratin 18 are elevated in serum from patients with lung cancer and helpful to predict the survival. *Lung Cancer* 2007; **56:** 399–404.

31. Meyn RE, Stephens LC, Hunter NR, Milas L. Apoptosis in murine tumors treated with chemotherapy agents. *Anticancer Drugs* 1995; **6:** 443-50.

32. Ellis PA, Smith IE, McCarthy K, Detre S, Salter J, Dowsett M. Preoperative chemotherapy induces apoptosis in early breast cancer. *Lancet* 1997; **349:** 849.

33. Green AM, Steinmetz ND. Monitoring apoptosis in real time. *Cancer J* 2002; **8:** 82-92.

research article

Clinical efficacy of local targeted chemotherapy for triple-negative breast cancer

Jinsong He, Xianming Wang, Hong Guan, Weicai Chen, Ming Wang, Huisheng Wu, Zun Wang, Ruming Zhou, Shuibo Qiu

The Center of Diagnosis and Treat of Breast Disease, The Second People's Hospital of Shenzhen City, Shenzhen, P. R. China

Received 24 February 2011
Accepted 14 March 2011

Correspondence to: Prof. Dr. Jinsong He, The Center of Diagnosis and Treat of Breast Disease, The Second People's Hospital of Shenzhen City, Shenzhen 518035, P.R. China. Phone: +86 755 8336 6388 8287; E-mail: hehesmiling@163.com or hjssums@sohu.com

Disclosure: No potential conflicts of interest were disclosed.

Background. The aim of the study was to evaluate the clinical efficacy of superselective intra-arterial targeted neoadjuvant chemotherapy in the treatment of estrogen receptor (ER)-negative, progesterone receptor (PR)-negative, and human epidermal growth factor receptor 2 (HER2)-negative (triple-negative) breast cancer.

Patients and methods. A total of 47 triple-negative breast cancer patients (29 at stage II, 13 at stage III and 5 at stage IV) were randomly assigned to two groups: targeted chemotherapy group (n=24) and control group (n=23). Patients in the targeted chemotherapy group received preoperative superselective intra-arterial chemotherapy with CEF regimen (C: cyclophosphamide [600 mg/m^2]; E: epirubicin [90 mg/m^2]; F: 5-fluorouracil [600 mg/m^2]), and those in the control group received routine neoadjuvant chemotherapy with CEF. The duration of the treatment, changes in lesions and the prognosis were determined.

Results. The average course of the treatment was 15 days in the targeted chemotherapy group which was significantly shorter than that in the control group (31 days) (P<0.01). The remission rate of lesions was 91.6% in the targeted chemotherapy group and 60.9% in the control group, respectively. Among these patients, 9 died within two years, including 2 (both at IV stage) in the targeted chemotherapy group and 7 (2 at stage II, 4 at stage III and 1 at stage IV) in the control group.

Conclusions. As an neoadjuvant therapy, the superselective intra-arterial chemotherapy is effective for triple-negative breast cancer, with advantages of the short treatment course and favourable remission rates as well as prognoses.

Key words: triple-negative breast cancer; targeted chemotherapy; prognosis

Introduction

Triple-negative breast cancer refers to breast cancers negative for estrogen receptor (ER), progesterone receptor (PR), and human epidermal growth factor receptor 2 (HER2), accounting for about 15% of breast cancers of all types.[1-4] Triple-negative breast cancer progresses rapidly and is susceptible to distant metastasis due to the lack of the effective targeted endocrine therapy and anti-HER-2 therapy, resulting in a high mortality. Patients with triple-negative breast cancer have a high risk for death, and no effective treatment has been developed yet.[4-6] The polymerase inhibition might be an effective treatment for triple-negative breast cancer, but it's still under study.[7] Since April 2006, superselective intra-arterial targeted neoadjuvant chemotherapy has been applied in our hospital for the short-course treatment of triple-negative breast cancer. The clinical efficacy of this method in the treatment of triple-negative breast cancer and its effect on the prognosis of this disease were analysed herein.

Patients and methods

General data

A total of 47 patients with triple-negative breast cancer were recruited from April 2006 to March 2010 from the Center of Breast Disease of our hospital. All patients underwent core needle biopsy, and the pathological examination was conducted

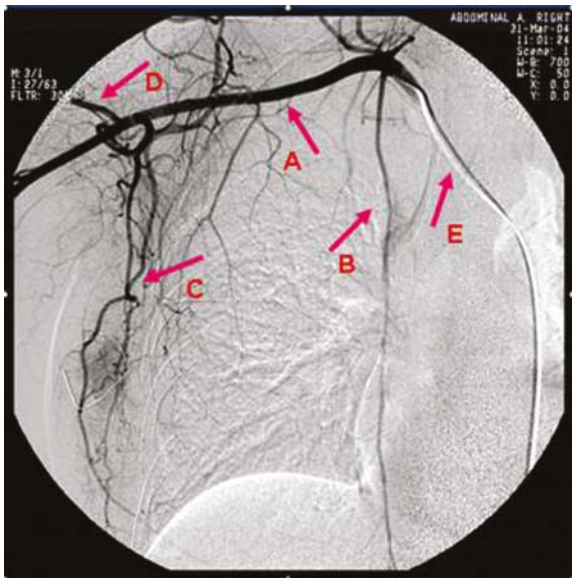

FIGURE 1. Blood vessel network under digital subtraction angiography. A = subclavian artery; B = internal mammary artery; C = lateral thoracic artery; D = circumflex scapular artery; E = Catheter

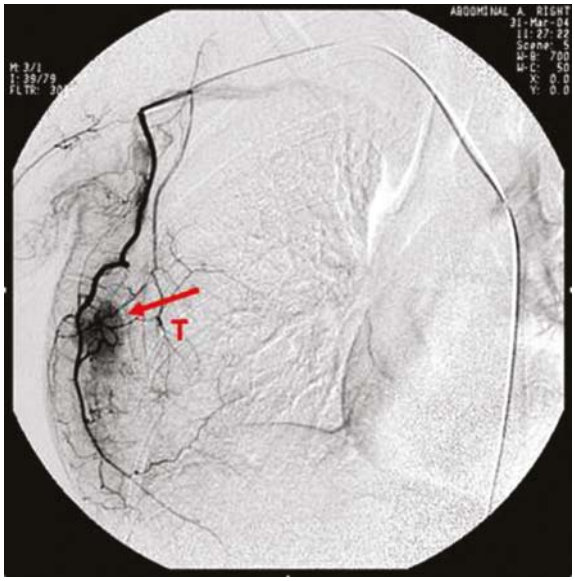

FIGURE 2. Breast cancer and its feeding arteries. T = tumour

to detect the ER, PR and HER-2, and the diagnosis of triple-negative breast cancer was confirmed. The cancers were at stage ⅡA-Ⅳ and primary invasive breast cancer. The median age was 41 years (range: 26-58 years).

These patients were randomly assigned into a targeted chemotherapy group and a control group. Before chemotherapy, all patients underwent ultrasonography of bilateral breasts, bilateral armpits and the liver, chest radiography and systemic bone scanning. For the enlarged lymph nodes, the fine needle aspiration biopsy was done to detect whether there was metastasis. There were 24 patients in the target chemotherapy group with a median age of 42 years (range: 28-58 years). Of them, 5 and 19 were negative and positive for regional lymph node metastasis, respectively. In respect of the TMN stage, there were 6, 8, 4, 2 and 4 cases at the stage of ⅡA, ⅡB, ⅢA, ⅢC and Ⅳ, respectively. In the control group (n=23), the median age of patients was 41 years (range: 26-55 years). Of them, 4 and 19 were negative and positive for regional lymph node metastasis, respectively. In respect of the TMN stage, there were 6, 9, 4, 3 and 1 cases at the stage of ⅡA, ⅡB, ⅢA, ⅢC and Ⅳ, respectively. There were no significant differences in the age or stage of cancers between both groups (P=0.643 and 0.514, respectively).

Neoadjuvant chemotherapy

Targeted chemotherapy group

Before surgery, superselective intra-arterial targeted neoadjuvant chemotherapy was performed.[8,9] The femoral artery is punctured with a Seldinger needle and a 5-6F catheter was inserted into ipsilateral subclavian artery. The blood vessel network of breast, feeding arteries of the cancer and blood supply to the cancer were presented under angiography (Figures 1, 2). The superselective catheterization was performed into a main feeding artery of the cancer, followed by infusion of half amount of the drug, and then into the main feeding artery (lateral thoracic artery or internal mammary artery) of the breast followed by infusion of 25% of the drug, and finally into the distal end of the cross between subclavian artery and vertebral artery followed by the infusion of the remaining drug (involving the whole blood vessel network of the breast and blood vessels in the armpit). Then, the blood flow of brachial artery was blocked by pneumatic tourniquet avoiding the entry of drug to the brachial artery. The duration of the whole perfusion was 3-5 h, and all patients treated with CEF regimen (C: cyclophosphamide [600 mg/m^2]; E: epirubicin [90 mg/m^2]; F: 5-fluorouracil [600 mg/m^2]). A cycle lasted 21 days.

Control group

Before surgery, routine intravenous chemotherapy was carried out. All patients received chemotherapy with CEF regimen (C: 600 mg/m^2 at day 1; E: 90 mg/m^2 at day 1; F: 600 mg/m^2 at day 1). A cycle lasted 21 days.

Surgery and post-operative adjuvant therapies

After 1-2 courses of chemotherapy, all patients received surgery. In the targeted chemotherapy group, 6 patients received classical radical mastectomy (Halsted), 10 modified radical mastectomy, 4 breast-conserving surgery and 4 palliative resection of breast cancer. In the control group, 9 patients received classical radical mastectomy (Halsted), 7 modified radical mastectomy, 2 breast-conserving surgery and 5 palliative resection of breast cancer. After surgery, adjuvant chemotherapy with previous regimen was performed for a total of 6 courses. In addition, 20 patients experienced radiotherapy. Clinical manifestations were observed during the study including changes in lesions, days of the treatment, complications (adverse effects were diagnosed according to Criteria for Acute and Subacute Toxicity by WHO), and the post-operative follow up was also carried out.

Statistical analysis and ethical consideration

Comparisons of means between two groups were done with t test and one way analysis of variance was used to analyse the difference in the means between multiple groups. A pairwise comparison was done with q test. The statistical analysis was performed with SPSS 10.0 statistic software package. A value of $P < 0.05$ was considered statistically significant. The study was carried out according to the Helsinki Declaration.

Results

Short-term efficacy and changes in TNM stage and N stage after treatment

In the targeted chemotherapy group, changes of local lesions were observed as early as 3 days after chemotherapy. Oedema at the local lesion was attenuated and accompanied by the occurrence of fold, the superficial varicosity was alleviated, and the adherence between cancers and chest wall was improved. The mass size was decreased, and the lesion was softened and could be moved. The exudate in the ulcerated site was reduced, and the skin colour was changed into brownness (Figures 3, 4). In the targeted chemotherapy group, nine patients achieved a clinical complete remission (cCR), thirteen patients achieved a partial remission (PR), one patient achieved state disease (SD), one patient achieved progress disease (PD); four patients achieved a pathological complete remission (pCR), and the remission rate (RR) was 91.67 % (22/24) (Figure 5~6). Residual carcinoma *in situ* was noted in 1 patient. The down-staging rate was 62.50% (15/24). In the control group, the changes of local lesions were observed at 10 days after chemotherapy. The mass was softened and tumour size was reduced, which was more obvious 30 days after chemotherapy. In the control group, there were 3, 11, 7, 2, and 1 patient with cCR, PR, SD, PD and pCR, respectively, and the RR was 60.87% (14/23). The down-staging rate was 39.13% (9/24). In the targeted chemotherapy group, of the 19 patients with an axillary lymph node metastasis, no metas-

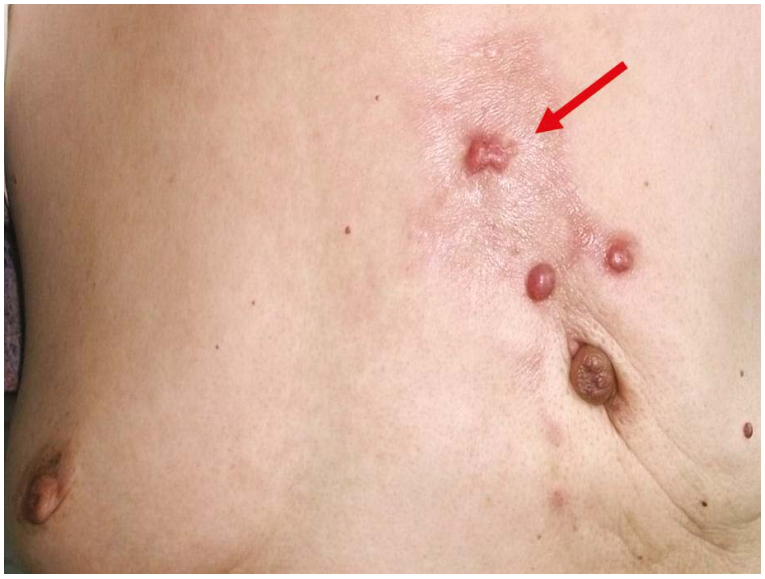

FIGURE 3. Lesions before targeted chemotherapy.

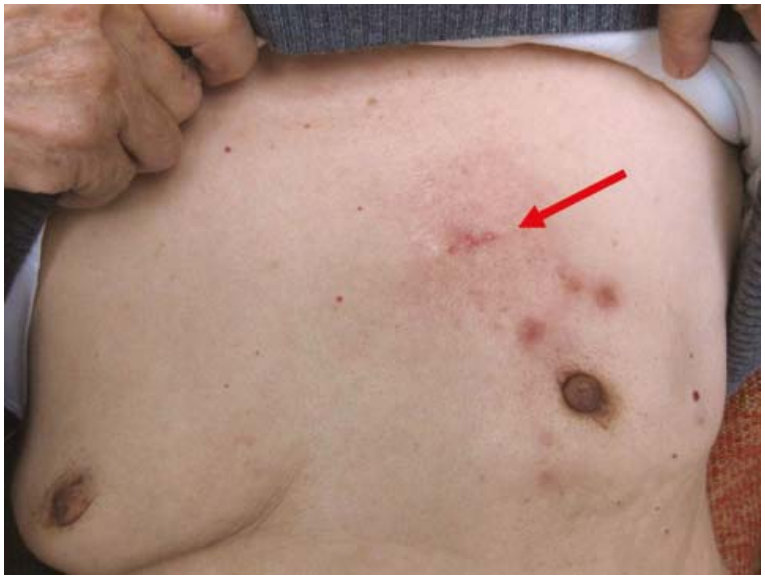

FIGURE 4. The lesions were markedly improved after targeted chemotherapy.

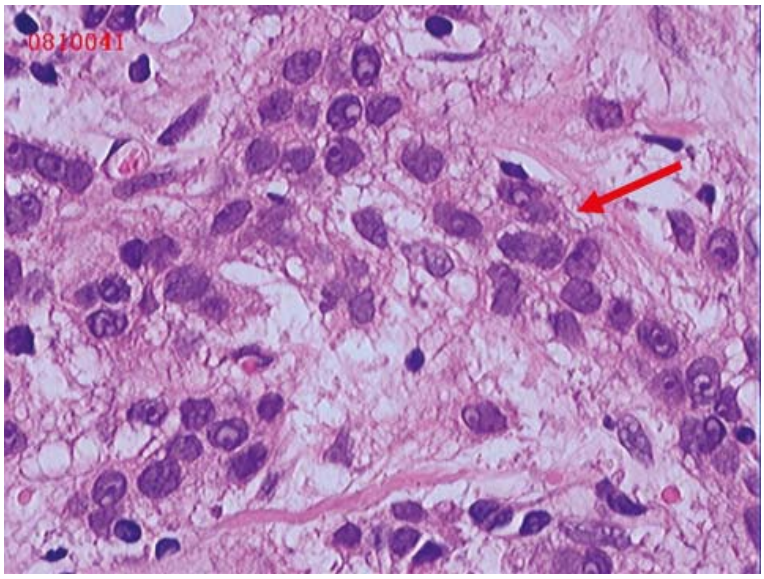

FIGURE 5. Pre-operative aspiration biopsy and pathological examination showed invasive ductal carcinoma (HE ×200).

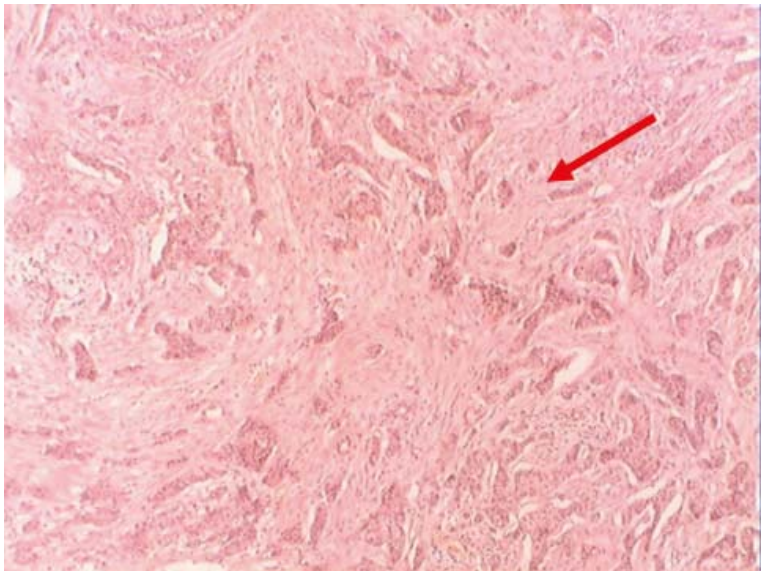

FIGURE 6. The residual cancer nests were not found after targeted chemotherapy (H&E×200).

tasis was found in regional lymph nodes in 7 patients after surgery. In the control group, of 19 patients with an axillary lymph node metastasis, no metastasis was found in regional lymph nodes in 7 patients after surgery. The negative change ratio in a lymph node metastasis was 47.37% (7/19) in the targeted chemotherapy group and 26.31% (5/19) in the control group. The statistical analysis showed there were significant differences in the down-staging rate and negative change ratio between both groups (P=0.023 and 0.041, respectively). The efficacy of targeted chemotherapy was superior to traditional chemotherapy (P=0.018). The targeted chemotherapy was also superior to traditional chemotherapy in terms of cCR and pCR (P=0.016 and 0.018).

Course of treatment

In the targeted chemotherapy group, 18 patients and 6 patients received surgery after 1 course and 2 courses of chemotherapy, respectively. The mean duration of the treatment was 15 days. In the control group, 8 patients and 15 patients received surgery after 1 course and 2 courses of chemotherapy, respectively. The mean course of the treatment was 31 days. A statistical analysis showed the mean course of the treatment in the targeted chemotherapy group was shorter than in the control group ($P<0.01$).

Toxicity of treatment

The grades of chemotherapy toxicity were 0 in 14 patients (58.3%), I in 7 patients (29.2%), II in 3 patients (12.5%) in the targeted chemotherapy group; 0 in 12 patients (52.2%), I in 7 patients (30.4%), II in 4 patients (17.4%) in the control group. There was no significant difference in the degree of drug toxicity between two groups ($P>0.05$). The toxicity of degree 0-1 can resolve spontaneously, and that of degree II can resolve within 1 week after the general treatment.

Follow up

The follow up period was 8-48 months after the surgery. A total of 41 patients (87.23%) completed the follow up and 6 were lost to the follow up. There were 22 patients (91.67%) in the targeted chemotherapy group and 19 patients (82.61%) in the control group completing a follow up. A total of 9 patients died within 2 years including 2 (at stage IV) in the targeted chemotherapy group and 7 in the control group (2 at stage II, 4 at stage III and 1 at stage IV).

Discussion

With the understanding of the genomic profile of breast cancer, the molecular biological types of breast cancer can be determined. Breast cancer of different subtypes may have significantly distinct

prognosis, different therapeutic strategies and marked difference in survival.[10-12] Patients with triple-negative breast cancer cannot benefit from the targeted endocrine therapy and anti-HER-2 treatment. Therefore, for such patients, the only alternative strategy is chemotherapy as an adjuvant therapy of surgery and radiotherapy. Studies have demonstrated triple-negative breast cancer is more sensitive to chemotherapeutic drugs than breast cancer of other subtypes.[13,14] However, the prognosis of triple-negative breast cancer is very poor and it is susceptible to recurrence, which may be contributed to the low pathological remission rate of triple-negative breast cancer. Therefore, in enhanced chemotherapy, the pathological remission rate is a critical factor in improving the prognosis of triple-negative breast cancer.

The sensitivity to chemotherapeutic drugs and local concentration are two crucial factors determining the fate of cancer cells (especially the tumour stem cells) and the subsequent pathological remission rate.[15] Traditionally, the pre-operative chemotherapy is carried out through intravenous infusion. Under this condition, the effective concentration of chemotherapeutic drugs in local lesion is relatively low and, therefore, the effectiveness will be achieved after prolonged courses of the treatment. In addition, intravenous chemotherapy may result in drug resistance of cancer cells. Nevertheless, in the intra-arterial chemotherapy, the effective concentration of chemotherapeutic drugs in local lesion, surrounding tissues and lymph nodes is significantly elevated.[16,17] Previously, the blood supply of breast cancer was considered to be mainly from internal mammary artery. Therefore, in superselective intra-arterial chemotherapy, the chemotherapeutic drugs were infused into internal mammary artery. However, in recent studies[18-20], results revealed the lateral thoracic artery was the dominant feeding artery of breast cancer followed by thoracic artery and subscapular artery. At the same time, the metastasis of breast cancer is done through ipsilateral axillary lymph nodes which are supplied by thoracic artery and subscapular artery. Therefore, the optimal target in superselective intra-arterial chemotherapy should be the blood vessel network in the breast cancer and the axillary arteries[8] and the area supplied by these blood vessels is also called target region. In the present study, superselective intra-arterial chemotherapy was performed and the effective concentration of chemotherapeutic drugs in the local target region was dramatically increased in unit time, resulting in increased time-density/intensity. Therefore, the primary lesion and surrounding potential lesions as well as lymph nodes were effectively chemically treated which further increased the pathological remission rate and reduced the local recurrence and the risk for distant metastasis.

The favourable sensitivity to chemotherapeutic drugs but poor prognosis of triple-negative breast cancer may be contributed to the difficult detection of local skin metastases, lymph node metastases or even distant micrometastases. In traditional chemotherapy, the effective concentration in local lesion is relatively low in unit time and subsequently the cancer cells can not be completely killed, which, however, may lead to drug resistance of cancer cells affecting the efficacy of chemotherapy. Our results showed the advantages of targeted chemotherapy in the increased efficacy, down-staging, improved lymph node metastasis, cCR, and pCR over traditional chemotherapy ($P<0.05$). Furthermore, the mean course of targeted chemotherapy was only 15 days which was also shorter than that in the control group (31 days). These results revealed the superselective intra-arterial chemotherapy could increase the local effective concentration of chemotherapeutic drugs, possess favourable efficacy demonstrated by the decrease in tumour size and rapidly control the disease progression, which are critical for the killing of cancer cells as soon as possible.

Pre-operative superselective intra-arterial chemotherapy, on one hand, can increase the local effective concentration after the regional infusion, and more cancer cells can be killed when completely contacting with drugs. As a result, the tumour could be shrunk in a large scale. Therefore, the man-made spread of cancer cells during operations and post-operative recurrence as well as metastasis are prevented. On the other hand, the infused drugs are transferred into the systemic circulation. Therefore, not only local chemotherapy but systemic chemotherapy is carried out. In the present study, there was no significant difference in the side effects of chemotherapy between both groups, which suggested the concentration of drugs in the systemic circulation was also comparative with that in traditional chemotherapy. This effect is critical for the control of subclinical lesion and benefits for the complete remission in pathology. Moreover, the mortality in the targeted chemotherapy was lower than that in the control group, which also demonstrated the advantage of targeted chemotherapy in improving the prognosis of triple-negative breast cancer.

Acknowledgment

This study was supported by Science and Technology Program of Guangdong Province (NO.73125) and Key Science and Technology Program of Shenzhen City (NO.200801004).

References

1. Bauer KR, Brown M, Cress RD, Parise CA, Caggiano V. Descriptive analysis of estrogen receptor (ER)-negative, progesterone receptor (PR)-negative, and HER2-negative invasive breast cancer, the so-called triple-negative phenotype: a population-based study from the California cancer Registry. *Cancer* 2007; **109:** 1721-8.
2. Cleator S, Heller W, Coombes RC. Triple-negative breast cancer: therapeutic options. *Lancet Oncol* 2007; **8:** 235-44.
3. Foulkes WD, Smith IE, Reis-Filho JS. Triple-negative breast cancer. *N Engl J Med* 2010, **363:** 1938-48.
4. Ovcaricek T, Frkovic SG, Matos E, Mozina B, Borstnar S. Triple negative breast cancer – prognostic factors and survival. *Radiol Oncol* 2011; **45:** 46-52.
5. Rakha EA, El-Sayed ME, Green AR, Lee AH, Robertson JF, Ellis IO. Prognostic markers in triple-negative breast cancer. *Cancer* 2007; **109:** 25-32.
6. Billar JA, Dueck AC, Stucky CC, Gray RJ, Wasif N, Northfelt DW, et al. Triple-negative breast cancers: unique clinical presentations and outcomes. *Ann Surg Oncol* 2010; **17(Suppl 3):** 384-90.
7. Anders CK, Winer EP, Ford JM, Dent R, Silver DP, Sledge GW, et al. Poly(ADP-Ribose) polymerase inhibition: "Targeted" therapy for triple-negative breast cancer. *Clin Cancer Res* 2010; **16:** 4702-10.
8. Wang XM, He JS, Tong JM. Clinical application of preoperative superselective intra-arterial chemotherapy in the treatment of late breast cancer cases. *Journal of Surgery Concepts & Practice* 2006; **11:** 136-8.
9. Zuo WS. *Modern molecular oncology of breast cancer.* 2nd edition. Shandong: Shandong Science & Technology Press; 2006. p. 974-9.
10. Huober J, von Minckwitz G, Denkert C, Tesch H, Weiss E, Zahm DM, et al. Effect of neoadjuvant anthracycline-taxane-based chemotherapy in different biological breast cancer phenotypes: overall results from the GeparTrio study. *Breast Cancer Res Treat* 2010; **124:** 133-40.
11. Yi SY, Ahn JS, Uhm JE, Lim do H, Ji SH, Jun HJ, et al. Favorable response to doxorubicin combination chemotherapy does not yield good clinical outcome in patients with metastatic breast cancer with triple-negative phenotype. *BMC Cancer* 2010; **10:** 527.
12. Bryan BB, Schnitt SJ, Collins LC. Ductal carcinoma in situ with basal-like phenotype: a possible precursor to invasive basal-like breast cancer. *Mod Pathol* 2006; **19:** 617-21.
13. Carey LA, Dees EC, Sawyer L, Gatti L, Moore DT, Collichio F, et al. The triple negative paradox: primary tumor chemosensitivity of breast cancer subtypes. *Clin Cancer Res* 2007; **13:** 2329-34.
14. Maegawa RO, Tang SC. Triple-negative breast cancer: unique biology and its management. *Cancer Invest* 2010; **28:** 878-83.
15. Ocvirk J. Advances in the treatment of metastatic colorectal carcinoma. *Radiol Oncol* 2009; **43:** 1-8.
16. Maurer CA, Borner M, Buchler MW. Regional chemotherapy of gastrointestinal cancer. *Digestive Surg* 1997; **14:** 9-22.
17. Miura T, Takeuchi I, Kikuoka S, Miura T. Intra-arterial infusion chemotherapy for advanced breast cancer – 5 cases of marked response. *Gan To Kagaku Ryoho* 2009; **36:** 2108-10.
18. Vanel D. Interventional radiology: the new daily work of the breast radiologist. *Eur J Radiol* 2002; **42:** 1.
19. Pacetti P, Mambrini A, Paolucci R, Sanguinetti F, Palmieri B, Della Seta R, et al. Intra-arterial chemotherapy: a safe treatment for elderly patients with locally advanced breast cancer. *In Vivo* 2006; **20:** 761-4.
20. Takizawa K, Shimamoto H, Ogawa Y, Yoshimatsu M, Yagihashi K, Nakajima Y, et al. Development of a new subclavian arterial infusion chemotherapy method for locally or recurrent advanced breast cancer using an implanted catheter-port system after redistribution of arterial tumor supply. *Cardiovasc Inter Rad* 2009; **32:** 1059-66.

case report

Giant Brunner's gland adenoma as an unusual cause of anaemia: report of a case

Ali Coskun[1], Nazif Erkan[1,2]

[1] Department of Surgery, Izmir Bozyaka Training and Research Hospital, Izmir, Turkey
[2] Department of Emergency Medicine, Izmir Bozyaka Training and Research Hospital, Izmir, Turkey

Received 27 July 2010
Accepted 14 September 2010

Correspondence to: Assoc. Prof. Nazif Erkan MD, 2040/5 Sok. No: 8 Flamingo 9 D.39 Mavişehir-Karşıyaka İzmir, Turkey. Phone: +90 505 5307807, Fax: +90 232 2277201; E-mail: naziferkan@gmail.com

Disclosure: No potential conflicts of interest were disclosed.

Background. Brunner's gland adenoma (BGA) is a rare benign duodenal tumour proliferating from Brunner's glands. Here, we present a giant BGA leading to anaemia, with its clinical, endoscopic, radiological, surgical and pathological findings.

Case report. A 48-year-old Turkish man complained of a six months history of vague epigastric discomfort, loss of appetite and nausea after meals without vomiting. The physical examination had no unremarkable finding. Laboratory findings, including liver function tests, were within normal limits except a hypochromic, microcytic anaemia. The upper gastrointestinal endoscopic examination revealed a lobulated, red, polypoid tumour with a smooth surface covered with normal mucosa. The tumour was located on the anterior surface of duodenal bulb and had a wide base measuring 3.5 x 4 cm in size. Endoscopic ultrasonography revealed a submucosal polypoid mass located at the anterior surface of duodenal bulb. The endoscopic excision was tried but was not successful. The patient was operated and transduodenal polypectomy was done. The postoperative period was uneventful and the pathologic diagnosis was assessed as Brunner's gland adenoma. During the follow-up period, the endoscopic examination was normal at 12th month postoperatively.

Conclusions. BGA is a rare benign cause of anaemia that can be treated with excellent results.

Key words: Brunner's gland; adenoma; anaemia

Introduction

Brunner's gland adenoma (BGA), also known as Brunneroma or polypoid hamartoma, is a rare benign duodenal tumour proliferating from Brunner's glands of duodenum. They are usually asymptomatic and discovered during endoscopy or on an upper gastrointestinal series.[1]

Here we present a giant BGA leading to anaemia, with its clinical, endoscopic, radiological, surgical and pathological findings.

Case Report

A 48-year-old Turkish man complained of a six months history of vague epigastric discomfort, loss of appetite and nausea after meals without vomiting. The physical examination had no unremarkable finding. Laboratory findings, including liver function tests, were within normal limits except a hypochromic, microcytic anaemia (Haemoglobin: 10 g/dl). The upper gastrointestinal endoscopic examination revealed a lobulated, red colour, polypoid tumour with a smooth surface covered with normal mucosa (Figure 1). The tumour located on the anterior surface of duodenal bulb had a wide base measuring 3.5 x 4 cm in size. Endoscopic ultrasonography revealed a submucosal polypoid mass located at the anterior surface of duodenal bulb (Figure 2).

The endoscopic excision was tried but was not successful and biopsy was made and it was reported as gastric metaplasia. The patient was operated. A duodenotomy was performed and anteriorly located tumour was totally excised. The postoperative period was uneventful and the pathologic diagnosis was assessed as Brunner's gland adenoma

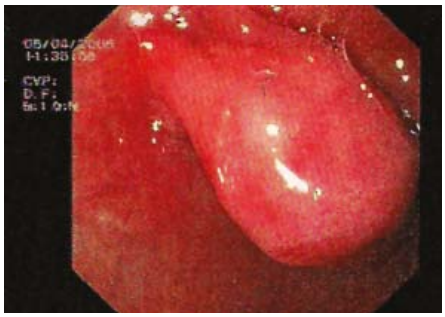

FIGURE 1. Upper GI endoscopic examination revealed a lobulated, red, polypoid tumour with a smooth surface covered with normal mucosa. The tumour located on the anterior surface of duodenal bulb, had a wide base, measuring 3.5 x 4 cm in size.

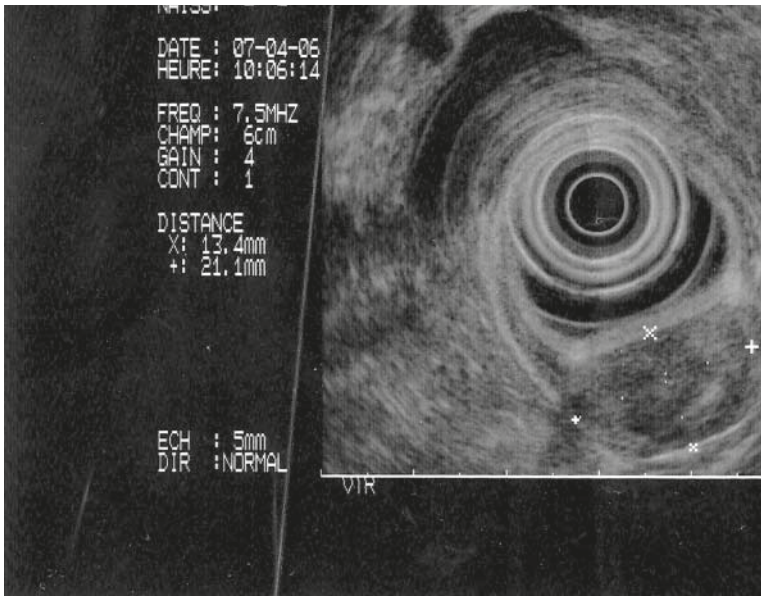

FIGURE 2. Endoscopic ultrasonography revealed a submucosal polypoid mass located at the anterior surface of duodenal bulb.

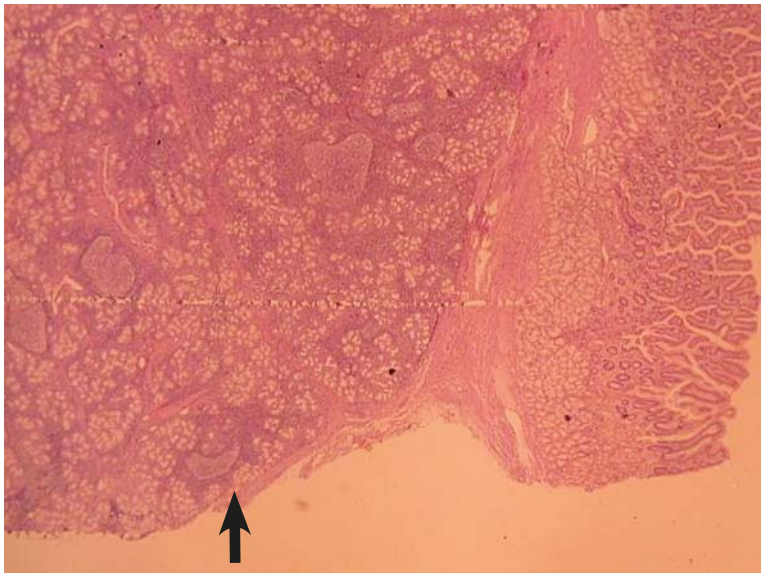

FIGURE 3. Light microscopy revealed hyperplasia of Brunner's glands within the *lamina propria* of the duodenum (dark arrow) and normal duodenal mucosa (white arrow) (H&Ex40).

(Figure 3). During the follow-up period, the endoscopic examination was normal at the 12 month postoperatively. He has been followed without any symptom for four years.

Discussion

Brunner's glands are alkaline secreting glands in the submucosal layer of the duodenum. They are branched acinotubular structure. Brunner first described glands in duodenal tissue in 1688. They secrete mucus, urogastrone and pepsinogen and their primary function appears to protect the surface epithelium from acid chyme from stomach. The majority of glands are located in the first portion of the duodenum with decreasing prevalence in the second and third portion of duodenum.[1,2]

Benign tumours of the duodenum are very rare, with an incidence of 0.008% in a single autopsy study and those BGA comprise 10.6 % of these tumours.[3,4] Since the original description of Brunner's gland hamartoma in 1876 by Salvioli[5], fewer than 200 cases have been reported in English literature.[6] Various nomenclatures have been used to describe these tumours including Brunner's gland hamartoma, adenoma and Brunneroma. As BGA grow, they typically form polypoid pedunculated masses. The pathogenesis of BGA remains unclear. It has been hypothesized that BGA is related to hyperacidity with compensatory growth of the alkaline-secreting Brunner's gland, or to Helicobacter pylori infection.[2,6] BGA has equivalent gender and race distribution with age of presentation typically in the fifth or sixth decade of life. BGA is often an incidental finding during esophago-gastro-duodenoscopy or imaging studies as majority of patients are asymptomatic. In these patients tumour tends to be smaller, which may account for their absence of symptoms.

In symptomatic patients, BGA presents with hemorrhagic or obstructive symptoms. A group of patients presented with tumour-related blood loss, which, in the majority, is chronic and does not result in hemodynamic instability. The BGA could lead to a gross upper gastrointestinal bleeding due to ulceration of the mucosa especially in tumours located in the first portion of the duodenum.[7] Another group of patients with BGA presented with prolonged histories of obstructive upper gastrointestinal symptoms such as epigastric pain, bloating and early satiety. Rare presentations include obstructive jaundice and intussusception due to localization and size of the tumour.[8] In our

patient, BGA is located in the first portion of duodenum, and leads to dyspeptic symptoms with anaemia due to a chronic blood loss.

The diagnosis of this lesion can be made like in other intestinal tumours radiologically or endoscopically.[9] Before endoscopy, small bowel series were the main tool for the diagnosis. The pedunculated BGA is featured by a well-defined smooth and round filling defect, whereas the nodular and diffuse varieties are seen as multiple filling defects in the duodenum, described as "Swiss cheese" in appearance**.** The description of BGA on computed tomography has been limited but varies from homogenous enhancement with intravenous contrast administration to heterogeneous lesions with solid and cystic components.[10] The endoscopic US examination clearly demonstrates heterogeneous lesions with solid and cystic components.[11] Endoscopy allows a direct visualization of the lesion, biopsy to rule out malignancy and the option of the endoscopic resection. Biopsies are typically indeterminate given the submucosal location of the lesion.[5,6,9] In our case, all diagnostic tools including upper gastrointestinal endoscopy and endoscopic US indicated a submucosal polypoid mass.

The pathologic features of these tumours are characteristic. The lack of dysplasia, unusual admixture of normal tissues including Brunner's glands, ducts, adipose tissue and lymphoid tissue consist the texture of pathology.[2] The differential diagnosis includes duplication cyst, leiomyoma, leiomyosarcoma, adenoma or adenocarcinoma, lymphoma, carcinoid tumours, heterotopic pancreatic or gastric tissue or gastrointestinal stromal tumours.[1,2,6]

The treatment can be different according to size, symptoms and suspicious of malignancy. The conservative management is advocated for asymptomatic diffuse hyperplasia because it is considered to have no neoplastic potential. Symptomatic and larger lesions leading to bleeding or obstruction should be excised either endoscopically or surgically. The endoscopic treatment is especially useful for pedunculated lesions. However, if endoscopic interventions fail, the surgical resection may be necessary in symptomatic patients or those in whom a malignancy is suspected.[2,7] In our case, the endoscopic removal was unsuccessful since the tumour was huge in size and in a broad wide-base. Then we made a transduodenal polpectomy.

In conclusion, BGA is a rare benign cause of anaemia that could be treated by the endoscopic or the surgical resection with an excellent outcome.

References

1. Rocco A, Borriello P, Compare D, De Collibus P, Pica L, Lacono A, et al. Large Brunner's gland adenoma: Case report and literature review. *World J Gastroenterol* 2006; **12:** 1966-8.
2. Levine JA, Burgart LJ, Batts KP, Wang KK. Brunner's gland hamartomas: Clinical presentation and pathological features of 27 cases. *Am J Gastroenterol* 1995; **90:** 290-4.
3. Nasio J. Tumors of the duodenum. *Semana Med* 1959; **115:** 411-8.
4. Botsford TW, Crowe P, Crocker DW. Tumors of the small intestine. A review of experience with 115 cases including a report of a rare case of malignant hemangioendothelioma *Am J Surg* 1962; **103:** 358-65.
5. Salvioli G. Contributione allo studio delgi: Lo Osservatore E. *Gazzelia Medicica de Torino* 1876; **12:**481.
6. Stewart ZA, Hruban RH, Fishman EF, Wolfgang CL. Surgical management of giant Brunner's gland hamartoma: case report and literature review. *World J Surg Oncol* 2009; **7:** 68-72.
7. Tan YM, Wong WK. Giant Bruneroma as an unusual cause of upper gastrointestinal haemorrhage: Report of a case. *Surg Today* 2002; **32:** 910-12.
8. Hol JW, Stuifbergen W, Tepen J, van Laarhoven C. Giant Brunner's hamartoma of the duodenum and obstructive jaundice. *Dig Surg* 2007; **24:** 452-5.
9. Sofic A, Beslic S, Kocijancic I, Sehovic N. CT colonography in detection of colorectal carcinoma. *Radiol Oncol* 2010; **44:** 19-23.
10. Patel ND, Levy AD, Mehrotra AK, Sobin LH. Brunner gland hyperplasia and hamartoma: Imaging features and clinicopathologic correlations. *Am J Rad* 2005;**187:** 715-22.
11. Hizawa Ki, Iwai K, Esaki M, Suekane H, Inuzuka S, Matsumoto T, et al. Endosographic features of Brunner's gland hamartomas which were subsequently resected endoscopically. *Endoscopy* 2002; **34:** 956-8.

research article

Target and peripheral dose from radiation sector motions accompanying couch repositioning of patient coordinates with the Gamma Knife® Perfexion™

Tuan-Anh Tran[1,2], Vincent Wu[1], Harish Malhotra[1,2,3], James P. Steinman[1,3], Dheerendra Prasad[1,4], Matthew B. Podgorsak[1,2,3]

[1] Department of Radiation Medicine, Roswell Park Cancer Institute, Buffalo, USA
[2] Department of Molecular and Cellular Biophysics and Biochemistry, Roswell Park Cancer Institute, Buffalo, USA
[3] Department of Physiology and Biophysics, State University of New York, Buffalo, USA
[4] Department of Neurosurgery, Roswell Park Cancer Institute, Buffalo, USA

Received 31 January 2011
Accepted 13 March 2011

Correspondence to: Tuan-Anh Tran, Ph.D., Roswell Park Cancer Institute, Elm and Carlton Streets, Buffalo, NY 14263, USA. E-mail: ttran3@buffalo.edu

Disclosure: No potential conflicts of interest were disclosed.

Background. The GammaPlan™ treatment planning system (TPS) does not fully account for shutter dose when multiple shots are required to deliver a patient's treatment. The unaccounted exposures to the target site and its periphery are measured in this study. The collected data are compared to a similar effect from the Gamma Knife® model 4C.

Materials and methods. A stereotactic head frame was attached to a Leksell® 16 cm diameter spherical phantom; using a fiducial-box, CT images of the phantom were acquired and registered in the TPS. Measurements give the relationship of measured dose to the number of repositions with the patient positioning system (PPS) and to the collimator size. An absorbed dose of 10 Gy to the 50% isodose line was prescribed to the target site and all measurements were acquired with an ionization chamber.

Results. Measured dose increases with frequency of repositioning and with collimator size. As the radiation sectors transition between the beam on and beam off states, the target receives more shutter dose than the periphery. Shutter doses of 3.53±0.04 and 1.59±0.04 cGy/reposition to the target site are observed for the 16 and 8 mm collimators, respectively. The target periphery receives additional dose that varies depending on its position relative to the target.

Conclusions. The radiation sector motions for the Gamma Knife® Perfexion™ result in an additional dose due to the shutter effect. The magnitude of this exposure is comparable to that measured for the model 4C.

Key words: gamma knife; perfexion; shutter effect; stereotactic radiosurgery; dosimetry

Introduction

The Gamma Knife® Perfexion™ (Elekta Instrument AB, Stockholm, Sweden) has 192 ^{60}Co sources mounted onto eight sectors, forming a partial conical shape inside the Gamma Knife unit.[1-5] The unit includes a Patient Positioning System (PPS) that automatically positions the patient's head to the coordinates of a treatment run by moving the entire couch apparatus to which the patient's head is attached. Before any patient motion (either to the initial treatment position, between consecutive shots, or to the setup position after the final shot), the eight sectors within the unit move to the shielded "sector off" position. When treatment begins, the PPS moves the framed head to the planned treatment coordinates, the radiation sectors move into the appropriate collimator position, and the prescribed dose is delivered.[1-5] The purpose of this study is to evaluate the extent of exposure to patients that is associated with these motions; in particular, with the motions associated with the transition of radiation sectors between the "sector off" position and the open collimator position. The

importance of correct treatment dose in radiation therapy[6], especially hypofractionated treatments[7], has prompted many studies into the accuracy of dose delivery with Gamma Knife radiosurgery.[8-11]

There are three sources of undocumented dose during a typical treatment with the Perfexion™: the transportation dose from leakage and scatter, the leakage and scatter dose during patient positioning between coordinates, and the shutter dose. The transportation dose results from the exposure the patient receives while moving between the setup and treatment position at the beginning and end of a run. Even though the sources are shielded in the "sector off" position during this phase, the shielding doors are open and the patient is exposed to leakage and scatter radiation. While the sectors are in the "off" position, when the PPS undergoes change in treatment coordinates, exposure will result from leakage and scatter from the sources. Finally, the shutter dose results from exposure when the radiation sectors move between the collimator position and the "sector off" position; this occurs before and after the PPS changes shot coordinates as well as before and after a treatment run.

There is considerable emphasis on conformal dose planning, with associated conformity indices providing a quantitative dosimetric quality measure for a radiosurgery treatment plan. Because of the irregular shape of many targets, treatment plans usually call for a considerable number of isocenters to deliver a conformal treatment, resulting in the use of multiple shots requiring multiple repositioning by the PPS with multiple sector transitions. The consequence is the potential for considerable, undocumented dose, the degree of which is evaluated in this work. With the introduction of the Perfexion™, there have been several studies comparing it to its predecessors.[1-3,12-14] In this study, we compare our results to a similar study analyzing added dose from repositioning with the Automatic Positioning System of the model 4C.[15]

Materials and methods

Setup for measurements with an ionization chamber

During the period over which measurements for this study were performed, the dose rate at the center of a spherical calibration phantom (Elekta, Atlanta, GA) for all sectors aligned with the 16 mm collimator ranged from 3.425 to 3.218 Gy/min. Rather than using the plastic connectors and red dosimetry adaptors to attach to the frame adaptor, a standard Elekta stereotactic frame (Leksell Coordinate Frame G, Elekta, Atlanta, GA) was applied to the phantom in order to more accurately simulate the conditions of a typical patient treatment. A CT fiducial box was attached to the framed phantom and subsequently imaged with a GE HiSpeed FX/i CT scanner (GE Healthcare) (Figure 1A, B). Images (1 mm slice thickness) were exported to and registered in the GammaPlan™ (Version 8.3.1, Elekta, Atlanta, GA) treatment planning system. The planning target was selected to be the center of the spherical phantom, where a dose of 10 Gy to the 50% isodose line was prescribed (Figure 2). For delivery of treatment plans, the frame adaptor was attached to the phantom and coupled to the PPS. Within the phantom, a calibrated 0.07 cm^3 cylindrical ionization chamber (model PR-05P, Capintec, Ramsey, NJ) was positioned using a chamber cassette and connected to an electrom-

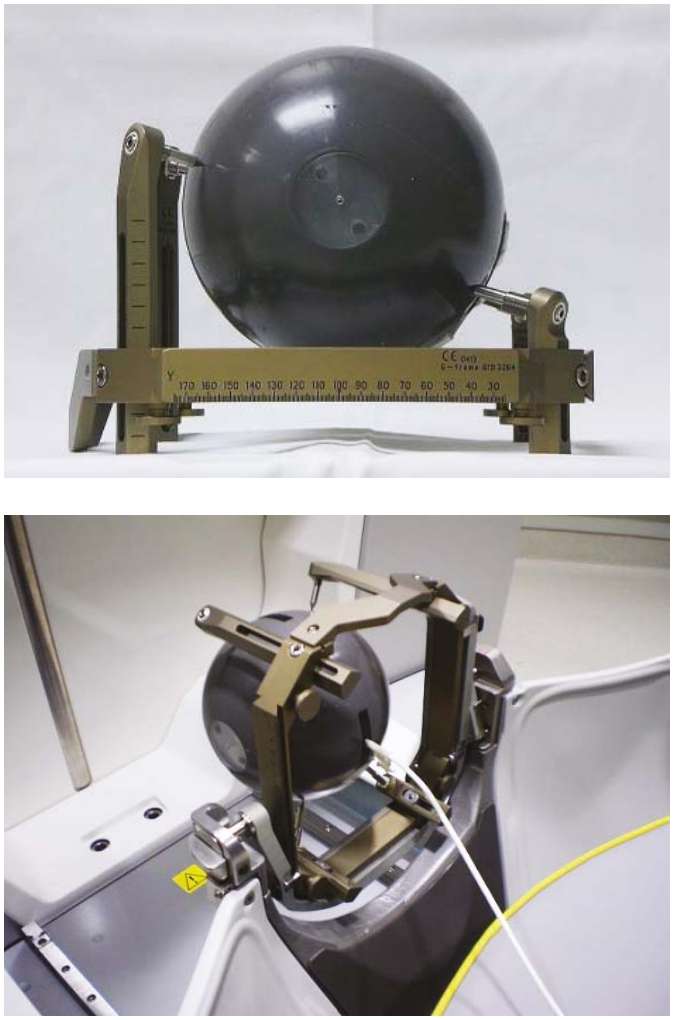

FIGURE 1. Setup of phantom for measurements. A: Framed phantom B: Phantom fixed to the PPS with a frame adaptor.

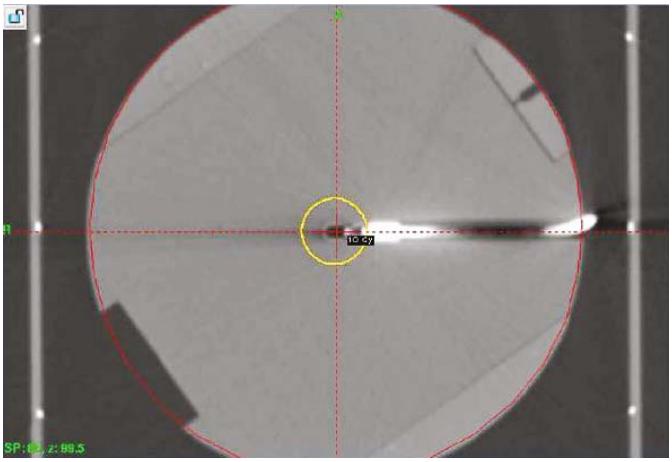

FIGURE 2. CT image of framed spherical phantom. The three fiducial marks are used to determine the treatment coordinates for the center of the spherical phantom. The phantom was imaged with an ionization chamber placed in the cylindrical cavity of the chamber cassette. The 50% isodose line for a shot with the 16 mm collimator is shown.

eter (35617EBS Programmable Dosimeter, Keithley Instruments, Cleveland, Ohio), enabling measurements of dose during irradiation of the phantom. All measurements were taken multiple times to enable statistical analysis. The error represented in all the presented data indicates the standard deviation of the mean of these multiple, independent measurements (Type A error evaluation). The collected shutter data are presented as a dose rate (Gy/min) in the graphs and tables. Representing the shutter effect as Gy/shot (or Gy/reposition) would not be reflective of the differences between the shutter effects for plans with various shots because of its dependence on the source activity, which decays exponentially with time. As the data were acquired over an extended period of time, it seemed most appropriate to compare the shutter effect in terms of a dose rate (Gy/min or cGy/min) that is normalized to the focus dose rate (with the 16 mm collimator). For the shutter dose at the target site, we also present the effect in Gy/shot to enable users of the Perfexion™ to compute the expected shutter dose for their unit by multiplying shutter dose per reposition values with the ratio of dose rates (dose rate on current day to dose rate on the day the original experiment was performed).

Measuring shutter dose to the target

Measurements of shutter doses were carried out for single run treatment plans developed to deliver the same dose to the isocenter with varying numbers of shots (1, 5, 20, 30, and 50) for the 8 and 16 mm collimators. Each run was timed with a stopwatch; the mean time difference between the single shot run and each multiple shot run was used to determine the shutter dose rate. Statistical analysis for the time measurements with the stopwatch were performed with Type A error analysis; the standard deviations of the mean times were calculated to indicate error in this study. The differences between the dose measured for the single shot run and the multiple shot runs for the same prescription dose represent the additional doses to the target site from radiation sector motions. This experimental design eliminates the transportation dose (defined above) because all plans require the same transport from the setup position to the "beam on" position and back. Therefore, the transport dose cancels when the shutter dose is calculated. The shutter effect for the 4 mm collimator was not measured at the target due to concerns with the partial volume effect associated with ionization chamber irradiation.

Measuring shutter dose to the periphery

The shutter effect at the periphery was measured to determine dose to normal tissue, or non-target sites, within the cranium. These measurements were taken for the 4, 8 and 16 mm collimators with the ion chamber. For this study, the spherical phantom had to be framed twice with different orientations to enable measurement of radiation dose along the x-axis (lateral) and the z-axis (cranial-caudal). As a result of the symmetric shape of the collimator assembly, additional dose along the y-axis (anterior-posterior) is expected to be the same as the dose along the x-axis. To measure the dose along the x-axis, a customized cassette with the insert for the ionization chamber was aligned in the transverse plane ensuring the alignment of the cylindrical cavity for the ionization chamber along the x-axis. Though use of the plastic connectors and red dosimetry adaptor allow orientation of the cylindrical cavity along the x- and z-axes for the Perfexion™, this is not possible with the similar calibration setup with the model 4C. Because we compare measurements of these two units, constancy between the methods of measurement is essential for proper evaluations. In addition, the red dosimetry adaptor has been shown to cause unintended attenuation of about 1.0%.[16] Any attenuation resulting from the frame posts will be the same for all measurements.

Measurements were acquired with the ionization chamber center positioned at 0, ±1.2, ±3.2 and ±6.2 cm from the target along the x-axis. Doses for 1, 5,

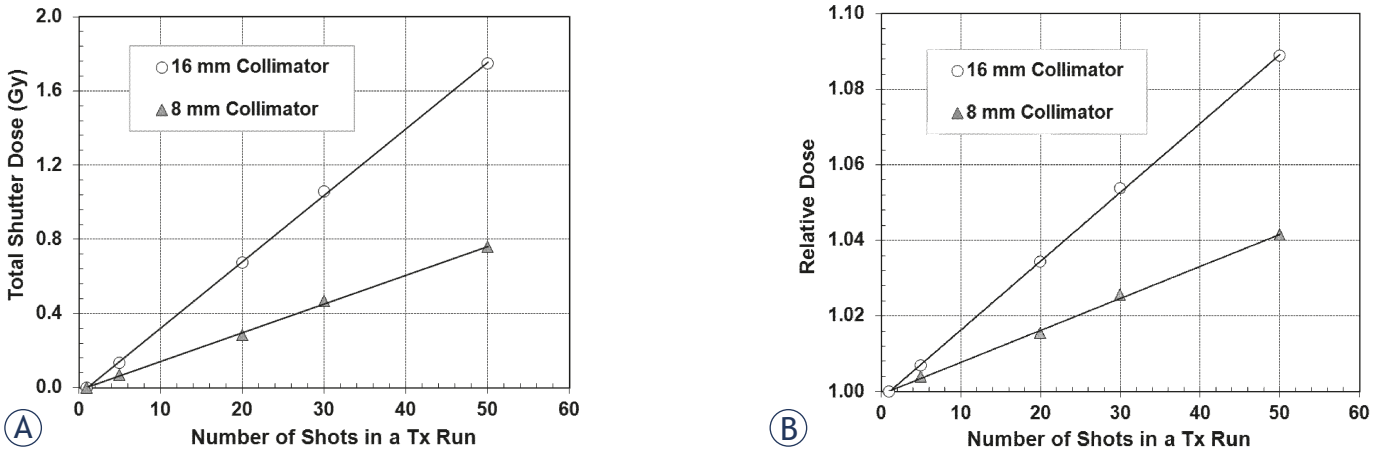

FIGURE 3. Shutter dose for the 8 and 16 mm collimators. A: The target position is the same for all measurements. Measured dose associated with PPS positioning increases with increase in the number of shots in a run and collimator size. B: The relative dose was calculated by normalizing the dose from the multiple shot plans to the single shot plan.

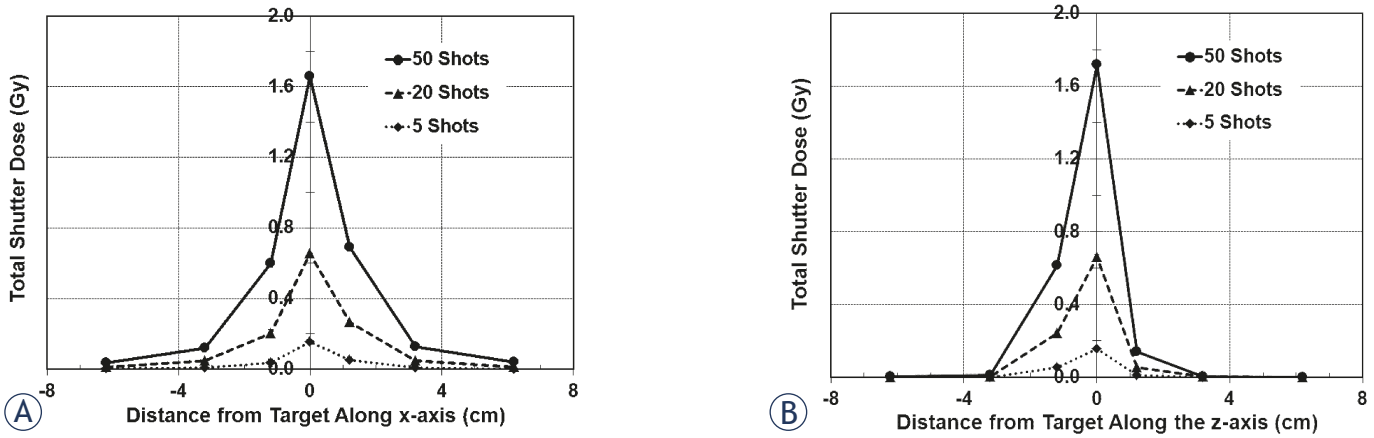

FIGURE 4. Total shutter dose for the 16 mm collimator. A: The shutter dose along the x-axis is greatest at the target site and falls off with distance; it will also increase with the number of shots. B: The shutter dose along the z-axis does not have the same symmetry as it does along the x-axis. The collimators are angled towards the inferior direction; this will increase exposure inferior to the target, as seen.

20 and 50 shot runs were measured at these points along the x-axis to determine the off axis shutter dose. Measurements along the z-axis required the cylindrical cavity to be aligned along the couch longitudinal axis. Along the z-axis, doses for 1, 5, 20 and 50 shot runs were obtained with the ionization chamber centered at 0, ±1.2, ±3.2 and ±6.2 cm from the target to determine the shutter effects to each position. Cylindrical Lucite rods (1, 2 and 3 cm long) of 6 mm diameter were used to position the chamber off-axis. The rods were inserted followed by the chamber, displacing the chamber from the phantom center by the length of the rod(s). With these rods, the chamber can be positioned at 1.2, 3.2 and 6.2 cm from the center of the phantom. The additional 0.2 cm comes from the incomplete insertion of the cylindrical rods at the end of the cavity (in the center of the spherical phantom).

Results

Shutter dose to the target

Figure 3A shows that shutter dose increases with frequency of repositioning and with collimator size. Dose increases of 1.59 ± 0.04 cGy and 3.53 ± 0.04 cGy per reposition were observed for the 8 and 16 mm collimators, respectively. In the extreme case of a 50 shot plan, this represents 75.6 and 174.7 cGy extra dose to the target, compared to the entire planned dose being delivered in a single shot. The shutter dose rate for each of the collimators is listed in Table 1 along with its value relative to the focus dose rate for the day of measurement (3.425 Gy/min for the 16 mm collimator). Figure 3B shows the relative shutter dose for the 8 and 16 mm collimators.

TABLE 1. Shutter and inter-shot transit dose rates at the target. The shutter dose rate is represented as a percent of the focus dose rate on the day of measurements (Perfexion™ had a focus dose rate of 3.425 Gy/min for the 16 mm collimator; model 4C had a focus dose rate of 2.254 Gy/min for 18 mm collimator helmet).

Perfexion™: Collimator Size and Shutter Dose Rates			
Collimator Size (mm)	**Shutter Dose Rate (cGy/min)**	**Percent of Focus Dose Rate (%)**	**Shutter Dose per Reposition (cGy)**
16	40.04 ± 0.51	11.69 ± 0.15	3.53 ± 0.04
8	39.52 ± 1.08	11.54 ± 0.31	1.59 ± 0.04
Model 4C: Collimator Size and Inter-shot Transit Dose Rates			
Collimator Size (mm)	**Transit Dose Rate (cGy/min)**	**Percent of Focus Dose Rate (%)**	**Transit Dose per Reposition (cGy)**
18	8.81 ± 0.41	3.91 ± 0.18	2.37 ± 0.00
14	6.98 ± 0.51	3.10 ± 0.23	1.94 ± 0.00
8	5.89 ± 0.51	2.62 ± 0.23	1.58 ± 0.00

Shutter dose to the periphery

Plotted in Figure 4A is the shutter dose along the x-axis for the 16 mm collimator measured using an ion chamber. There are three separate data sets; each represents a different number of shots in a single run. The greatest shutter dose is at the target site, and falls off nearly symmetrically with increasing distance from the target site. Shutter dose to the periphery increases with increasing number of shots in a run, as is the case with shutter dose to the target site. The average shutter dose per reposition at the target is 3.70 ± 0.04 cGy and falls off symmetrically with distance along the x-axis. Table 2 gives the transit dose rates along the x-axis. Also listed are the percent dose rates (shutter dose rate as a function of the dose rate at the focus point on the day of measurement, which is 3.351 Gy/min for the 16 mm collimator).

Along the z-axis, there is not the same symmetry in shutter dose as seen with dose measurements along the x-axis (Figure 4B). The dose is still highest in magnitude at the target site and falls-off on each side; however, the falloff is steeper in the superior region from the target. The shutter dose per reposition is 3.78 ± 0.10 cGy for the target, while at 6.2 cm on each side of the target, it is nearly zero. Table 2 lists the shutter dose rates along the z-axis; also presented is the percent of the focus dose rate on the day of measurement (3.366 to 3.362 Gy/min with the 16 mm collimator). These measurements were also taken for the 8 mm collimator to determine the shutter effects from the radiation sector motions to these collimators. Figure 5 shows the total shutter dose for the x- and z-axes and Table 3 shows the dose rates for each position measured.

The average shutter dose rates were calculated and plotted for positions along both axes for the 16 mm collimator (Figure 6A). The difference in dose profiles in each axis can be attributed to the inferiorly focused orientation of the beamlets. The discrepancy in transit doses at the target site is due to the non-isotropic isodose distribution at isocenter, where the dose is weighted more in the superior direction. When the ionization chamber is placed at the target, the exposure integrated over the collecting volume will be greater with the ionization chamber oriented in the z-direction (cranial-caudal) than if oriented along the x-direction (left-right). The average shutter dose rates were also calculated and plotted for positions along both axes for the 8 mm collimator (Figure 6B).

Discussion

Measured data

The shutter dose to the target increases with increasing number of shots and collimator size, as shown in Figure 3A. The measured doses for the multiple shot plans were normalized to the expected dose (measured for the single shot plan) and graphed in Figure 3B. There are several factors that contribute to the observed deviation in relative shutter effect for the 16 and 8 mm collimator. The shutter time is longer for the 16 mm collimator (5.38 seconds) than the 8 mm collimator (2.39 seconds), and the collimator size is considerably larger. This means once the sources begin to align with the open collimators, it takes longer to reach alignment, thus depositing more unaccounted dose. These factors contribute a greater measured shutter effect for the 16 mm col-

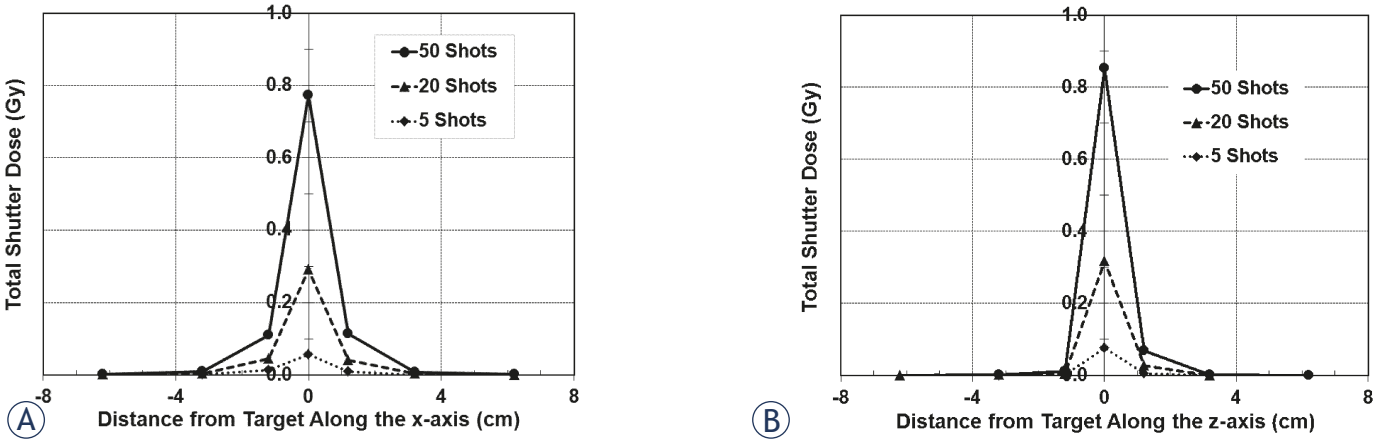

FIGURE 5. Total shutter dose for the 8 mm collimator. A: Measurements along the x-axis. B: Measurements along the z-axis.

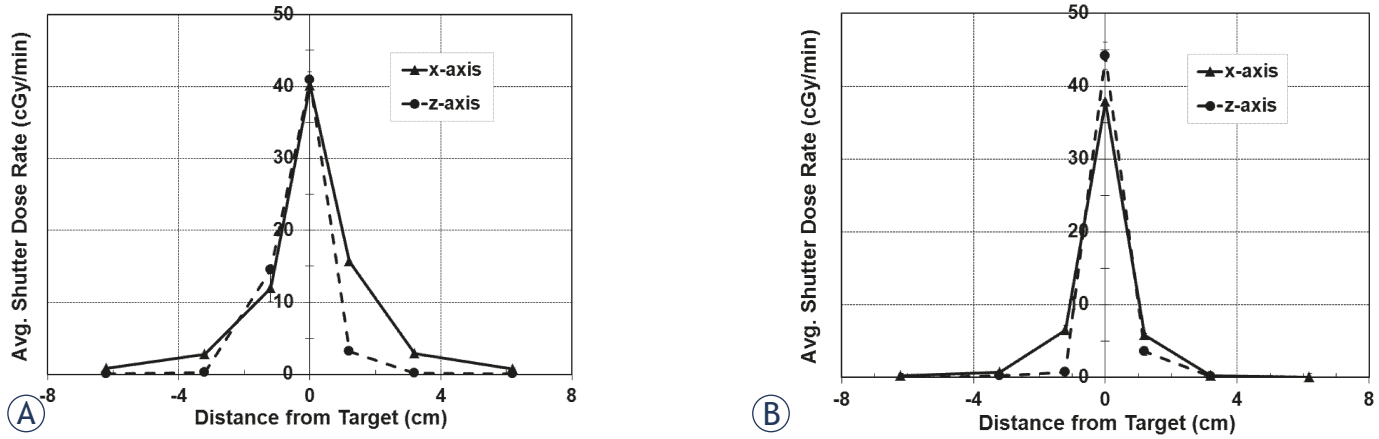

FIGURE 6. A comparison of the average shutter dose rates along the x- and z-axes for the A: 16 mm and B: 8 mm collimators. The difference in dose rates at target site may be due to the orientation of the ionization chamber for each measurement.

limator. Another source of contribution to the shutter dose for the 16 mm collimator is an additional source of radiation. As the sources move from the "sector off" position to the 16 mm collimator position, the sources must flash over the open 4 mm collimator; when the sources retract after the shot is complete, there is another flashing occurrence over the 4 mm collimator. Thus the effective shutter dose from use of the 16 mm collimator comes from both the 4 mm and 16 mm collimators. This passing motion would contribute additional dose, resulting in a larger relative shutter effect from the 16 mm collimator measurements than expected.

Multiple shots in a run will result in additional, unaccounted exposure of surrounding normal tissue from the shutter effect because the GammaPlan™ software does not fully account for the sector motions accompanying PPS repositioning. This is especially true for plans that require larger collimator sizes and greater number of shots. The amount of peripheral exposure during repositioning will depend on location – proximity to the target site means greater exposure from the shutter effect.

There are other considerations that may change the total unaccounted dose during treatment. The PPS does not change coordinates until the sectors reach the "sector off" position; this minimizes the exposure from leakage and scatter dose. Because our experimental design does not include actual position change through PPS motions, there may be added dose from leakage and scatter when there are changes in treatment coordinates during an actual treatment. The activity of the sources affects the leakage and scatter radiation to the patient during coordinate repositioning; higher activity sources will contribute more unintended exposure to the patient during positioning than lower activity sources.

The shutter dose rate is dependent on the activity of the sources in a predictable manner over time. It may also depend on the time it takes for the sectors to move from the open collimator position to

TABLE 2. Shutter dose rates (Perfexion™) and Inter-shot Transit dose rates (model 4C) along the x and z-axes. The shutter dose rate is also represented as a percentage of the focus dose rate on the day of measurement (Perfexion™ had focus dose rates ranging from 3.366 to 3.351 Gy/min for the 16 mm collimator; model 4C had a focus dose rate of 2.220 Gy/min for 18 mm collimator helmet).

Dose Rates Along the x-axis				
	Perfexion™ (16 mm Collimator)		Model 4C (18 mm Collimator)	
Position (cm)	Shutter Dose Rate (cGy/min)	Percent of Focus Dose Rate (%)	Transit Dose Rate (cGy/min)	Percent of Focus Dose Rate (%)
-6.2	0.91 ± 0.08	0.27 ± 0.02	0.36 ± 0.06	0.16 ± 0.03
-3.2	2.88 ± 0.08	0.85 ± 0.02	0.70 ± 0.04	0.32 ± 0.02
-1.2	12.51 ± 2.63	3.72 ± 0.62	6.11 ± 1.85	2.75 ± 0.83
0	41.80 ± 0.55	12.42 ± 0.12	7.72 ± 0.08	3.48 ± 0.04
1.2	16.30 ± 0.07	4.84 ± 0.02	5.28 ± 2.45	2.38 ± 1.10
3.2	3.03 ± 0.08	0.90 ± 0.02	0.59 ± 0.02	0.27 ± 0.01
6.2	0.79 ± 0.12	0.23 ± 0.02	0.36 ± 0.04	0.16 ± 0.02
Dose Rates Along the z-axis				
	Perfexion™ (16 mm Collimator)		Model 4C (18mm Collimator)	
Position (cm)	Shutter Dose Rate (cGy/min)	Percent of Focus Dose Rate (%)	Transit Dose Rate (cGy/min)	Percent of Focus Dose Rate (%)
-6.2	0.05 ± 0.03	0.02 ± 0.01	0.00 ± 0.00	0.00 ± 0.00
-3.2	0.28 ± 0.04	0.08 ± 0.01	0.10 ± 0.10	0.05 ± 0.05
-1.2	15.09 ± 0.28	4.48 ± 0.08	Not Measured	Not Measured
0	42.63 ± 1.12	12.66 ± 0.33	8.66 ± 0.19	3.90 ± 0.08
1.2	3.27 ± 0.21	0.97 ± 0.06	1.37 ± 0.30	0.62 ± 0.14
3.2	0.15 ± 0.03	0.04 ± 0.01	1.88 ± 0.14	0.85 ± 0.06
6.2	0.03 ± 0.02	0.01 ± 0.00	3.34 ± 0.04	1.51 ± 0.02

the off position; this value may not be the same for all Perfexion™ units. In an actual patient treatment, the unaccounted dose will also depend upon the time needed for the PPS to transit between treatment coordinates. With the hybrid shot capability of the Perfexion™, shutter dose may depend on the combination of collimation that makes up a shot.[17] Finally, the maximum number of shots used in this study is 50 in a single treatment run. If more shots and runs are required, the unaccounted dose may be more than reported here.

For these measurements, the target site for all shots is fixed to the unit isocenter at (100, 100, 100). However, a typical treatment plan will have shots that are distributed to cover a volume that encompasses the target site, where none of the shots are overlapping. The excess target and peripheral dose rates for each collimator can be applied to each shot of a treatment plan to determine the overall distribution of excess dose from shutter with the Perfexion™. The shape of a treatment target can vary extensively; in addition, treatments will also depend on the bias of the planner. Because there are no standard treatment plans for an irregularly shaped target and because of the subjectivity with planning, formulating a treatment plan for a hypothetical target volume gives no indication on the effect of shutter to other treatment plans. Rather, the additional target and peripheral dose from shutter per shot for each collimator can be used and applied to the position of each shot to determine the distribution of additional dose from shutter. That is, using the coordinates of each shot, the shutter dose profile can be applied to their respective shot to map the shutter dose distribution for a treatment volume. Figures 4, 5 and 6 show the shutter dose profiles and display the shutter effects to regions peripheral to the target site.

Perfexion™ *vs.* model 4C

Gamma Knife radiosurgery is a highly precise stereotactic tool for the treatment of intracranial disease.[18-22] The introduction of the Automatic

Positioning System (APS) with the model C appreciably streamlined the dose delivery process by enabling delivery of multiple shots within a single treatment run.[19,20,23] The APS is an analogous device to the PPS; it repositions the patient's head to allow therapeutic dose delivery to target site(s), though with a much smaller coordinate repositioning range than the PPS.[1-3] Repositioning with the APS also has an element that contributes unaccounted exposure – the intershot transit effect.[13] A similar study was conducted with the APS of the Gamma Knife® model 4C using an ionization chamber as the dosimeter.[15] As a part of this work, we compare the shutter effect of the Perfexion™ with the inter-shot transit effect of the model 4C previously measured.

With the model 4C, inter-shot transit dose rates were measured for the 8, 14 and 18 mm collimators. To compare the data from the model 4C with the Perfexion™, the shutter and transit dose rates were normalized using the calibrated focus dose rates for the day of measurement. Table 1 shows the transit and shutter dose rates relative to the focus dose rates. For all collimator sizes, the Perfexion™ has a greater shutter dose rate than the transit dose rate of the model 4C; however, the shutter doses are comparable to the transit doses. The differences between the dose rates can be attributed to the shorter time for the radiation sectors to move from a collimator to the "sector off" position (for the Perfexion™) than the time for the couch to move from the focus to defocus position (of the model 4C). Though the design of each model is different, the shutter doses are comparable to the intershot transit doses. Figure 7 shows the relative shutter and transit doses to the target for each model; the added dose is collimator and shot dependent. Comparing the additional dose measured for the 8 mm collimator for both models, the doses per reposition are nearly identical (Table 1). Of course, if the calibrated focus dose rate of the model 4C were the same as the Perfexion™ (2.254 versus 3.425 Gy/min, respectively) then the added dose would probably be larger for the model 4C. The activity of the sources will affect the unaccounted dose.

In Table 2, the shutter dose rates for the 16 mm collimator of the Perfexion™ and the transit dose rates for 18 mm collimator helmet of the model 4C are compared along the x- and z-axes. As a fraction of the focus dose rate, the shutter effect for

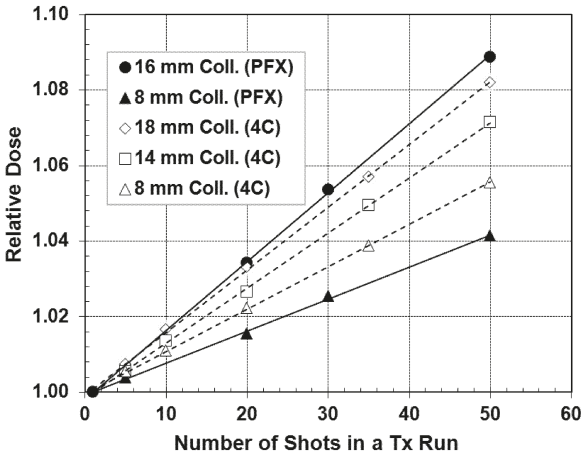

FIGURE 7. Shutter and inter-shot transit dose at the target site for the Gamma Knife® Perfexion™ (PFX) and model 4C (4C), respectively. The shutter and inter-shot transit doses are not accounted for by the treatment planning system.

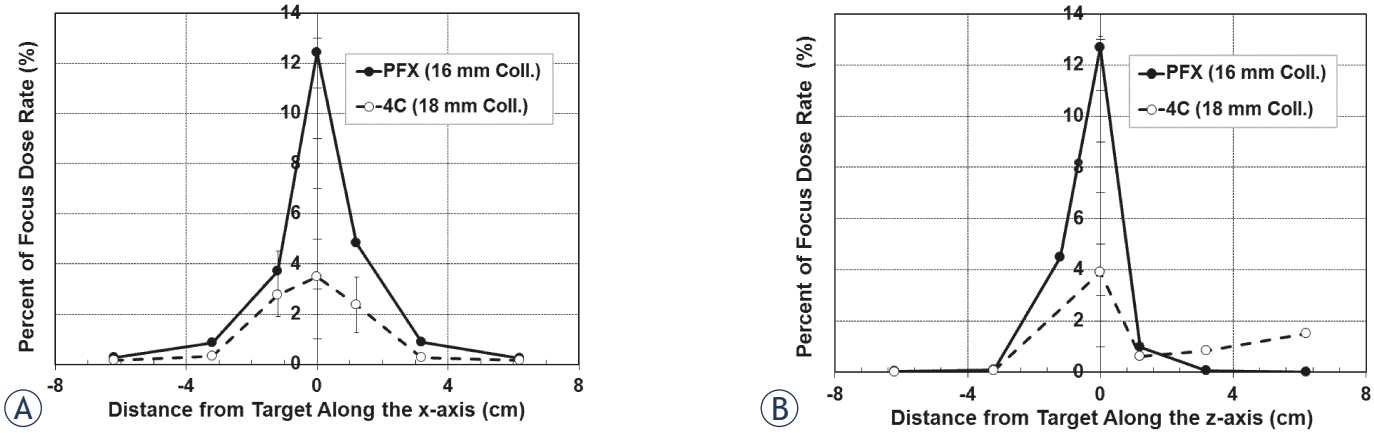

FIGURE 8. A comparison of the shutter dose rate (as a percent of the focus dose rate with the 16 mm collimator) for the Perfexion™ to the inter-shot transit dose rate (as a percent of the focus dose rate with the 18 mm collimator) for the model 4C. A: Along the x-axis, the shutter and transit dose rates are similar in behavior, but the shutter effect with the Perfexion™ is greater than the transit effect with the model 4C. B: The effect is different between the two models in the superior region, along the z-axis. The dose falls off from the target position then increases with the model 4C; the falloff of the shutter dose is sharper in the superior region for the Perfexion™. This can be attributed to the difference in machine design and treatment coordinate change between the two models.

TABLE 3. Shutter Dose Rates along the x-axis for the 4 and 8 mm collimators. For these measurements, the focus dose rate ranged from 3.230 to 3.221 Gy/min. The shutter dose rate is represented as a percent of the focus dose rate on the day of measurement for the 16 mm collimator.

Dose Rates Along the x-axis				
	4 mm Collimator		8 mm Collimator	
Position (cm)	Shutter Dose Rate (cGy/min)	Percent of Focus Dose Rate (%)	Shutter Dose Rate (cGy/min)	Percent of Focus Dose Rate (%)
-6.2	0.00 ± 0.09	0.00 ± 0.01	0.22 ± 0.22	0.07 ± 0.09
-3.2	0.65 ± 0.04	0.20 ± 0.02	0.74 ± 0.09	0.23 ± 0.04
-1.2	4.96 ± 0.16	1.53 ± 0.07	6.50 ± 0.65	2.01 ± 0.25
0	Not Measured	Not Measured	37.86 ± 0.28	11.72 ± 0.14
1.2	1.74 ± 0.25	0.54 ± 0.09	5.81 ± 0.27	1.80 ± 0.11
3.2	0.35 ± 0.13	0.11 ± 0.05	0.18 ± 0.29	0.06 ± 0.07
6.2	-0.23 ± 0.15	-0.07 ± 0.05	0.03 ± 0.07	0.01 ± 0.02
Dose Rates Along the z-axis				
	4 mm Collimator		8 mm Collimator	
Position (cm)	Shutter Dose Rate (cGy/min)	Percent of Focus Dose Rate (%)	Shutter Dose Rate (cGy/min)	Percent of Focus Dose Rate (%)
-6.2	-0.08 ± 0.17	-0.03 ± 0.05	-0.03 ± 0.58	-0.01 ± 0.15
-3.2	0.03 ± 0.12	0.01 ± 0.02	0.24 ± 0.57	0.07 ± 0.23
-1.2	2.15 ± 0.11	0.66 ± 0.05	0.66 ± 0.57	0.21 ± 0.23
0	Not Measured	Not Measured	44.16 ± 1.84	13.67 ± 0.83
1.2	0.12 ± 0.01	0.04 ± 0.01	3.57 ± 0.57	1.10 ± 0.23
3.2	0.06 ± 0.22	0.02 ± 0.05	0.08 ± 0.57	0.02 ± 0.22
6.2	0.16 ± 0.22	0.05 ± 0.06	-0.05 ± 0.57	-0.01 ± 0.19

the Perfexion™ is larger than the transit effect of the model 4C along the x-axis. However, along the z-axis, the corresponding effect is more substantial for the model 4C in regions superior to the target than with the Perfexion™. This can be attributed to the helmet and repositioning design of the model 4C. Greater transit dose rates are seen at more superior regions within the phantom because of proximity to the sources. Also, as the helmet moves away from and towards the sources during repositioning, the unfocused beam will intersect the fiberglass helmet cap (where there is little attenuation of the beam) exposing the superior region of the phantom or patient to unintended radiation.[24-25] The transit dose increases at positions closer to the crown of the head because of the poorly shielded 23 cm diameter opening at the helmet's apex, which results in more exposure from leakage and scatter to the superior regions of the phantom.[15,24] This is the reason for the behavior of the increased transit dose towards the superior portion of the z-axis for the model 4C. With the Perfexion™, this is not observed because the radiation sectors are the components of the unit that move in order to reduce exposure during repositioning, not the couch.

Figure 8A and 8B plot the behavior of the shutter and transit effect as a function of the calibrated focus dose rate along both x- and z-axes for their respective model. Figure 8A shows a similar trend between each model, with the major difference seen with magnitude. In Figure 8B, a difference in the region superior to the target can be seen, which can be attributed to the difference in design of each model. The model 4C has a poorly shielding helmet cap that allows contribution of additional dose. In terms of limiting the shutter dose to the target, there is an improvement with the latest model. Additional dose to the target site is not a vital issue because when planning a treatment, the limitation is the dose to the peripheral structure, especially critical structures. The focus on shutter dose is therefore not because of significant concern of added dose to the target, but rather, additional dose to the periphery of the target. Accounting for this shutter effect would better document dose to

peripheral structures as well as improve dosimetric accuracy of the treatment plan.

Previous studies

A study of the relative output factors of the 4 and 8 mm collimators of the Perfexion™ was reported by Novotny *et al*.[9] To correct for the relative output factors, the authors also report the transition doses (which we define as the shutter dose) for all three collimators in this study: 0.98, 1.51, and 3.46 cGy for the 4, 8 and 16 mm collimators, respectively.[9] This was measured with an ionization chamber in the spherical phantom using the red dosimetry adaptor. These values are consistent with our values for shutter measured with the 8 and 16 mm collimators (1.59 and 3.53 cGy per reposition, respectively, as seen in Table 1); however, no dose rate for the original experiment is reported in their article so we are unable to conclusively compare our data.

In the Perfexion™ manual, a value is given for the shutter dose for the 4 mm collimator; however, there are no indications of the method used to obtain this value. The magnitude of the shutter effect for a dose rate of 3.0 Gy/min is 0.005 Gy per reposition (or 0.5 cGy/reposition). This value is approximately half the value of that reported by Novotny *et al*.

Ruschin *et al*. conducted a thorough investigation of peripheral dose from the treatment of large lesions with the Perfexion™.[11] They conducted measurements studying the effect of the target's volume and collimator size on peripheral exposures.[11] Many of these plans were generated with a significant number of shots to adequately cover the target site with the appropriate dose prescription, but contribution from the shutter effect is not considered in their study. Given the positions of each shot, the values we measured for peripheral shutter dose can be used to determine the overall shutter dose distribution and contribution to their measured data.

Conclusions

For multiple shot runs, radiation sector motions result in additional dose to the target site and its periphery due to the shutter effect. The relationship between unaccounted dose and collimator size, shutter dose and number of repositions, and the positional dependence of the shutter dose to the focus are reported. The shutter dose rates are greater with the Perfexion™ than with the model 4C, but the shutter doses are comparable to the intershot transit dose. Though regarded as a highly accurate modality for intracranial radiosurgery, there is still potential for substantial unaccounted dose during treatment resulting from radiation sector motions accompanying PPS repositioning. This may be important for treatment areas around critical structures within the brain. Further characterization of exposure from the radiation sector motions accompanying movement of the PPS and better documentation of these radiation doses would improve the accuracy of the calculated treatment plans.

Acknowledgment

The authors would like to thank Mary Elizabeth Jurca, RN for her assistance with equipment acquisition and scheduling throughout this study.

References

1. Lindquist C, Paddick I. The Leksell Gamma Knife Perfexion and comparisons with its predecessors. *Neurosurgery* 2007; **61:** 130-40.
2. Lindquist C, Paddick I. The Leksell Gamma Knife Perfexion and comparisons with its predecessors. *Neurosurgery* 2008; **62:** 721-32.
3. Sheehan J. Gamma Knife surgery: past to perfexion. *J Neurosurg* 2008; **109:** 1.
4. Ma L, Verhey L, Chuang C, Deschovich M, Smith V, Huang K, et al. Effect of composite sector collimation on average dose fall-off for Gamma Knife Perfexion. *J Neurosurg* 2008; **109:** 15-20.
5. Regis J, Tamaura M, Guillot C, Yomo S, Muraciolle X, Nagaje M, et al. Radiosurgery with the world's first fully robotized Leksell Gamma Knife PerfeXion in clinical use: a 200-patient perspective, randomized, controlled comparison with the Gamma Knife 4C. *Neurosurgery* 2009; **64:** 346-55.
6. Stavrev P, Schinkel C, Stavreva N, Fallone BG. How well are clinical gross tumor volume DVHs approximated by an analytical function? *Radiol Oncol* 2009; **43:** 132-5.
7. Strojnik A. Search of the shortest regimen: fractionation of a fully isoeffective combination of hyperfractionated and hypofractionated treatment. *Radiol Oncol* 2008; **42:** 170-2.
8. Ma L, Kjall P, Novotný Jr J, Nordstrom H, Johansson J, Verhey L. A simple and effective method for validation and measurement of collimator output factors for Leksell Gamma knife® Perfexion™. *Phys Med Biol* 2009; **54:** 3897-907.
9. Novotný Jr J, Bhatnager JP, Quader MA, Bednarz G. Measurement of relative output factors for the 8 and 4 mm collimators of the Leksell Gamma Knife Perfexion by film dosimetry. *Med Phys* 2009; **36:** 1768-74.
10. Yang DY, Sheehan J, Liu YS, ChangLai SP, Pan HC, Chen CJ, et al. Analysis of factors associated with volumetric data errors in gamma knife radiosurgery. *Stereotact Funct Neurosurg* 2009; **87:** 1-7.
11. Ruschin M, Nordstrom H, Kjall P, Cho YB, Jaffray D. Investigation of intracranial peripheral dose arising from the treatment of large lesions with Leksell Gamma Knife® Perfexion. *Med Phys* 2009; **36:** 2069-73.
12. Novotný Jr J, Bhatnagar JP, Niranjan A, Quader MA, Huq MS, Bednarz G, et al. Dosimetric comparison of the Leksell Gamma Knife Perfexion and 4C. *J Neurosurg* 2008; **109:** 8-14.
13. Yomo S, Tamura M, Carron R, Porcheron D, Regis J. A quantitative comparison of radiosurgical treatment parameters in vestibular schwannomas: the Leksell gamma Knife Perfexion versus Model 4C. *Acta Neurochir* **152:** 47-55.

14. Niranjan A, Novotný Jr J, Bhatnagar J, Flickinger JC, Kondziolka D, Lundsford LD. Efficiency and dose planning comparisons between the Perfexion and 4C Gamma Knife units. *Stereotact Funct Neurosurg* 2009; **87:** 191-8.

15. Tran T, Stanley TR, Malhotra MK, deBoer SF, Prasad D, Podgorsak MB. Target and peripheral dose during patient repositioning with the gamma knife automatic positioning system (APS) device. *J Appl Clin Med Phys* 2010; **10:** 88-98.

16. Bhatnagar JP, Novotný Jr J, Quader MA, Bednarz G, Huq MS. Unintended attenuation in the Gamma Knife Perfexion calibration-phantom adaptor and its effect on dose calibration. *Med Phys* 2009; **36:** 1208-11.

17. Petti PL, Larson DA, Kunwar S. Use of hybrid shots in planning Perfexion Gamma Knife treatments for lesions close to critical structures. *J Neurosurg* 2008; **109:** 34-40.

18. Lindquist C. Gamma knife radiosurgery. *Sem Radiat Oncol* 1995; **5:** 197-202.

19. Tlachacova D, Schmitt M, Novotný J, Novotný Jr J, Majali M, Liscák R. A comparison of the gamma knife model C and the automatic positioning system with Leksell model B. *J Neurosurg* 2005; **102(Suppl):** 25-8.

20. Kondziolka D, Maitz AH, Niranjan A, Flickinger JC, Lunsford LD. An evaluation of the model C gamma knife with automatic patient positioning. *Neurosurgery* 2002; **50:** 429-32.

21. Kuo JS, Yu C, Giannotta SL, Petrovich Z, Apuzzo MLJ. The Leksell gamma knife model U versus model C: a quantitative comparison of radiosurgical treatment parameters. *Neurosurgery* 2004; **55:** 168-73.

22. Goetsch SJ. Risk analysis of Leksell gamma knife model C with the automatic positioning system. *Int J Radiat Oncol Biol Phys* 2002; **52:** 869-77.

23. Chiou TSM. Patient treated by model-C gamma knife with APS are less exposed to non-therapeutic irradiation. *Minim Invas Neurosurg* 2008; **51:** 47-50.

24. Bradford CD, Morabito B, Shearer DR, Noren G, Chougule P. Radiation-induced epilation due to couch transit dose for the Leksell gamma knife model C. *Int J Radiat Oncol Biol Phys* 2002; **54:** 1134-9.

25. Watanabe Y, Gerbi BJ. Radiation exposure during head repositioning with the automatic positioning system for gamma knife radiosurgery. *Int J Radiat Oncol Biol Phys* 2007; **68:** 1207-11.

research article

Thyroid volume's influence on energy deposition from ^{131}I calculated by Monte Carlo (MC) simulation

Ali Asghar Mowlavi[1,2], Maria Rosa Fornasier[1], Mario de Denaro[1]

[1] Department of Medical Physics, A.O.U. "Ospedali Riuniti di Trieste", Trieste, Italy
[2] Physics Department, School of Sciences, Sabzevar Tarbat Moallem University, Sabzevar, Iran

Received 12 May 2010
Accepted 2 December 2010

Correspondence to: Maria Rosa Fornasier, Department of Medical Physics, Via della Pietà 19, 34129 Trieste, Italy. Phone: +390403992381; E-mail: mariarosa.fornasier@aots.sanita.fvg.it

Disclosure: No potential conflicts of interest were disclosed.

Background. It is well known that the success of the radiomethabolic ^{131}I treatment of hyperthyroidism could depend on the absorbed dose to the thyroid. It is, thus, very important to calculate the individual radiation dose as accurately as possible for different masses of thyroid lobes. The aim of this work is to evaluate the influence of thyroid volume on the energy deposition from beta and gamma rays of ^{131}I by Monte Carlo (MC) simulation.

Materials and methods. We have considered thyroid lobes having an ellipsoidal shape, with a density of 1.05 g/cm^3 and the material composition suggested by International Commission on Radiological Protection (ICRP). We have calculated the energy deposition of ^{131}I rays for different volumes of thyroid lobes by using the MCNPX code, with a full transport of beta and gamma rays.

Results and conclusions. The results show that the total energy deposition has a significant difference, till 11%, when the lobe's volume varies from 1 ml to 25 ml, respect to the value presented in MIRDOSE for a 10 g sphere. The absorbed energy fraction increases by volume, because the increasing volume to surface ratio of ellipsoidal lobe causes the decrease of beta ray fraction escaping from the lobe.

Key words: thyroid gland; ^{131}I radionuclide; total energy deposition; MCNPX code

Introduction

Thyroid gland consists of two linked lobes and is located in the middle of the low neck, overlying the trachea. Radioactive iodine ^{131}I has become the most widely used therapy for patients with hyperthyroidism due to Graves' disease.[1] This kind of therapy has largely replaced surgery as the definitive treatment for such benign disease in contrast with malignant ones[2-4], because it is easier than surgery to perform and has proved to be more effective. A number of dosing regimens have been proposed, ranging from those based on thyroid volume evaluation and Iodine test-activity uptake determination – for high precision dosimetry –, to large, fixed activities of ^{131}I administration, intended to cause hypothyroidism soon after treatment.[1-3] Physicians generally determine the ^{131}I activity on an empirical basis: the decision is based on the volume of the thyroid evaluated by scintigraphy, SPECT, MRI or ultrasonic methods and, sometimes, on the basis of $^{131}I/^{123}I$ test-activity uptake at 24 hours post-administration.[5]

It is well known that the success of this therapy could depend on the absorbed dose to the thyroid: it is thus very important to calculate the individual radiation dose as accurately as possible for different mass of thyroid lobe. Many authors have developed algorithms for the calculation of the radiation absorbed dose to a target organ, starting from a basic absorbed dose rate equation represented by the Medical Internal Radiation Dose (MIRD) models.[6] Traino *et al.* evaluated the influence of the volume reduction on the calculation of the absorbed dose to the thyroid by presenting a mathematical model.[1] The aim of this work is to evaluate the influence of thyroid volume on the energy deposition from ^{131}I by Monte Carlo (MC) simulation.

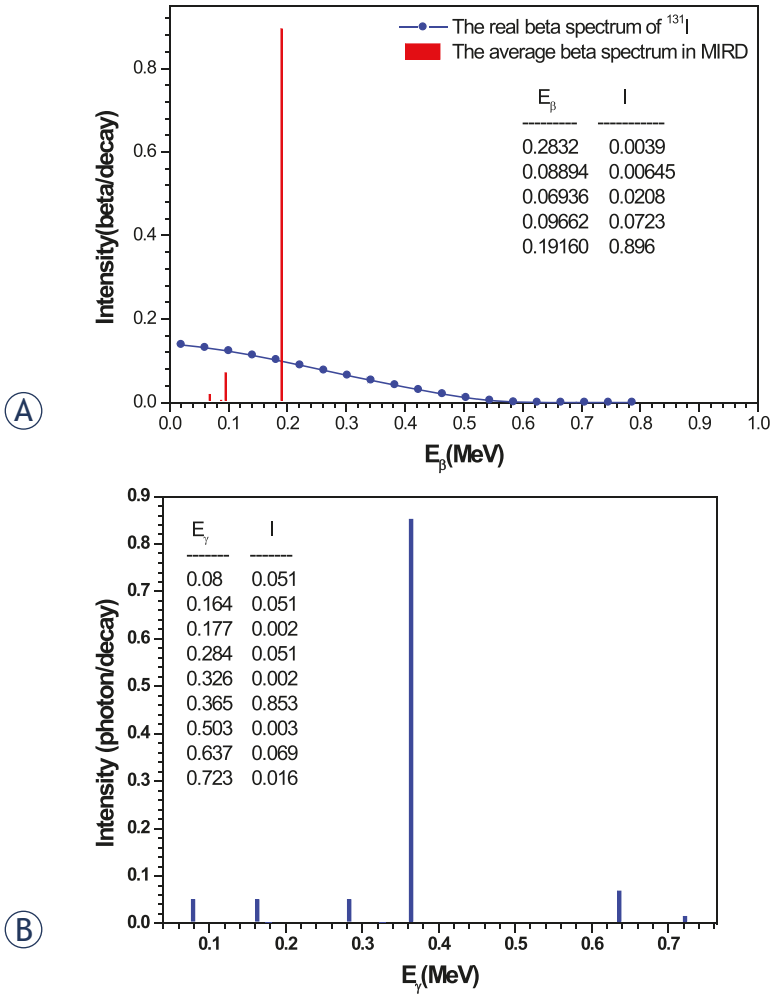

FIGURE 1. Radiation spectra of ^{131}I radionuclide: a) the real beta spectrum and the average beta spectrum used in MIRD, b) the photons spectrum.

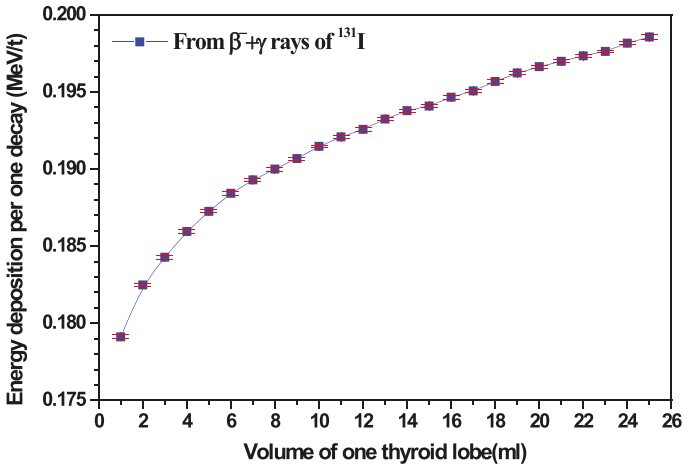

FIGURE 2. Variation of total energy deposition per decay against the volume of thyroid lobe.

Materials and methods

MCNPX is a general purpose, continuous and discrete energy, generalized-geometry, time-dependent code to simulate particles transport, based on Monte Carlo method. It is an extremely useful tool for radiations transport simulation and tracks about 40 particles including some light ions.[7] The code is written in Fortran 90 and contains flexible source and tally options; it utilizes the latest nuclear cross section libraries with a data library of photons cross-section ranging from 1 keV to 100 GeV.

This code has been used to calculate the energy deposition from beta and gamma rays of ^{131}I for a thyroid lobe of ellipsoidal shape, with the major axis two times of the minor axis, 1.05 g/cm^3 density and with a mass varying from 1 g to 25 g.

In running MCNPX code, we have considered the "full transport" for both gamma and beta rays; that is, we have considered that beta rays do not deposit their energy in a starting point, but they undergo many Coulomb interactions, so that a significant portion of their energy, near the surface of lobes, escapes and is stored out of the thyroid lobes.

Figure 1A shows the real beta spectrum of ^{131}I that we have used for our simulation, and the average beta spectrum used in MIRD, according to the Evaluated Nuclear Structure Data File (ENSDF) decay data. In the MIRD format, the beta spectrum includes 5 discrete lines, each representing the average beta energy and the yield for ^{131}I beta radiations.[8] As well as, the gamma spectrum is presented in Figure 1B.

The adult 70 kg human MIRD5 phantom has been used: the source organ was the thyroid gland with a uniform ^{131}I distribution; the neck has been simulated with more detailed organs including skin, adipose layer under the skin, bone, spinal cord, thyroid lobes, and the remaining part as soft tissue. We have considered for soft tissue 1.05 g/cm^3 density and the ICRP composition.

As it is well known, the basic formula for absorbed dose rate used in MIRD formulation is:

$$\frac{dD}{dt} = w\left(\sum_i n_i E_i \Phi_i\right)\frac{A}{m} \qquad [1]$$

where w is a proportional constant, A is the radionuclide activity within the source organ, n_i is the number of radiations with energy E_i emitted per one decay, Φ_i is the fraction of energy emitted in the source that is absorbed in the target organ, and m is the mass of the target. When the thyroid is considered both as source and target organ, the

beta and gamma rays absorption fraction (Φ_i) depends on thyroid volume.

We have selected σ as proper parameter to evaluate, by rewriting of Equation [1]:

$$\frac{dD}{dt} = \sigma \frac{A}{m} \quad ; \quad \sigma = w\left(\sum_i n_i E_i \Phi_i\right) \qquad [2]$$

The activity administrated for hyperthyroidism and thyroid cancer therapy is varying inversely with σ. In many literatures, such as MIRDOSE code, σ is taken as a constant value 0.0313 (mGy g MBq^{-1} s^{-1}), calculated by MC method for gamma rays and considering all beta energy deposited in a thyroid lobe of spherical shape, with fixed mass of 10 g. We have calculated the total (beta and gamma) energy deposition and σ for different volumes of thyroid lobes.

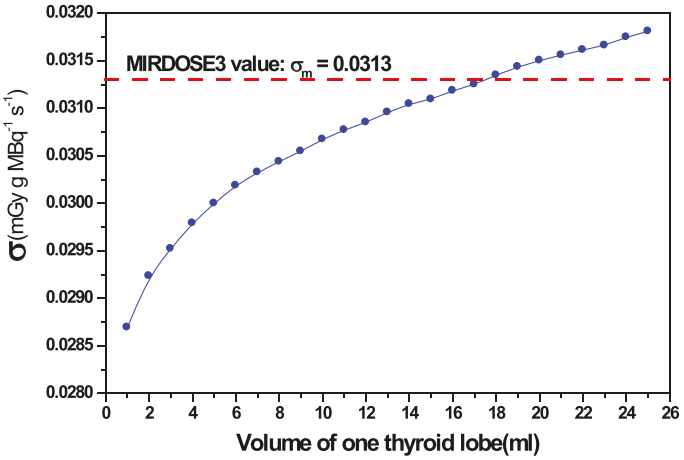

FIGURE 3. Influence of the thyroid lobe volume on value.

Results and discussion

Figure 2 shows the variation of the total energy deposition per decay of ^{131}I for both beta and gamma rays against the volume of thyroid.

The total energy deposition per decay is the term in brackets $\left(\sum_i n_i E_i \Phi_i\right)$ and it increases by volume, because the increasing volume to surface ratio of ellipsoidal lobe causes the decrease of radiations fraction escaping from the lobe (Figure 2).

The calculated value of σ against the thyroid volume lobe has been presented in Figure 3. It can be seen that σ has a significant difference with the previous constant value, ranging from 10% to -1% when the lobe's volume varies from 1 ml to 25 ml. For a 10 g lobe, our calculation shows about 2.2% difference with MIRDOSE3 σ value. This difference comes from two main sources: the first is the beta spectrum, as we have used the spectrum of ^{131}I taken from a reference published by Eckerman *et al.* in 1994 in Health Physics[9,10], with a mean beta energy of 0.1822 MeV per disintegration; the second is due to considering in our calculation the full beta and gamma transport in an ellipsoidal thyroid lobe (Figure 3).

We have used the photon energy deposition tally, called F6:p in MCNPX code, to calculate the photon energy deposition per unit of mass, in the other organs of the body, due to a decay in the source organ. It is clear that the result is proportional to the dose organ per one decay in the source.

The energy deposition in other organs of neck as a function of the thyroid lobe volume per decay

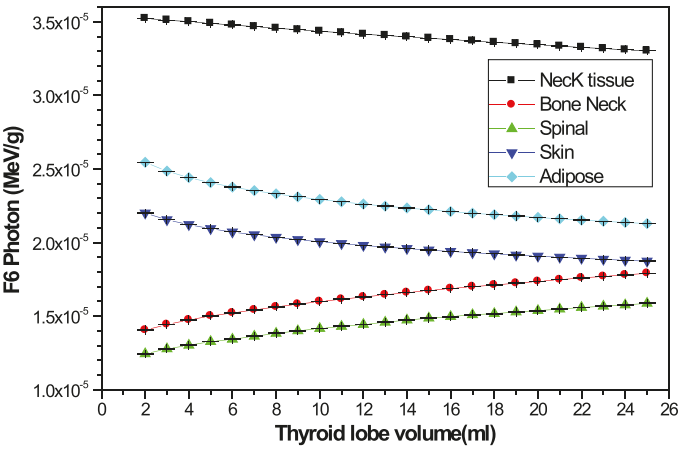

FIGURE 4. The variation of the energy deposition in other organs of neck respect to the thyroid lobe volume, per decay.

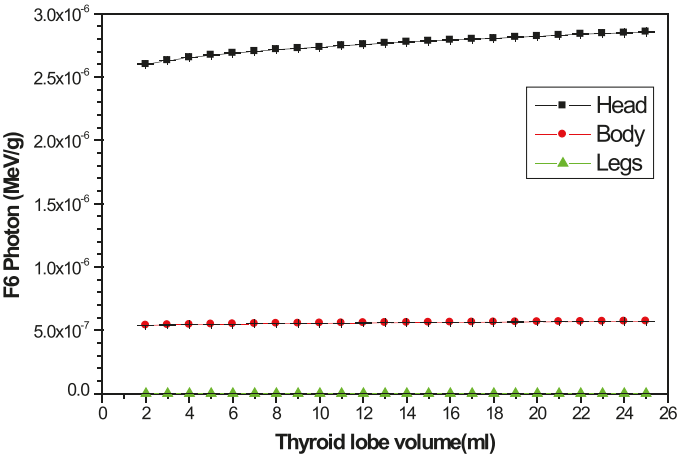

FIGURE 5. The variation of the energy deposition to head, body and legs respect to the thyroid lobe volume, per decay.

of ^{131}I has been shown in Figure 4. As it is predictable, by increasing the lobe volume the dose in the bone and spinal cord increases but for other organs it decreases. The energy depositions per decay to organs far from the thyroid, including head, body and legs have been presented in Figure 5.

Conclusions

The result shows that considering the lobe volume or mass has a significant effect over the absorbed dose calculation in thyroid gland. So, an accurate determination of the active volume of thyroid is very important in activity evaluation for radiomethabolic therapy by Iodine-131. As well as, according to our calculation, we suggest re-evaluating the Φ_i value for gamma and beta sources when the source organ is the same as target and its volume or mass variation among different patients is considerable.

Acknowledgements

The authors would like to thank Prof. G. Furlan and Prof. D. Treleani head of TRIL program at ICTP, Trieste, Italy, for their support to this work.

References

1. Traino AC, di Martino F, Lazzeri M, Stabin MG. Influence of thyroid volume reduction on calculated dose in radioiodine therapy of Graves' hyperthyroidism. *Phys Med Biol* 2000; **45:** 121-29.
2. Becker DV. Choice of therapy for Graves' hyperthyroidism. *N Eng J Med* 1989; **311:** 454-66.
3. Farrar JJ, Toft AD. Iodine-131 treatment of hyperthyroidism. *Clin Endocrinol Oxf* 1991; **35:** 207-12.
4. Vardar E, Erkan N, Bayol U, Yılmaz C, Dogan M. Metastatic tumours to the thyroid gland: report of 3 cases and brief review of the literature. *Radiol Oncol* 2011; **45:** 53-8.
5. Van Isselt JW, de Klerk JMH, Van Rijk PP, Van Gils APG, Polman LJ, Kamphuis C, Meijer R, Beekman FJ. Comparison of methods for thyroid volume estimation in patients with Graves' disease. *Eur J Nucl Med Mol Imaging* 2003; **30:** 525-31.
6. Snyder W, Ford M, Warner G. Estimates of absorbed fractions for monoenergetic photon sources uniformly distributed in various organs of a heterogeneous phantom: MIRD pamphlet no. 5. *J Nucl Med* 1969; **10** (Suppl 3)**:** 5-52.
7. Waters L S. *MCNPX User's Manual, version 2.3.0*. Los Alamos; 2002.
8. http://www.orau.org/ptp/PTP%20Library/library/DOE/bnl/nuclidedata/MIRI131.htm
9. Eckerman KF, Westfall RJ, Ryman JC, Cristy M. Availability of nuclear decay data in electronic form, including beta spectra not previously published. *Health Phys* 1994; **67:** 338-45.
10. Cember H, Johnson TE. *Introduction to health physics*. New York: McGraw-Hill; 2009.

special communication

Croatian Society of Radiology (1928-2008), the Croatian Medical Association - 80 years of existence and activity

Slavko Simunic[1], Kresimir Glavina[1], Nada Besenski[2], Ratimira Klaric-Custovic[3]

[1] Department of Diagnostic and Interventional Radiology, University Clinical Centre Osijek, Osijek, Croatia
[2] Department of Diagnostic and Interventional Radiology, University Clinical Centre Split, Split, Croatia
[3] Department of Diagnostic and Interventional Radiology, University Hospital "Sestre milosrdnice", Zagreb, Croatia

Received 22 September 2010
Accepted 14 November 2010

Correspondence to: Prof. Slavko Šimunić, MD, PhD, Department of Diagnostic and Interventional Radiology, University Clinical Centre Osijek, Osijek, Croatia. E-mail: slavko.simunic@xnet.hr

Disclosure: No potential conflicts of interest were disclosed.

Often and in various connotations one can hear or read the following syntagma: "Let's leave the past in the past - and turn to the future". Even more frequent and numerous are opposite opinions, *e.g.* "There is no future without past", "Future is built on past" or "Remembering our past – reaching for our future", and many more.

Key words: radiology; history; Croatian Medical Association, Croatian Society of Radiology

The first practical use of X-rays in medicine

In the very same year (1895) as Francis Joseph I, the Austro-Hungarian emperor, ceremonially opened a new building of the Croatian National Theatre in Zagreb, Wilhelm Konrad Röntgen, a German physicist (Lennep 1845 – Munich 1923), in his experimental laboratory in Würzburg discovered the radiation until then unknown, which he called X-rays. As a proof then, he also published the first roentgenogram – an image of his wife's hand with a ring on the middle finger. He was awarded the first Nobel Prize in physics (1901) for this extraordinary discovery, and the newly discovered rays were named the Roentgen rays in his honour. The discovery gave origin to a new profession (science) radiology (roentgenology), which enabled a fresh impetus in the development not only of medicine, but of many other human activities.

The first practical use of X-rays in medicine in this region was recorded in Rijeka (1897), when a roentgen apparatus was acquired, Prof. Dr. Peter Salcher presented at the Naval Academy an X-ray of a hand with a ring on the baroness Vranyczány's finger. Thereafter followed Ogulin, Šibenik and Srijemska Mitrovica (1898), Zagreb (1901), Osijek (1902) and Lepoglava (1904) – let us remember that the Paulists of Lepoglava, in rivalry with the Jesuits, started providing university education (1656) with lectures in logic. The roentgen apparatuses were then obtained in Pula, Split, Dubrovnik, Bjelovar (1905), and Varaždin, Karlovac, Vinkovci and Nova Gradiška (1911), and Sisak (1912). We may also mention that the roentgen radiation was for the first time used for the research in palaeontology by Prof. Dragutin Gorjanović-Kramberger (1902), a Croatian natural scientist of world-renowned, a geologist, palaeontologist and anthropologist, for taking X-ray of the Krapina early man's jaw.[1]

Organizations in Croatia

Organised medical work in Croatia started with the establishment of the **Društvo slavonskih liječnika** (*Slavonian Medical Association)* in Osijek (1874), that started publishing the **Glas slavonskih liječnika** (*Slavonian Medical Journal*) (1877) – the today's "Medicinski vjesnik" (*Medical Journal),* published by the University Hospital Osijek, the Faculty of Medicine in Osijek, and other regional medical centres. A few months later, in the same year (1874), the **Sabor liečnika kraljevine Hrvatske i Slavonije**

(*Medical Association of the Kingdom of Croatia and Slavonia)* was founded in Zagreb, and started publishing the **Liečnički viestnik** (*Medical Journal)* (1877) – the today's "Liječnički vjesnik" (*Medical Journal of the Croatian Medical Association)*, the gazette of the Croatian Medical Association.[1] From the 1920s, the Association was called the **Hrvatski liječnički zbor** *(Croatian Medical Association)*, and from 1945 to 1992 it operated under the name the **Zbor liječnika Hrvatske** (*Medical Association of Croatia)*, becoming the member of the Savez lekarskih/liječničkih društava Jugoslavije (*Union of Medical Associations of Yugoslavia)*.

As the aggression on Croatia started (1991), the Medical Association of Croatia freezed (on 26th February 1991), and subsequently broke off all the relations (on 30th September 1991) with the Union of Medical Associations of Yugoslavia. We were also obligated to do so by the UN Security Council Resolution no. 757/1992, stating that "*....any activity in the area of science, technology, information sciences, education, culture and sports, even publishing activity, with the SFRY /Socialist Federative Republic of Yugoslavia/ shall be suspended...*". In that period, and observing the then-valid and customary schedule of rotating the seats of the leadership of a particular professional association during a 4-year mandate, Zagreb was the seat of the Yugoslav Society of Cardiology, the Yugoslav Association of Pulmonology and Phthisiology, the Association of Yugoslav Clinical Cytology, the Yugoslav Association of Anaesthesiologists, the Yugoslav Association of Dermatology, and the Yugoslav Society of Radiology and Nuclear Medicine. All the presidents, vice-presidents and secretaries of these associations resigned their duties, and on behalf of their respective associations renounced any further cooperation. The **Section of radiology** of the Medical Association of Croatia, in accordance with this, broke off (on 4th October 1991) the cooperation with the Yugoslav Society of Radiology and Nuclear Medicine, and returned the mandate for presiding the Society for the period 1988 – 1992, and renounced to the obligation of organising the 14th Congress of the Yugoslav Society of Radiology and Nuclear Medicine planned for 1992, informing about it all the professional associations of the then Yugoslav republics and provinces.

Following the disintegration of the Socialist Federative Republic of Yugoslavia, and the founding of the Republic of Croatia, with its international recognition, the conditions were met for the direct membership of Croatian professional associations in international professional institutions, so that the Croatian Medical Association also became a full member of the **World Medical Association** (1992), *i.e.* the **Croatian Medical Association**.

Although the radiology profession and science in this region was being applied soon after the respective discovery (Rijeka 1897), the roentgenologists / radiologists were formally organised only in 1928, through the foundation of the **Society of Roentgenology** (1928-1935), which changed the name into the **Section of Radiology, Electrophysiology and Balneology** (1935-1945). After the Second World War, the Society was reorganised again and the name changed to the **Section of Radiology and Nuclear Medicine** (1945-1984), having radiologists, radiotherapeutists, oncologists and nuclear medicine practitioners as members. The development of nuclear medicine and the growing number of educated nuclear medicine practitioners lead to the separation of these experts into two independent sections, so that ours changed the name into the **Section of Radiology** of the Medical Association of Croatia (1984 – 1992).

As the Croatian Medical Association became a member of the World Medical Association, all the Sections were entitled to a higher level of membership, *i.e.* to receive the title of a society, so that on this basis the present-day **Hrvatsko društvo radiology (HDR) – The Croatian Society of Radiology (CSR)** was founded and named at the Founding Assembly held on 22nd April 1992, in the Great Hall of the Croatian Medical Association, being the successor of all the already mentioned Associations of Radiology in Croatia.

Since the foundation (1928) until the present day, the Sections / Societies were headed by presidents: Prof. Dr. Laza Popović (1928-1945), Prof. Dr. Ferdo Petrovčić (1945- 1958), Prof. Dr. Vladimir Gvozdanović (1958-1960), Prof. Dr. Silvije Kadrnka (1960-1965), Ass. Prof. Dr. Sc. Ivo Belančić (1965-1967), Prim. Dr. Karlo Strohal (1967-1971), Prof. Dr. Sc. Šime Čičin-Šain (1971-1976), Prof. Dr. Sc. Duško Katunarić (1976-1986), Prof. Dr. Sc. Davorin Kovačević (1986-1992), Prof. Dr. Sc. Slavko Šimunić (1992-1996), Prof. Dr. Sc. Nada Bešenski (1996-2004), Prof. Dr. Sc. Ratimira Klarić-Čustović (2004-2008), and Prof. Dr. Sc. Boris Brkljačić (from 2008 on).

Immediately after its foundation, the CSR obtained right to apply for an independent direct membership in international institutions. Firstly, all the required documentation for the membership in the **European Association of Radiology - EAR** was collected and submitted (a written application

and an explanation in English, an English version of the Statute of the Croatian Medical Association and the Rules of Procedure of the Society, and the list of the Society's members). The application was examined in the General Assembly of the European Association of Radiology at the time of the European Congress of Radiology, in Vienna 1993. The application was granted unanimously, and the CSR became a regular and full member of the EAR.

An application for the membership of the **International Society of Radiology – ISR** followed. In accordance with the same procedure, the application waited for the General Assembly and the International Congress of Radiology to be held – in Singapore 1994, when the CSR became a member of this society as well.

Professional activities

The Croatian radiologists have always had a significant impact on the organization and participation in various radiology events in the then Yugoslavia: the 1st Yugoslav Meeting on Radiology (Split, 1930), organised by Prim. Dr. Jakša Račić; the 2nd Yugoslav Meeting on Radiology (Belgrade, 1935), in the organisation participated the following colleagues from Croatia: Prof. Dr. Ernst Mayerhofer – the dean of the Faculty of Medicine / Zagreb, Prof. Dr. Laza Popović, radiologist / Zagreb, Dr. Milan Smokvina, radiologist / Zagreb, and Dr. Stevo Radojević, radiologist / Zagreb. After the Second World War, meetings were held every four years, by rotation in the republics' capitals. The 1st Scientific Meeting of Radiologist of the Federal People's Republic of Yugoslavia (FNRY) – (Belgrade 1950); the 2nd Scientific Meeting of Radiologists of FNRY (Zagreb 1953). Thereafter, the meetings were named congresses: the 3rd Congress of Radiology of FNRY (Ljubljana 1956); the 4th Congress of Radiology of FNRY (Skopje 1960); the 5th Congress of Radiology of Yugoslavia (Belgrade 1964). Because of the two Scientific Meetings held earlier (Split 1930, and Belgrade 1935), the next congress was titled the 8th Congress of Radiology of Yugoslavia (Pula 1968); and the 9th Congress of Radiology of Yugoslavia (Ljubljana 1972). Out of the total of 228 lectures held on that congress, 55 lectures (24 %) were from Croatia. At the 10th Congress of Radiology of Yugoslavia (Sarajevo 1976), out of the total of 245 lectures held, 65 lectures (26%) were from Croatia. At the 11th Congress of Radiology of Yugoslavia (Novi Sad 1980), out of the total of 396 lectures held, 97 lectures (25%) were from Croatia. At the 12th Congress of Radiology of Yugoslavia (Belgrade 1984), out of the total of 325 lectures held, 97 lectures (20%) were from Croatia. And at the 13th Congress of Radiology of Yugoslavia (Ohrid 1988), out of the total of 496 lectures held, 97 lectures (20%) were from Croatia. The 14th Congress of Radiology of Yugoslavia (1992) was supposed to be held in organisation of the Croatian radiologists, but due to the known war situation, Croatia renounced the task.

In the period from 1978 to 1992, and owing to Prof. Dr. Sc. Duško Katunarić and Prim Dr. Krešo

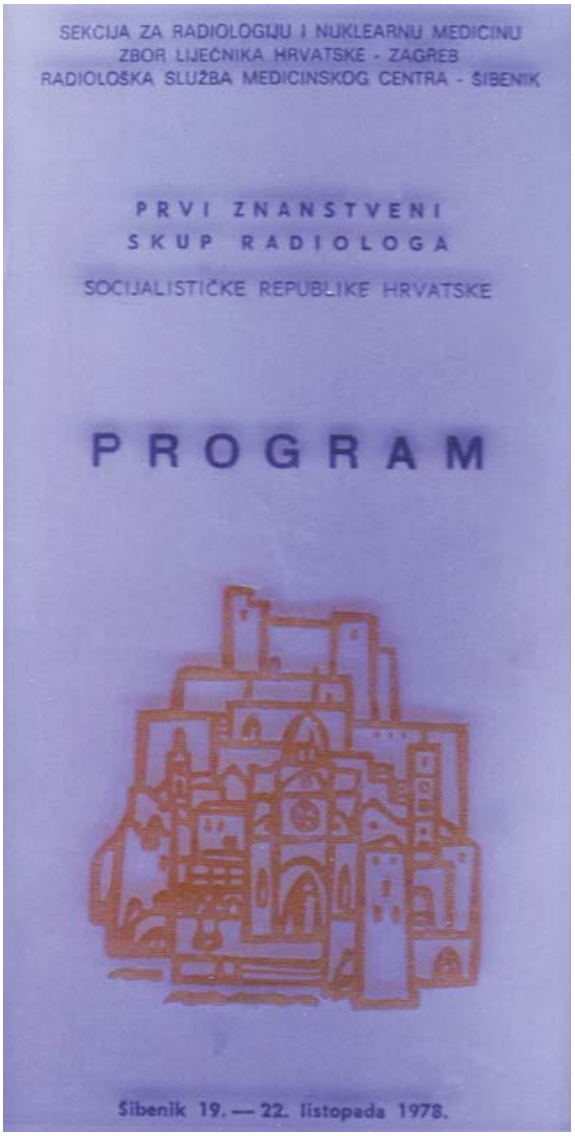

FIGURE 1. Programme of the First scientific meeting of radiologists of the Croatia, Šibenik, October 19-22, 1978.

Pavleković, the president and the secretary respectively of the then Section of Radiology, the Section organised **Scientifics Meetings of Radiologists of Croatia** in various towns in Croatia, followed an alternating "continent – seaside" territorial principle. Even though in those times the meetings were of mere republic-importance, they had wide reverberation across the entire then Yugoslavia, both among the participants and the lecturers, so those meetings were considered to be at the "level" of a congress. There were ten meetings held in total: in Šibenik (1978) (Figure 1), Plitvička jezera (1979), Split (1981), Osijek (1982), Pula (1985), Karlovac (1986), Opatija (1987), Požega (1989), Zadar (1990) and Varaždin (1992). The total of 776 lectures were held at the meetings (752 national authors and 24 foreign authors – 5 from Germany, 5 from Switzerland, 2 from Italy, 2 from Norway, 2 from the USA, 1 from France, 1 from Belgium, 1 from Sweden), and 102 lectures at three Courses (on Radiology of Kidney, on Radiology of Mediastinum, and on CT in Neuroradiology).

With the development of radiology and an increasing number of specialists in radiology, as well as their professional and scientific orientation, the conditions were met, as per the Statute of the Croatian Medical Association and the Rules of Procedure of the Croatian Society of Radiology, for the establishment of particular sections. Firstly, the **Section of Neuroradiology** (1933) was founded – the first president was Prof. Dr. Sc Nada Bešenski. Then followed the establishment of the **Junior Radiologists Forum** (1994) – encouraged by the Junior Radiologist Forum (JRF) of the European Association of Radiology – the first president was Dr. Franka Jelavić – Kojić. The third to be established was the **Section of Ultrasound in Medicine** (1994) – the first president was Prof. Dr. Sc. Ivo Drinković. Then the **Section of Interventional Radiology** (2000) – the first president was Prof. Dr. Sc. Josip Mašković, and the **Section of Thoracic Radiology** (2001) – the first president was Prof. Dr. Sc. Zlata Herceg – Ivanovi.

On several occasions the Section / the Society took part in specialised programmes of the international fair "Medicine and Technology" at the Zagreb Fair. The *Symposium on Interventional Radiology* (1981) – chaired by S. Šimunić; the *Symposium on Percutaneous Transluminal Angioplasty – PTA* (1983) – chaired by S. Šimunić / M. Šesto, (a book was published: "*PTA renalnih, perifernih i koronarnih* arterija. Šimunić S, Šesto M, editors. Zagreb; 1985"); the *Symposium on Percutaneous Organ and Organic Systems Drainage* (1985) – organized / chaired by S. Šimunić / I. Obrez – Ljubljana; the *Symposium on MRI in Clinical Medicine* (1988) – chaired by S. Šimunić / D. Ivančević; the *Symposium on Rationalization of Diagnostic Procedures in Radiology, Nuclear Medicine and Ultrasound* (1987) – chaired by S. Šimunić / S. Franić; the *Symposium on Algorithm of Diagnostic Procedures in Neuroradiology* (1999) – chaired by S. Šimunić / N. Bešenski; the *Symposium on Teleradiology* (1999) – chaired by A. Hebrang / S. Šimunić and assoc.

The emergence of therapeutic procedures in interventional radiology and our first experiences were presented at the CSR expert meeting: the *Round Table on Interventional Radiology* (1980) – chaired by S. Šimunić, also published in a book: "*Okrugli stol o intervencijskoj radiologiji*. Šimunić S, Gürtl R, editors, 1981".

The CSR has had an intensive, long-term cooperation with members of other professions and institutions. It has endeavoured to approach and solve a number of common problems with the related Radiation Protection Association. It used to cooperate, at the time, with radiologists of the Department of Roentgenology and Physical Therapy of the Faculty of Veterinary Medicine in Zagreb (Prof. Dr. Sc. Mensur Šehić). With the Ministry of Health and Social Welfare of the Republic of Croatia and the Croatian Institute for Health Insurance, the CSR discussed various professional, status and organisational issues on the regular basis. Expert meetings are well-attended and held regularly (9-10 times per year), in cooperation with other clinical professions (internal medicine specialists, paediatricians, neurosurgeons, urologists, orthopaedists, otorhinolaryngologists, etc.)

Various business partners, manufacturers and suppliers of equipment, accessories and expandable supplies presented to us regular basis novelties in their assortment of products: Siemens, General Electric, Philips, Shimadzu, Bayer Health Care, Schering, Farma, Sonimed, Thomy Frey East, Mark/De Plano, Medtronic, OptiMed, Bard, Abbot, Bracco, Cook and many others.

A long-term professional, loyal and friendly cooperation with the Hungarian Radiological Society ("Societatis Radiologorum Hungarorum") was particularly emphasized, dating back since 1985, when the *Vereinbarung über die Ungarischen und Jugoslawischen Radiologischen Gesellschaften* was signed (signatories: *Gy Vargha and B. Fornet – Budapest; M. Radojević – Skopje; S. Šimunić – Zagreb and L. Popović – Novi Sad.* At the same year, during the International Fair "Medicine and Technology", at the Zagreb Fair, within the frame-

work of professional events at the Symposium on Percutaneous Organ and Organic Systems Drainage, the lectures were given by Gy Vargha and T. Baranyai (Debrecen), L. Horváth (Pécs) and Lélek (Zalaegerszeg). The cooperation was continued through regular joint Croatian-Hungarian Radiological Symposiums: Kőszeg (1999) and Opatija (2000), after which Slovenia also joined this cooperation, so the symposia were thereafter held under the name Hungarian-Croatian-Slovenian Radiological Symposia: Pécs (2001), Maribor (2002), Koprivnica (2003), Héviz (2004), Maribor (2005). It was at that point decided that the symposia were to be held biannually from then: Vukovar (2007) and Kehidakustanyi (2009). The participants of the meeting in Vukovar visited and paid respects by placing wreaths at the Stone Cross, on the confluence of Vuka and Danube, and at the Memorial Cemetery of the Homeland War victims on Ovčara.[2]

The CSR gave an appreciation award to the Hungarian Radiological Society for the close long-term cooperation, and the same award was also given to the following individuals: Gy Vargha, G. Vadon, J. Kénez, B. Fornet, and L. Hórvath at the congress in Tihany, in 1996. N. Bešenski was awarded a certificate - Honorary Member of the Hungarian Society of Neuroradiology (7th Annual Meeting of the Hungarian Society of Neuroradiology - Györ 1997).

The following colleagues were declared honorary members of the Societatis Radiologorum Hungarorum: N. Bešenski (Zagreb), K. Glavina (Osijek), S. Šimunić (Zagreb / Osijek), I. Lovasić (Rijeka) and B. Brkljačić (Zagreb).

It has become customary to participate in one another's national, i.e. Croatian and Hungarian, radiology congresses: in Miskolc 1994, Opatija 1994; Tihany 1996, Osijek 1998[3], Pécs 1998, Split 2002[4], etc., but also in the Hungarian Society of Neuroradiology congresses.

The cooperation with the Združenje radiologov Slovenije (the Slovenian Association of Radiology) went back long ago. There used to be held (1958-1971) joint meetings of Croatian and Slovenian radiologists. The last one, the sixth expert meeting, was held in Zagreb, in 1971. At that point, the cooperation was developed on Croatian and Slovenian national radiology congresses: in Portorož 1996, Portorož 2000, Ljubljana 2004, Ptuj 2008. Moreover, the Croatian radiologists cooperated occasionally on expert meetings with the University Medical Center Ljubljana and the Maribor General Hospital / University Medical Centre Maribor. On the occasion of the 100th anniversary of the Röntgen's discovery, the Medicohistorical Section of the Slovenian Medical Association published a book including an article by Croatian authors: "Lovasić I, Šimunić S, Borković Z, Pavan G. *Prve rentgenske snimke i prvi rentgen aparati u Hrvatskoj*. (*The first roentgen rays and roentgen apparatuses in Croatia).* Maribor; 1995" (Figure 2). The international radiology cooperation to be mentioned is the participation of the Croatian delegation at the Founding Conference of the Radiological Society of Bosnia and Herzegovina (Sarajevo 1996). The Society was

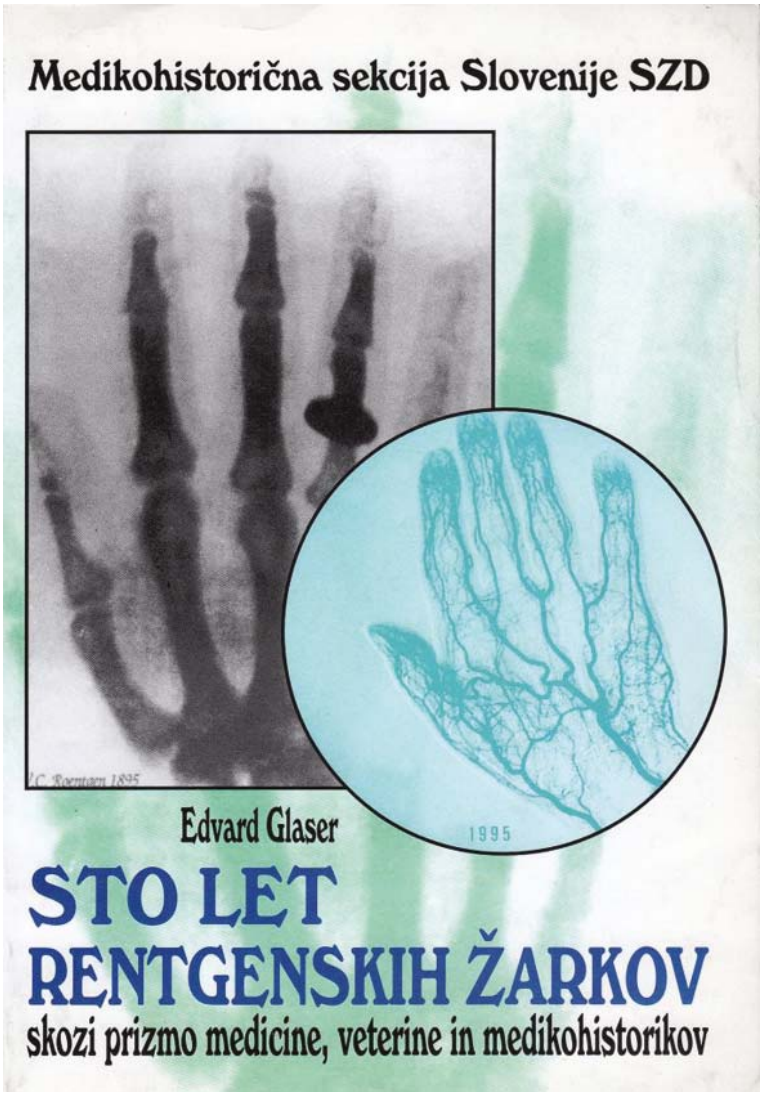

FIGURE 2. The book of Edvard Glaser. *Sto let rentgenskih žarko kozi prizmom medicine, veterine in medikohistorikov [100 years of the x-rays through the prism medicine, veterinary nad medical historyans]*. Glaser E, editor. Maribor: Medikohistorična sekcija Slovenije, SZD [Section for the history of medicine, Slovenian Medical Society]; 1998.[5]

TABLE 1. Publications of radiology that were published in Croatia with help of Croatian radiology experts and teachers

Radojević S, Nikolić S. *Grizlica kolačića i želuca [Ulcus duodeni et ventriculi]*. Zagreb: Centralni rentgenološki institut Medicinskog fakulteta u Zagrebu [Central Roentgen Institute of Medical Faculty Zagreb]; 1927. (Figure 3)
Popović L, Smokvina M. *Pregled naše rentgenološke literature*. Zagreb: Centralni rentgenološki institut Medicinskog fakulteta u Zagrebu; 1927.
Smokvina M. *Klinička rentgenologija, kosti i zglobovi [Clinical roentgenology, bones and joints]*. Zagreb: Yugoslav Academy of Sciences and Arts; 1959. (Figure 4)
Hodges FJ, Lampe I, Floyd HF. *Radiology for Medical Students. [Radiologija za studente medicine]*. 4th Edition. Chicago: Year Book Medical Publisher Inc.;1964; Zagreb: Školska knjige Zagreb; 1976
Petrovčić F. *Leksikon radioloških pojmova*. Zagreb: Leksikografski zavod M. Krleža Zagreb; 1977.
Okrugli stol o intervencijskoj radiologiji. Šimunić S, Gürtl R, editors. Zagreb: Zavod za radiologiju KBC Zagreb; 1981.[6]
Intervencijska radiologinja – perkutana transluminalna angioplastika renalnih, koronarnih i perifernih arterija. Šimunić S, Šesto M, editor. Zagreb: Sekcija za radiologiju, Kardiološka i nefrološka sekcija Zbora liječnika Hrvatske; 1985.[7]
Intervencijska radiologija. Mašković J, Boschi S, Stanić I, editors. Split; Sekcija za radiologiju Zbora liječnika Hrvatske – Podružnica Split; 1986.[8]
Plavšić B. *Radiologija probavnog kanala*. Zagreb: Školska knjiga Zagreb; 1986.
Petrovčić F. *Opća radiologija*. Zagreb: Sveučilišna naklada, Liber Zagreb; 1986.
Hebrang A, Petrovčić F. *Radijacija i zaštita u medicinskoj dijagnostici*. Zagreb, Beograd: Medicinska knjiga; 1987.
Bešenski N, Škegro N. *Radiografska tehnika skeletal.* Zagreb: Školska knjiga Zagreb; 1987.
Škarica R, Potočki K. *Radiološki atlas reumatskih bolesti.* Zagreb, Beograd: Medicinska knjiga; 1989.
Plavšić B. *Radiologija probavnog kanala.* 2nd edition. Zagreb: Školska knjiga Zagreb; 1990.
Radiologija. Agbaba M, Lovrenčić M, editors. 1st edition. Zagreb: Medicinska naklada Zagreb; 1994.
WHO Scientific Group on Clinical Diagnostic Imaging. *[Izbor dijagnostike u kliničkoj praksi – Izbor radioloških dijagnostičkih postupaka]*. Hebrang A, translator and editor. Zagreb: HZZO; 1996.
Frković M. *Radiološki atlas probavnog sustava djece*. Zagreb: Informator; 1998.
Strugačevac P. *Teorijska osnova imaging CT tehnike*. Osijek: KB Osijek; 1999.
Brkljačić B. *Dopler krvnih žila*. Zagreb: Medicinska naklada Zagreb; 2000.
Radiologija. Hebrang A, Lovrenčić M, editors. 2nd edition. Zagreb: Medicinska naklada Zagreb; 2001.
Chapman S, Nakilney R. *Pomoć u radiološkoj diferencijalnoj dijagnostici.* [Translation from English]. Gotovac N, editor. Požega: Self-published; 2005.
Pichler E. *Ultrazvučni atlas dojke-diferencijalna dijagnoza i intervencije*. Zagreb: Školska knjiga Zagreb; 2005.
Pavić L, Radoš M. *Mali medicinski leksikon magnetne rezonancije*. Zagreb: Školska knjiga Zagreb; 2005.
Seminari iz kliničke radiologije. Janković S, editor. Split: MF Split; 20905.
Stojanović J. *Trzajna ozljeda-riješena enigma*. Zagreb: Sveučilišna tiskara; 2006.
Radiologija. Hebrang A, Klarić-Čustović R, editors. Zagreb: Medicinska naklada Zagreb; 2007.[9,10]
Miletić D. *Skeletna radiografija*. Rijeka: Glosa; 2008.
Odabrana poglavlja intervencijske radiologije. Mašković J, Janković S, editors. Split: MF Split; 2008.
Dentalna radiografija. Janković S, Miletić D, editors. Split: MF Split; 2009.
Brkljačić B. *Vaskularni ultrazvuk*. Zagreb: Medicinska naklada Zagreb; 2010.

after that admitted to the European Association of Radiology (1999). The Croatian radiologists participated in congresses of the Radiological Society of the Medical Association of Bosnia and Herzegovina (Sarajevo 1999, Tuzla 2003, Sarajevo 2007).

The Croatian radiologists participated almost on the regular basis with lectures in congresses of the European Association of Radiology (ECR) in Vienna, as well as in the International Congress of Radiology (ICR). They, for example, held five lectures and presented two posters in the Vienna ECR '93, while young radiologists, members of the CSR's Junior Radiologists Forum, won three Winners of the Day medals.

We have been participating already for decades in expert meetings of the ALPE-ADRIA bordering countries, Austria, Italy, Slovenia and Croatia, held in various towns. The examples of our participation are the following: "Gvozdanović V, Nutrizio V, Šimunić S. La nostra esperienza con Emi Scanner. Padova; 1975", and "Gvozdanović V, Nutrizio V, Šimunić S, Marinšek Čičin-Šain V. CT in the Diagnostic Acousticus Neurinoma".

There are meetings of the Cardiovascular and Interventional Radiological Society of Europe (CIRSE), whose members are: Z. Čačić, A. Hebrang, J. Mašković, S. Šimunić, L. Camby-Sapunar, V. Vidjak, V. Tkalec, held every second year in various European towns, with the participation of a dozen or more Croatian radiologists.

Our teachers and the then authorities on radiology (S. Kadrnka, M. Smokvina, V. Gvozdanović, D. Katunarić, M. Bašić), owing to their personal acquaintances and friendships, to relations and cooperation with leading European and other authorities on radiology, organised in those times the following participation and lectures: "Jirout J. Pneumomyelography of the Cervical Spine. Prague; 1965"; "Vieten H. Die Methoden der Kontrastmitteldarstellung des Herzens und der großen Gefäße deren Indikationen und Gefahren. Düsseldorf ; 1967"; "Wellauer J. Kontrastmittel Probleme in der modernen Röntgendiagnostik. Zurich; 1967"; Bodar P. La radiologie du grêle (maladie de Crohn-Tuberculose-Tumeurs"). Louvain, Belgium; 1968"; Oliva L. Studio radiologico dell'incontinenza urinaria femminile. Siena; 1968".

In more recent times, and through the offices of D. Kovačević, M. Lovrenčić, N. Bešenski, S. Šimunić, V. Vidjak, B. Brkljačić and others, we were hosts to S. Wallace (Houston/USA), Pocajt (Maribor), D. Pavčnik (Ljubljana), H. Hricak and A. Margulis (San Francisco/USA), J. Matela (Maribor),

L. Hórvath, C. Focafy, M. Kovey (Pécs/Hungary); Ufflacker (Charleston/USA), and others.

The CSR and its members were entrusted the organisation of the "Workshop – New Application of CT and MRI" – Elscint, Zagreb, 1996; "Visiting Junior Radiologists to Eastern Europe", Zagreb, 1995, 1997; a "Crash Course in CT", on the occasion of the acquisition of a large number of CT devices by the Ministry of Health of the Republic of Croatia, and the Croatian Institute for Health Insurance.

It is worth remembering, recording and saving from oblivion the works on radiology, from the old days, but also from the most recent times, written by radiology experts and teachers. Among them, the book of Hodges *et al* was the first comprehensive teaching material and great help to students in acquiring necessary knowledge, in addition to lectures, seminars and exercises for the Radiology course (Table 1).

In addition to the publications listed in Table 1, the CSR members radiologists published countless number of articles and chapters in journals, encyclopaedias, and books, both in Croatia and around the world, those being not only in the field of radiology but also in other professions: Marotti M, Klarić-Čustović R, Lovrenčić M, Krolo I, Papa J, Agbaba M, Radanović B, Mandić A, Štern-Padovan R, Mašković J, Sučić Z, Čavka K, Glavina K, Borković Z, Ivanovi-Herceg Z, Camby-Sapunar L, Brkljačić B, Kalousek M, Brajša M, Drinković I, Jakovac I, Gürtl R, Klenkar M, Čičin-Šain Š, Marinšek- Čičin-Šain V, Sabolić A, Prpić-Hartl V, Bešenski N., S. Šimunić and many more.

The then Section of Radiology, in cooperation with the central health institutions (the then University Hospital "Dr. M. Stojanović" in Zagreb, and the University Hospital Centre Zagreb), organized memorial meetings: a **Memorial Meeting Dedicated to the 5th Anniversary of he Death of Prof. dr. Silvije Kadrnka (1902-1965)** – in 1970, and an **In Memoriam Symposium "Vladimir Gvozdanović"** (1914-1979) – in 1987.

A **Celebration of the 65th Anniversary of the Croatian Society of Radiology (1928-1993)** was held, with art programme and a performance by the Physicians Singers of Zagreb choir, and a historical overview in presence of numerous members of the CSR and the invitees. On that occasion, the first logo of the CSR was also presented, designed by Krešimir Ivanček, academic painter – graphic artist, Studio Color Soft, of Bjelovar, and after our ideas and efforts made by Prim. Dr. Luka Ježek, the Head of the Department of Radiology in the Bjelovar General Hospital.

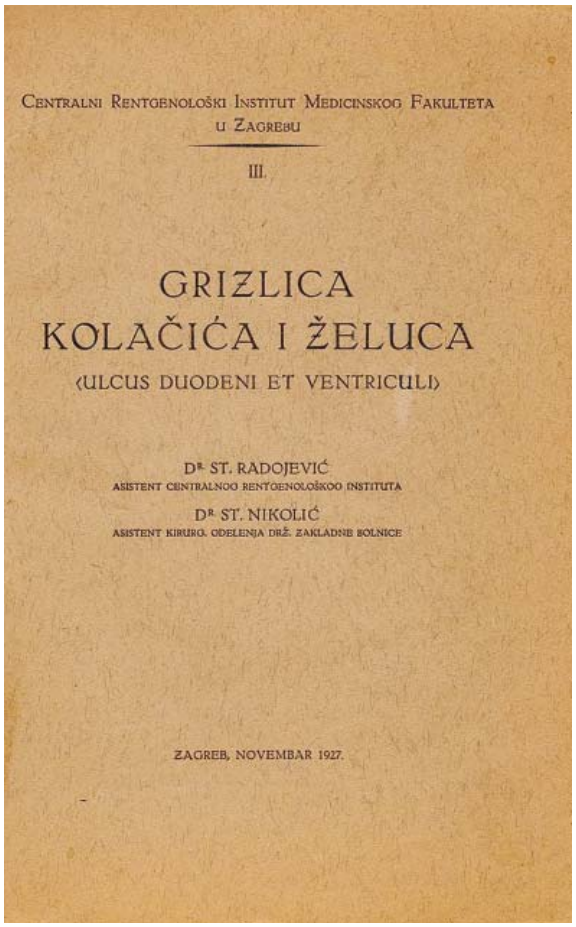
CENTRALNI RENTGENOLOŠKI INSTITUT MEDICINSKOG FAKULTETA U ZAGREBU

III.

GRIZLICA KOLAČIĆA I ŽELUCA

(ULCUS DUODENI ET VENTRICULI)

Dr. ST. RADOJEVIĆ
ASISTENT CENTRALNOG RENTGENOLOŠKOG INSTITUTA

Dr. ST. NIKOLIĆ
ASISTENT KIRURG. ODELENJA DRŽ. ZAKLADNE BOLNICE

ZAGREB, NOVEMBAR 1927.

FIGURE 3. The book of Stevo Radojević and St. Nikolić. Radojević S, Nikolić S. *Grizlica kolačića i želuca [Ulcus duodeni et ventriculi]*. Zagreb: Centralni rentgenološki institut Medicinskog fakulteta u Zagrebu [Central Roentgen Institute of Medical Faculty Zagreb]; 1927.

There was also held a **Celebration of the 100th Anniversary of the X-rays Discovery (1985-1995)**. The Society thus joined marking of that event, remembered all around the world. On that occasion the Technical Museum Zagreb organised an exhibition on the **Röntgen Rays Discovery 1985-1995** (Figure 5); and an article: "Lovrenčić M, Marotti M, Bašić M. *Iz povijesti medicinske primjene rentgenskih zraka u dijagnostičke svrhe u Hrvatskoj (From the history of medical application of roentgen rays for diagnostic purposes in Croatia)"* was published, among others, in the accompanying book.[11]

Professional journals

Before the Second World War, a journal **Radiološki glasnik** *(Journal of Radiology)* used to be published for some time. The journal **Radiologia Iugoslavica** used to be published from 1966-1992, being a gazette of the Yugoslav Society of Radiology and Nuclear Medicine. Out of 16 members of the Colegium Redactorum until 1974, there were seven (44%) members from Croatia: Bašić M, Gvozdanović V, Mark B, Martinčić N, Petrovčić F, Smokvina M and Špoljar M. Just as an example of the participation of Croatian radiologists in the journal, let us mention that out of the total of 9 articles in one particular issue (*Radiol Yugosl* 8(1); 1974) 4 of them (44%) were from Croatia. In the period from 1974-1990, out of the total of 27 Editorial Board members, 5 of them (18 %) were from Croatia: Ivančević D, Lovrenčić M, Popović S, Spaventi Š, Leković A, and out of the total of 24 Advisory Board members, 5 of them (21%) were from Croatia: Kovačević D, Šimonović I, Šimunić S, Dujmović M, Lovasić I. Just as an example of the participation of Croatian radiologists in the journal, let us mention that out of the total of 27 articles in one particular issue (24[4];1990), 10 of them (37%) were from Croatia.

A joint journal has been published since 1992 – **Radiology and Oncology**, a journal devoted to the publication of original contributions in diagnostic and interventional radiology, CT, US, MR, nuclear medicine, radiotherapy, clinical and experimental oncology, radiobiology, radiophysics and radiation protection. The founders and publishers are the Slovenian Association of Radiology, the Slovenian Nuclear Medicine Society, the Slovenian Society for Radiotherapy and Oncology and the Slovenian Cancer Society, and the **Croatian Medical Association / Croatian Society of Radiology**. The associated societies are also the Societas Radiologorum Hungarorum and the Friuli-Venezia Giulia regional group of La Società italiana per la radiologia medica (SIRM). The first editor-in-chief for many years was Tomaž Benulič (now editor-in-chief-emeritus). He was succeeded by Gregor Serša. Out of the 38 Editorial Board members (1992-2008), 9 of them (24%) were from Croatia: Bešenski N, Boko H, Drinković I, Hebrang A, Lovrenčić M, Osmak M, Papa J, Šimunić S, Lovasić I. The other members were from Slovenia, Hungary, Austria, Italy, USA, Australia, the Netherlands, Canada and Germany. Since year 2008, out of the total of 30 Editorial Board members, 3 of them (10%) are from Croatia: Osmak M, Štern-Padovan R, Miletić D. The journal is published 4 times per year, only in the English language.[12]

Current activities and congresses

Regular monthly expert meetings (8-10 times per year) are held as a rule in the Great Hall of the Croatian Medical Association, in Šubićeva Street in Zagreb. These meetings used to be held occasionally also in institutions out of Zagreb: in Bjelovar, Sisak, Karlovac, Varaždin, Krapinske toplice and even in Osijek, Split and Pula.

Since the independence of Croatia and the founding of the Croatian Society of Radiology, five Elective Assemblies were held: 1992, 1996, 2000, 2004 and 2008. Thus, the conditions were met (64 years from its foundation and continuous activities, and 95 years from the first practical application of X-rays in Croatia) for holding national radiology congresses.

The First Congress of the Croatian Society of Radiology with International Participation was held in Opatija, from 11th – 15th October 1994, in the Adriatic Hotel. On behalf of the European Association of Radiology, the Congress was greeted by the then president, Lodovico dalla Palma (Trieste), and other invitees and guests. Out of the total of 155 lectures and 14 workshops, there were sixteen lectures (10%) and seven workshops (50%) from abroad. Beside the Croatian and foreign expert lectures, part of the lectures was dedicated also to historic topics on the development of radiology in the region: Šimunić S. (part of Croatia); Ježek L. (Bjelovar), Kačić P. (Dubrovnik) and Lovasić I. (Rijeka). There was a book also published on that occasion: *"Dijagnostička i intervencijska radiologija (Diagnostic and interventional radiology).* Lovasić I, Dujmović M, Budiselić B, Riman S, editors.[13]

The Second Congress of the Croatian Society of Radiology with International Participation was held in Osijek, from 23rd – 25th April 1998, in the Croatian Army Hall.[3] Out of the total of 150 lectures and 38 posters, there were 20 lectures (13%) and 13 posters (34%) from abroad. On the same occasion a book by Frković M was presented: *"Radiološki atlas probavnog sustava djece (A radiological atlas of the children digestive track)"*, and also a satellite mini-symposium was held*: "Nonionic Radiological Diagnostic Contrast Medium – OPTIRAY (Ioversol)"*, by the company Byk-Gulden, Konstanz, Germany. In addition to the expert topics, the Congress also discussed historic issues related to radiology in the re-

gion: Glavina K, Vugrinec M, Dlouhy B, Sontacchi B. The second section of lectures was dedicated to current organisational developments in radiology and radiation protection legislation (Hebrang A, Grgić S, Kubelka D, Vekić B). The proceedings were also published, including lectures and summaries.

The Third Congress of the Croatian Society of Radiology with International Participation was held in Split, from 5th – 8th June 2002, in the Marjan Hotel. Out of the total of 176 lectures and 80 posters, there were 53 lectures (30%) and 13 posters (16%) from abroad. On the occasion of the congress, a special issue of Acta Clinica Croatica (*Acta Clin Croat* 2002; 41[Suppl 1]: 1-126.) was published, which included 19 congress articles.[4]

The Fourth Congress of the Croatian Society of Radiology with International Participation was held in Zagreb, from 11th – 14th October 2006, in the Westin Hotel. Out of the total of 177 lectures and 51 posters, there were 34 lectures (19%) and 3 posters (6%) from abroad. The medical journal published a special issue (*Lijec Vjesn* 2006; 128[Suppl 7]: 5-107.) with summaries of lectures and posters. (12)

Key note lectures

The topics of expert meetings and other events in radiology were various and the intention was to follow all the new events. It is evident from the archive material that various techniques were discussed as early as in 1964: lympho-gamma-scintigraphy (Spaventi Š, Bosnar M); lymphography technique with oil contrast medium (Temer B, Beronić I), roentgen cinematography (Katunarić D), on the principles of logetron work (Katunarić D.), on rotation and pendulum roentgen therapy (Bašić M), and a Report on the 1st Symposium on Radiology Protection (Petrovčić F), held in Portorož, was submitted.

A number of interesting radiology cases from daily practice (Hočušćak I) were discussed at the meeting held in the Varaždin General Hospital in 1965, and a lecture was given with reference to the World Congress of Radiology in Rome (Katunarić D).

More than 40 years ago (1967) the application of ultrasound in diagnosis had been discussed (Ašperger Z).

Lectures on radiology were not seldom programmed together with other clinical professions, as *e.g.* a lecture on "Three Cases of Urological Diagnostics" (Kos V. and assoc. radiologists and Čečuk LJ and assoc. urologists – 1968). Or cooperation between internal medicine-radiology for the lecture: "Brachial angiography" (Čustović F, Gvozdanović V, Šimunić S – 1968); "Unusual form of congenital lymphoedema" (cooperation of radiology-surgery Prpić-Hartl V. Pasini M – 1968); "A case of morbus Klippel-Trenaunay-Weber" (Lovrenčić M, Georgijević A – 1968).

Particularly interesting lectures were given by clinicians from other branches before radiological audience: "Coordinated findings of radiologists and clinicians in pulmology" (internal medicine specialist Harambašić H – 1968); "Biliary tract dis-

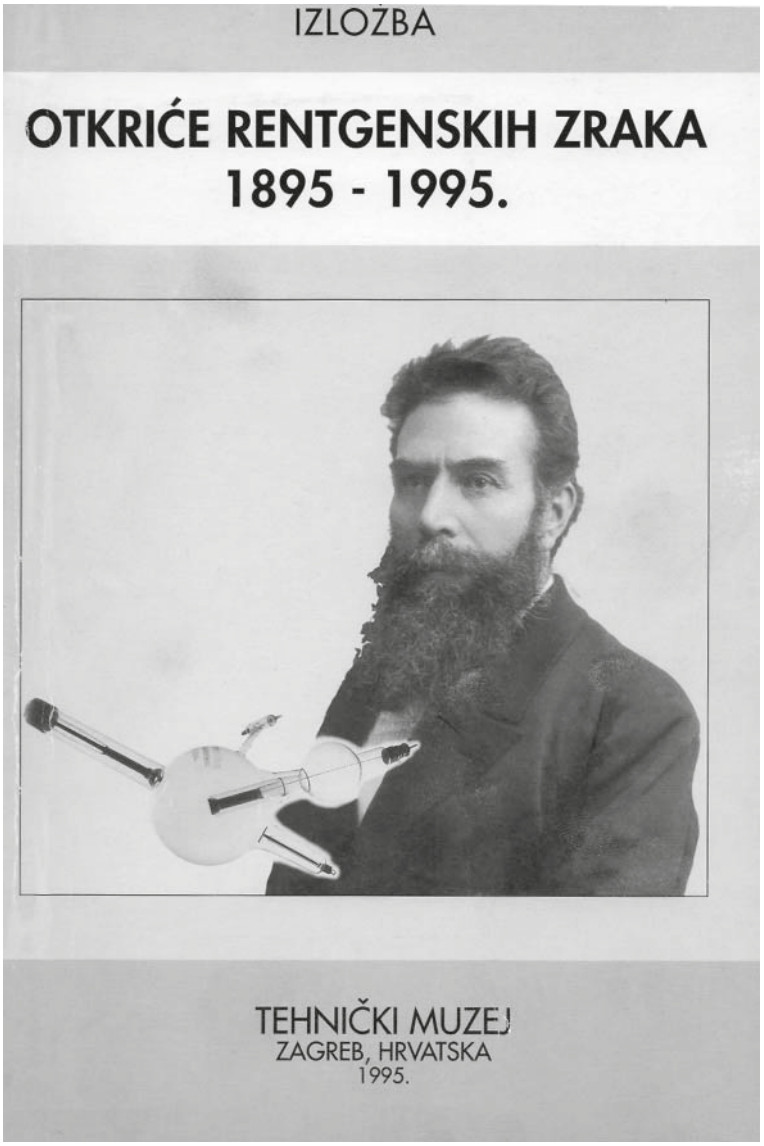

FIGURE 4. Izložba. Otkriće rentgenskih zraka 1895-1995". [Exhibition, Discovery of x-Ray, 1895-1995]. Zagreb 14.12.1995 – 18.02.1996. Zagreb: Tehnički muzej Zagreb [Technical museum Zagreb]; 1995.

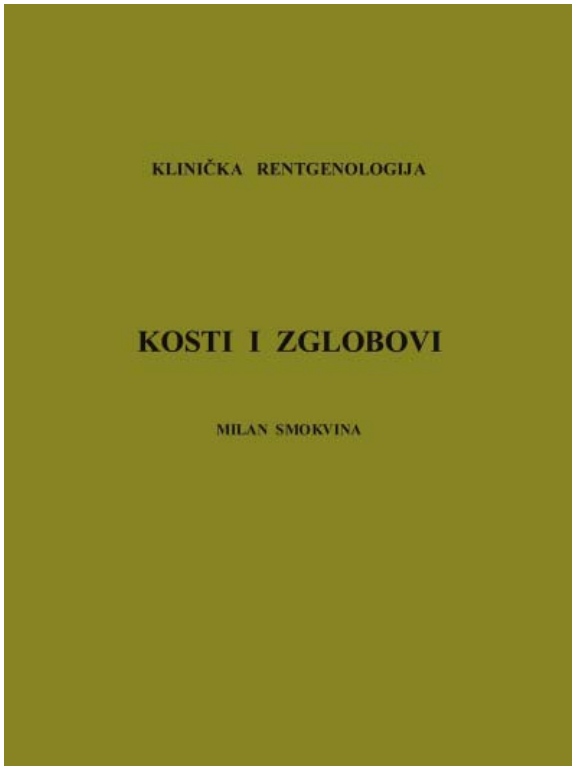

FIGURE 5. The book of Milan Smokvina. Clinical roentgenology, bones and joints. Smokvina M, editor. Zagreb: Yugoslav Academy of Sciences and Arts; 1959.

eases and role of roentgen diagnostics as viewed through the prism of clinicians" (internal medicine specialist Čerlek S – 1968); "Clinical aspects of chronic gastritis" (internal medicine specialist Kallai L – 1968).

A lecture on "Lumbar myelography without anaesthesia using Mallinckrodt contrast media Conray 60" was held on an expert meeting in Pula (1969).

On pneumogynecography technique and application: lectured by Gjurin B – 1969; on transhepatic cholangiography: Temer B – 1969; on testicular lymphography: Agbaba M and assoc. – 1969.

On the occasion of a visit paid by the colleagues from Ljubljana, two reports were submitted from the 12th International Congress of Radiology – Tokyo 1969, Tabor L from Ljubljana and Gvozdanović V from Zagreb.

In a whole-evening expert programme on "bronchitis", the topic was discussed by pulmonologists and radiologists from the aspect of the clinical picture, the problems of public health service, the role of functional analysis of breathing and roentgen diagnostics – 1970).

In a review of the 2nd Diagnostic Course of the International Society of Lymphology (Davos 1971), Mihajlović N, Šimunić S, and Agbaba M talked about the organisation of the course, the lymphogram analysis, new nomenclature and new views in lymphography diagnostics.

Cooperations

In working and cooperating with many companies, manufacturers and suppliers of the necessary working material, there are occasionally held joined meetings aimed at providing information on new products, technologies and methods. A round table on enteroclysis was held (1992): "The small barium enema (enteroclysis) with barium and methylcellulose" and "Die Technik der radiologischen Dündarmdiagnostik – Enteroclysis", with companies Nicholas GmbH Sulzbach and Aspro-Nicholas Vienna, with the participation of lecturers: Antes G (Sulzbach) and Holacky (Vienna), and the radiologists: Mandić A, Dolenčić P, Frković M, Kapetanović D and Tonković V, and the internal medicine specialists: Papa B, Vucelić B and Bilić A of Zagreb.

Another round table was held (1992) on "Ultrasound in algorithm of diagnostic and interventional procedures in renal disease". Introductory lectures were held by Odak D: "Ultrasound diagnostics in inflammatory and obstructive renal diseases"; Drinković I: "Ultrasound diagnostics of expansive renal processes and intervention ultrasound"; and Brkljačić B: "Possibilities of application of Doppler and colour-Doppler in renal diseases". Sabljar-Matovinović M, Mrklić B, Agbaba M, Hebrang A, Marotti M and Kunštek N participated in the discussion.

The CSR occasionally cooperates with the Slovenian colleagues – radiologists. Pavčnik D (1993), of the Institute of Diagnostic and Interventional Radiology, the University Clinical Center Ljubljana, filled the whole-evening programme with lectures on intravascular stents, microcatheters, subselective angiographies, transcatether embolizations and fibrinolysis and vena cava filters.

An ever-topical issue of the protection of patients and personnel from ionizing radiation was covered in two whole-evening programmes (1993) by the most competent experts in the field: Hebrang A and Gunarić M – the Ministry of Health of the Republic of Croatia; Milković-Kraus S, Cerovac H and Cesar D – the Institute for Medical Research and

Occupational Health; Pokupec R – the Department of Ophthalmology, University Hospital Centre Zagreb; Vekić B – the Ruđer Bošković Institute; and Marović F – the Ministry of Labour and Social Welfare of the Republic of Croatia.

The CSR contributed also to the celebration on the occasion of the 150th anniversary of the Bjelovar General Hospital and Radiology Activities (1995), when the lectures were, beside the hosts (Ježek L and assoc.), held by Marotti M and assoc; and Papa J and assoc.

The CSR and the Radiological Diagnostics Department of the Karlovac General Hospital organised a joint expert meeting (1995), with the programme prepared by the hosts, which covered the historic development of radiology in Karlovac (Pavan G); algorithm of radiological examinations in abdominal tumour diagnostics (Pavan G and assoc.); ten years of the ultrasound application in Karlovac (Popović A and assoc.); the value of ultrasound in diagnostics of choledocholithiasis (Baškot A and assoc.).

Along with one of the expert programmes (1995), an occasional Christmas meeting was held, with a lecture on the comparison between CT and DSA in evaluating the degree of the extension of bronchial carcinoma (Marušić P and assoc.), and an occasional Christmas address was given by Msgr. Matija Stepinec, the parish priest of St. Peter's Parish in Zagreb; it was followed by a "Little Christmas Concert" (Snježana Arbanas, soprano, medical student ABD, accompanied by piano played by Hlavomirka Bledšnajder, BAMus).

In one of the meetings (1996), the Ministry of Health informed the CSR's members about the condition of the radiological equipment in the Republic of Croatia, in comparison with other countries (Hebrang A); about the ionizing radiation legislation in force in relation to world standards (Grgić S and assoc.), and about the results of the checks performed on medical sources of radiation (Tonković V).

The cooperation with colleagues radiologists – veterinary surgeons has already been pointed, but let us mention also that the CSR (1966) took part in the celebration on the occasion of the 65th anniversary of the foundation and work of the Department of Roentgenology and Physical Therapy of the Faculty of Veterinary Medicine in Zagreb, when an overview of the historical development of the Department, and scientific and professional cooperation with human medicine were presented (Šehić M).

The CSR and the Croatian Radiation Protection Association (1966) held a joint meeting, with two particularly attractive, interesting and unusual lectures: "Control without destruction in industry" (Krstelj V, Dean of the Faculty of Mechanical Engineering and Naval Architecture in Zagreb), and "Non-destructive methods in research and protection of works of art" (Braun M, Director of the Institute for the Conservation of Objects of Art, Zagreb).

The Society members had an opportunity to listen to and experience another interesting and unusual programme when the then Section of Radiology was led by the president (1976-1986) Prof. Duško Katunarić (1923-1986), and when Tomislav Ladan (1932-2008), a Croatian writer, linguist, translator, polyglot and lexicographer, held a lecture titled: "Literature and medicine".

This overview of the 80 years of work is a mere attempt to remember, burdened with the present, the "good old times" and save from oblivion at least one part of our rich radiological heritage. We are well aware of many shortcomings this overview may have, being the result of unpreserved documentation from early stages, but also due to the "holes" in the memory of the past not so long ago.

References

1. Belicza B, Tucak A. Glasnik društva Slavonskih liječnika. Najstariji liječnički časopis. Glasilo liječničke udruge u Hrvatskoj 1877-1878. *Lijec Vjesn* 2003; **125:** 213-22.
2. Šimunić S, Horvát L, Glavina K, Fornet B, Bešenski N, Vargha G, te al. Croatian-Hungarian radiological coopereation. *Coll Antropol* 2003; **2:** 823-6.
3. Drugi kongres Hrvatskog društva radiologa [The 2nd Congress of the Croatian Society of Radiology]. Knjiga sažetaka [Book of Abstracts], Osijek, April 23rd-25th, 1998.
4. Treći kongres Hrvatskog društva radiologa [The 3rd Congress of the Croatian Society of Radiology]. Split, June 5th-8th, 2002; *Acta Clin Croat* 2002; **41(Suppl I):** 1-126.
5. *Sto let rentgenskih žarko kozi prizmom medicine, veterine in medikohistorikov [100 years of x-rays through the prism medicine, veterinary nad medical historyans].* Glaser E, editor. Maribor: Medikohistorična sekcija Slovenije, SZD [Section for the history of medicine, Slovenian Medical Society]; 1998.
6. Okrugli stol o intervencijskoj radiologiji. Šimunić S, Gürtl R, editora. Zagreb: Zavod za radiologiju KBC Zagreb; 1981.
7. *Intervencijska radiologinja – perkutana transluminalna angioplastika renalnih, koronarnih i perifernih arterija.* Šimunić S, Šesto M, editor. Zagreb: Sekcija za radiologiju, Kardiološka i nefrološka sekcija Zbora liječnika Hrvatske; 1985.
8. *Intervencijska radiologija.* Mašković J, Boschi S, Stanić I, editors. Split; Sekcija za radiologiju Zbora liječnika Hrvatske – Podružnica Split; 1986.
9. *Radiologija.* Hebrang A, Klarić-Čustović R, editors. Zagreb: Medicinska naklada Zagreb; 2007.

10. Šimunić S, Glavina K, Lovrenčić M. Radiology. Hebrang A, Klarić-Čustović R. Radiologija, editor. Zagreb: Medicinska naklada Zagreb, 2007. *Coll Antropol* 2007; **31:** 641-4.

11. *Izložba. Otkriće rentgenskih zraka 1895-1995" [Exhibition, Discovery of x-Ray, 1895-1995]. Zagreb 14.12.1995 – 18.02.1996.* Zagreb: Tehnički muzej Zagreb [Technical Museum Zagreb]; 1995.

12. Pavcnik D. 60 years of the Slovenian Association of Radiology 1950-2010, *Radiol Oncol* 2009; **43:** 137-43.

13. *Prvi kongres Hrvatskog društva radiologaM. Opatija / Rijeka 13.-15.10.1994.* [The 1st Congress of the Croatian Society of Radiology]. Lovasić I, Dujmović M, Budiselić B, Riman S, editors. Rijeka: Dijagnostička i intervencijska radiologija, Hrvatsko društvo radiologa, Klinički zavod za radiologiju Medicinskog fakulteta u Kliničkom bolničkom centru Rijeka; 1994.

14. *Četvrti kongres Hrvatskog društva radiologa, Zagreb 11.-14.10.2006.* [The 4th Congress of the Croatian Society of Radiology]. Knjiga sažetaka [Abstract Book]. *Lijec Vjesn* 2006; **128 (Suppl 7):** 1-107.

Radiol Oncol 2011; 45(2): 75-81.
doi:10.2478/v10019-011-0005-8

Mikrosatelitna nestabilnost pri raku debelega črevesa in danke

Horvat M, Štabuc B

Izhodišča. Rak debelega črevesa in danke (RDČD) je tretji najpogostejši rak na svetu. V 75% nastane sporadično, v 25% kot ena izmed dednih oblik ali kot posledica kronične vnetne črevesne bolezni. Kancerogeneza poteka več let. Vzrok RDČD je v 85% kromosomska nestabilnost (CIN) in v 15% mikrosatelitna nestabilnost (MSI-H), kjer predstavlja dedni nepolipozni rak debelega črevesa in danke (HNPCC) 10-20%. Mikrosatelitna zaporedja (MZ) so kratka ponavljajoča se zaporedja dolžine do šestih nukleotidov po celotnem genomu. Mikrosatelitna stabilnost (MSS) pomeni, da so MZ enaka v posameznikovi tumorski in zdravi celici, mikrosatelitna nestabilnost (MSI-H) pa pomeni, da se MZ razlikujejo v posameznikovi tumorski in zdravi celici. Vzrok MSI-H je okvarjen mehanizem, ki preverja natančnost podvajanja (*mismatch repair* - MMR), kjer so najpomembnejši proteini MSH2, MLH1 in MSH6.

Zaključki. Zdi se, da je MSI-H pomemben prognostični dejavnik pri RDČD in pomemben prediktivni dejavnik učinkovitosti kemoterapevtskega zdavljenja RDČD. Klinične raziskave so za enkrat dale nasprotujoče si rezultate pri različnih vrstah kemoterapevtskega zdravljenja RDČD, dopolnilnega in paliativnega, zato bo MSI-H predmet nadaljnega raziskovanja. Prihodnost sistemskega zdravljenja raka je v individualizirani terapiji odvisni od molekularnih značilnosti, kot je MSI-H pri RDČD.

Radiol Oncol 2011; 45(2): 82-90.
doi: 10.2478/v10019-011-0004-9

Analiza zaznavanja perifernega arterijskega pretoka na modelu svinje

Meng Q, Ding W, Yang B, Fu N, Lu G

Izhodišča. Namen raziskave je bil zaznati periferni arterijski pretok z ultrazvočno preiskavo na modelu svinje in ugotoviti možnosti diagnoze žilne bolezni glede na vrsto, lokacijo in njeno stopnjo.

Materiali in metode. Po zažemanju okončine, injiciranju adrenalina ali zbadanju stene arterije na šestih svinjah, smo sledili pretoke v eksterni iliakalni arteriji, iliakalni arteriji ali femoralni arteriji.

Rezultati. S povečanjem zažemanja zadnje okončine smo spremenili vrh sistolnega pretoka (*peak systolic velocity* – PSV) ipsilateralne iliakalne arterije s 36,33±1,77 cm/s na 59,72±2,67 cm/s, minimalni pretok po prvem valu (*minimum post-principal wave velocity* – MPV) pa iz 13,68±1,11 cm/s na -7,48±0,82 cm/s. Vrh diastolnega pretoka (*peak diastolic velocity* – PDV) smo na ta način spremenili iz 19,31±0,86 cm/s na 8,98±0,45 cm/s, končni diastolični pretok (*end diastolic velocity* – EDV) pa iz 13,2±0,45 cm/s na 0. S povečanjem odmerka injiciranega epinefrina smo PSV povečali iz 36,33±1,77 cm/s na 43,97±2,15 cm/s, vendar se je za tem znižal na 35,43±3,01 cm/s, med tem ko se je MPV negativno povečal na -23,53±0,82 cm/s, potem ko se je zmanjšal iz 13,68±1,11 cm/s na 0. PDV in EDV sta se počasi znižala na 0. S povečanjem zažemanja in zbadanjem arterijske stene, se je PSV zniževal in imel negativno korelacijo s stopnjo zažemanja (R=0,983; R2=0,967). MPV se je počasi povečeval, a se je njegova smer obrnila, ko se je povečevala stopnja zažemanja, nato se je zmanjševal, ko je bil pretok zmanjšan za 2/3.

Zaključki. Hitrost perifernega pretoka krvi je posledica več dejavnikov: iztisnega volumna srca, žilnega upora, volumna krvi v obtoku in prožnosti žil. Žilni upor ima velik učinek na diastolični val, kjer oblikovanje povratnega vala kaže na povečan upor v perifernem pretoku.

Radiol Oncol 2011; 45(2): 91-96.
doi:10.2478/v10019-011-0007-6

Primerjava CT in MRI diagnostike cerebrospinalnega izliva povzročenega z multiplimi zlomi možganskega dna

Wang X, Xu M, Liang H, Xu L

Izhodišča. Multipli zlomi možganskega dna z izlivom cerebrospinalne tekočine so pogosti zapleti ob mehanski poškodbi možgan, ki zahtevajo kirurški poseg. Zaradi velikokrat kompleksnih poškodb možganskega dna je preoperativna radiološka diagnostika zelo težka. V klinični diagnostiki sedaj pogosto uporabljamo večrezni spiralni CT in MRI. Namen raziskave je bil primerjati zanesljivost cisternografije z večreznim spiralnim CT-jem in MRI-jem pri ugotavljanju cerebrospinalnega izliva.

Metode. V raziskavo smo vključili 23 bolnikov z multiplimi zlomi možganskega dna po mehanski poškodbi glave. Retrospektivno smo analizirali radiološke in kirurške izvide. Pri 12 bolnikih smo naredili preiskavo s 64-reznim CT in nato tridimenzionalno rekonstrukcijo. Pri preostalih 11 bolnikih pa smo naredili preiskavo z MRI in cisternografijo. Mesto cerebrospinalnega izliva sta ugotavljala dva izkušena radiologa, specialista neuroradiologije. Vse bolnike smo operirali, kirurško ponovno določili mesto cerebrospinalnega izliva in naredili rekonstrukcijo. Rezultat zdravljenja smo ocenili kot uspešen, če po kirurškem posegu ni bilo več cerebrospinalnega izliva.

Rezultati. Po kirurškem posegu smo ocenili, da smo pri 9. od 12. bolnikih že preoperativno natančno določili mesto cerebrospinalnega izliva s CT-jem, pri dveh bolnikih tega nismo uspeli zaradi multiplih poškodb, pri enem pa je bila diagnoza lažno pozitivna. Preopearativna smo mesto cerebrospinalnega izliva natančno določili z MRI-jem pri 10 od 11 bolnikih.

Zaključki. MRI cisternografija je sodobnejša diagnostična metoda glede na večrezni CT, ki ju uporabljamo pri multiplih zlomih možganskega dna. Sočasna uporaba obeh metod bi lahko izboljšala natančnost opredelitve cerebrospinalnega izliva.

Radiol Oncol 2011; 45(2): 97-101.
doi:10.2478/v10019-011-0011-x

Difuzijske razlike med pilocitnimi astrocitomi in ependimomi z drugo stopnjo malignosti

Pavliša G, Pavliša G, Radoš M

Izhodišča. Namen raziskave je bil ugotoviti razliko v difuzijskih lastnostih cerebelarnega pilocitnega astrocitoma in ependimoma z drugo stopnjo malignosti pri slikanju z magnetno resonanco (MR).

Bolniki in metode. V prospektivno raziskavo smo vključili 12 bolnikov s pilocitnim astrocitomom in 5 bolnikov z ependimomom. Primerjali smo jih na osnovi difuzijskih koeficientov ob slikanju z MR.

Rezultati. Vrednosti difuzijskih koeficientov so bile značilno višje pri pilocitnih astrocitomih kot pri ependimomih, brez prekrivanja vrednosti med obema vrstama tumorjev.

Zaključki. Rezultati nakazujejo možnost preoperativnega razlikovanja pilocitnih astrocitomov in ependimomov druge stopnje malignosti na osnovi difuzijskih razlik v kombinaciji s standardnim magnetnoresonančnim slikanjem.

Radiol Oncol 2011; 45(2): 102-115.
doi:10.2478/v10019-011-0015-6

CD133/prominin1 je prognostičen za preživetje bolnikov z glioblastoma, vendar obratno korelira z izražanjem cisteinskih katepsinov

Ardebili SY, Zajc I, Gole B, Campos B, Herold-Mende C, Drmota S, Lah TT

Izhodišča. CD133 je označevalec populacije glioblastomskih (GBM) matičnih celic in normalnih nevralnih matičnih celic (NNSC). Želeli smo odkriti, ali sta migracijski potencial in diferenciacija teh matičnih celic povezana z izražanjem CD133 in s katepsinskimi proteazami.

Materiali in metode. Ovrednotili smo invazivnost normalnih NNSC, GBM/CD133+ matičnih celičnih linij in GBM sferoidov v 3D kolagenu ter v enem sloju rastočih U87-MG celic in normalnih astrocitov v 2D Matrigelu. Spremembe v aktivnosti in v izražanju katepsinov B, L in S, ki smo jih izmerili na nivoju mRNA, smo primerjali z invazivnostjo in izražanjem CD133 v 26 gliomih in s preživetjem teh bolnikov.

Rezultati. Povprečen delež CD133+ celic iz vzorcev GBM je bil 9,6%. Preživetje bolnikov z višjim izražanjem CD133 mRNA je bilo statistično značilno krajše ($p<0,005$). Invazijski potencial v povezavi s proteolizno razgradnjo matriksa je bil višji pri NNSC in GBM sferoidih v primerjavi s sferoidi GBM CD133+ matičnih celic. V kliničnih vzorcih gliomov nismo opazili korelacij med izražanjem CD133 mRNA in katepsini, opazili pa smo obratno sorazmerje z njihovimi aktivnostmi.

Zaključki. Raziskava potrjuje, da je CD133 napovedni kazalec za preživetje GBM bolnikov. Dokazali smo, da NNSC bolje in na drugačen način invadirajo kolagen kakor GBM matične celice. To spoznanje lahko vpliva na načrtovanje novih zdravil, vključno proteazne inhibitorje, katerih tarča bi bile le invazivne tumorske matične celice. Povečana katepsinska aktivnost v CD133 negativnih celicah nakazuje na njihovo vlogo v invazivnih GBM.

Radiol Oncol 2011; 45(2): 116-122.
doi:10.2478/v10019-011-0006-7

Bolnicam s karcinomom dojke kemoterapija poveča nivo s kaspazami cepljenega citorkeratina 18 v serumu

Ulukaya E, Karaagac E, Ari F, Oral AY, Adim SA, Tokullugil AH, Evrensel T

Izhodišča. Kemoterapija povzroča apoptozo tumorskih celic, zato bi lahko pri bolnikih z rakom z merjenjem apoptoze ugotavljali učinkovitost zdravljenja prej kot s konvencionalnimi metodami.

Bolniki in metode. Apoptozo smo ugotavljali s pomočjo novega specifičnega biomarkerja, s kaspazami cepljenega citokeratina 18 (antigena M30). Uporabili smo test ELISA. V raziskavo smo vključili 37 bolnic z malignimi (metastatskimi ali nemetastatskimi) tumorji dojke, 35 bolnic z benignimi spremembami v dojki in 34 zdravih žensk. Bolnice z rakom so dobivale neoadjuvantno kemoterapijo, fluorouracil, epirubicin in cyclophosphamide ali epirubicin skupaj z docetexelom. Antigen M30 smo bolnicam z malignimi tumorji določili pred kemoterapijo ter 24 in 48 ur po njej.

Rezultati. Ugotovili smo, da se osnovne vrednosti apoptoze v skupinah bolnic z nemetastatskimi malignimi ali benigni spremembami niso statistično značilno razlikovale od bazične vrednosti pri zdravih ženskah ($p>0,05$). Statistično značilno večje pa so bile bazične vrednosti antigena M30 pri metastatski skupini bolnic v primerjavi s kontrolno skupino ($p<0,05$). Bazični nivo M30-antigena je bil približno 3-krat višji pri bolnicah regresijo tumorja.

Zaključki. V raziskavi se je M30-antigen v serumu bolnic z rakom dojke po kemoterapiji povečal. Tako bi merjenje tega antigena pomagalo pri zgodnjem napovedovanju učinkovitosti kemoterapevtskega zdravljenja, vendar je potrebno rezultate potrditi v večji raziskavi.

Radiol Oncol 2011; 45(2): 123-128.
doi:10.2478/v10019-011-0014-7

Klinična učinkovitost lokalne tarčne kemoterapije pri trojno negativnem raku dojke

He J, Wang X, Guan H, Chen W, Wang M, Wu H, Wang Z, Zhou R, Qiu S

Izhodišča. Namen raziskave je bil oceniti klinično učinkovitost predoperativne superselektivne intraarterialne tarčne kemoterapije pri zdravljenju raka dojke, ki ne izraža estrogenskih receptorjev (ER), progesteronskih (PR) in HER2 receptorjev in ki ga imenujemo trojno negativni rak dojke.

Bolniki in metode. V raziskavo smo zajeli 47 bolnic s trojno negativnim rakom dojke (29 z bolezenskim stadijem II, 13 s III in 5 s stadijem IV). Randomizirano so bile razvrščene v dve skupini: skupino, ki je prejemala tarčno kemoterapijo (n=24), in kontrolno skupino (n=23). Bolnice s tarčno kemoterapijo so citostatike prejemale predoperativno superselektivno intraarterialno po shemi CEF (C: ciklofosfamid [600 mg/m^2]; E: epirubicin [90 mg/m^2]; F: 5-fluorouracil [600 mg/m^2]). Bolnice v kontrolni skupini pa so prejemale enako shemo predoperativne kemoterapije, vendar intravenozno. Ugotavljali smo trajanje zdravljenja, spremembe tumorjev in potek bolezni.

Rezultati. Pri bolnicah s tarčno kemoterapijo je povprečno predoperativno zdravljenje trajalo 15 dni in je bilo značilno krajše kot pri bolnicah v kontrolni skupini, kjer je trajalo 31 dni (P<0,01). Odgovor na zdravljenje je bil pri bolnicah s tarčno kemoterapijo 91,6% in pri bolnicah v kontrolni skupini 60,9%. V prvi skupini sta 2 bolnici umrli v času dveh let (obe sta imele bolezenski stadij IV), v kontrolni skupini pa je umrlo 7 bolnic (2 s stadijem II, 4 s III in 1 s stadijem IV).

Zaključki. Superselektivna intraarterialna predoperativna kemoterapija je učinkovita pri trojno negativnem raku dojke. Čas predoperativnega zdravljenja je krajši, odgovor na zdravljenje je večji in potek bolezni bolj ugoden v primerjavi z intravenoznim predoperativnim zdravljenjem.

Radiol Oncol 2011; 45(2): 129-131.
doi:10.2478/v10019-010-0053-5

Prikaz primera redkega vzroka za anemijo: adenom Brunnerjevih žlez

Coskun A, Erkan N

Izhodišča. Adenomi Brunnerjevih žlez so redki benigni tumorji, ki izvirajo iz teh žlez v dvanajstniku.

Prikaz primera. Opisujemo primer 48-letnega turškega bolnika, ki je navajal blago tiščanje v žlički, izgubo apetita in slabost brez bruhanja, ki se je pojavljala po zaužitju hrane. Težave so trajale pol leta. V laboratorijskih izvidih je izstopala hipokromna mikrocitna anemija. Z ezofagogastroduodenoskopijo in endoskopskim UZ smo odkrili lobuliran, rdeč polipoiden tumor, pokrit z normalno sluznico, ki je ležal na sprednji steni dvanajstnika. Tumor smo poskušali odstraniti endoskopsko, vendar poseg ni uspel, potrebna je bila transduodenalna polipektomija. Histološki izvid je pokazal, da je imel bolnik adenom Brunnerjevih žlez. Leto dni po posegu je bil bolnik brez težav, endoskopski izvid dvanajstnika je bil v mejah normale.

Zaključki. Adenom Brunnerjevih žlez je redek vzrok za anemijo. Rezultati zdravljenja tega tumorja so odlični.

Radiol Oncol 2011; 45(2): 132-142.
doi:10.2478/v10019-011-0012-9

Absorbirana doza na tarčo in njeno okolico kot posledica premikanja obsevalnih sektorjev zaradi repozicioniranja bolnika pri obsevalni aparaturi Gamma Knife® Perfection™

Tran TA, Wu V, Malhotra H, Steinman JP, Prasad D, Podgorsak MB

Izhodišča. Načrtovalni sistem za obsevanje GammaPlan™ ne upošteva v celoti zaslonske doze v primeru, ko je potrebnih več delnih obsevanj tarče za določeno obsevalno zdravljenje. V raziskavi smo izmerili neupoštevane ekspozicije na tarčo in na okolico tarče. Dobljene podatke smo primerjali s podobnim učinkom pri obsevalni aparaturi Gamma Knife® model 4C.

Materiali in metode. Stereotaktični okvir za glavo smo pritrdili na Leksellov® sferični fantom s premerom 16 cm; ob uporabi fiducijske kocke smo posneli CT slike in jih prenesli v načrtovalni sistem za obsevanje. Meritve dajejo odnos med izmerjeno dozo in številom repozicioniranj z bolnikovim pozicionirnim sistemom (PPS) ter z velikostjo kolimatorja. Predpisana absorbirana doza na tarčo je bila 10 Gy za 50% izodozo, vse meritve pa so bile opravljene z ionizacijsko celico.

Rezultati. Izmerjena absorbirana doza narašča s frekvenco repozicioniranja in z velikostjo kolimatorja. Kadar obsevalni sektorji prehajajo med fazo, ko imamo ekspozicijo (*beam on*), in fazo, ko je nimamo (*beam off*), prejme tarča več zaslonske doze kot njena okolica. Za kolimator velikosti 16 mm smo izmerili dozo na tarčo 3,53±0,04 cGy/repozicijo, za kolimator velikosti 8 mm pa 1,59±0,04 cGy/repozicijo. Okolica tarče prejme dodatno dozo, ki je odvisna od relativne lege glede na tarčo.

Zaključki. Posledica premikov obsevalnih sektorjev pri obsevalni aparaturi Gamma Knife® Perfection™ je dodatna doza zaradi t.i. zaslonskega učinka. Velikost te ekspozicije je primerljiva s tisto, ki je izmerjena pri modelu 4C.

Radiol Oncol 2011; 45(2): 143-146.
doi:10.2478/v10019-011-0008-5

Vpliv ščitničnega volumna na odlaganje energije izotopa ^{131}I izračunan z Monte Carlo simulacijo

Mowlavi AA, Fornasier MR, de Denaro M

Izhodišča. Znano je, da je lahko uspeh radiometaboličnega zdravljenja hipertiroidizma z izotopom ^{131}I odvisen od absorbirane doze v ščitnici. Zato je zelo pomembno, da izračunamo za različne mase ščitničnih režnjev radiacijsko dozo, ki jo prejme bolnik, tako natančno, kot je mogoče. Namen raziskave je bil z Monte Carlo simulacijo oceniti vpliv ščitničnega volumna na odlaganje energije žarkov beta in gama pri sevanju izotopa ^{131}I.

Materiali in metode. Ščitnične režnje smo opisali kot elipsoide z gostoto 1,05 g/cm^3 in sestavo po priporočilih Mednarodne komisije za radiološko zaščito (ICRP). Izračunali smo odloženo energijo žarkov izotopa ^{131}I za različne volumne ščitničnih režnjev s kodo MCNPX ter upoštevali popolni transport žarkov beta in gama.

Rezultati in zaključki. Rezultati kažejo, da se je skupna odložena energija pomembno razlikovala – do 11%, ko se je volumen ščitničnega režnja spreminjal od 1 ml do 25 ml. Vrednost energije smo izračunali s programom MIRDOSE za 10 g kroglo. Delež absorbirane energije je naraščal z volumnom, ker povečano razmerje volumna glede na površino elipsoidnega režnja povzroči padec deleža žarkov beta, ki ubežijo iz ščitničnega režnja.

Fundacija "Docent dr. J. Cholewa"
je neprofitno, neinstitucionalno in nestrankarsko
združenje posameznikov, ustanov in organizacij, ki želijo
materialno spodbujati in poglabljati raziskovalno
dejavnost v onkologiji.

Dunajska 106
1000 Ljubljana

ŽR: 02033-0017879431

Activity of "Dr. J. Cholewa" Foundation for Cancer Research and Education - a report for the second quarter of 2011

The Dr. J. Cholewa Foundation for Cancer Research and Education is a non-profit, non-government and non-political association of individuals, institutions and organisations with the aim to support various initiatives in cancer research, prevention and education. Its target audience includes medical and other professionals, and general population. The Foundation distributes various grants and other forms of help to applicants wishing to extend existing or gain new knowledge in oncology. It also helps professional and other associations in Slovenia to organise scientific and other meetings of specific interest in different fields of advanced cancer research. On the other hand, it also supports Slovenian Cancer Association to publish various cancer information and cancer awareness brochures and booklets for general public. Importantly, the Foundation continues to support the publication of "Radiology and Oncology" international medical scientific journal that is edited, published and printed in Ljubljana, Slovenia. "Radiology and Oncology" is an open access journal, available free of charge on its website.

Within its possibilities, the Foundation supports the implementation of all advances in cancer therapy and education into everyday hospital, ambulatory and health promotion practice. Several new activities are to be added to its routine in the near future, as the need for up to date prevention and early detection measures available to Slovenian patients has grown substantially in the last few years, with a number of changes in incidence and prevalence rates of various types of cancer.

The Foundation continues with its activities in 2011 with the aim to spread the latest scientific information about cancer to specialists and other professionals in Slovenia, with important part of its activities being the education and information of general public about prevention, early detection and treatment of cancer. Hopefully, these activities may lead to greater application of the latest cancer diagnostic, therapy and education methods to medical, nursing and public environment in Slovenia.

Andrej Plesničar, MD, MSc
Tomaž Benulič, MD, MSc
Prof. Borut Štabuc, MD, PhD

Prsni ekspanderji in vsadki za rekonstrukcijo dojk

Contour Profile® Gel Family
The CPG® 300 Series

Smooth Tissue Expander Family.
Veliko število različnih oblik.

Siltex® Contour Profile® Style
6300 Tall Height

Zastopa in prodaja:

LABORMED

Labormed d.o.o. Ljubljana

Tel.: 01/436 49 00 | www.labormed.si | info@labormed.si

the power *to transform*®

MENTOR

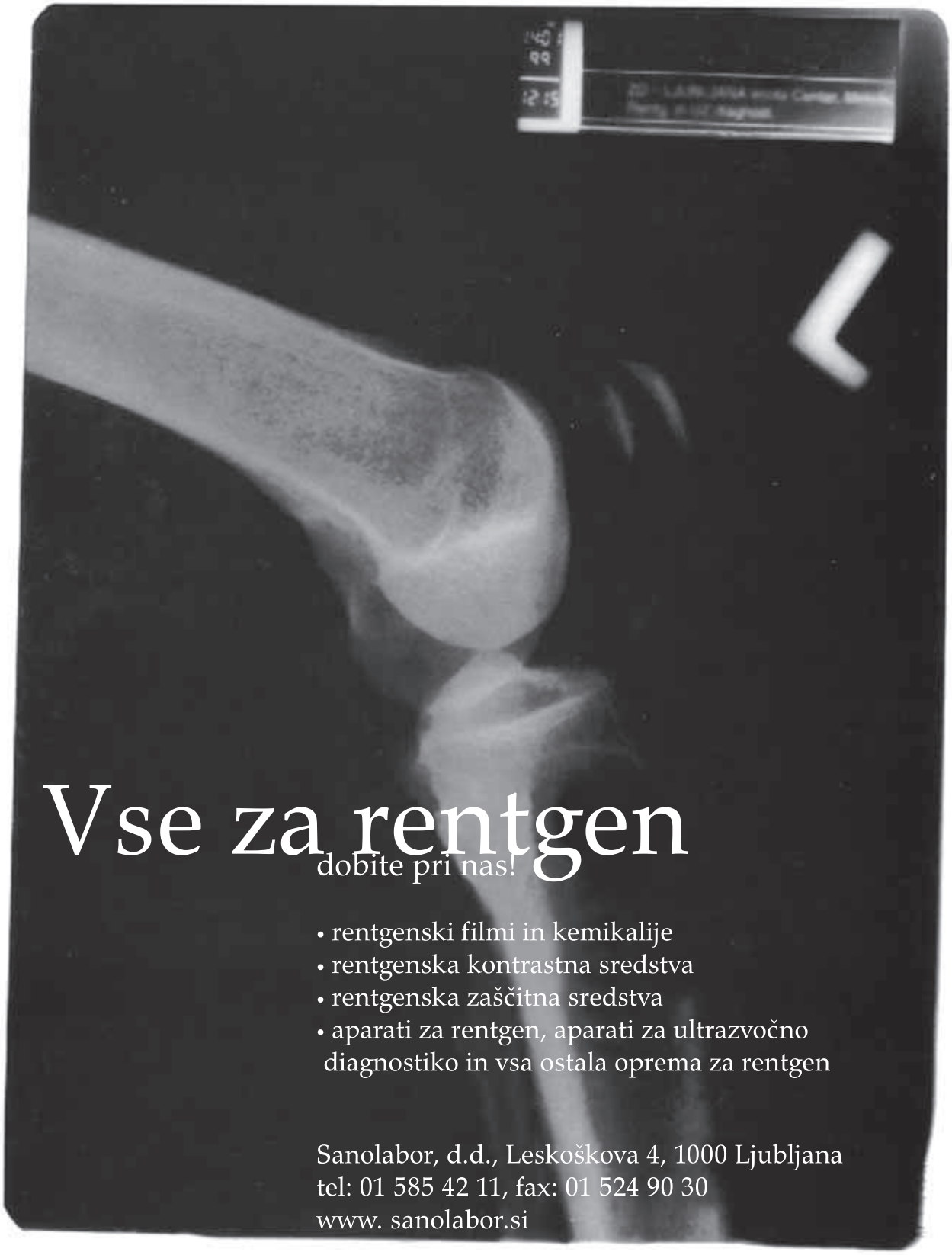

Vse za rentgen

dobite pri nas!

- rentgenski filmi in kemikalije
- rentgenska kontrastna sredstva
- rentgenska zaščitna sredstva
- aparati za rentgen, aparati za ultrazvočno diagnostiko in vsa ostala oprema za rentgen

Sanolabor, d.d., Leskoškova 4, 1000 Ljubljana
tel: 01 585 42 11, fax: 01 524 90 30
www. sanolabor.si

Sanolabor

Zadeli smo pravo tarčo

Izredno učinkovito zdravljenje prvega reda pri nedrobnoceličnem pljučnem raku z mutacijo EGFR

Iressa je prva in edina tarčna monoterapija, ki dokazano podaljša preživetje brez napredovanja bolezni v primerjavi z dvojno kemoterapijo kot zdravljenje prvega reda pri bolnikih z napredovalim nedrobnoceličnim pljučnim rakom z mutacijo EGFR. [1]

IRESSA® (GEFITINIB)
SKRAJŠAN POVZETEK GLAVNIH ZNAČILNOSTI ZDRAVILA

1. Povzetek glavih značilnosti zdravila Iressa (gefitinib). Junij 2009.

Sestava: Filmsko obložene tablete vsebujejo 250 mg gefitiniba. **Indikacije:** zdravljenje odraslih bolnikov z lokalno napredovalim ali metastatskim nedrobnoceličnim pljučnim rakom z aktivacijskimi mutacijami EGFR-TK **Odmerjanje in način uporabe:** Zdravljenje z gefitinibom mora uvesti in nadzorovati zdravnik, ki ima izkušnje z uporabo zdravil proti raku. Priporočeno odmerjanje zdravila IRESSA je ena 250-mg tableta enkrat na dan. Tableto je mogoče vzeti s hrano ali brez nje, vsak dan ob približno istem času. **Kontraindikacije:** preobčutljivost za zdravilno učinkovino ali katerokoli pomožno snov, dojenje **Opozorila in previdnostni ukrepi:** Pri 1,3 % bolnikov, ki so dobivali gefitinib, so opažali intersticijsko bolezen pljuč (IBP). Ta se lahko pojavi akutno in je bila v nekaterih primerih smrtna. Če se bolniku poslabšajo dihalni simptomi, npr. dispneja, kašelj in zvišana telesna temperatura, morate zdravljenje z zdravilom IRESSA prekiniti in bolnika takoj preiskati. če je potrjena IBP, morate terapijo z zdravilom IRESSA končati in bolnika ustrezno zdraviti. čeprav so bile nepravilnosti testov jetrnih funkcij pogoste, so jih redko zabeležili kot hepatitis. Zato so priporočljive redne kontrole delovanja jeter. V primeru blagih do zmernih sprememb v delovanju jeter je treba zdravilo IRESSA uporabljati previdno. Če so spremembe hude, pride v poštev prekinitev zdravljenja. Zdravilo IRESSA vsebuje laktozo. Bolniki z redko dedno intoleranco za galaktozo, laponsko obliko zmanjšane aktivnosti laktaze ali malabsorpcijo glukoze2galaktoze ne smejo jemati tega zdravila. Bolnikom naročite, da morajo takoj poiskati zdravniško pomoč, če se jim pojavijo kakršnikoli očesni simptomi, huda ali dolgotrajna driska, navzea, bruhanje ali anoreksija, ker lahko vse te posredno povzročijo dehidracijo. **Medsebojno delovanje zdravile:** Induktorji CYP3A4 lahko povečajo presnovo gefitiniba in zmanjšajo njegovo koncentracijo v plazmi. Zato lahko sočasna uporaba induktorjev CYP3A4 (npr. fenitoina, karbamazepina, rifampicina, barbituratov ali zeliščnih pripravkov, ki vsebujejo šentjanževko/Hypericum perforatum) zmanjša učinkovitost zdravljenja in se ji je treba izogniti. Pri posameznih bolnikih, ki imajo genotip slabih metabolizatorjev s CYP2D6, lahko zdravljenje z močnim zaviralcem CYP3A4 poveča koncentracijo gefitiniba v plazmi. Na začetku zdravljenja z zaviralcem CYP3A4 je treba bolnike natančno kontrolirati glede neželenih učinkov gefitiniba. Pri nekaterih bolnikih, ki so jemali varfarin skupaj z gefitinibom, so se pojavili zvišanje internacionalnega normaliziranega razmerja (INR) in/ali krvavitve. Bolnike, ki sočasno jemljejo varfarin in gefitinib, morate redno kontrolirati glede sprememb protrombinskega časa (PC) ali INR. Zdravila, ki občutno in dolgotrajno zvišajo pH v želodcu npr. zaviralci protonske črpalke in antagonisti H2, lahko zmanjšajo biološko uporabnost gefitiniba in njegovo koncentracijo v plazmi in tako zmanjšajo učinkovitost. Redno jemanje antacidov, uporabljenih blizu časa jemanja zdravila IRESSA, ima lahko podoben učinek. **Neželeni učinki:** V kumulativnem naboru podatkov kliničnih preskušanj III. faze so bili najpogosteje opisani neželeni učinki, ki so se pojavili pri več kot 20 % bolnikov, driska in kožne reakcije (vključno z izpuščajem, aknami, suho kožo in srbenjem). Neželeni učinki se ponavadi pojavijo prvi mesec zdravljenja in so praviloma reverzibilni. Ostali pogostejši neželeni učinki so: anoreksija, konjunktivitis, blefaritis in suho oko, krvavitev, npr. epistaksa in hematurija, intersticijska bolezen pljuč (1,3 %), navzea, bruhanje, stomatitis, dehidracija, suha usta, nepravilnosti testov jetrnih funkcij, bolezni nohtov, alopecija, asimptomatično laboratorijsko zvišanje kreatinina v krvi, proteinurija, astenija, pireksija. **Vrsta in vsebina ovojnine:** škatla s 30 tabletami po 250 mg gefitiniba **Način izdajanja zdravila:** samo na recept **Datum priprave besedila:** junij 2009 **Imetnik dovoljenja za promet:** AstraZeneca AB, S-151 85, Sodertalje, Švedska Pred predpisovanjem, prosimo, preberite celoten povzetek glavnih značilnosti zdravila. **Dodatne informacije so na voljo pri:** AstraZeneca UK Limited, Podružnica v Sloveniji, Verovškova 55, 1000 Ljubljana, telefon: 01/51 35 600.

AstraZeneca
ONKOLOGIJA

IRESSA®
gefitinib

Merck Serono Onkologija | ključ je v kombinaciji

Erbitux 5 mg/ml raztopina za infundiranje (Skrajšan povzetek glavnih značilnosti zdravila)

Sestava: En ml raztopine za infundiranje vsebuje 5 mg cetuximaba in pomožne snovi. Cetuksimab je himerno monoklonsko IgG1 protitelo. **Terapevtske indikacije:** Zdravilo Erbitux je indicirano za zdravljenje bolnikov z metastatskim kolorektalnim rakom z ekspresijo receptorjev EGFR in nemutiranim tipom KRAS v kombinaciji s kemoterapijo in kot samostojno zdravilo pri bolnikih, pri katerih zdravljenje z oksaliplatinom in irinotekanom ni bilo uspešno. Zdravilo Erbitux je indicirano za zdravljenje bolnikov z rakom skvamoznih celic glave in vratu v kombinaciji z radioterapijo za lokalno napredovalo bolezen in v kombinaciji s kemoterapijo na osnovi platine za ponavljajočo se in/ali metastatsko bolezen. **Odmerjanje in način uporabe:** Zdravilo Erbitux pri vseh indikacijah infundirajte enkrat na teden. Pred prvo infuzijo mora bolnik prejeti premedikacijo z antihistaminikom in kortikosteroidom. Začetni odmerek je 400 mg cetuksimaba na m2 telesne površine. Vsi naslednji tedenski odmerki so vsak po 250 mg/m2. **Kontraindikacije:** Zdravilo Erbitux je kontraindicirano pri bolnikih z znano hudo preobčutljivostno reakcijo (3. ali 4. stopnje) na cetuksimab. **Posebna opozorila in previdnostni ukrepi:** Če pri bolniku nastopi blaga ali zmerna reakcija, povezana z infundiranjem, lahko zmanjšate hitrost infundiranja. Priporočljivo je, da ostane hitrost infundiranja na nižji vrednosti tudi pri vseh naslednjih infuzijah. Če se pri bolniku pojavi huda kožna reakcija (≥ 3. stopnje po kriterijih US NCI-CTC), morate prekiniti terapijo s cetuksimabom. Z zdravljenjem smete nadaljevati le, če se je reakcija izboljšala do 2. stopnje. Zaradi možnosti pojava znižanja nivoja magnezija v serumu se pred in periodično med zdravljenjem priporoča določanje koncentracije elektrolitov. Če se pojavi sum na nevtropenijo, je potrebno bolnika skrbno nadzorovati. Potrebno je upoštevati kardiovaskularno stanje bolnika in sočasno dajanje kardiotoksičnih učinkovin kot so fluoropirimidini. **Interakcije:** farmakokinetične značilnosti cetuksimaba ostanejo nespremenjene po sočasni uporabi enkratnega odmerka irinotekana, tudi farmakokinetika irinotekana je nespremenjena pri sočasni uporabi cetuksimaba. Pri kombinaciji s fluoropirimidini se je povečala pogostnost srčne ishemije, vključno z miokardnim infarktom in kongestivno srčno odpovedjo ter pogostnost sindroma dlani in stopal. V kombinaciji s kemoterapijo na osnovi platine se lahko poveča pogostnost hude levkopenije ali hude nevtropenije. **Neželeni učinki:** Zelo pogosti (≥ 1/10): hipomagneziemija, povečanje ravni jetrnih encimov, kožne reakcije, blage ali zmerne reakcije povezane z infundiranjem, blag do zmeren mukozitis. Pogosti (≥ 1/100, < 1/10): dehidracija, hipokalciemija, anoreksija, glavobol, konjunktivitis, driska, navzeja, bruhanje, hude reakcije povezane z infundiranjem, utrujenost. **Posebna navodila za shranjevanje:** Shranjujte v hladilniku (2 °C - 8 °C). **Pakiranje:** 1 viala z 20 ml ali 100 ml raztopine. **Način in režim izdaje:** H. **Imetnik dovoljenja za promet:** Merck KGaA, 64271 Darmstadt, Nemčija. **Datum zadnje revizije besedila:** november 2010.

Pred predpisovanjem zdravila natančno preberite celoten Povzetek glavnih značilnosti zdravila. Podrobne informacije o zdravilu so objavljene na spletni strani Evropske agencije za zdravila (EMEA) http://www.emea.europa.eu.

Dodatne informacije so na voljo pri: Merck d.o.o., Dunajska cesta 119, 1000 Ljubljana, tel.: 01 560 3810, faks: 01 560 3831, el. pošta: info@merck.si

www.merckserono.net

www.Erbitux-international.com

Merck Serono

Merck Serono is a division of Merck.

MERCK

Samo za strokovno javnost PM-ONC-12/10/25.11.2010

POVZETEK GLAVNIH ZNAČILNOSTI ZDRAVILA

Ime zdravila: Temodal 20 mg, 100 mg, 140mg, 180 mg, 250 mg, Temodal 2,5 mg/ml prašek za raztopino za infundiranje **Kakovostna in količinska sestava:** Vsaka kapsula zdravila Temodal vsebuje 20 mg, 100 mg, 140 mg, 180 mg ali 250 mg temozolomida. Ena viala vsebuje 100 mg temozolomida Po rekonstituciji 1 ml raztopine za infundiranje vsebuje 2,5 mg temozolomida. Pomožna snov: Ena viala vsebuje 2,4 mmol natrija. **Terapevtske indikacije:** Zdravilo Temodal 2,5 mg/ml je indicirano za zdravljenje: odraslih bolnikov z novo diagnosticiranim multiformnim glioblastomom, sočasno z radioterapijo (RT) in pozneje kot monoterapija in otrok, starih 3 leta in več, mladostnikov in odraslih bolnikov z malignimi gliomi, npr. multiformnimi glioblastomi ali anaplastičnimi astrocitomi, ki se po standardnem zdravljenju ponovijo ali napredujejo. **Odmerjanje in način uporabe:** Zdravilo Temodal 2,5 mg/ml smejo predpisati le zdravniki, ki imajo izkušnje z zdravljenjem možganskih tumorjev. *Odrasli bolniki z novo diagnosticiranim multiformnim glioblastomom* Zdravilo Temodal 2,5 mg/ml se uporablja v kombinaciji z žariščno radioterapijo (faza sočasne terapije), temu pa sledi do 6 ciklov monoterapije (monoterapijska faza) z temozolomidom (TMZ). *Faza sočasne terapije* TMZ naj bolnik jemlje v odmerku 75 mg/m2 na dan 42 dni, sočasno z žariščno radioterapijo (60 Gy, danih v 30 delnih odmerkih). Zmanjševanje odmerka ni priporočeno, vendar se boste vsak teden odločili o morebitni odložitvi jemanja TMZ ali njegovi ukinitvi na podlagi kriterijev hematološke in nehematološke toksičnosti. TMZ lahko bolnik jemlje ves čas 42-dnevnega obdobja sočasne terapije (do 49 dni), če so izpolnjeni vsi od naslednjih pogojev:

- absolutno število nevtrofilcev (ANC – Absolute Neutrophil Count) ≥ 1,5 x 109/l;
- število trombocitov ≥ 100 x 109/l;
- skupna merila toksičnosti (SMT) za nehematološko toksičnost ≤ 1. stopnje (z izjemo alopecije, navzee in bruhanja).

Med zdravljenjem morate pri bolniku enkrat na teden pregledati celotno krvno sliko.

Faza monoterapije Štiri tedne po zaključku faze sočasnega zdravljenja s TMZ in RT naj bolnik jemlje TMZ do 6 ciklov monoterapije. V 1. ciklu (monoterapije) je odmerek zdravila 150 mg/m2 enkrat na dan 5 dni, temu pa naj sledi 23 dni brez terapije. Na začetku 2. cikla odmerek povečajte na 200 mg/m2, če je SMT za nehematološko toksičnost za 1. cikel stopnje ≤ 2 (z izjemo alopecije, slabosti in bruhanja), absolutno število nevtrofilcev (ANC) ≥ 1,5 x 109/l in število trombocitov ≥ 100 x 109/l. Če odmerka niste povečali v 2. ciklu, ga v naslednjih ciklih ne smete povečevati. Ko pa odmerek enkrat povečate, naj ostane na ravni 200 mg/m2 na dan v prvih 5 dneh vsakega naslednjega cikla, razen če nastopi toksičnost. Zmanjšanje odmerka in ukinitev zdravila med fazo monoterapije opravite, kot je opisano v preglednicah 2 in 3. Med zdravljenjem morate 22. dan pregledati celotno krvno sliko (21 dni po prvem odmerku TMZ). *Odrasli in pediatrični bolniki, stari 3 leta ali več, s ponavljajočim se ali napredujočim malignim gliomom:* Posamezen cikel zdravljenja traja 28 dni. Bolniki, ki še niso bili zdravljeni s kemoterapijo, naj jemljejo TMZ v odmerku 200 mg/m2 enkrat na dan prvih 5 dni, temu pa naj sledi 23-dnevni premor (skupaj 28 dni). Pri bolnikih, ki so že bili zdravljeni s kemoterapijo, je začetni odmerek 150 mg/m2 enkrat na dan, v drugem ciklu pa se poveča na 200 mg/m2 enkrat na dan 5 dni, če ni bilo hematoloških toksičnih učinkov. **Kontraindikacije:** Preobčutljivost za zdravilno učinkovino ali katerokoli pomožno snov. Preobčutljivost za dakarbazin (DTIC). **Posebna opozorila in previdnostni ukrepi:** *Pljučnica, ki jo povzroča Pneumocystis carinii* Pilotno preskušanje podaljšane 42-dnevne sheme zdravljenja je pokazalo, da pri bolnikih, ki so sočasno prejemali TMZ in RT, obstaja še posebej veliko tveganje za nastanek pljučnice zaradi okužbe s Pneumocystis carinii (PCP). *Malignosti* Zelo redko so poročali tudi o primerih mielodisplastičnega sindroma in sekundarnih malignostih, vključno z mieloidno levkemijo. Antiemetično zdravljenje Navzea in bruhanje sta pogosto povezana z zdravljenjem s TMZ. *Antiemetično zdravljenje* se lahko da pred uporabo TMZ ali po njej. *Odrasli bolniki z novo diagnosticiranim multiformnim glioblastomom* Antiemetična profilaksa je priporočljiva pred začetnim odmerkom sočasne faze in je močno priporočljiva med fazo monoterapije. *Ponavljajoči se ali napredujoči maligni gliom* Pri bolnikih, ki so močno bruhali (stopnja 3 ali 4) v prejšnjih ciklih zdravljenja, je potrebno antiemetično zdravljenje. *Laboratorijske vrednosti* Pred jemanjem zdravila morata biti izpolnjena naslednja pogoja za laboratorijske izvide: ANC ≥ 1,5 x 109/l in število trombocitov ≥ 100 x 109/l. Na 22. dan (21 dni po prvem odmerku) ali v roku 48 ur od navedenega dne, morate pregledati celotno krvno sliko in jo nato spremljati vsak teden, dokler ni ANC > 1,5 x 109/l in število trombocitov > 100 x 109/l. Če med katerimkoli ciklom ANC pade na < 1,0 x 109/l ali število trombocitov na < 50 x 109/l, morate odmerek zdravila v naslednjem ciklu zmanjšati za eno stopnjo (glejte poglavje 4.2). Stopnje odmerka so 100 mg/m2, 150 mg/m2 in 200 mg/m2. Najmanjši priporočeni odmerek je 100 mg/m2. *Pediatrična uporaba* Kliničnih izkušenj z uporabo TMZ pri otrocih, mlajših od 3 let, ni. Izkušnje z uporabo tega zdravila pri starejših otrocih in mladostnikih so zelo omejene. *Starejši bolniki* (stari > 70 let) Videti je, da je pri starejših bolnikih tveganje za nevtropenijo ali trombocitopenijo večje, kot pri mlajših. Zato je pri uporabi zdravila TMZ pri starejših bolnikih potrebna posebna previdnost.

Moški bolniki Moškim, ki se zdravijo s TMZ je treba svetovati, naj ne zaplodijo otroka še šest mesecev po prejetem zadnjem odmerku in naj se pred zdravljenjem posvetujejo o možnostih za shranitev zmrznjene sperme. *Natrij* To zdravilo vsebuje 2,4 mmol natrija na vialo. To je treba upoštevati pri bolnikih na nadzorovani dieti z malo natrija. **Medsebojno delovanje z drugimi zdravili in druge oblike interakcij:** Študije medsebojnega delovanja so izvedli le pri odraslih. V ločeni študiji 1. faze, sočasna uporaba TMZ in ranitidina ni povzročila spremembe obsega absorpcije temozolomida ali izpostavljenosti njegovem aktivnem presnovku monometiltriazenoimidazol karboksamidu (MTIK). Analiza populacijske farmakokinetike v preskušanjih 2. faze je pokazala, da sočasna uporaba deksametazona, proklorperazina, fenitoina, karbamazepina, ondansetrona, antagonistov receptorjev H2 ali fenobarbitala ne spremeni očistka TMZ. Sočasno jemanje z valprojsko kislino je bilo povezano z majhnim, a statistično pomembnim zmanjšanjem očistka TMZ. Študij za določitev učinka TMZ na presnovo ali izločanje drugih zdravil niso izvedli. Ker pa se TMZ ne presnavlja v jetrih in se na beljakovine veže le v majhni meri, je malo verjetno, da bi vplival na farmakokinetiko drugih zdravil.

Uporaba TMZ v kombinaciji z drugimi mielosupresivnimi učinkovinami lahko poveča verjetnost mielosupresije. **Neželeni učinki:** Pri bolnikih, ki se zdravijo s TMZ v kombinaciji z RT ali monoterapijo po RT zaradi novo diagnosticiranega multiformnega glioblastoma ali z monoterapijo pri bolnikih s ponavljajočim se ali napredujočim gliomom, so bili zelo pogosti neželeni učinki podobni; slabost, bruhanje, zaprtje, neješčnost, glavobol in utrujenost. Pri bolnikih z novo diagnosticiranim glioblastomom multiforme na monoterapiji so zelo pogosto poročali o konvulzijah, medtem ko je bil izpuščaj opisan zelo pogosto pri bolnikih z novo diagnosticiranim multiformnim glioblastomom, ki so prejemali TMZ sočasno z RT, ter pri tistih, ki so zdravilo prejemali v obliki monoterapije, pogosto pa pri tistih s ponavljajočim se gliomom. Pri obeh indikacijah so o večini hematoloških neželenih reakcij poročali pogosto ali zelo pogosto. **Imetnik dovoljenja za promet:** Schering-Plough Europe, Rue de Stalle 73, Bruselj Belgija **Način in režim izdaje zdravila:** Zdravilo Temodal 20 mg, 100 mg, 140mg, 180 mg, 250 mg se izdaja na recept (Rp/Spec), Temodal 2,5 mg/ml prašek za raztopino za infundiranje pa je namenjeno uporabi samo v bolnišnicah (H). **Datum priprave informacije:** februar 2010

1. Stupp R, et.al. Effects of radiotherapy with concomitant and adjuvant temozolomide versus radiotherapy alone on survival in glioblastoma in a randomised III study: 5-year analysis of the EORTC-NCIC trial
2. Povzetek temeljnih značilnosti zdravila Temodal

5 jakosti v 5 barvah za lažje in natančnejše dnevno odmerjanje[2]

250 mg	180 mg	140 mg	100 mg	20 mg

Schering-Plough CE AG
Dunajska cesta 22, 1000 Ljubljana
tel: 01 300 10 70
fax: 01 300 10 80

Schering-Plough

Resnični napredek

Pomembno izboljšanje preživetja potrjeno tudi ob daljšem spremljanju bolnikov[1]

Temodal®
temozolomide
capsules

SKRAJŠAN POVZETEK GLAVNIH ZNAČILNOSTI ZDRAVILA

Samo za strokovno javnost.

Ime zdravila: Tarceva 25 mg/100 mg/150 mg filmsko obložene tablete
Kakovostna in količinska sestava: Ena filmsko obložena tableta vsebuje 25 mg, 100 mg ali 150 mg erlotiniba (v obliki erlotinibijevega klorida).
Terapevtske indikacije: Nedrobnocelični rak pljuč: Zdravilo Tarceva je indicirano za samostojno vzdrževalno zdravljenje bolnikov z lokalno napredovalim ali metastatskim nedrobnoceličnim rakom pljuč s stabilno boleznijo po 4 ciklih standardne kemoterapije na osnovi platine v prvi liniji zdravljenja. Zdravilo Tarceva je indicirano tudi za zdravljenje bolnikov z lokalno napredovalim ali metastatskim nedrobnoceličnim rakom pljuč po neuspehu vsaj ene predhodne kemoterapije. Pri predpisovanju zdravila Tarceva je treba upoštevati dejavnike, povezane s podaljšanim preživetjem. Koristnega vpliva na podaljšanje preživetja ali drugih klinično pomembnih učinkov zdravljenja niso dokazali pri bolnikih z EGFR-negativnimi tumorji. Rak trebušne slinavke: Zdravilo Tarceva je v kombinaciji z gemcitabinom indicirano za zdravljenje bolnikov z metastatskim rakom trebušne slinavke. Pri predpisovanju zdravila Tarceva je treba upoštevati dejavnike, povezane s podaljšanim preživetjem. Koristnega vpliva na podaljšanje preživetja niso dokazali za bolnike z lokalno napredovalo boleznijo.
Odmerjanje in način uporabe: Zdravljenje z zdravilom Tarceva mora nadzorovati zdravnik z izkušnjami pri zdravljenju raka. Zdravilo Tarceva vzamemo najmanj eno uro pred zaužitjem hrane ali dve uri po tem. Kadar je potrebno odmerek prilagoditi, ga je treba zmanjševati v korakih po 50 mg. Pri sočasnem jemanju substratov in modulatorjev CYP3A4 bo morda potrebna prilagoditev odmerka. Pri dajanju zdravila Tarceva bolnikom z jetrno okvaro je potrebna previdnost. Če se pojavijo hudi neželeni učinki, pride v poštev zmanjšanje odmerka ali prekinitev zdravljenja z zdravilom Tarceva. Uporaba zdravila Tarceva pri bolnikih s hudo jetrno ali ledvično okvaro ter pri otrocih ni priporočljiva. Bolnikom kadilcem je treba svetovati, naj prenehajo kaditi, saj so plazemske koncentracije erlotiniba pri kadilcih manjše kot pri nekadilcih. Nedrobnocelični rak pljuč: Priporočeni dnevni odmerek zdravila Tarceva je 150 mg. Rak trebušne slinavke: Priporočeni dnevni odmerek zdravila Tarceva je 100 mg, v kombinaciji z gemcitabinom. Pri bolnikih, pri katerih se kožni izpuščaj v prvih 4 do 8 tednih zdravljenja ne pojavi, je treba ponovno pretehtati nadaljnje zdravljenje z zdravilom Tarceva.
Kontraindikacije: Preobčutljivost za erlotinib ali katero koli pomožno snov.
Posebna opozorila in previdnostni ukrepi: Močni induktorji CYP3A4 lahko zmanjšajo učinkovitost erlotiniba, močni zaviralci CYP3A4 pa lahko povečajo toksičnost. Sočasnemu zdravljenju s temi zdravili se je treba izogibati. Bolnikom, ki kadijo, je treba svetovati, naj prenehajo kaditi, saj so plazemske koncentracije erlotiniba pri kadilcih zmanjšane v primerjavi s plazemskimi koncentracijami pri nekadilcih. Verjetno je, da je velikost zmanjšanja klinično pomembna. Pri bolnikih, pri katerih se akutno pojavijo novi in/ali poslabšajo nepojasnjeni pljučni simptomi, kot so dispneja, kašelj in vročina, je treba zdravljenje z zdravilom Tarceva prekiniti, dokler ni znana diagnoza. Bolnike, ki se sočasno zdravijo z erlotinibom in gemcitabinom, je treba skrbno spremljati zaradi možnosti pojava toksičnosti, podobni intersticijski bolezni pljuč. Če je ugotovljena intersticijska bolezen pljuč, zdravilo Tarceva ukinemo in uvedemo ustrezno zdravljenje. Pri približno polovici bolnikov, ki so se zdravili z zdravilom Tarceva, se je pojavila driska (vključno z zelo redkimi primeri, ki so se končali s smrtnim izidom). Zmerno do hudo drisko zdravimo z loperamidom. V nekaterih primerih bo morda potrebno zmanjšanje odmerka. V primeru hude ali dolgotrajne driske, navzeje, anoreksije ali bruhanja, povezanih z dehidracijo, je treba zdravljenje z zdravilom Tarceva prekiniti in dehidracijo ustrezno zdraviti. O hipokaliemiji in ledvični odpovedi so poročali redko. Posebno pri bolnikih z dejavniki tveganja (sočasno jemanje drugih zdravil, simptomi, bolezni ali drugi dejavniki, vključno z visoko starostjo) moramo, če je driska huda ali dolgotrajna oziroma vodi v dehidracijo, zdravljenje z zdravilom Tarceva prekiniti in bolnikom zagotoviti intenzivno intravensko rehidracijo. Dodatno je treba pri bolnikih s prisotnim tveganjem za razvoj dehidracije spremljati ledvično delovanje in serumske elektrolite, vključno s kalijem. Pri uporabi zdravila Tarceva so poročali o redkih primerih jetrne odpovedi. K njenemu nastanku je lahko pripomogla predhodno obstoječa jetrna bolezen ali sočasno jemanje hepatotoksičnih zdravil. Pri teh bolnikih je treba zato premisliti o rednem spremljanju jetrnega delovanja. Dajanje zdravila Tarceva je treba prekiniti, če so spremembe jetrnega delovanja hude. Bolniki, ki prejemajo zdravilo Tarceva, imajo večje tveganje za razvoj perforacij v prebavilih, ki so jih opazili občasno (vključno z nekaterimi primeri, ki so se končali s smrtnim izidom). Pri bolnikih, ki sočasno prejemajo zdravila, ki zavirajo angiogenezo, kortikosteroide, nesteroidna protivnetna zdravila (NSAID) in/ali kemoterapijo na osnovi taksanov, ali so v preteklosti imeli peptični ulkus ali divertikularno bolezen, je tveganje večje. Če pride do tega, je treba zdravljenje z zdravilom Tarceva dokončno ukiniti. Poročali so o primerih kožnih bolezni z mehurji in luščenjem kože, vključno z zelo redkimi primeri, ki so nakazovali na Stevens-Johnsonov sindrom/toksično epidermalno nekrolizo in so bili v nekaterih primerih smrtni. Zdravljenje z zdravilom Tarceva je treba prekiniti ali ukiniti, če se pri bolniku pojavijo hude oblike mehurjev ali luščenja kože. Zelo redko so poročali o primerih perforacije ali ulceracije roženice; opazili so tudi druge očesne bolezni. Zdravljenje z zdravilom Tarceva je treba prekiniti ali ukiniti, če se pri bolnikih pojavijo akutne očesne bolezni, kot je bolečina v očeh, ali se le-te poslabšajo. Tablete vsebujejo laktozo in jih ne smemo dajati bolnikom z redkimi dednimi stanji: intoleranco za galaktozo, laponsko obliko zmanjšane aktivnosti laktaze ali malabsorpcijo glukoze/galaktoze.
Medsebojno delovanje z drugimi zdravili in druge oblike interakcij: Erlotinib se pri ljudeh presnavlja v jetrih z jetrnimi citokromi, primarno s CYP3A4 in v manjši meri s CYP1A2. Presnova erlotiniba zunaj jeter poteka s CYP3A4 v črevesju, CYP1A1 v pljučih in CYP1B1 v tumorskih tkivih. Z zdravilnimi učinkovinami, ki se presnavljajo s temi encimi, jih zavirajo ali pa so njihovi induktorji, lahko pride do interakcij. Erlotinib je srednje močan zaviralec CYP3A4 in CYP2C8, kot tudi močan zaviralec glukuronidacije z UGT1A1 *in vitro*. Pri kombinaciji ciprofloksacina ali močnega *zaviralca CYP1A2* (npr. fluvoksamina) z erlotinibom je potrebna previdnost. V primeru pojava neželenih učinkov, povezanih z erlotinibom, lahko odmerek erlotiniba zmanjšamo. Predhodno ali sočasno zdravljenje z zdravilom Tarceva ni spremenilo očistka prototipov *substratov CYP3A4*, midazolama in eritromicina. Inhibicija glukoronidacije lahko povzroči interakcije z zdravili, ki so *substrati UGT1A1* in se izločajo samo po tej poti. Močni *zaviralci aktivnosti CYP3A4* zmanjšajo presnovo erlotiniba in zvečajo koncentracije erlotiniba v plazmi. Pri sočasnem jemanju erlotiniba in močnih zaviralcev CYP3A4 je zato potrebna previdnost. Če je treba, odmerek erlotiniba zmanjšamo, še posebno pri pojavu toksičnosti. Močni *spodbujevalci aktivnosti CYP3A4* zvečajo presnovo erlotiniba in pomembno zmanjšajo plazemske koncentracije erlotiniba. Sočasnemu dajanju zdravila Tarceva in induktorjev CYP3A4 se je treba izogibati. Pri bolnikih, ki potrebujejo sočasno zdravljenje z zdravilom Tarceva in močnim induktorjem CYP3A4, je treba premisliti o povečanju odmerka do 300 mg ob skrbnem spremljanju njihove varnosti. Zmanjšana izpostavljenost se lahko pojavi tudi z drugimi induktorji, kot so fenitoin, karbamazepin, barbiturati ali šentjanževka. Če te zdravilne učinkovine kombiniramo z erlotinibom, je potrebna previdnost. Kadar je mogoče, je treba razmisliti o drugih načinih zdravljenja, ki ne vključujejo močnega spodbujanja aktivnosti CYP3A4. Bolnikom, ki jemljejo *kumarinske antikoagulante*, je treba redno kontrolirati protrombinski čas ali INR. Sočasno zdravljenje z zdravilom Tarceva in *statinom* lahko poveča tveganje za miopatijo, povzročeno s statini, vključno z rabdomiolizo; to so opazili redko. Sočasna uporaba *zaviralcev P-glikoproteina*, kot sta ciklosporin in verapamil, lahko vodi v spremenjeno porazdelitev in/ali spremenjeno izločanje erlotiniba. Za erlotinib je značilno zmanjšanje topnosti pri pH nad 5. *Zdravila, ki spremenijo pH v zgornjem delu prebavil*, lahko spremenijo topnost erlotiniba in posledično njegovo biološko uporabnost. Učinka antacidov na absorpcijo erlotiniba niso proučevali, vendar je ta lahko zmanjšana, kar vodi v nižje plazemske koncentracije. Kombinaciji erlotiniba in zaviralca protonske črpalke se je treba izogibati. Če menimo, da je uporaba antacidov med zdravljenjem z zdravilom Tarceva potrebna, jih je treba jemati najmanj 4 ure pred ali 2 uri po dnevnem odmerku zdravila Tarceva. Če razmišljamo o uporabi ranitidina, moramo zdravili jemati ločeno: zdravilo Tarceva je treba vzeti najmanj 2 uri pred ali 10 ur po odmerku ranitidina. V študiji faze Ib ni bilo pomembnih učinkov *gemcitabina* na farmakokinetiko erlotiniba, prav tako ni bilo pomembnih učinkov erlotiniba na farmakokinetiko gemcitabina. Erlotinib poveča koncentracijo platine. Pomembnih učinkov *karboplatina* ali paklitaksela na farmakokinetiko erlotiniba ni bilo. *Kapecitabin* lahko poveča koncentracijo erlotiniba. Pomembnih učinkov erlotiniba na farmakokinetiko kapecitabina ni bilo.
Neželeni učinki: *Zelo pogosti neželeni učinki* so kožni izpuščaj in driska, kot tudi utrujenost, anoreksija, dispneja, kašelj, okužba, navzea, bruhanje, stomatitis, bolečina v trebuhu, pruritus, suha koža, suhi keratokonjunktivitis, konjunktivitis, zmanjšanje telesne mase, depresija, glavobol, nevropatija, dispepsija, flatulenca, alopecija, okorelost, pireksija, nenormalnosti testov jetrne funkcije. *Pogosti neželeni učinki* so krvavitve v prebavilih, epistaksa, keratitis, paronihija, fisure na koži. *Občasno* so poročali o perforacijah v prebavilih, hirzutizmu, spremembah obrvi, krhkih nohtih, odstopanju nohtov od kože, blagih reakcijah na koži (npr. hiperpigmentacija), spremembah trepalnic, hudi intersticijski bolezni pljuč (vključno s smrtnimi primeri). *Redko* pa so poročali o jetrni odpovedi. *Zelo redko* so poročali o Stevens-Johnsonovem sindromu/toksični epidermalni nekrolizi ter o ulceracijah in perforacijah roženice.
Režim izdaje zdravila: H/Rp. **Imetnik dovoljenja za promet:** Roche Registration Limited, 6 Falcon Way, Shire Park, Welwyn Garden City, AL7 1TW, Velika Britanija. **Verzija:** 2.0/10. **Informacija pripravljena:** maj 2011.

014-11-TAR

DODATNE INFORMACIJE SO NA VOLJO PRI:
Roche farmacevtska družba d.o.o.
Vodovodna cesta 109, 1000 Ljubljana.
Povzetek glavnih značilnosti zdravila je dosegljiv na www.roche.si ali www.onkologija.si.

Roche

Tarceva®
erlotinib

ČAS ZA ŽIVLJENJE.

DOKAZANO PODALJŠA PREŽIVETJE PRI BOLNIKIH:

- z lokalno napredovalim ali metastatskim nedrobnoceličnim rakom pljuč[1]
- z metastatskim rakom trebušne slinavke[1]

[1] Povzetek glavnih značilnosti zdravila TARCEVA, www.ema.europa.eu

odprto

Novartis Oncology prinaša spekter inovativnih zdravil, s katerimi poskuša spremeniti življenje bolnikov z rakavimi in hematološkimi obolenji.

Ta vključuje zdravila kot so Glivec® (imatinib), Tasigna® (nilotinib), Afinitor® (everolimus), Zometa® (zoledronska kislina), Femara® (letrozol), Sandostatin® LAR® (oktreotid/i.m. injekcije) in Exjade® (deferasiroks).

Novartis Oncology ima tudi obširen razvojni program, ki izkorišča najnovejša spoznanja molekularne genomike, razumskega načrtovanja in tehnologij za odkrivanje novih učinkovin.

glivec imatinib

Tasigna nilotinib

AFINITOR (everolimus) tablete

ZOMETA zoledronska kislina

Femara letrozol

Sandostatin LAR oktreotid/i.m. injekcije

EXJADE deferasiroks

NOVARTIS ONCOLOGY

Novartis Pharma Services Inc. • Podružnica v Sloveniji • Tivolska cesta 30 • 1000 Ljubljana

Samo za strokovno javnost.

NVS-JA-01/11-SI

Že več kot desetletje prinašamo rešitve v Vaš laboratorij!

Za področja:

- bioznanosti **SYNGENE, INVITROGEN, BIOTEK**
  diagnostike **MINERVA, MEDAC, BIOTEK**
- gojenja celičnih kultur **INVITROGEN-GIBCO, TPP, SANYO**
- merjenja absorbance, fluorescence in luminiscence
  BIOTEK, SHIMADZU
- pipetiranja **BIOHIT** in **BIOTEK**
- laboratorijske opreme in instrumentov **SANYO, SHIMADZU**
- čiste vode za laboratorije **ELGA LABWATER**
- HPLC in GC instrumentov, kolon, vial in filtrov
  PHENOMENEX, CHROMACOL/NATIONAL SCIENTIFIC, SHIMADZU

KEMOMED
Prinašamo rešitve

SVETOVANJE, TRGOVINA, TRŽENJE d.o.o. • Kališka 9 • PE: Stritarjeva 5 • 4000 KRANJ • Slovenija
T: +386 4 20 15 050 • F: +386 4 20 15 055 • e-mail: info@kemomed.si • www.kemomed.si

Megace®

megestrolacetat 40mg/ml
peroralna suspenzija

učinkovita in preizkušena možnost zdravljenja anoreksije-kaheksije

Megace®

... še vedno EDINO ZDRAVILO, ki je v Sloveniji registrirano za zdravljenje anoreksije-kaheksije pri bolnikih z napredovalim rakom [1,2] - predpisovanje na zeleni recept v breme ZZZS [6]

Megace®

- **izboljša apetit [1,5]**
- **pomaga ohraniti in pridobiti telesno težo [3,4,5]**
- **izboljša splošno počutje bolnikov [3,4]**

SKRAJŠAN POVZETEK GLAVNIH ZNAČILNOSTI ZDRAVILA: MEGACE 40 mg/ml peroralna suspenzija

Sestava: 1 ml peroralne suspenzije vsebuje 40 mg megestrolacetata. **TERAPEVTSKE INDIKACIJE:** Zdravljenje anoreksije-kaheksije ali nepojasnjene, pomembne izgube telesne mase pri bolnikih z AIDS-om. Zdravljenje anorektično-kahektičnega sindroma pri napredovalem raku. **ODMERJANJE IN NAČIN UPORABE:** Pri aidsu je priporočeni začetni odmerek Megace za odrasle 800 mg (20 ml peroralne suspenzije) enkrat na dan eno uro pred jedjo ali dve uri po jedi in se lahko med zdravljenjem prilagodi glede na bolnikov odziv. V raziskavah bolnikov z aidsom so bili klinično učinkoviti dnevni odmerki od 400 do 800 mg/dan (10 do 20 ml), uporabljani štiri mesece. Pri anorektično-kahektičnem sindromu zaradi napredovalega raka je priporočljiv začetni odmerek 200 mg (5 ml) na dan; glede na bolnikov odziv ga je mogoče povečati do 800 mg na dan (20 ml). Običajni odmerek je med 400 in 800 mg na dan (10–20 ml). V raziskavah bolnikov z napredovalim rakom so bili klinično učinkoviti dnevni odmerki od 200 do 800 mg/dan (5 do 20 ml), uporabljani najmanj osem tednov. Pred uporabo je potrebno plastenko s suspenzijo dobro pretresti. Uporaba pri otrocih: Varnosti in učinkovitosti pri otrocih niso dokazali. Uporaba pri starostnikih: Zaradi pogostejših okvar jeter, ledvic in srčne funkcije, pogostejših sočasnih obolenj ali sočasnega zdravljenja z drugimi zdravili je odmerek za starejšega bolnika treba določiti previdno in običajno začeti z najnižjim odmerkom znotraj odmernega intervala. **KONTRAINDIKACIJE:** Preobčutljivost za megestrolacetat ali katerokoli pomožno snov. **POSEBNA OPOZORILA IN PREVIDNOSTNI UKREPI:** Uporaba gestagenov med prvimi štirimi meseci nosečnosti ni priporočljiva. Pri bolnikih s tromboflebitisom v anamnezi je treba zdravilo Megace uporabljati previdno. Zdravljenje z zdravilom Megace se lahko začne šele, ko so bili vzroki hujšanja, ki jih je mogoče zdraviti, ugotovljeni in obravnavani. Megestrolacetat ni namenjen za profilaktično uporabo za preprečitev hujšanja. Učinki na razmnoževanje virusa HIV niso ugotovljeni. Med zdravljenjem z megestrolacetatom in po prekinitvi kroničnega zdravljenja je treba upoštevati možnost pojava zavore nadledvične žleze. Morda bo potrebno nadomestno zdravljenje s stresnimi odmerki glukokortikoidov. Megestrolacetat se v veliki meri izloči prek ledvic. Ker je verjetnost zmanjšanega delovanja ledvic pri starostnikih večja, je pri določitvi odmerka potrebna previdnost, prav tako je koristno spremljanje ledvične funkcije. Peroralna suspenzija vsebuje saharozo. Bolniki z redko dedno intoleranco za fruktozo, malabsorpcijo glukoze/galaktoze ali pomanjkanjem saharoza-izomaltaze ne smejo jemati tega zdravila. Peroralna suspenzija vsebuje tudi majhne količine etanola (alkohola), in sicer manj kot 100 mg na odmerek. **INTERAKCIJE:** Aminoglutetimid: poročali so o zmanjšanju koncentracije progestogena v plazmi z možno izgubo terapevtskega delovanja zaradi inducirane presnove. Sočasno jemanje megestrolacetata (v obliki peroralne suspenzije) in zidovudina ali rifabutina ne povzroča sprememb farmakokinetičnih parametrov. **NEŽELENI UČINKI:** Pogosti (≥ 1/100, < 1/10): navzea, bruhanje, driska, flatulenca, izpuščaj, metroragija, impotenca, astenija, bolečina, edem. Neznana pogostnost (pogostnosti ni mogoče oceniti iz razpoložljivih podatkov): poslabšanje osnovne bolezni (širjenje tumorja), adrenalna insuficienca, kušingoidni izgled, Cushingov sindrom, diabetes mellitus, motena toleranca za glukozo, hiperglikemija, spremembe razpoloženja, sindrom karpalnega kanala, letargija, srčno popuščanje, tromboflebitis, pljučna embolija (v nekaterih primerih usodna), hipertenzija, navali vročine, dispneja, zaprtje, alopecija, pogosto uriniranje. **Vrsta ovojnine in vsebina:** Plastenka z 240 ml suspenzije. **Režim izdaje:** Rp/Spec. **Imetnik dovoljenja za promet:** Bristol-Myers Squibb spol. s r.o., Olivova 4, Praga 1, Češka; **Odgovoren za trženje v Sloveniji:** PharmaSwiss d.o.o., Ljubljana, tel: 01 236 4 700, faks: 01 236 4 705; MGS-120609. **Pred predpisovanjem preberite celoten povzetek glavnih značilnosti zdravila!**

Reference: 1. Povzetek glavnih značilnosti zdravila Megace – 12. junij 2009; **2.** Register zdravil Republike Slovenije XII – leto 2010; **3.** Beller, E., 1997. Ann Oncol 8: 277-283; **4.** Čufer, T, 2002. Onkologija 9(2): 73-75; **5.** Yavuzsen, T., 2005. J Clin Oncol 23(33): 8500-8511; **6.** Bilten Recept 8(2), 8.12.2010

MEG0211-01; februar 2011

Bristol-Myers Squibb

PharmaSwiss
Choose More Life

TANTUM® VERDE

Lajšanje bolečine in oteklin pri vnetju v ustni votlini in žrelu, ki nastanejo zaradi okužb in stanj po operaciji in kot posledica radioterapije (t.i. radiomukozitis).

Tantum Verde 1,5 mg/ml oralno pršilo, raztopina

Kakovostna in količinska sestava
1 ml raztopine vsebuje 1,5 mg benzidaminijevega klorida, kar ustreza 1,34 mg benzidamina. V enem razpršku je 0,17 ml raztopine. En razpršek vsebuje 0,255 mg benzidaminijevega klorida, kar ustreza 0,2278 mg benzidamina. En razpršek vsebuje 13,6 mg 96 odstotnega etanola, kar ustreza 12,728 mg 100 odstotnega etanola, in 0,17 mg metilparahidroksibenzoata (E218).

Terapevtske indikacije
Samozdravljenje: lajšanje bolečine in oteklin pri vnetju v ustni votlini in žrelu, ki so lahko posledica okužb in stanj po operaciji. Po nasvetu in navodilu zdravnika: lajšanje bolečine in oteklin v ustni votlini in žrelu, ki so posledica radiomukozitisa.

Odmerjanje in način uporabe
Uporaba 2- do 6-krat na dan (vsake 1,5 do 3 ure). Odrasli: 4 do 8 razprškov 2- do 6-krat na dan. Otroci od 6 do 12 let: 4 razprški 2- do 6-krat na dan. Otroci, mlajši od 6 let: 1 razpršek na 4 kg telesne mase; do največ 4 razprške 2 do 6-krat na dan.

Kontraindikacije
Znana preobčutljivost za zdravilno učinkovino ali katerokoli pomožno snov.

Posebna opozorila in previdnostni ukrepi
Pri manjšini bolnikov lahko resne bolezni povzročijo ustne/žrelne ulceracije. Če se simptomi v treh dneh ne izboljšajo, se mora bolnik posvetovati z zdravnikom ali zobozdravnikom, kot je primerno. Zdravilo vsebuje aspartam (E951) (vir fenilalanina), ki je lahko škodljiv za bolnike s fenilketonurijo. Zdravilo vsebuje izomalt (E953) (sinonim: izomaltitol (E953)). Bolniki z redko dedno intoleranco za fruktozo ne smejo jemati tega zdravila. Uporaba benzidamina ni priporočljiva za bolnike s preobčutljivostjo za salicilno kislino ali druga nesteroidna protivnetna zdravila. Pri bolnikih, ki imajo ali so imeli bronhialno astmo, lahko pride do bronhospazma. Pri takih bolnikih je potrebna previdnost.

Medsebojno delovanje z drugimi zdravili in druge oblike interakcij
Pri ljudeh raziskav o interakcijah niso opravljali.

Nosečnost in dojenje
Tantum Verde z okusom mentola 3 mg pastile se med nosečnostjo in dojenjem ne smejo uporabljati.

Vpliv na sposobnost vožnje in upravljanja s stroji
Uporaba benzidamina lokalno v priporočenem odmerku ne vpliva na sposobnost vožnje in upravljanja s stroji.

Neželeni učinki
Bolezni prebavil Redki: pekoč občutek v ustih, suha usta.
Bolezni imunskega sistema Redki: preobčutljivostna reakcija.
Bolezni dihal, prsnega koša in mediastinalnega prostora Zelo redki: laringospazem.
Bolezni kože in podkožja Občasni: fotosenzitivnost. Zelo redki: angioedem.

Rok uporabnosti
4 leta. Zdravila ne smete uporabljati po datumu izteka roka uporabnosti, ki je naveden na ovojnini. Posebna navodila za shranjevanje Za shranjevanje pastil niso potrebna posebna navodila. Plastenko z raztopino shranjujte v zunanji ovojnini za zagotovitev zaščite pred svetlobo. Shranjujte pri temperaturi do 25°C. Shranjujte v originalni ovojnini in nedosegljivo otrokom.

www.tantum-verde.si
CSC Pharma, d.o.o., Jana Husa 1a, 1000 Ljubljana, www.csc-pharma.si

Imetnik dovoljenja za promet
CSC Pharma d.o.o.
Jana Husa 1a
1000 Ljubljana

CSC ANGELINI

NA **VMESNI LISTI**[1]!

S klinično dokazano učinkovitostjo

EDINI **Prosure®**

2 TETRAPAKA NA DAN VSAJ 8 TEDNOV

Klinične raziskave pri bolnikih z rakom so pokazale, da *Prosure*®:

- **Izboljša apetit in poveča količino zaužite hrane.**[2,3,10,11]
- **Pripomore k pridobivanju telesne teže.**[2,3,7-9]
- **Poveča mišično maso.**[2,3,7,8]
- **Poveča fizično moč.**[6]
- **Omogoča večjo fizično dejavnost.**[3,4,5]
- **Izboljša kakovost življenja.**[2,5,6,8,10]
- **Ublaži vnetni odziv bolnikovega imunskega sistema na onkološko bolezen.**[8,10,12]

POMEMBEN JE **VSAK** KORAK!

1. Le na osnovi predpisa pooblaščenega zdravnika, za določeno skupino bolnikov in določen produkt. Za podrobnosti si oglejte spletno stran **www.zzzs.si**. **2.** Fearon K C H et al. Gut. 2003;52:1479-1486. **3.** Barber MD. et al. Brit J Can. 1999; 81:80-86. **4.** Moses AWG. et. al. Br J Can. 2004;90:996-1002. **5.** Bauer JD et al. Support Care Cancer. 2005;13:270-274. **6.** Von Meyenfeldt M. et.al. Proc Am Soc Clin Oncol. 2002;21:385A. **7.** Weed HG. et.al. Proc Am Soc Clin Oncol. 2005; 8112A. **8.** Read JA. et al. Support Care Cancer. 2007;15:301-307. **9.** Bayram I. et al. Pediatr Blood Cancer. 2009;52:571-574. **10.** Guarcello M. et. al. Nutr Ther & Metab. 2006;24:168-175. **11.** Jatoi A. et. al. Journal of Cl Oncology. 2004;22:2469-2476. **12.** Ryan A et al. Ann Surg. 2009;249:355-363.

Prosure®
Živeti življenje

NJUT0422011

Abbott
A Promise for Life

Pri zdravljenju raka jajčnikov, raka dojk, diseminiranega plazmocitoma ali Kaposijevega sarkoma zagotavlja CAELYX® v primerjavi s standardnim doksorubicinom: **primerljivo učinkovitost z manj kardiotoksičnosti, mielosupresije, alopecije in slabosti.**[1,2]

1. Immordino M. et al. Int J Nanomedicine 2006; 1(3): 297-315.
2. Caelyx SmPC: November 2010.

Skrajšano navodilo za predpisovanje

CAELYX® - 2 mg/ml koncentrat za raztopino za infundiranje **SESTAVA:** doksorubicinijev klorid, α-(2-[1,2-distearoil-sn-glicero(3)fosfooksi]etilkarbamoil)-ω-metoksipoli(oksietilen)-40 natrijeva sol, hidrogeniran sojin fosfatidilholin, holesterol, amonijev sulfat, saharoza, histidin, voda za injekcije, klorovodikova kislina, natrijev hidroksid. **INDIKACIJE:** metastatski rak dojk (bolnice s povečanim tveganjem za nastanek bolezni srca), napredovali rak jajčnikov (neuspešna prva platinska kemoterapija), napredujoči diseminirani plazmocitom (kombinacija z bortezomibom) pri bolnikih, ki so pred tem že prejeli najmanj eno terapijo in so imeli presaditev kostnega mozga ali niso primerni zanjo, z AIDS povezani Kaposijev sarkom (bolniki z majhnim št. celic CD_4 in razširjeno mukokutano ali visceralno boleznijo). **ODMERJANJE:** **rak dojk/jajčnikov:** 50 mg/m² i.v./4 tedne, **diseminirani plazmocitom:** 1 urna i.v. infuzija 30 mg/m² na 4. dan 3 tedenske sheme zdravljenja z bortezomibom, takoj po infuziji bortezomiba. **Kaposijev sarkom:** 20 mg/m² i.v./2-3 tedne, presledki naj ne bodo krajši od 10 dni. Zdravila ne smete dati v obliki bolusne injekcije ali nerazredčene raztopine. Priporočamo priključitev infuzijske linije zdravila prek stranskega nastavka na i.v. infuzijo 5 % glukoze. Infuzija lahko teče v periferno veno. Linijskih filtrov ne smete uporabljati. Za prilagajanje odmerkov glejte SmPC. Zdravljenje bolnikov mlajših od 18 let ni priporočljivo. **KONTRAINDIKACIJE:** preobčutljivost za učinkovino ali katerokoli pomožno snov, z AIDS povezan Kaposijev sarkom, ki bi ga bilo mogoče učinkovito zdraviti lokalno ali s sistemskim interferonom alfa. **POSEBNA OPOZORILA:** za oceno delovanja srca uporabljajte EKG, merjenje iztisnega deleža levega prekata, endomiokardno biopsijo. Če izvid pokaže možno okvaro srca v povezavi s terapijo, morate skrbno pretehtati koristnost nadaljnje terapije. Ocena delovanja levega prekata je nujna pred dajanjem zdravila, ki presega kumulativni odmerek antraciklinov 450 mg/m². Potrebne so redne preiskave krvne slike. Trdovratna mielosupresija lahko vodi do sekundarnih okužb ali krvavitev. Zdravila CAELYX® ne smete prosto zamenjevati z drugimi pripravki doksorubicinijevega klorida. Že nekaj minut po začetku infuzije zdravila se lahko pojavijo resne, včasih življenje ogrožajoče infuzijske reakcije alergijskega ali anafilaktoidnega tipa. Zelo redko se lahko pojavijo konvulzije, ki jih običajno odpravimo z začasno prekinitvijo infuzije, običajno že brez dodatne terapije, kljub temu pa morate imeti vedno pri roki ustrezna zdravila in opremo za urgentno zdravljenje. Pri večini bolnikov lahko kemoterapijo nadaljujete po pomiritvi vseh simptomov. Infuzijske reakcije se le redko ponovijo po prvem ciklusu kemoterapije. Da bi tveganje za njihov pojav zmanjšali, začetnega odmerka ne smete infundirati hitreje kot 1 mg/min. Zdravilo vsebuje saharozo in odmerek dajete v 5 % (50 mg/ml) raztopini glukoze za infundiranje. **INTERAKCIJE:** previdnost je potrebna med sočasno uporabo zdravil, za katera je znano, da medsebojno delujejo s standardnim doksorubicinijevim kloridom. Med sočasno uporabo drugih citotoksičnih zdravil je potrebna previdnost. **NOSEČNOST IN DOJENJE:** zdravila ne smete uporabljati med nosečnostjo, razen če je nujno potrebno. Ženskam v rodni dobi morate svetovati, naj ne zanosijo, medtem, ko one ali njihov partner prejemajo zdravilo in še šest mesecev po prenehanju zdravljenja. Zaradi možnosti resnih neželenih učinkov pri dojenčku mora ženska pred začetkom zdravljenja nehati dojiti. S HIV okužene ženske naj ne dojijo. **VPLIV NA SPOSOBNOST VOŽNJE:** Med uporabo zdravila so redko opažali omotico in zaspanost, taki bolniki naj ne vozijo in ne upravljajo s stroji. **NEŽELENI UČINKI:** faringitis, folikulitis, okužbe, razjede, levkopenija, anemija, nevtropenija, trombocitopenija, anoreksija, parestezije, somnolenca, nevropatija, solzenje, zamegljen vid, prekatne aritmije, epistaksa, slabost, stomatitis, bruhanje, zaprtje, driska, dispepsija, palmarno-plantarna eritrodizestezija, alopecija, izpuščaj, suha koža, obarvanje kože, eritem, dermatitis, bolezni nohtov, luskasta koža, krči v nogah, astenija, mukozitis, bolečine, edem, herpes, alergijske reakcije, dehidracija, kaheksija, tesnoba, depresija, nespečnost, glavobol, omotica, hipertonija, konjunktivitis, srčno-žilne bolezni, vazodilatacija, dispneja, kašelj, ezofagitis, gastritis, disfagija, suha usta, napenjanje, gingivitis, motnje okusa, pruritus, kožne bolezni, potenje, akne, mialgija, disurija, bolezni sluznic, mrzlica, bolehnost, hujšanje, pljučnica, nazofaringitis, limfopenija, hipokaliemija, hiperkaliemija, hipomagneziemija, hiponatremija, hipokalcemija, nevralgija, disgevzija, letargija, hipoestezija, sinkopa, disestezija, hipotenzija, zariplost, hipertenzija, flebitis, petehije, artralgija, mišični krči, pireksija, gripi podobna bolezen, zvišana koncentracija aspartat aminotransferaze, kreatinina v krvi, alanin aminotransferaze, zmanjšana iztisna frakcija srca, zmedenost, retinitis, glositis, akutne reakcije povezane z infuzijami. **IMETNIK DzP:** Janssen-Cilag International NV, Turnhoutseweg 30, B-2340 Beerse, Belgija; Predstavnik v Sloveniji: Johnson & Johnson d.o.o., Šmartinska 53, Ljubljana **REŽIM IZDAJE:** H **DATUM REVIZIJE:** 11. 11. 2010

Janssen, farmacevtski del Johnson & Johnson d.o.o., Šmartinska 53, 1000 Ljubljana, tel: 01 401 18 00

Samo za strokovno javnost

janssen
PHARMACEUTICAL COMPANIES OF Johnson&Johnson

CAE-SLO-A-015-210311

Skrajšan povzetek glavnih značilnosti zdravila

IME ZDRAVILA
Votrient 200 mg filmsko obložene tablete
Votrient 400 mg filmsko obložene tablete

KAKOVOSTNA IN KOLIČINSKA SESTAVA
Ena Votrient 200 mg filmsko obložena tableta vsebuje 200 mg pazopaniba (v obliki pazopanibijevega klorida).
Ena Votrient 400 mg filmsko obložena tableta vsebuje 400 mg pazopaniba (v obliki pazopanibijevega klorida).

Seznam pomožnih snovi

Jedro tablete
magnezijev stearat, mikrokristalna celuloza, povidon (K30), natrijev karboksimetilškrob (vrsta A)
Obloga tablete
hipromeloza, rdeči železov oksid (E172), makrogol 400, polisorbat 80, titanov dioksid (E171)

FARMACEVTSKA OBLIKA
Votrient 200 mg filmsko obložene tablete so rožnate filmsko obložene tablete v obliki kapsule z oznako GS JT na eni strani.
Votrient 400 mg filmsko obložene tablete so bele filmsko obložene tablete v obliki kapsule z oznako GS UHL na eni strani.

KLINIČNI PODATKI
Terapevtske indikacije
Zdravilo Votrient je indicirano kot zdravilo prvega izbora za zdravljenje napredovalega karcinoma ledvičnih celic (renal cell carcinoma - RCC) in pri bolnikih, ki so zaradi napredovale bolezni predhodno prejemali zdravljenje s citokini.

Odmerjanje in način uporabe

Zdravljenje z zdravilom Votrient sme uvesti le zdravnik, ki ima izkušnje z uporabo protitumorskih zdravil.

Odrasli

Priporočeni odmerek pazopaniba je 800 mg enkrat na dan.

Prilagoditev odmerka

Odmerek je treba prilagajati postopoma, z višanjem odmerka v korakih po 200 mg in pri tem upoštevati prenašanje zdravila pri posameznem bolniku zaradi nadzora neželenih učinkov. Odmerek pazopaniba ne sme preseči 800 mg.

Pediatrična populacija

Uporabe pazopaniba ne priporočamo pri otrocih in mladostnikih, mlajših od 18 let, zaradi nezadostnih podatkov o varnosti in učinkovitosti.

Starostniki

Podatkov o uporabi pazopaniba pri bolnikih, starih 65 let in starejših, je malo. V kliničnih študijah RCC, izvedenih s pazopanibom, se varnost uporabe pazopaniba pri bolnikih, starih vsaj 65 let, v celoti klinično ni pomembneje razlikovala od varnosti pri mlajših bolnikih. Klinične izkušnje ne kažejo na razlike v odzivu pri starostnikih in mlajših bolnikih, vendar pa večje občutljivosti posameznih starostnikov ni mogoče izključiti.

Okvara ledvic

Pazopanib in njegovi presnovki se le v majhnem obsegu izločajo preko ledvic, zato je verjetnost, da bi okvara ledvic klinično pomembno vplivala na farmakokinetiko pazopaniba, majhna. Pri bolnikih s kreatininskim očistkom, večjim od 30 ml/min, odmerka ni treba prilagajati. Pri bolnikih s kreatininskim očistkom, manjšim od 30 ml/min, je potrebna previdnost, saj pri tej skupini bolnikov ni izkušenj z uporabo pazopaniba.

Okvara jeter

Pri bolnikih z okvaro jeter varnosti in farmakokinetike pazopaniba niso popolnoma raziskali. Pri bolnikih z blago ali zmerno okvaro jeter je treba pazopanib uporabljati previdno in bolnike skrbno nadzirati zaradi možne večje izpostavljenosti bolnikov zdravilu. Pri bolnikih z blago okvaro jeter zaradi nezadostnih podatkov ne moremo podati priporočil za zmanjšanje odmerka. Pri bolnikih z zmerno okvaro jeter je priporočljivo, da se odmerek zmanjša na 200 mg enkrat na dan.
Pri bolnikih s hudo okvaro jeter je uporaba pazopaniba kontraindicirana.

Način uporabe

Bolnik mora pazopanib jemati brez hrane, vsaj eno uro pred ali dve uri po jedi. Votrient filmsko obložene tablete mora bolnik pogoltniti cele z vodo. Ne sme jih razpolavljati ali zdrobiti.

Kontraindikacije

Preobčutljivost za zdravilno učinkovino ali katerokoli pomožno snov.
Huda okvara jeter.

Posebna opozorila in previdnostni ukrepi

Učinki na jetra

Med uporabo pazopaniba so poročali o primerih odpovedi jeter (vključno s smrtnimi izidi). Pri bolnikih z že obstoječo okvaro jeter varnost in farmakokinetika pazopaniba nista povsem ugotovljeni. Pri bolnikih z blago do zmerno okvaro jeter je treba pazopanib uporabiti previdno in ob natančnem spremljanju. Za bolnike z zmerno okvaro jeter je priporočljiv manjši odmerek pazopaniba 200 mg enkrat na dan. Zaradi nezadostnih podatkov pri bolnikih z blago okvaro jeter priporočil za prilagoditev odmerka ni mogoče podati. Pri bolnikih s hudo okvaro jeter je uporaba pazopaniba kontraindicirana. V kliničnih študijah s pazopanibom so poročali o zvišanju vrednosti serumskih aminotransferaz (ALT in AST) in zvišanju vrednosti bilirubina. V večini primerov so poročali o posameznih primerih zvišanja vrednosti ALT in AST, brez sočasnega zvišanja vrednosti alkalne fosfataze ali bilirubina. Pred uvedbo zdravljenja s pazopanibom je treba opraviti serumske jetrne teste in jih nato med prvimi 4 meseci zdravljenja ponavljati vsaj enkrat na 4 tedne ali kot je to klinično indicirano. Po tem času je treba vrednosti nadzirati še občasno.
• Pri bolnikih, ki imajo le zvišane vrednosti aminotransferaz ≤ 8 X vrednosti zgornje meje normalnih vrednosti (ZMN), se zdravljenje s pazopanibom lahko nadaljuje. Pri teh bolnikih je treba delovanje jeter spremljati tedensko, dokler se vrednosti aminotransferaz ne vrnejo na stopnjo 1 ali izhodiščne vrednosti.
• Pri bolnikih, ki imajo vrednosti aminotransferaz > 8 X vrednosti ZMN, je treba zdravljenje s pazopanibom prekiniti, dokler se vrednosti ne vrnejo na stopnjo 1 ali izhodiščne vrednosti. Če je pričakovana korist ponovne uvedbe zdravljenja s pazopanibom večja od tveganja za pojav hepatotoksičnih učinkov, je treba uvesti zdravljenje s pazopanibom z zmanjšanim odmerkom in tedensko opravljati serumske jetrne teste v trajanju 8 tednov. Če se po ponovni uvedbi zdravljenja s pazopanibom vrednosti aminotransferaz zopet povečajo na > 3 X vrednosti zgornje meje normalnih vrednosti, je treba zdravljenje s pazopanibom ukiniti.
• Če se zvišanje vrednosti aminotransferaz za > 3 X vrednosti zgornje meje normalnih vrednosti pojavi skupaj z zvišanjem vrednosti bilirubina za > 2 X vrednosti zgornje meje normalnih vrednosti, je treba določiti frakcijo bilirubina. Če je delež direktnega (konjugiranega) bilirubina > 35 % skupnega bilirubina, je treba zdravljenje s pazopanibom ukiniti.

Hipertenzija

V kliničnih študijah s pazopanibom so se pojavili primeri hipertenzije, vključno z na novo diagnosticiranimi simptomatskimi epizodami zvišanega krvnega tlaka (hipertenzivna kriza). Pred uvedbo zdravljenja s pazopanibom mora biti vrednost krvnega tlaka dobro nadzorovana. Bolnike je treba nadzirati glede pojava hipertenzije in po potrebi uvesti zdravljenje s standardnimi zdravili za zdravljenje hipertenzije. Stopnje zvišanega krvnega tlaka (sistolični krvni tlak ≥ 150 ali distolični krvni tlak ≥ 100 mm Hg) so se pojavile kmalu po uvedbi zdravljenja (v 39 % primerov se je pojavila do 9. dneva zdravljenja in v 88 % primerov se je pojavila v prvih 18 tednih po uvedbi zdravljenja). Če se vrednost krvnega tlaka kljub zdravljenju z antihipertenzivi ne normalizira, je treba odmerek pazopaniba zmanjšati. Če so prisotne zvišane vrednosti krvnega tlaka (140/90 mm Hg) ali če je arterijska hipertenzija huda in se krvni tlak kljub zdravljenju z antihipertenzivi in zmanjšanju odmerka pazopaniba ne zmanjša, je treba zdravljenje s pazopanibom prekiniti.

Podaljšanje intervala Q-T in torsade de pointes

V kliničnih študijah s pazopanibom so poročali o pojavu podaljšanja intervala Q-T in tahikardiji torsade de pointes. Pri bolnikih, ki so kdaj že imeli težave s podaljšanjem intervala Q-T, pri bolnikih, ki se zdravijo z zdravili za zdravljenje srčnih aritmij ali drugimi zdravili, ki lahko podaljšajo interval Q-T, ter bolnikih, ki imajo relevantne bolezni srca, je treba pazopanib uporabljati previdno. Pred začetkom zdravljenja s pazopanibom je priporočljivo izvesti elektrokardiografsko preiskavo srca in jo nato med zdravljenjem občasno ponavljati ter skrbeti za ravnovesje elektrolitov (npr. kalcij, magnezij, kalij) znotraj mej normalnih vrednosti.

Arterijska tromboza

V kliničnih študijah s pazopanibom so poročali o pojavu miokardnega infarkta, ishemične kapi in tranzitorne ishemične atake. Pri bolnikih, pri katerih obstaja večje tveganje za pojav kateregakoli od teh stanj, je treba pazopanib uporabljati previdno. Odločitev o uvedbi zdravljenja je treba sprejeti na osnovi ocene razmerja med koristjo in tveganjem pri vsakem posameznem bolniku.

Hemoragični dogodki

V kliničnih študijah s pazopanibom so poročali o pojavu hemoragičnih dogodkov. Pri bolnikih z anamnezo izkašljevanja krvi, cerebralne krvavitve ali klinično pomembne gastrointestinalne krvavitve v zadnjih 6 mesecih uporaba pazopaniba ni priporočljiva. Pri bolnikih s pomembnim tveganjem za pojav krvavitev je treba pazopanib uporabljati previdno.

Perforacije in fistula v gastrointestinalnem traktu

V kliničnih študijah s pazopanibom so poročali o pojavu perforacij ali fistule v gastrointestinalnem traktu. Pri bolnikih s tveganjem za pojav perforacije ali fistule v gastrointestinalnem traktu je treba pazopanib uporabljati previdno.

Celjenje ran

Formalne študije o vplivu pazopaniba na celjenje ran niso bile izvedene. Ker lahko zaviralci žilnega endotelnega rastnega faktorja (VEGF;"vascular endothelial growth factor") vplivajo na celjenje ran, je treba zdravljenje s pazopanibom prekiniti vsaj 7 dni pred načrtovanim kirurškim posegom. Odločitev o nadaljevanju zdravljenja s pazopanibom po opravljenem kirurškem posegu je treba sprejeti na osnovi klinične presoje ustreznosti celjenja rane. Pri bolnikih, pri katerih se rana ponovno odpre, je treba zdravljenje s pazopanibom prekiniti.

Srčno popuščanje

Pri bolnikih z zmernim do hudim srčnim popuščanjem varnosti in farmakokinetike pazopaniba niso raziskovali.

Hipotiroidizem

V kliničnih študijah s pazopanibom so poročali o primerih zmanjšanega delovanja ščitnice. Pred uvedbo zdravljenja s pazopanibom je priporočljivo z laboratorijskimi preiskavami ovrednotiti delovanje ščitnice. Bolnike s hipotiroidizmom je treba pred uvedbo zdravljenja s pazopanibom zdraviti v skladu z ustaljeno prakso. Med zdravljenjem s pazopanibom je treba vse bolnike skrbno nadzirati glede pojava znakov ali simptomov zmanjšanega delovanja ščitnice. Periodično je treba opravljati laboratorijske preiskave delovanja ščitnice in po potrebi ukrepati v skladu z ustaljeno medicinsko prakso.

Proteinurija

V kliničnih študijah s pazopanibom so poročali o pojavu proteinurije. Pred začetkom zdravljenja in periodično med zdravljenjem je priporočljivo opraviti preiskave urina, bolnike pa je treba nadzirati glede poslabšanja proteinurije. V primeru pojava proteinurije stopnje 4 je treba zdravljenje s pazopanibom prekiniti.

Nosečnost

Predklinične študije na živalih so pokazale reproduktivno toksičnost. Če se pazopanib uporablja med nosečnostjo, ali če bolnica med zdravljenjem s pazopanibom zanosi, ji je treba pojasniti možno tveganje za plod. Ženskam v rodni dobi je treba pojasniti, da med zdravljenjem s pazopanibom ne smejo zanositi.

Interakcije

Sočasnemu zdravljenju z močnimi zaviralci CYP3A4, P-glikoproteina (P-gp) ali proteina BCRP se je treba izogniti, ker obstaja tveganje večje izpostavljenosti pazopanibu. Pretehtati je treba uporabo drugih sočasno uporabljanih zdravil, ki imajo majhen potencial za zaviranje CYP3A4, P-gp ali BCRP, ali takšnega potenciala sploh nimajo.

Sočasnemu zdravljenju z induktorji CYP3A4 se je treba izogibati zaradi tveganja za zmanjšanje izpostavljenosti pazopanibu.
Pri sočasni uporabi pazopaniba in substratov za uridin-difosfat-glukuroniziltransferazo 1A1 (UGT1A1) (npr. irinotekan) je potrebna previdnost, ker je pazopanib inhibitor UGT1A1.
Med zdravljenjem s pazopanibom bolnik ne sme uživati soka grenivke.

Medsebojno delovanje z drugimi zdravili in druge oblike interakcij

Vpliv drugih zdravil na pazopanib

Študije in vitro kažejo, da oksidativna presnova pazopaniba v človeških jetrnih mikrosomih poteka predvsem s CYP3A4 in le v manjši meri s CYP1A2 in CYP2C8. Zaviralci in induktorji CYP3A4 torej lahko vplivajo na presnovo pazopaniba.

Zaviralci CYP3A4, P-gp, BCRP:

Pazopanib je substrat CYP3A4, P-gp in BCRP. Pri sočasni uporabi pazopaniba in zdravil iz skupine močnih zaviralcev CYP3A4 (npr. ketokonazol, itrakonazol, klaritromicin, atazanavir, indinavir, nefazodon, nelfinavir, ritonavir, sakvinavir, telitromicin, vorikonazol) se koncentracije pazopaniba lahko povečajo. Sok grenivke vsebuje zaviralec CYP3A4 in tudi lahko poveča koncentracije pazopaniba v plazmi.
Pri uporabi lapatiniba (ki je substrat in šibek zaviralec CYP3A4 in P-gp ter močen zaviralec BCRP) v odmerku 1500 mg skupaj s pazopanibom v odmerku 800 mg, sta se srednji vrednosti $AUC_{(0-24)}$ in C_{max} pazopaniba povečali za približno od 50 % do 60 % v primerjavi z uporabo pazopaniba samega v odmerku 800 mg. Zavrtje P-gp in/ali BCRP z lapatinibom je verjetno pripomoglo k večji izpostavljenosti pazopanibu.
Sočasna uporaba enega odmerka kapljic za oči pazopanib (v majhnem odmerku 400 µg (80 µl 5 mg/ml)) z močnim zaviralcem CYP3A4 in zaviralcem P-gp ketokonazolom je pri zdravih prostovoljcih povečala $AUC_{(0-t)}$ za 2,2-krat in C_{max} za 1,5-krat. Zavrtje P-gp in/ali BCRP s ketokonzolom je verjetno pripomoglo k večji izpostavljenosti pazopanibu. Trenutno ni mogoče dati priporočil za odmerjanje bodisi močnih specifičnih zaviralcev CYP3A4 bodisi ketokonazola.
Pri sočasni uporabi pazopaniba skupaj z zaviralci CYP3A4, P-gp in BCRP, kot je lapatinib, se koncentracije pazopaniba v plazmi povečajo. Sočasna uporaba z močnimi zaviralci P-gp ali BCRP lahko tudi spremeni izpostavljenost pazopanibu in njegovo porazdelitev, vključno s porazdelitvijo v osrednje živčevje.
Sočasni uporabi z močnimi zaviralci CYP3A4, P-gp ali BCRP se je zato treba izogibati. Priporočljivo je izbrati alternativno sočasno zdravilo, ki ne zavira ali ima minimalen vpliv na zaviranje CYP3A4, P-gp ali BCRP.
Induktorji CYP3A4, P-gp, BCRP: Induktorji CYP3A4, kot je rifampicin, lahko zmanjšajo koncentracije pazopaniba v plazmi. Sočasna uporaba pazopaniba z močnimi induktorji P-gp ali BCRP lahko spremeni izpostavljenost pazopanibu in njegovo porazdelitev, vključno s porazdelitvijo v osrednje živčevje. Priporočljivo je izbrati alternativno sočasno zdravilo, ki ne inducira ali ima minimalen vpliv na indukcijo encima ali transporterja.

Vpliv pazopaniba na druga zdravila

Študije in vitro s humanimi jetrnimi mikrosomi so pokazale, da pazopanib zavira encime CYP 1A2, 3A4, 2B6, 2C8, 2C9, 2C19 in 2E1. Morebitna indukcija CYP3A4 je pri človeku bila dokazana *in vitro* s humanim PXR. Klinične farmakološke študije z uporabo pazopaniba v odmerku 800 mg enkrat na dan so pokazale, da pazopanib pri bolnikih z rakom nima klinično pomembnih učinkov na farmakokinetiko kofeina (preiskovani substrat za CYP1A2), varfarina (preiskovani substrat za CYP2C9) ali omeprazola (preiskovani substrat za CYP2C19).
Pri sočasni uporabi pazopaniba sta se srednji vrednosti AUC in C_{max} midazolama (preiskovani substrat za CYP3A4) povečali za približno 30 %, razmerje koncentracij dekstrometrofana in dekstrofana v urinu po peroralni uporabi dekstrometorfana (preiskovani substrat za CYP2D6) pa se je povečalo za od 33 % do 64 %. Pri sočasni uporabi pazopaniba v odmerku 800 mg enkrat na dan in paklitaksela v odmerku 80 mg/m^2 (substrat za CYP3A4 in CYP2C8) enkrat na teden, se je srednja vrednost AUC paklitaksela povečala za 25 %, C_{max} paklitaksela pa za 31 %.
Glede na vrednosti IC50 in vitro in vrednosti C_{max} v plazmi in vivo lahko presnovka pazopaniba GSK1268992 in GSK1268997 pripomoreta k neto zaviralnemu vplivu pazopaniba na BCRP. Poleg tega ni mogoče izključiti zavrtja BCRP in P-gp s pazopanibom v prebavilih. Previdnost je potrebna, če je pazopanib uporabljen hkrati z drugimi peroralnimi substrati BCRP in P-gp.
In vitro je pazopanib zavrl humani transportni polipeptid za organske anione (OATP1B1). Vpliva pazopaniba na farmakokinetiko substratov OATP1B1 (npr. rosuvastatina) ni mogoče izključiti.

Vpliv hrane na pazopanib

Pri uporabi pazopaniba skupaj z obrokom z veliko ali majhno vsebnostjo maščob sta se vrednosti AUC in C_{max} pazopaniba povečali za približno 2-krat. Bolnik mora pazopanib jemati vsaj eno uro pred ali dve uri po jedi.

Plodnost, nosečnost in dojenje

Nosečnost

Ni zadostnih podatkov o uporabi pazopaniba pri nosečnicah. Študije na živalih so pokazale vpliv na sposobnost razmnoževanja. Možno tveganje za ljudi ni znano.
Pazopanib se med nosečnostjo ne sme uporabljati, razen če klinično stanje bolnice zahteva zdravljenje s pazopanibom. Če se pazopanib uporablja med nosečnostjo, ali če bolnica med zdravljenjem s pazopanibom zanosi, ji je treba pojasniti možno tveganje za plod.
Ženski v rodni dobi je treba svetovati uporabo primerne metode kontracepcije in pojasniti, da med zdravljenjem s pazopanibom ne sme zanositi.

Dojenje

Varnost uporabe pazopaniba med dojenjem ni bila dokazana. Ni znano, če se pazopanib izloča z materinim mlekom. Podatki o izločanju pazopaniba z mlekom pri živalih niso na voljo. Tveganja za dojenega otroka ni mogoče izključiti. Med zdravljenjem s pazopanibom mora bolnica prenehati dojiti.

Plodnost

Študije na živalih kažejo, da zdravljenje s pazopanibom lahko vpliva na plodnost moških in žensk.

Vpliv na sposobnost vožnje in upravljanja s stroji

Študij o vplivu na sposobnost vožnje in upravljanja s stroji niso izvedli. Iz farmakologije pazopaniba se škodljiv vpliv na tovrstne aktivnosti ne more predvideti. Pri presojanju bolnikove sposobnosti za opravila, ki zahtevajo presojo motorične ali kognitivne funkcije, je treba upoštevati tako klinično stanje bolnika kot profil neželenih učinkov pazopaniba. Bolniki naj ne vozijo in ne upravljajo s stroji, če so omotični, utrujeni ali šibki.

Neželeni učinki

Pri celotnem vrednotenju varnosti in prenašanja pazopaniba pri osebah s karcinomom ledvičnih celic (skupaj n=586) so upoštevani združeni podatki iz ključne študije RCC (VEG105192, n=290), podaljška študije (VEG107769, n=71) in podporne študije II. faze (VEG102616, n=225).
Najpomembnejši resni neželeni učinki so tranzitorna ishemična ataka, ishemična kap, ishemija miokarda, diskfunkcija srca, gastrointestinalna perforacija in fistula, podaljšanje intervala Q-T ter krvavitve v pljučih, prebavilih in možganih. O vseh neželenih učinkih so poročali pri manj kot 1 % zdravljenih bolnikov.
Dogodki, ki so bili povezani s smrtnim izidom, in bi lahko bili povezani z uporabo pazopaniba so gastrointestinalna krvavitev, pljučna krvavitev/hemoptiza, nenormalno delovanje jeter, perforacija črevesa in ishemična možganska kap.
Najpogostejši neželeni učinki (ki so se pojavili vsaj pri 10 % bolnikov) katerekoli stopnje so bili: driska, sprememba barve las, hipertenzija, navzea, utrujenost, anoreksija, bruhanje, disgevzija, zvišanje vrednosti alanin-aminotransferaze in zvišanje vrednosti aspartat-aminotransferaze.
Z zdravljenjem povezani neželeni učinki, o katerih so poročali pri bolnikih s karcinomom ledvičnih celic, so v nadaljevanju navedeni po MedDRA podatkovni bazi glede na organske sisteme, pogostnosti in stopnjo resnosti. Pogostnost je navedena v skladu z naslednjim dogovorom:

Zelo pogosti ≥ 1/10
Pogosti ≥1/100 do <1/10
Občasni ≥ 1/1.000 do <1/100
Redki ≥1/10.000 do <1/1.000
Zelo redki < 1/10.000
Neznana (ni mogoče oceniti iz razpoložljivih podatkov)

Kategorije pogostnosti so bile določene na osnovi absolutne pogostnosti iz kliničnih študij.
V razvrstitvah pogostnosti znotraj posameznega organskega sistema so neželeni učinki navedeni po padajoči resnosti.

Tabela 1: Z zdravljenjem povezani neželeni učinki, o katerih so poročali v študijah pri bolnikih s karcinomom ledvičnih celic (n=586)

Organski sistem	Pogostnost (vse stopnje)	Neželeni učinki	Vse stopnje n (%)	Stopnja 3 n (%)	Stopnja 4 n (%)
Bolezni krvi in limfatičnega sistema	Pogosti	trombocitopenija	25 (4 %)	3 (< 1 %)	3 (< 1 %)
	Pogosti	nevtropenija	17 (3 %)	4 (< 1 %)	2 (< 1 %)
	Pogosti	levkopenija	14 (2 %)	1 (< 1 %)	0
Bolezni endokrinega sistema	Pogosti	hipotiroidizem	23 (4 %)	0	0
Presnovne in prehranske motnje	Zelo pogosti	zmanjšan apetit[e]	122 (21 %)	6 (1 %)	0
	Občasni	hipofosfatemija	4 (< 1 %)	2 (< 1 %)	0
	Občasni	hipomagneziemija	3 (< 1 %)	0	0
Bolezni živčevja	Zelo pogosti	disgevzija[c]	92 (16 %)	0	0
	Pogosti	glavobol	41 (7 %)	0	0
	Pogosti	omotica	19 (3 %)	0	1 (< 1 %)
	Pogosti	letargija	12 (2 %)	1 (< 1 %)	0
	Pogosti	parestezija	12 (2 %)	2 (< 1 %)	0
	Občasni	periferna senzorična nevropatija	5 (< 1 %)	0	0
	Občasni	hipestezija	4 (< 1 %)	0	0
	Občasni	tranzitorna ishemična ataka	3 (< 1 %)	2 (< 1 %)	0
	Občasni	cerebrovaskularni incident	1 (< 1 %)	0	1 (< 1 %)
	Občasni	ishemična možganska kap	1 (< 1 %)	0	0
Očesne bolezni	Občasni	sprememba barve trepalnic	3 (< 1 %)	0	0
Srčne bolezni	Občasni	bradikardija	3 (< 1 %)	0	0
	Občasni	disfunkcija srca	4 (< 1 %)	1 (< 1 %)	1 (< 1 %)
	Občasni	miokradni infarkt	2 (< 1 %)	0	2 (< 1 %)
	Občasni	ishemija miokarda	1 (< 1 %)	1 (< 1 %)	0
Žilne bolezni	Zelo pogosti	hipertenzija	225 (38 %)	34 (6%)	0
	Pogosti	navali vročine	11 (2 %)	0	0
	Občasni	zardevanje	5 (< 1 %)	0	0
	Občasni	krvavitev	1 (< 1 %)	0	0
	Občasni	hipertenzivna kriza	1 (< 1 %)	0	1 (< 1 %)
Bolezni dihal, prsnega koša in mediastinalnega prostora	Pogosti	krvavitev iz nosu	16 (3 %)	0	0
	Pogosti	disfonija	15 (3 %)	0	0
	Občasni	pljučna embolija	4 (< 1 %)	1 (< 1 %)	3 (< 1 %)
	Občasni	hemoptiza	3 (< 1 %)	0	0
	Občasni	pljučna krvavitev	1 (< 1 %)	0	0
Bolezni prebavil	Zelo pogosti	driska	286 (49 %)	19 (3 %)	2 (< 1 %)
	Zelo pogosti	navzea	161 (27 %)	3 (< 1 %)	0
	Zelo pogosti	bruhanje	89 (15 %)	7 (1 %)	1 (< 1 %)
	Zelo pogosti	bolečina v trebuhu[a]	60 (10 %)	8 (1 %)	0
	Pogosti	dispepsija	24 (4 %)	2 (< 1 %)	0
	Pogosti	stomatitis	24 (4 %)	0	0
	Pogosti	flatulenca	20 (3 %)	0	0
	Pogosti	distenzija trebuha	15 (3 %)	0	0
	Občasni	razjede v ustih	4 (< 1 %)	1 (< 1 %)	0
	Občasni	pogosta črevesna motiliteta	3 (< 1 %)	0	0
	Občasni	gastrointestinalna krvavitev	3 (< 1 %)	1 (< 1 %)	0
	Občasni	krvavitev iz danke	3 (< 1 %)	1 (< 1 %)	0
	Občasni	perforacija debelega črevesa	2 (< 1 %)	1 (< 1 %)	0
	Občasni	krvavitev v ustih	2 (< 1 %)	0	0
	Občasni	enterokutana fistula	1 (< 1 %)	0	0
	Občasni	hematemeza	1 (< 1 %)	0	0
	Občasni	hematohezija	1 (< 1 %)	0	0
	Občasni	hemoroidalna krvavitev	1 (< 1 %)	0	0
	Občasni	perforacija ileuma	1 (< 1 %)	0	1 (< 1 %)
	Občasni	melena	1 (< 1 %)	0	0
	Občasni	krvavitev v požiralniku	1 (< 1 %)	0	1 (< 1 %)
	Občasni	pankreatitis	1 (< 1 %)	0	0
	Občasni	peritonitis	1 (< 1 %)	0	0
	Občasni	retroperitonealna krvavitev	1 (< 1 %)	0	0
	Občasni	krvavitev v zgornjih prebavilih	1 (< 1 %)	0	0
Bolezni jeter, žolčnika in žolčevodov	Pogosti	nenormalno delovanje jeter	20 (3 %)	6 (1 %)	0
	Pogosti	hiperbilirubinemija	18 (3 %)	2 (< 1 %)	1 (< 1 %)
	Občasni	hepatotoksičnost	5 (< 1 %)	3 (< 1 %)	0
	Občasni	zlatenica	2 (< 1 %)	1 (< 1 %)	0
	Občasni	odpoved jeter	1 (< 1 %)	0	1 (< 1 %)
	Občasni	hepatitis	1 (< 1 %)	1 (< 1 %)	0
Bolezni kože in podkožja	Zelo pogosti	sprememba barve las	231 (39 %)	1 (< 1 %)	0
	Pogosti	kožni izpuščaj	52 (9 %)	3 (< 1 %)	0
	Pogosti	alopecija	50 (9 %)	0	0
	Pogosti	sindrom palmarno-plantarne eritrodisestezije	43 (7 %)	7 (1 %)	0
	Pogosti	hipopigmentacija kože	25 (4 %)	0	0
	Pogosti	rdečina	15 (3 %)	0	0
	Pogosti	srbenje	13 (2 %)	0	0
	Pogosti	depigmentacija kože	13 (2 %)	0	0
	Pogosti	suha koža	12 (2 %)	0	0
	Pogosti	čezmerno znojenje	9 (2 %)	0	0
	Občasni	fotosenzibilnostna reakcija	7 (1 %)	0	0
	Občasni	eksfoliacija kože	7 (1 %)	0	0
	Občasni	vezikulozni izpuščaj	3 (< 1 %)	0	0
	Občasni	generalizirano srbenje	2 (< 1 %)	1 (< 1 %)	0
	Občasni	papulozni izpuščaj	2 (< 1 %)	0	0
	Občasni	plantarni eritem	1 (< 1 %)	0	0
	Občasni	eritematozni izpuščaj	1 (< 1 %)	0	0
	Občasni	generaliziran izpuščaj	1 (< 1 %)	0	0
	Občasni	makulozni izpuščaj	1 (< 1 %)	0	0
	Občasni	pruritični izpuščaj	1 (< 1 %)	0	0
Bolezni mišično-skeletnega sistema in vezivnega tkiva	Pogosti	mialgija	15 (3 %)	2 (< 1 %)	0
	Pogosti	mišični krči	12 (2 %)	0	0
Bolezni sečil	Pogosti	proteinurija	40 (7 %)	5 (< 1 %)	0
	Občasni	krvavitev v sečila	1 (< 1 %)	0	0
Motnje reprodukcije in dojk	Občasni	menoragija	1 (< 1 %)	0	0
	Občasni	metroragija	1 (< 1 %)	0	0
	Občasni	krvavitev iz nožnice	1 (< 1 %)	0	0
Splošne težave in spremembe na mestu aplikacije	Zelo pogosti	utrujenost	139 (24 %)	16 (3 %)	0
	Pogosti	astenija	41 (7 %)	8 (1 %)	0
	Pogosti	vnetje sluznic	27 (5 %)	2 (< 1 %)	0
	Pogosti	edem[b]	19 (3 %)	0	0
	Pogosti	bolečina v prsnem košu	14 (2 %)	2 (< 1 %)	0
	Občasni	motnje sluznic	1 (< 1 %)	0	0
Preiskave	Zelo pogosti	zvišanje vrednosti alanin-aminotransferaze	83 (14 %)	28 (5 %)	4 (< 1 %)
	Zelo pogosti	zvišanje vrednosti aspartat-aminotransferaze	72 (12 %)	17 (3 %)	3 (< 1 %)
	Pogosti	zmanjšanje telesne mase	38 (6 %)	2 (< 1 %)	0
	Pogosti	zvišanje vrednosti kreatinina v krvi	13 (2 %)	2 (< 1 %)	0
	Pogosti	zvišanje vrednosti bilirubina v krvi	11 (2 %)	1 (< 1 %)	1 (< 1 %)
	Pogosti	zmanjšanje števila belih krvnih celic[d]	10 (2 %)	1 (< 1 %)	0
	Pogosti	zvišanje vrednosti lipaze	9 (2 %)	4 (< 1 %)	1 (< 1 %)
	Pogosti	zvišan krvni tlak	6 (1 %)	0	0
	Pogosti	zvišanje tiroideo-stimulirajočega hormona v krvi	6 (1 %)	0	0
	Pogosti	zvišanje gama-glutamiltransferaze	6 (1 %)	1 (< 1 %)	1 (< 1 %)
	Pogosti	zvišanje jetrnih encimov	6 (1 %)	2 (< 1 %)	0
	Občasni	aspartat-aminotransferaza	5 (< 1 %)	2 (< 1 %)	0
	Občasni	zvišanje sečnine v krvi	5 (< 1 %)	1 (< 1 %)	0
	Občasni	podaljšanje Q-T na elektrokardiogramu	5(< 1 %)	1 (< 1 %)	0
	Občasni	zvišanje amilaze v krvi	4 (< 1 %)	0	0
	Občasni	znižanje glukoze v krvi	4 (< 1 %)	0	0
	Občasni	alanin-aminotransferaza	3 (< 1 %)	2 (< 1 %)	0
	Občasni	zvišana aktivnost transaminaz	3 (< 1 %)	1 (< 1 %)	0
	Občasni	zvišan diastolični krvni tlak	2 (< 1 %)	0	0
	Občasni	nenormalni test delovanja ščitnice	2 (< 1 %)	0	0
	Občasni	zvišan sistolični krvni tlak	1 (< 1 %)	0	0
	Občasni	nenormalni test delovanja jeter	1 (< 1 %)	0	0

Naslednji izrazi so združeni:
[a] bolečine v trebuhu, bolečine v zgornjem delu trebuha in bolečine v spodnjem delu trebuha
[b] edemi, periferni edemi, edemi v predelu oči, lokalizirani edemi in edem obraza
[c] dizgevzija, agevzija in hipogevzija
[d] zmanjšanje števila levkocitov, zmanjšanje števila nevtrofilcev in zmanjšanje števila levkocitov
[e] zmanjšanje apetita in anoreksija

Preveliko odmerjanje

V kliničnih študijah so ovrednotili uporabo pazopaniba v odmerkih do 2000 mg. Pri tem se toksični učinki, ki bi bili povezani z velikostjo odmerka, niso pojavili.
Specifični antidot za primere prevelikega odmerjanja pazopaniba ne obstaja. Zdravljenje v primeru prevelikega odmerjanja mora vključevati splošne podporne ukrepe.

Inkompatibilnosti

Navedba smiselno ni potrebna.

Vrsta ovojnine in vsebina

Plastenke iz polietilena visoke gostote (HDPE) z za otroke varno zaporko, ki vsebujejo 30 ali 90 tablet.

IMETNIK DOVOLJENJA ZA PROMET

Glaxo Group Limited / Berkeley Avenue / Greenford / Middlesex / UB6 0NN / Velika Britanija

Referenca:

1. Sternberg CN,et al.Pazopanib locally advanced or metastatic renal cell carcinoma:Results of a randomized
Phase III trial. J ClinOncol2010,28(6):1061-8
2. Votrient, povzetek glavnih značilnosti zdravila, 2011.
3. Kumar R, et al. Myelosuppression and kinase selectivity of multikinase angiogenesis inhibitors. Br J Cancer 2009; 101:1717–1723.
4. Karaman MW, et al. A quantitative analysis of kinase inhibitor selectivity. Nat Biotechnol 2008; 26: 127–132.

DATUM ZADNJE REVIZIJE BESEDILA
01.02.2011
Režim izdaje: Rp/Spec
<Podrobne informacije o zdravilu so objavljene na spletni strani Evropske agencije za zdravila http://www.ema.europa.eu/.>

Votrient®
pazopanib

Učinkovito upočasni napredovanje raka ledvičnih celic*

gsk GlaxoSmithKline

SLO/PAZ/0001/11

Votrient je potenten in selektiven tirozin kinazni inhibitor, zdravilo za zdravljenje bolnikov z napredovalim karcinomom ledvičnih celic v prvi liniji, ki:

- signifikantno podaljša čas do napredovanja bolezni
- ima nizko pojavnost neželenih učinkov stopnje 3 in 4, kot so mukozitis/stomatitis, sindrom roka-noga, utrujenost
- ohranja kvaliteto življenja bolnika. [1,3,4]

*vs placebo.

SAMO ZA STROKOVNO JAVNOST

Oncology
Trusted Generics: Total Care

The Fresenius Kabi oncology portfolio

- Devices, i.v. solutions and drugs
- Parenteral and enteral nutrition
- Compounding services and home care

Safety in the pharmacy

- Colour safety concept extended to generic oncology portfolio
- Clear, safe and easily understandable system

Controlling the supply chain, bringing value

- State of the art production facilities and processes
- Audited and approved by international regulatory bodies including the FDA, MHRA, WHO and TGA

Enhancing data provision

- Dedicated oncology research and development ensures high quality products

FRESENIUS KABI
caring for life

medias international

Zastopnik za Slovenijo:
Medias International d.o.o. , Trgovanje in trženje z medicinskim materialom
Leskoškova cesta 9D , 1000 Ljubljana, Slovenija
Tel.: 01/ 52 02 300, Faks: 01/ 52 02 495, E-pošta: info@medias-int.si
www.medias-int.si

Preprečuje CINV* od samega začetka

z zdravilom EMEND v kombinaciji z drugimi antiemetiki

* - s kemoterapijo povzročena navzea in bruhanje

06-12-EMD-11-SLO-022-J

EMEND 80 mg trde kapsule EMEND 125 mg trde kapsule **SKRAJŠAN POVZETEK GLAVNIH ZNAČILNOSTI ZDRAVILA Pred predpisovanjem, prosimo, preberite celoten Povzetek glavnih značilnosti zdravila, ki ga dobite pri naših strokovnih sodelavcih! Sestava:** Ena EMEND 125 mg trda kapsula vsebuje 125 mg aprepitanta in 125 mg saharoze. Ena EMEND 80 mg trda kapsula vsebuje 80 mg aprepitanta in 80 mg saharoze. **Terapevtske indikacije:** Preprečevanje akutne in zapoznele navzee in bruhanja povezanih z zelo emetogeno kemoterapijo raka s cisplatinom pri odraslih. Preprečevanje navzee in bruhanja, povezanih z zmerno emetogeno kemoterapijo raka pri odraslih. Zdravilo EMEND 125 mg/80 mg se daje v sklopu kombiniranega zdravljenja. **Odmerjanje in način uporabe:** Zdravilo EMEND se daje 3 dni po shemi zdravljenja, ki vključuje kortikosteroid in antagonist 5-HT3. Priporočeno odmerjanje zdravila EMEND je 125 mg peroralno (p.o.) enkrat dnevno eno uro pred pričetkom kemoterapije prvi dan ter 80 mg (p.o.) enkrat na dan drugi in tretji dan. Fosaprepitant 115 mg, liofilizirano predzdravilo aprepitanta v obliki 15-minutne infuzije, lahko prvi dan, 30 minut pred kemoterapijo nadomesti uporabo zdravila EMEND (125 mg). Zdravilo EMEND se lahko jemlje s hrano ali brez. Trdo kapsulo je treba pogoltniti celo. Pri starostnikih, bolnikih z okvaro ledvic in pri bolnikih s končno ledvično odpovedjo, ki se zdravijo s hemodializo, bolnikih z blago okvaro jeter ter glede na spol odmerka ni treba prilagajati. Pri bolnikih z zmerno okvaro jeter je število podatkov omejeno, pri bolnikih s hudo okvaro jeter pa podatkov ni. Pri teh bolnikih je treba aprepitant uporabljati previdno. Uporabe pri bolnikih, ki so mlajši od 18 let, zaradi nezadostnih podatkov o varnosti in učinkovitosti ne priporočamo. **Kontraindikacije:** Preobčutljivost za zdravilno učinkovino ali katerokoli pomožno snov. Sočasno jemanje s pimozidom, terfenadinom, z astemizolom ali s cisapridom. **Posebna opozorila in previdnostni ukrepi:** Zdravilo EMEND je treba uporabljati previdno pri bolnikih, ki sočasno jemljejo peroralne zdravilne učinkovine, ki se primarno presnavljajo s CYP3A4 in z ozkim terapevtskim območjem, kot so ciklosporin, takrolimus, sirolimus, everolimus, alfentanil, diergotamin, ergotamin, fentanil in kinidin. Previdnost je še posebej potrebna pri sočasnem dajanju irinotekana, saj lahko kombinacija poveča toksični učinek. Pri sočasni uporabi zdravila EMEND z alkaloidi rženega rožička (ergot alkaloid) svetujemo previdnost zaradi morebitnega tveganja za pojav z ergot alkaloidi povezanih toksičnih učinkov. Sočasna uporaba zdravila EMEND z varfarinom zmanjša protrombinski čas, izražen kot INR. Pri bolnikih, ki se kontinuirano zdravijo z varfarinom, je treba INR skrbno spremljati med zdravljenjem z zdravilom EMEND in še 2 tedna po vsakem 3-dnevnem ciklusu zdravljenja navzee in bruhanja zaradi kemoterapije z zdravilom EMEND. Med jemanjem zdravila EMEND in še 28 dni po koncu jemanja se lahko zmanjša učinkovitost hormonskih kontraceptivov. Med zdravljenjem z zdravilom EMEND in 2 meseca po zadnjem odmerku zdravila EMEND je treba uporabljati alternativno ali dodatno kontracepcijsko metodo. Sočasnemu jemanju zdravila EMEND in zdravilnih učinkovin, ki močno inducirajo aktivnost CYP3A4 (npr. rifampicin, fenitoin, karbamazepin, fenobarbital), se je treba izogibati, ker kombinacija povzroči zmanjšanje plazemskih koncentracij aprepitanta. Sočasna uporaba zdravila EMEND in zeliščnih pripravkov, ki vsebujejo šentjanževko, ni priporočljiva. Potrebna je previdnost pri sočasni uporabi zdravila EMEND in zdravilnih učinkovin, ki zavirajo aktivnost CYP3A4 (npr. ketokonazol, itrakonazol, vorikonazol, posakonazol, klaritromicin, telitromicin, nefazodon in zaviralci proteaz), ker se zaradi kombinacije pričakuje zvišanje plazemskih koncentracij aprepitanta. Zdravilo EMEND vsebuje saharozo. Bolniki z redkimi dednimi motnjami – fruktozno intoleranco, malabsorpcijo glukoze in galaktoze ali insuficienco saharaze-izomaltaze – ne smejo jemati tega zdravila. **Medsebojno delovanje z drugimi zdravili in druge oblike interakcij:** Aprepitant (125 mg/80 mg) je substrat, zmerni zaviralec in induktor CYP3A4. Aprepitant je tudi induktor CYP2C9. Med zdravljenjem se CYP3A4 inhibira. Po koncu zdravljenja pa zdravilo EMEND povzroči blago indukcijo CYP2C9, CYP3A4 in glukuronidacije. Aprepitant nima medsebojnega vpliva z digoksinom, zato verjetno ne intereagira s P-glikoproteinskim prenašalcem. Kot blag induktor CYP2C9, induktor CYP3A4 in glukuronidacije lahko aprepitant zniža plazemske koncentracije substratov, ki se izločajo po teh poteh. Ta učinek se lahko pokaže šele po koncu zdravljenja z zdravilom EMEND. Za substrate CYP2C9 in CYP3A4 je indukcija prehodna, največji učinek pa je dosežen v 3-5 dneh po koncu 3 dnevnega zdravljenja z zdravilom EMEND. Učinek traja nekaj dni, potem pa počasa upada in je klinično nepomemben v dveh tednih po koncu zdravljenja. V tem obdobju svetujemo previdnost pri dajanju peroralnih zdravilnih učinkovin, ki se presnavljajo s CYP2C9. *Kortikosteroidi:* Pri sočasnem jemanju je treba običajni peroralni odmerek deksametazona zmanjšati za približno 50 %, običajni intravenski odmerek metilprednizolona zmanjšati za približno 25 % in običajni peroralni odmerek metilprednizolona zmanjšati za približno 50 %. *Kemoterapevtiki:* Pri bolnikih, ki poleg zdravila EMEND peroralno prejemajo kemoterapevtike, ki se primarno ali delno presnavljajo s CYP3A4 (npr. etopozid, vinorelbin), svetujemo previdnost.. Pri takih bolnikih bo morda potreben dodatni nadzor. *Imunosupresivi:* Zmanjšanja odmerka imunosupresivov, ki se presnavljajo s CYP3A4 (npr. ciklosporin, takrolimus, everolimus in sirolimus), ne priporočamo. *Midazolam:* Pri sočasni uporabi z zdravilom EMEND (125mg / 80 mg) je treba upoštevati možne učinke zvišanih plazemskih koncentracij midazolama in drugih benzodiazepinov, ki se presnavljajo predvsem s CYP3A4 (alprazolam, triazolam). *Tolbutamid:* Zdravilo EMEND je pri jemanju po shemi 125 mg prvi dan ter 80 mg/dan drugi in tretji dan zmanjšal AUC tolbutamida (ki je substrat za CYP2C9), ki so ga bolniki prejemali v enkratnem odmerku 500 mg per os pred začetkom 3 dnevne sheme odmerjanja zdravila EMEND ter 4., 8. in 15. dan. *Antagonisti 5 HT_3:* V kliničnih raziskavah medsebojnega delovanja aprepitant ni imel klinično pomembnih učinkov na farmakokinetiko ondansetrona, granisetrona in hidrodolasetrona. *Ketokonazol:* Pri enkratnem odmerku 125 mg aprepitanta 5. dan 10 dnevnega zdravljenja s ketokonazolom (ki je močan zaviralec CYP3A4) 400 mg na dan, se je AUC aprepitanta povečal za približno 5 krat, srednji končni razpolovni čas aprepitanta pa se je podaljšal za približno za 3 krat. *Rifampicin:* Pri enkratnem odmerku 375 mg aprepitanta 9. dan 14 dnevnega zdravljenja z rifampicinom (ki je močan induktor CYP3A4) 600 mg na dan, se je AUC aprepitanta zmanjšal za 91 %, srednji končni razpolovni čas aprepitanta pa se je skrajšal za 68 %. **Neželeni učinki:** Pri bolnikih, zdravljenih z aprepitantom, so opazili naslednje neželene učinke, ki so se pojavljali pogosteje kot pri standardni terapiji: Pogosti (>1/100, <1/10): anoreksija, glavobol, omotica, kolcanje, konstipacija, driska, dispepsija, spahovanje, astenija/utrujenost, zvišanje ALT, zvišanjeAST. Občasni (>1/1.000, <1/100): kandidoza, okužbe s stafilokoki, anemija, febrilna nevtropenija, povečanje telesne mase, polidipsija, dezorientacija, evforija, anksioznost, neobičajne sanje, motnje mišljenja, letargija, zaspanost, konjunktivitis, tinitus, bradikardija, palpitacije, bolezen srca in ožilja, zardevanje/navali vročine, faringitis, kihanje, kašelj, zatekanje izcedka iz nosu v žrelo, draženje žrela, perforirajoč duodenalen ulkus, navzea, bruhanje, refluks kisline, motnje okusa, neugodje v epigastriju, obstipacija, gastroezofagalna refluksna bolezen, bolečine v trebuhu, suha usta, enterokolitis, vetrovi, stomatitis, napihnjen trebuh, trdo blato, nevtropenični kolitis, izpuščaji, akne, fotosenzitivnost, prekomerno znojenje, mastna koža, srbenje, lezije kože, srbeči izpuščaj, mišični krči, bolečine v mišicah, mišična oslabelost, poliurija, disurija, polakisurija, edem, nelagodje v prsnem košu, splošno slabo počutje, žeja, mrzlica, motnja hoje, zvišanje alkalne fosfataze, hiperglikemija, mikrohematurija, hiponatriemija, zmanjšanje telesne mase, zmanjšano število nevtrofilcev. Poročali so o enem primeru angioedema in urtikarije. Pri enem bolniku, ki je dobival aprepitant ob kemoterapiji zaradi raka, so poročali o pojavu Stevens-Johnsonovega sindroma. V obdobju trženja zdravila so poročali še o (pogostnost je neznana): pruritus, izpuščaj, urtikarija, preobčutljivostne reakcije, vključno z anafilaktičnimi reakcijami. EMEND 80mg trde kapsule EMEND 125 mg trde kapsule **Imetnik dovoljenja za promet:** Merck Sharp & Dohme Ltd., Hertford Road, Hoddesdon, Hertfordshire EN 11 9BU, Velika Britanija **Način in režim izdaje zdravila:** Predpisovanje in izdaja zdravila je le na zdravniški recept. **Datum zadnje revizije besedila:** 01/2010

Samo za strokovno javnost.

EMEND® (aprepitant, MSD)

IVEMEND® (fosaprepitant dimeglumin, MSD)

Preventivno od začetka

MSD

Merck Sharp & Dohme, inovativna zdravila d.o.o.
Šmartinska cesta 140, 1000 Ljubljana; telefon: 01/ 5204 201, faks: 01/ 5204 349

Tiskano v Sloveniji, junij 2011.

Antraciklinska ekstravazacija lahko nastopi kadarkoli.

savene™
deksrazoksan

Edini dokazani antidot pri ekstravazaciji antraciklinov v okolno tkivo, ki ga je odobrila EMEA.

Bodite pripravljeni!

Savene™ – Povzetek informacij o predpisovanju zdravila (izdelan na podlagi Povzetka glavnih značilnosti zdravila - SPC). Za celotne informacije o predpisovanju zdravila glejte SPC.
Vsaka škatlica zdravila Savene™ vsebuje 10 vial Savene™ praška (deksrazoksan) (10 x 500 mg) in 3 vrečke Savene™ puferske raztopine za redčanje (3 x 500 ml) za infuzijo. Indikacije: Zdravljenje ekstravazacije antraciklinov. Odmerjanje in način uporabe: Z aplikacijo zdravila Savene™ je treba začeti čim prej in najpozneje v šestih urah po opaženi ekstravazaciji. Zdravilo Savene™ se daje kot intravenska infuzija enkrat na dan 3 zaporedne dni, glede na telesno površino: 1. dan 1000 mg/m^2; 2. dan 1000 mg/m^2; 3. dan 500 mg/m^2. Pri bolnikih s telesno površino, ki presega 2 m^2, enkratni odmerek ne sme preseči 2000 mg. Ledene obloge ali druge pripomočke za hlajenje je treba odstraniti s prizadetega predela najmanj 15 min pred aplikacijo. Pred infuzijo je treba Savene™ prašek še pred nadaljnjim redčenjem, s pufersko raztopino za redčenje, rekonstituirati s sterilno vodo. Uporaba zdravila Savene™ ni priporočljiva pri otrocih in bolnikih z okvarjenim delovanjem ledvic in jeter. Varnost in učinkovitost zdravila nista bili ovrednoteni pri starejših bolnikih. Kontraindikacije: Preobčutljivost za aktivno učinkovino ali katerokoli sestavino zdravila, ženske v rodni dobi, ki ne uporabljajo kontracepcije, dojenje in sočasno cepljenje s cepivom proti rumeni mrzlici. Opozorila in previdnostni ukrepi: Po končanem zdravljenju je treba prizadeti predel redno nadzorovati, dokler se stanje ne izboljša. Redno je treba izvajati tudi hematološke preiskave. Zdravilo Savene™ se sme aplicirati samo pod nadzorom zdravnika, ki ima izkušnje z uporabo kemoterapevtikov za zdravljenje raka. Pri bolnikih z znanimi motnjami v delovanju jeter je pred vsako aplikacijo zdravila Savene™ priporočljivo izvajati rutinske teste jetrne funkcije. Pri bolnikih z okvarjenim delovanjem ledvic je treba opazovati znake hematološke toksičnosti. Za moške je priporočljivo, da med zdravljenjem in do 3 mesece po njem ne zaplodijo otroka. Ženske v rodni dobi morajo med zdravljenjem uporabljati kontracepcijsko zaščito. To zdravilo običajno ni priporočljivo v kombinaciji z živimi oslabljenimi cepivi ali s fenitoinom. Bolniki, ki prejmejo Savene™, ne smejo sočasno prejemati dimetil sulfoksida (DMSO). Ker vsebuje Savene™ redčilo kalij, (98 mg/500 ml), je treba pri bolnikih s tveganjem za pojav hiperkaliemije skrbno nadzorovati plazemske vrednosti kalija. Ker vsebuje tudi natrij (1,61 g/500 ml), lahko škoduje bolnikom, ki so na dieti z nizko vsebnostjo natrija. Interakcije: Interakcije, značilne za vse citotoksike, ki lahko medsebojno učinkujejo tudi s peroralnimi antikoagulanti. Pri sočasni uporabi imunosupresivov kot sta ciklosporin in takrolimus je potrebna posebna pozornost zaradi obsežne imunosupresije. Nosečnost in dojenje: Nosečnice ne smejo prejemati zdravila Savene™, razen če to ni nujno potrebno. Ženske v rodni dobi morajo med zdravljenjem uporabljati kontracepcijska sredstva. Doječe matere morajo med zdravljenjem z zdravilom Savene™ prenehati dojiti. Stranski učinki: Zelo pogosti: navzea, bolečina na mestu vboda, pooperativna okužba. Pogosti: bruhanje, driska, stomatitis, suha usta, pireksija, flebitis na mestu vboda, eritem na mestu vboda, utrujenost, induracija na mestu vboda, oteklina na mestu vboda, periferni edem, somnolenca, okužba, nevtropenična okužba, zaplet rane, zmanjšanje telesne teže, izguba teka, mialgija, omotičnost, izguba senzibilitete, sinkopa, tremor, nožnična krvavitev, dispneja, pljučnica, izpadanje las, srbečica, flebitis, površinski tromboflebitis, venska tromboza udov, tromboza. Vsi neželeni učinki so opisani kot hitro reverzibilni. Redko so poročali o povečanih koncentracijah jetrnih encimov (ALT/AST). Imetnik dovoljenja za promet: SpePharm Holding B.V., Kingsfordweg 151, NL – 1043 GR Amsterdam, Nizozemska. Številka dovoljenja za promet: EU/1/06/350/001.

SpePharm

www.medis.si

MEDIS

Instructions for authors

The editorial policy

Radiology and Oncology is a multidisciplinary journal devoted to the publishing original and high quality scientific papers, professional papers, review articles, case reports and varia (editorials, short communications, professional information, book reviews, letters, etc.) pertinent to diagnostic and interventional radiology, computerized tomography, magnetic resonance, ultrasound, nuclear medicine, radiotherapy, clinical and experimental oncology, radiobiology, radiophysics and radiation protection. Therefore, the scope of the journal is to cover beside radiology the diagnostic and therapeutic aspects in oncology, which distinguishes it from other journals in the field.

The Editorial Board requires that the paper has not been published or submitted for publication elsewhere; the authors are responsible for all statements in their papers. Accepted articles become the property of the journal and, therefore cannot be published elsewhere without the written permission of the editors.

Submission of the manuscript

The manuscript written in English should be submitted electronically to: gsersa@onko-i.si. In the case the figures are too big to be submitted electronically, authors are asked to send along the printed copy of the manuscript, together with all the files on CD, to the editorial office. The type of computer and word-processing package should be specified (Word for Windows is preferred).

Editorial Office Radiology and Oncology
Zaloska cesta 2
P.O. Box 2217
SI-1000 Ljubljana
Slovenia
Phone: +386 (0)1 5879 434,
Tel./Fax: +386 (0)1 5879 434,
E-mail: gsersa@onko-i.si

All articles are subjected to the editorial review and the review by independent referees. Manuscripts which do not comply with the technical requirements stated herein will be returned to the authors for the correction before peer-review. The editorial board reserves the right to ask authors to make appropriate changes of the contents as well as grammatical and stylistic corrections when necessary. Page charges will be charged for manuscripts exceeding the recommended page number, as well as additional editorial work and requests for printed reprints. All articles are published printed and on-line as the open access. To support the open access policy of the journal, the authors are encouraged to pay the open access charge of 500 EUR.

Preparation of manuscripts

Radiology and Oncology will consider manuscripts prepared according to the Uniform Requirements for Manuscripts Submitted to Biomedical Journals by International Committee of Medical Journal Editors (http://www.icmje.org/). The manuscript should be typed double-spaced with a 3-cm margin at the top and left-hand side of the sheet. The manuscript should be written in grammatically and stylistically correct language. Abbreviations should be avoided. If their use is neccessary, they should be explained at the first time mentioned. The technical data should conform to the SI system. The manuscript, including the references, must not exceed 15 typewritten pages, and the number of figures and tables is limited to 8. If appropriate, organize the text so that it includes: Introduction, Materials and methods, Results and Discussion. Exceptionally, the results and discussion can be combined in a single section. Start each section on a new page, and number each page consecutively with Arabic numerals.

The Title page should include a concise and informative title, followed by the full name(s) of the author(s); the institutional affiliation of each author; the name and address of the corresponding author (including telephone, fax and E-mail), and an abbreviated title. This should be followed by the abstract page, summarizing in less than 250 words the reasons for the study, experimental approach, the major findings (with specific data if possible), and the principal conclusions, and providing 3-6 key words for indexing purposes. Structured abstracts are preferred. Slovene authors are requested to provide title and the abstract in Slovene language in a separate file. The text of the research article should then proceed as follows:

Introduction should summarize the rationale for the study or observation, citing only the essential references and stating the aim of the study.

Materials and methods should provide enough information to enable experiments to be repeated. New methods should be described in detail.

Results should be presented clearly and concisely without repeating the data in the figures and tables. Emphasis should be on clear and precise presentation of results and their significance in relation to the aim of the investigation.

Discussion should explain the results rather than simply repeating them and interpret their significance and draw conclusions. It should discuss the results of the study in the light of previously published work.

Illustrations and tables must be numbered and referred to in the text, with the appropriate location indicated. Graphs and photographs, provided electronically, should be of appropriate quality for good reproduction. Color graphs and photographs are encouraged. Picture size must be 2.000 pixels on the longer side. In photographs, mask the identities of the patients. Tables should be typed double-spaced, with a descriptive title and, if appropriate, units of numerical measurements included in the column heading.

References must be numbered in the order in which they appear in the text and their corresponding numbers quoted in the text. Authors are responsible for the accuracy of their references. References to the Abstracts and Letters to the Editor must be identified as such. Citation of papers in preparation or submitted for publication, unpublished observations, and personal communications should not be included in the reference list. If essential, such material may be incorporated in the appropriate place in the text. References follow the style of Index Medicus. All authors should be listed when their number does not exceed six; when there are seven or more authors, the first six listed are followed by "et al.". The following are some examples of references from articles, books and book chapters:

Dent RAG, Cole P. *In vitro* maturation of monocytes in squamous carcinoma of the lung. *Br J Cancer* 1981; **43**: 486-95.

Chapman S, Nakielny R. *A guide to radiological procedures.* London: Bailliere Tindall; 1986.

Evans R, Alexander P. Mechanisms of extracellular killing of nucleated mammalian cells by macrophages. In: Nelson DS, editor. *Immunobiology of macrophage.* New York: Academic Press; 1976. p. 45-74.

Authorization for the use of human subjects or experimental animals

Manuscripts containing information related to human or animal use should clearly state that the research has complied with all relevant national regulations and institutional policies and has been approved by the authors' institutional review board or equivalent committee. These statements should appear in the Materials and methods section (or for contributions without this section, within the main text or in the captions of relevant figures or tables).

When reporting experiments on human subjects, authors should indicate whether the procedures followed were in accordance with the Helsinki Declaration. Patients have the right to privacy; therefore the identifying information (patient's names, hospital unit numbers) should not be published unless it is essential. In such cases the patient's informed consent for publication is needed, and should appear as an appropriate statement in the article.

The research using animal subjects should be conducted according to the EU Directive 2010/63/EU and following the Guidelines for the welfare and use of animals in cancer research (*Br J Cancer 2010; 102: 1555 – 77*). Authors must identify the committee approving the experiments, and must confirm that all experiments were performed in accordance with relevant regulations.

Transfer of copyright agreement

For the publication of accepted articles, authors are required to send the Transfer of Copyright Agreement to the publisher on the address of the editorial office. A properly completed Transfer of Copyright Agreement, signed by the Corresponding Author on behalf of all the authors, must be provided for each submitted manuscript. A form can be found on the journal's webpage.

Conflict of interest

When the manuscript is submitted for publication, the authors are expected to disclose any relationship that might pose real, apparent or potential conflict of interest with respect to the results reported in that manuscript. Potential conflicts of interest include not only financial relationships but also other, non-financial relationships. In the Acknowledgement section the source of funding support should be mentioned. The Editors will make effort to ensure that conflicts of interest will not compromise the evaluation process of the submitted manuscripts; potential editors and reviewers will exempt themselves from review process when such conflict of interest exists. The statement of disclosure must be in the Cover letter accompanying the manuscript or submitted on the form available on http://www.icmje.org/coi_disclosure.pdf

Page proofs will be sent by E-mail or faxed to the corresponding author. It is their responsibility to check the proofs carefully and return a list of essential corrections to the editorial office within three days of receipt. Only grammatical corrections are acceptable at this time.

Reprints: The electronic version of the published papers will be available on www.versitaopen.com free of charge.

Lilly Onkologija

Vsaka odprta vrata lahko pomenijo novo odkritje.

Z več kot 60 tarčnimi zdravili v razvoju, se naša prizadevanja v iskanju pristopov zdravljenja po meri bolnika, šele pričenjajo.

Lilly Onkologija

Niti dva bolnika z rakom nista enaka. Zato si Lilly Onkologija prizadeva, da razvije tako edinstvene pristope zdravljenja, kot so edinstveni ljudje, ki zdravljenje potrebujejo. Veliko smo prispevali k izboljšanju izidov zdravljenja in – z vsakimi vrati, ki jih odpremo – naredimo še en korak naprej. Naša prizadevanja v zagotavljanju zdravljenja po meri bolnika se nadaljujejo.

Znanost približujemo posamezniku.

SIALM00022

Lilly

Odgovori, ki štejejo.

Radiology and Oncology | Ljubljana | Slovenia | www.versitaopen.com

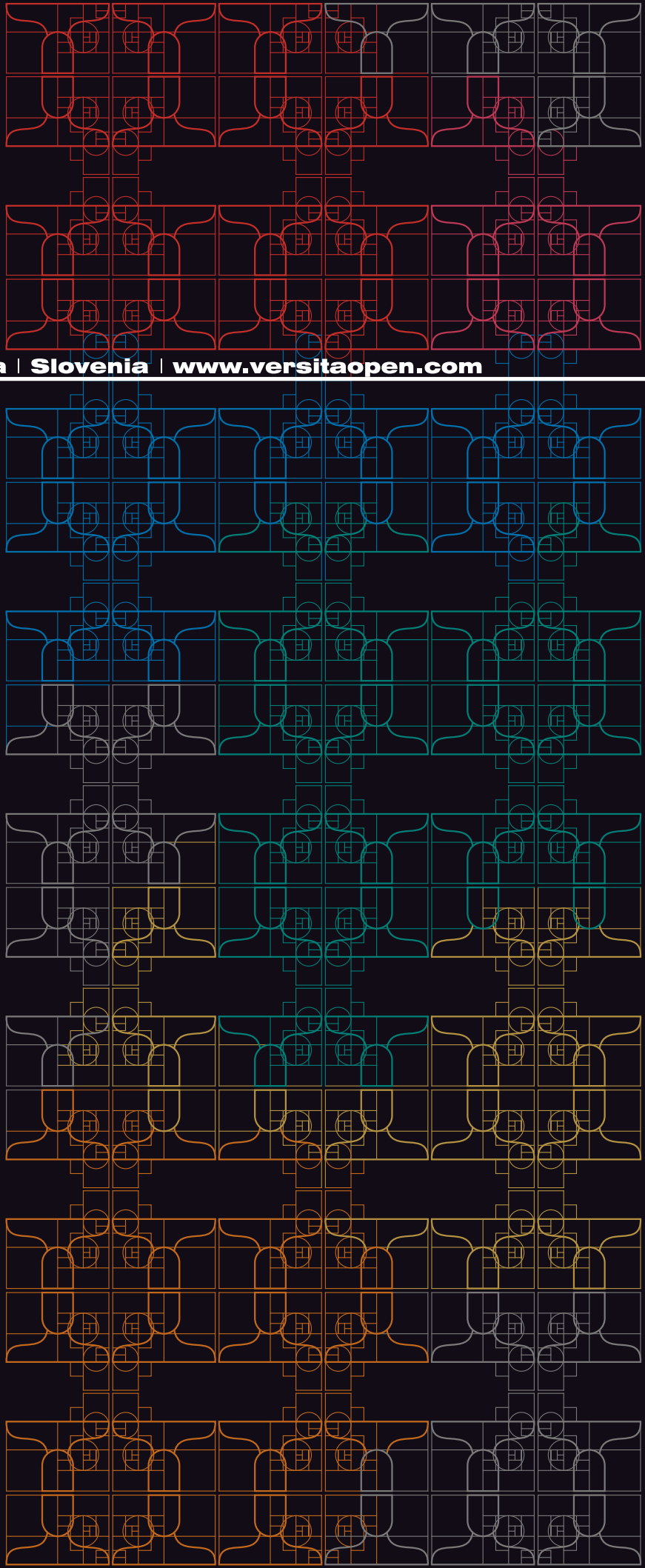

ISSN 1318 - 2099